WGIBAR 2018 REPORT

ICES INTEGRATED ECOSYSTEM ASSESSMENTS STEERING GROUP

ICES CM 2018/IEASG:04

REF ACOM AND SCICOM

Interim Report of the Working Group on the Integrated Assessments of the Barents Sea (WGIBAR)

9-12 March 2018

Tromsø, Norway

ICES
International Council for the Exploration of the Sea

CIEM
Conseil International pour l'Exploration de la Mer

International Council for the Exploration of the Sea
Conseil International pour l'Exploration de la Mer

H. C. Andersens Boulevard 44–46
DK-1553 Copenhagen V
Denmark
Telephone (+45) 33 38 67 00
Telefax (+45) 33 93 42 15
www.ices.dk
info@ices.dk

Recommended format for purposes of citation:

ICES. 2018. Interim Report of the Working Group on the Integrated Assessments of the Barents Sea (WGIBAR). WGIBAR 2018 REPORT 9-12 March 2018. Tromsø, Norway. ICES CM 2018/IEASG:04. 210 pp. https://doi.org/10.17895/ices.pub.8267

Contents

Executive summary

The Working Group Report of the Working Group on the Integrated Assessments of the Barents Sea (WGIBAR), chaired by Elena Eriksen (Norway) and Anatoly Filin (Russia), met in Tromsø, Norway, on 9–12 March 2018. The meeting was attended by 21 participants from 4 institutes and 2 countries.

The group updated most of the time-series data and established additional time-series for the oceanographic conditions (currents, temperature, and salinity (1980–2017), meso zooplankton (1989–2017) and 0-group fish (six fish species, 1980–2017), based on WGIBAR-subareas for the Barents Sea. The group discussed the 2017 state and changes of the Barents Sea ecosystem (see short summery below). The group discussed also different ecosystem models and their use in the IEA, and the group will be a platform for evaluation, testing, and development of ecosystem models. WGIBAR working group provide knowledge of the status, changes, relationships, and processes in the ecosystems to the Joint Russian-Norwegian Fisheries Commission, the Joint Russian-Norwegian Environmental Commission, the Norwegian Ministry of Climate and Environment and different ICES working groups.

Since the 1980s, the Barents Sea has gone from a situation with high fishing pressure, cold conditions and low demersal fish stock levels, to the current situation with high levels of demersal fish stocks, reduced fishing pressure and warm conditions. The current situation is unprecedented, and the Barents Sea appears to be changing rapidly. The main points for 2017 are:

- The air and water temperatures remained higher than average and typical of warm years, yet lower than temperature in 2016. In autumn, the area covered by Atlantic waters (>3°C) was large than in 2016; areas covered by Arctic and cold bottom waters (<0°C) were small but larger than in 2016. Ice coverage was much lower than normal, but higher than in 2016; the lowest value (1%) observed in September.
- Spatially integrated net primary production has increased over the years. A noteworthy increase is observed in the eastern regions where sea ice coverage has diminished over the years. An increase in ice-free areas, and length of the growing season, provide improved habitat for phytoplankton growth.
- Mesozooplankton biomass during autumn was higher than in autumn 2016 in the eastern Barents Sea and on the Central Bank, but lower on the Great Bank. Zooplankton biomasses in the Central Bank and Great Bank subareas have shown declining trends since the peak in 1995. An increasing trend in krill biomass has been observed during the last decades – and the level in 2017 was above the long-term average. Amphipods are still considered to be at a low level - although some large catches were made north and east of Svalbard. Jellyfish biomass was at third highest level since 1980.
- The capelin stock has recovered after a mini-collapse in 2015–2016, and the biomass of young herring is the highest since 2005. Polar cod and blue whiting biomass is low. Cod and haddock biomass have decreased in recent years following a peak around 2013, but is still above the long-term mean. The 2016 and 2017 year classes of haddock seem strong and could be of the same order of magnitude as the strong 2004–2006 year classes. *Sebastes mentella*, Greenland halibut and long rough dab biomass is stable at or above the long-term mean.
- Assessments of the benthos biomass in 2017 were very high but this most likely related with overestimation of the biomass due to the technical causes

during the benthic monitoring like in 2012. The distribution area of the invasive snow crab was larger than in previous years, and for the first time recorded northeast of Svalbard. The shrimp, *Pandalus borealis*, population was within the long-term mean and stable.

- The summer abundance of minke whales in the Barents Sea is now about 50 000 animals and has been quite stable or increasing over the period. The sighting rate from the 2017 survey is the highest recorded which might confirm the apparent increasing trend at present. In 2017, 1518 individuals of nine species of marine mammals were observed during the Barents Sea Ecosystem Survey (BESS), August-October 2017 and an additional 46 individuals were not identified to species level.
- A large-scale monitoring of marine litter performed in the joint Norwegian–Russian ecosystem monitoring surveys in the period from 2010 to 2017. During the time-series, plastic dominated number of observations with marine litter, as 72% of surface observations, 94% of pelagic trawls, and 86% of bottom trawls contained plastic. In 2017, marine litter on the surface (floating) and taken by trawls dominated by plastic. Wood was registered in the 28.4% of stations, while textile, paper, rubber and metal was observed occasionally.

1 Administrative details

Working Group name

The Working Group on the Integrated Assessments of the Barents Sea (WGIBAR)

Year of Appointment within the current cycle

2016

Reporting year within the current cycle

2

Chairs

Elena Eriksen (Norway)

Anatoliy Filin (Russia)

Meeting venues and dates

9-12 March 2018, Tromsø, Norway, (21 participants)

16–18 March 2017, Murmansk, Russia (25 participants)

2 Terms of Reference a) – d)

ToR	Description	Background	Science Plan topics addressed	Duration	Expected Deliverables
a	Prepare relevant datasets that can be used to describe and analyse fluctuations and changes in the Barents Sea ecosystem	Science and advisory requirements		Year 1,2 and 3	Updated multivariate datasets (Year 1,2 and 3). Develop new spatially disaggregated time-series (Year 1 and 2)
b	Prepare an annual report on the status and trends of the Barents Sea ecosystem based on integrated analysis of multivariate datasets and other relevant information	Science and advisory requirements		Year 1, 2 and 3	Annual reports of the status, drivers, pressures, trophic interactions and expected changes
c	Identify knowledge gaps and priority research items that when addressed, can improve future integrated ecosystem assessments	Science and advisory requirement		Year 1, 2 and 3	Annual status reports
d	Explore the use of available ecosystem and multi-species models as an analytical tool in integrated ecosystem assessment for the Barents Sea	Science and advisory requirements		Year 1, 2	Annual meting report
e	Provide recommendations to improve the monitoring of the Barents Sea ecosystem for integrated ecosystem assessments	Science and advisory requirements		Year 1	Annual meeting reports

3 Summary of Work plan

Year 1	Prepare relevant datasets and other relevant information, including pollution that can be used to describe fluctuations and changes in the Barents Sea ecosystem and prepare an annual report on the status and trends of the Barents Sea ecosystem based on integrated analysis of multivariate datasets. Present and discuss available ecosystem and multispecies models as an analytical tool in integrated ecosystem assessment for the Barents Sea Identify knowledge gaps and priority research items that can improve future integrated ecosystem assessments and provide recommendations to improve the monitoring Map collaboration partners, their needs and advantage from the cooperation.
Year 2	Prepare relevant datasets and other relevant information that can be used to describe fluctuations and changes in the Barents Sea ecosystem and prepare an annual report on the status and trends of the Barents Sea ecosystem based on integrated analysis of multivariate datasets. Identify knowledge gaps and priority research items that can improve future integrated ecosystem assessments. Explore the use of the ecosystem /multispecies models as an analytical tool in integrated ecosystem assessment for the Barents Sea.
Year 3	Prepare relevant datasets and other relevant information that can be used to describe fluctuations and changes in the Barents Sea ecosystem and prepare an annual report on the status and trends of the Barents Sea ecosystem based on integrated analysis of multivariate datasets. Identify knowledge gaps and priority research items that when addressed, can improve future integrated ecosystem assessments. Summarize literature from the last few years on the Barents Sea ecosystem.

4 List of Outcomes and Achievements of the WG in this delivery period

WGIBAR prepared relevant datasets and other relevant information, including pollution, to describe fluctuations and changes in the Barents Sea ecosystem and prepared an annual report "The state and trends of the Barents Sea ecosystem", which is available on the ICES WGIBAR community page as separate document.

Since the 1980s, the Barents Sea has gone from a situation with high fishing pressure, cold conditions and low demersal fish stock levels, to the current situation with high levels of demersal fish stocks, reduced fishing pressure and record warm conditions. The main points for 2016 are listed in executive summary.

New spatial time-series for oceanography, mesoplankton and 0-group fish were prepared for the WGIBAR annual meeting. These new time-series are based on subareas defined in 2017 (see report from WGIBAR 2017). Description and estimation of new time-series were included in the report or as working document (Annex 4).

Most of the scientific work relevant for WGIBAR is done by other projects at IMR/PINRO or other institutions. Because of the way WGIBAR is funded there is little intersessional work done by WGIBAR as a group.

4.1 List of relevant publications

Dalpadado P., Hop H., Rønning J., Pavlov V., Sperfeld E., Buchholz F., Rey A., Wold A. 2016. Distribution and abundance of euphausiids and pelagic amphipods in Kongsfjorden, Isfjorden, and Rijpfjorden (Svalbard) and changes in their relative importance as key prey in a warming marine ecosystem. Polar Biology DOI 10.1007/s00300-015-1874-x

Eriksen, E., Gjøsæter, H., Prozorkevich, D., Shamray, E., Dolgov, A., Skern-Mauritzen, M., Stiansen, J.E., Kovalev, Yu., Sunnanaa K. 2017. From single species surveys towards monitoring of the Barents Sea ecosystem. Progress in Oceanography http://dx.doi.org/10.1016/j.pocean.2017.09.007

Eriksen, E, Bogstad, B., Dolgov, A.V., and Beck, I.M. 2017. Cod diet as an indicator of Ctenophora abundance dynamics in the Barents Sea. Marine Ecology Progress Series, https://doi.org/10.3354/meps12199

Eriksen, E., Skjoldal, H.R. Gjøsæter, H. and Primicerio R. 2017. Spatial and temporal changes in the Barents Sea pelagic compartment during the recent warming. Progress in Oceanography 151: 206-226, http://dx.doi.org/10.1016/j.pocean.2016.12.009

Jørgensen 2017. Trawl and temperature pressure on Barents benthos. FEATURE ARTICLE – ICES, 11 July 2017.

Jørgensen, LL., Archambault P., Blicher M., Denisenko N., Guðmundsson G., Iken K., Roy V., Sørensen J., Anisimova N., Behe C., Bluhm B.A., Denisenko S., Denisenko N., Metcalf V., Olafsdóttir S., Schiøtte T., Tendal O., Ravelo A.M., Kędra M., Piepenburg D. 2017. "Benthos" In: CAFF. State of the Arctic Marine Biodiversity Report. Conservation of Arctic Flora and Fauna, Akureyri Iceland

Gjøsæter, H., Wiebe, P. H., Knutsen, T., and Ingvaldsen, R. 2017. Evidence of diel vertical migration of mesopelagic sound-scattering organisms in the Arctic. Frontiers in Marine Science.

Haug, T., Bogstad, B., Chierici, M., Gjøsæter, H., Hallfredsson, E. H., Høines, Å. S., Hoel AH., Ingvaldsen R.B., Jørgensen L.L., Knutsen T., Loeng H., Naustvoll L.J., Røttingen I., Sunnanå K., Loeng, H. 2017. Future harvest of living resources in the Arctic Ocean north of the Nordic and Barents Seas: A review of possibilities and constraints. Fisheries Research, 188, 38-57.

Ingvaldsen, R. B., Gjøsæter, H., Ona, E., and Michalsen, K. 2017. Atlantic cod (Gadus morhua) feeding over deep water in the high Arctic. Polar Biology.

Knutsen, T., Wiebe, P. H., Gjøsæter, H., Ingvaldsen, R., and Lien, G. 2017. High Latitude Epipelagic and Mesopelagic Scattering Layers - A Reference for Future Arctic Ecosystem Change. Frontiers in Marine Science.

5 Progress report on ToRs a) –e)

5.1 Progress report on ToR a

We updated most of the time-series data compiled for the first meeting sets (ICES 2014a) prior to or during the meeting of this year. We have established additional time-series for the oceanographic conditions (currents, temperature and salinity (1980–2017), mesozooplankton (1989–2017) and 0-group fish (six fish species, 1980–2017), based on new subareas for the Barents Sea (WGIBAR report 2017). These new spatial time–series are presented as working document in Annex 4.

The Integrated multivariate (PCA and RDA) analyses were performed for different purposes. The time-series were standardized to zero mean and unit variance. Analyses of temporal development of abiotic variables (1979–2017) showed shift from a cold to a warm regime and 2017 is a warm year. Further, abiotic time-series were combined with biotic (plankton and juveniles, organisms drifted with the currents into the Barents Sea) and analyses showed increasing of biomasses with the warming (1986–2017).

5.2 Progress report on ToR b

The followed presentations focusing of status of different ecosystem components and pressures were given during the meeting:

Hydrography, Alexander Trofimov

The situation for 2017 was presented for the following parameters: temperature (water and air), salinity, sea ice coverage, NAO index, index for storm activity, Atlantic water inflow, and areas of Atlantic, Arctic and mixed waters.

Plankton, Espen Bagøien

The situation was presented with the most recent data on net primary productivity as estimated by using satellite data, biomass of mesozooplankton, occurrence of *Calanus glacialis* and *Calanus finmarchicus* in sections, abundance of euphasiids, abundance of amphipods, and abundance of jellyfish.

0-group fish, Elena Eriksen

Abundance and distribution of 0-group of cod, haddock, NSS herring, capelin polar cod, and redfish was presented. Anomalies for average 0-group body length was also presented for these species (except redfish).

Pelagic fish, Georg Skaret/Harald Gjøsæter

Status and development of the stocks were presented for capelin and polar cod as well as the juvenile part of the NSS herring stock, and the part of the blue whiting stock residing in the Barents Sea. The abundance time-series of blue whiting is this year re-calculated with a revised target strength, which is considerable higher than the values used previously (https://www.hi.no/tokt/okosystemtokt_i_barentshavet/survey_reports/survey_report_2017/nb-no), resulting in a major downscaling of the blue whiting abundance during the whole time-series.

It was noted that the estimate of capelin obtained in autumn 2017 did not fit well with the estimate obtained in 2016. Either the 2016 estimate was an underestimate, the 2017 estimate an overestimate, or a combination of these two. It was also noted that the polar cod estimate in 2016 seems out of phase with those in 2015 and 2017; in 2016 the polar cod stock was estimated six times higher than in 2015 and five times higher than in

2017. Since more than 90% of the stock estimated in 2016 consisted of the 2015 year class, the estimate is not incompatible with the 2015 estimate, but if the 2017 estimate is correct, either there has been unusually high mortality from age one to age two of the 2015 year class, or major parts of this year class has migrated out of the surveyed area. These facts cause problems for the integrated analyses.

Demersal fish, Bjarte Bogstad

Status and development of the stocks was presented for cod, haddock, deep-sea (beaked) redfish, long rough dab, and saithe. Data on diet and fish growth were presented as well as for cod, capelin, and polar cod.

Slope communities, Elvar Hallfredsson

The continental slope between the Barents Sea and the Norwegian Sea contains unique fauna of fish and other organisms, and fish communities at the slope differ from the shelf ecosystem of the Barents Sea, and the pelagic ecosystems of the Norwegian Sea and the Central Arctic Ocean. Still the slope communities are affected by and affect the surrounding areas e.g. through species Greenland halibut and beaked redfish with distribution into these ecoregions as well as the slope. At the moment, the continental slope is not comprehensively covered by the ecoregion ICES working groups WGINOR[1], WGIBAR and WGICA[2], and this should be addressed.

Benthos, Lis Lindal Jørgensen/Natalia Strelskova

Status and trends of the benthos biomass and snow crab, and shrimp population abundances were presented. Two interaction drivers was discussed 1) Fisheries (temperature) and snowcrab impact on benthos, 2) temperature impact on the snow crab distribution of the Barents Sea.

Marine mammals, Mette Skern-Mauritzen

Status and trends of the marine mammal observation based on ecosystem survey in August-September 2017 and monitoring survey 2017. The main groups of humpback and fin whales were feeding at concentrations of capelin, primarily in areas south of Spitsbergen and on the Great Bank, other marine mammals in the Barents Sea were observed at concentrations of polar cod, capelin, herring, and cod fish.

Non-commercial fish, Elena Eriksen

Distribution of different zoogeographic groups of non-commercial fish species was presented for 2004–2017. Time-series of abundance indices for the same groups were also presented.

Marine litter, Elena Eriksen

Results from monitoring of marine litter based on ecosystem survey and Mariano program were presented. Summary of the newly published work, summarizing marine litter monitoring in the Barents Sea were also presented.

During the meeting a report "The state and trends of the Barents Sea ecosystem" was drafted and is presented as a separate document, available for the scientific community

[1] Working Group on the Integrated Assessments of the Norwegian Sea

[2] ICES/PICES/PAME Working Group on Integrated Ecosystem Assessment (IEA) for the Central Arctic Ocean

and others on the WGIBAR community page. The main findings are summarized in the executive summary.

The WGIBAR report "The state and trends of the Barents Sea ecosystem"is used in the status report for the Norwegian-Russian environmental commission, and by the Work Programme for the Norwegian - Russian environmental cooperation associated with the Joint Russian Norwegian Environmental Commission. In addition, several annual reports made separately in Norwegian and Russian by IMR and PINRO make use of the WGIBAR report on the state of the Baltic Sea. Furthermore, the Arctic Fisheries Working Group (AFWG), the main stock assessment working group for the Barents Sea use information from the report in their report each year.

5.3 Progress report on ToR c

During the WGIBAR meeting in 2016 and updated in 2017, the following research questions relevant for the state of the Barents Sea and management were identified:

The Barents Sea has been on a warming trend since 1980 with shorter oscillations between warm and cooler years. 2016 was the warmest year on record exceeding 2006 and 2012 as the two most recent warm years. The warming has been associated with an expansion of Atlantic and mixed (0–3°C) water masses and a near disappearance of Arctic water (defined as water with sub-zero temperature) and strong reduction in winter sea ice.

The oceanographic changes that are taking place has implications for all life forms in the Barents Sea both in the water and on the seafloor. There are many research questions related to distribution and population dynamics of single species and their interactions in foodwebs and communities. One particular question concerns the dominant herbivore copepod in the northern Barents Sea, *Calanus glacialis*, which has its habitat in the cold Arctic water. How will this copepod cope under warmer conditions with less sea ice and extended period of predation by planktivorous fish? Some model predictions are that *C. glacialis* will not do well and lead to a decrease in production of large mesozooplankton in the northern Barents Sea (Slagstad *et al.,* 2011).

Associated with the decline in Arctic water, the transitional mixed water (0–3°C) has increased. An important question is whether this habitat is suboptimal for both *C. finmarchicus*, which thrives on the warm side, and *C. glacialis*, which is found in cold Arctic water. The declining trend in mesozooplankton biomass on the Central and Great Banks may be an indication that change in oceanographic conditions associated with warming has made these waters less favorable for the Calanus species.

Russian and joint time-series reveal an increasing trend in krill (euphausids) over the last 10–15 years. This is likely related to warming and improved habitat conditions for advected krill, notably *Meganyctiphanes norvegica* and *Thysanoessa inermis* (Eriksen *et al.,* 2016, 2017). The increased amount of krill plays important roles in the ecosystem as food for a range of consumers, including fish, seabirds, and marine mammals. We need a better understanding of the spatial ecology and trophic role of the dominant krill species in the Barents Sea ecosystems. This includes to what extent the krill species reproduce in the Barents Sea, as opposed to being advected in from the adjacent Norwegian Sea.

Pelagic hyperiid amphipods, notably the large Arctic species *Themisto libellula*, have shown an opposite trend to that of krill, with a pronounced decrease in the Barents Sea over the most recent decades. Like for the krill species, we need better understanding of the biology and ecology of the dominant pelagic amphipods in the Barents Sea. They

are to large extent omnivores and carnivores and play dual roles as prey for and food competitors with planktivorous fish such as capelin, juvenile herring, and polar cod.

The cod stock is still at a high level and capelin, which is a key prey item, is increasing from a low level. Increased overlap between cod and capelin in summer, where cod has been able to follow capelin on its seasonal feeding migration to the northern Barents Sea, has resulted in increased predation by cod which eventually lead to the collapse of the capelin stock in 2015. The estimated consumption of capelin by cod in 2016 was still fairly high although cod has been shifting to take more alternative prey composed of other fish species and benthos. One important research issue is to what extent the large cod stock will prevent the recovery of the capelin stock by continuing to exert strong predation pressure. Another issue is the predation pressure from cod on the alternative prey. These include small Arctic fish (sculpins, snailfish, eelpouts, and others) which may not be so abundant and form high biomass. Will the large cod stock deplete these prey resources over the next few years, and will this in turn affect the feeding conditions and the overall status of the cod stock? May we witness a marked decrease in the condition and size of the cod stock in near future? These are questions that require our attention as we plan cruises and research activities.

The reasons for the discrepancies between the 2016 and 2017 estimates of Barents Sea capelin should be investigated further.

5.4 Progress report on ToR d

As of now, WGIBAR consists of researchers from IMR and PINRO, the institutions that do most of the monitoring of the Baltic Sea ecosystem. In addition, professors from The arctic University of Tromsø, Raul Primicerio and Torstein Pedersen participated actively in the group.

Mette Skerm -Mauritzen held a presentation about ICES expectations to Integrated Ecosystem Assessment (IEA) groups and experiences from other IEA with ecosystem modelling.

Benjamin Planque held presentation about principal Component Analysis (PCA) has been used as a standard tool in many ICES-IEA groups to summarize ecosystem trajectories and reveal relationships between various ecosystem components.

Torstein Pedersen held a presentation suggesting potential use of EwE in WGIBAR and how information from WGIBAR could be used in EwE-modelling. It was stressed that we are now experiencing environmental conditions (e.g. temperature) outside the time-range where reliable time-series exists, and thus it is challenging to use earlier time-series to understand and predict the present and future ecosystem responses. An Ecopath model comprising about 115 ecological groups have been constructed and this model have been tested for a case study regarding multi-stressor effects from changes in primary production, increase in snow crab biomass and exploitation level in the cod fishery. Modelling scenarios indicated that effects of increasing snow crab abundance affected relatively few groups, but there were negative effects on some prey groups and their predators while some predators on snow crabs (e.g. thorny ray and cod) were positively affected. It is now worked on documentation, assessment of uncertainty and publication of the model.

Anatoly Filin presented the results of using of STOCOBAR multispecies model for the evaluations of cod response to the ecosystem changes in the Barents Sea. This includes studies on cannibalism in cod, an impact of temperature and capelin abundance on cod stock as well as evaluation of long-term consequences of different scenarios of climate

change for the cod stock dynamics. Impact of capelin on cod is imitated through the changes in cod growth, feeding, maturation, and natural mortality induced by cannibalism. Temperature scenarios for the model runs can be created both outside and inside of the model. STOCOBAR is the most suitable for the scenario modelling. It may be useful for evaluation of long-term consequences of climate change in the Barents Sea. The uncertainties are associated with such kind of studies were also considered. Ecosystem change scenarios for the STOCOBAR simulations can include outputs from the other ecosystem and multispecies models. This may be used as a basis for development of multi-model evaluations.

The group agreed that the use of ecosystem models would be useful. The WGIBAR group is a group with expertise of oceanography, plankton, fish, benthos, seabirds, and marine mammals biology and ecology, with expertise within stock dynamics and assessment, and therefore this is an excellent platform for evaluation of ecosystem models. Some results from "Atlantis" models will be presented and discussed during the annual meetings. The group will continue to use PCA for visualization of big datasets of time-series and also spatial data. The group will continue to search for other methods to analyse big datasets.

5.5 Progress report on ToR e

The ecosystem survey is a cooperation between IMR and PINRO and has been run annually in August–October since 2004. The ecosystem survey covers the whole Barents Sea shelf and samples all main ecosystem components allowing the study of spatial overlaps and interactions (Annex 5 in the report "State and trends in the Barents Sea 2017"). Eriksen *et al.* (2017) described the development of Barents Sea monitoring from single species (or fishery) surveys focused on target species/groups to integrated ecosystem surveys aimed to describe the status and main changes in the Barents Sea ecosystem.

Parts of the text in this report are modified from the latest ecosystem survey report (which is available on https://www.hi.no/tokt/okosystemtokt_i_barentshavet/survey_reports/survey_report_2017/nb-no).

In 2017, the timing and the survey design was optimal. However due to various reasons, coverage of 0-group fish was insufficient.

WGIBAR recommends keeping BESS survey design as in previous year, including standard investigations at the same level.

WGIBAR suggests to extent the survey area in the northern Barents Sea, especially in the northeast and in Svalbard (Spitsbergen) area. Better coverage of the northern parts will provide more information about key species such as Greenland halibut, polar cod, and snow crab and the arctic community.

WGIBAR suggests evaluating methodological challenges with benthos and plankton sampling in the Barents Sea.

WGIBAR recommends increasing survey coverage during the winter survey for demersal fish (NOR-RU Q1 (Btr)) so that most of the ice free area is covered, especially east of Svalbard (Spitsbergen).

References:

Eriksen, E., Gjøsæter, H., Prozorkevich, D., Shamray, E., Dolgov, A., Skern-Mauritzen, M., Stiansen, J.E., Kovalev, Yu., Sunnanaa K. 2017. From single species surveys towards monitoring

of the Barents Sea ecosystem. Progress in Oceanography http://dx.doi.org/10.1016/j.pocean.2017.09.007

5.6 Cooperation

Cooperation with other WGs

- Stock assessment groups in particular the Arctic Fisheries Working Group (AFWG) and the Working Group on Widely Distributed Stocks (WGWIDE);
- Other IEA groups in particular the Working Group on the Integrated Assessments of the Norwegian Sea (WGINOR) and the ICES/PICES/PAME Working Group on Integrated Ecosystem Assessment (IEA) for the Central Arctic Ocean (WGICA);
- The Working Group on Multispecies Assessment Methods (WGSAM);
- At the moment the continental slope is not comprehensively covered by the ecoregion working groups WGINOR, WGIBAR and WGICA in ICES, and this should be addressed.

Cooperation with Management structures

The Joint Russian-Norwegian Fisheries Commission, in charge of joint fisheries management in the Barents Sea.

The Joint Russian-Norwegian Environmental Commission, in charge of joint environmental management in the Barents Sea.

The Norwegian Ministry of Climate and Environment, in charge of Norwegian holistic ecosystem-based management plan for the Norwegian part of the Barents Sea. The Ministry supports the WG report preparation and publish Annex 5 on Barents Portal (http://www.barentsportal.com/barentsportal/index.php/en/).

Cooperation with other IGOs

Relevant groups within the Arctic Council. PAME/ICES workshop (Seattle);

Norwegian monitoring group under the Norwegian Management Plan;

Norwegian Fishery reference fleet (coastal and sea).

6 Revisions to the work plan and justification

ToR d (multispecies) will be prolonged to 2019 to consider updates on modelling activity.

7 Next meeting

Next WGIBAR meeting will be held in Russia in February-March 2019.

Annex 1: List of participants

Name	Address	E-mail
Espen Bagøien	Institute of Marine Research, Norway	espen.bagoien@hi.no
Bjarte Bogstad	Institute of Marine Research, Norway	bjarte.bogstad@hi.no
Elena Eriksen	Institute of Marine Research, Norway	elena.eriksen@hi.no
Anatoly Filin	Knipovich Polar Research Institute of Marine Fisheries and Oceanography, Russia	filin@pinro.ru
Dmitry Prozorkevich	Knipovich Polar Research Institute of Marine Fisheries and Oceanography, Russia	dvp@pinro.ru
Yury Kovalev	Knipovich Polar Research Institute of Marine Fisheries and Oceanography, Russia	kovalev@pinro.ru
Hein Rune Skjoldal	Institute of Marine Research, Norway	hein.rune.skjoldal@hi.no
Aleksandr Trofimov	Knipovich Polar Research Institute of Marine Fisheries and Oceanography, Russia	trofimov@pinro.ru
Harald Gjøsæter	Institute of Marine Research, Norway	harald@hi.no
Vidar Lien	Institute of Marine Research, Norway	vidar.lien@ hi.no
Irina Prokopchuk	Knipovich Polar Research Institute of Marine Fisheries and Oceanography, Russia	irene_pr@pinro.ru
Padmini Dalpadado	Institute of Marine Research, Norway	padmini.dalpadado@hi.no
Raul Primicerio	The Arctic University of Norway, Norway	raul.primicerio@uit.no
Mette Skern-Mauritzen	Institute of Marine Research, Norway	mette.mauritzen@hi.no
Maria Fossheim	Institute of Marine Research, Norway	maria.fossheim@hi.no
Bérengère Husson	Institute of Marine Research, Norway	Berengere.Husson@hi.no
Torstein Pedersen	The Arctic University of Norway, Norway	torstein.pedersen@uit.no
Per Fauchald	Norwegian Institute for Nature Research, Norway	per.fauchald@nina.no

Annex 2: Recommendations

Recommendation	Adressed to
Take to account the changes in the Barents Sea ecosystem and ecosystem components. "State and trends of the Barents Sea ecosystem 2017" reported in Annex 5.	AFWG, WGWIDE, WGHARP and NIPAG

Annex 3: Agenda for WGIBAR 2018

14:00–14:10 Opening of WGIBAR meeting, adopting of the agenda and practical information (E. Eriksen/A. Filin)

14:10–19:00 Prepare an annual report on the status and trends of the Barents Sea ecosystem based on integrated analysis of multivariate datasets and other relevant information (Tor b).

Ecosystem status and trends (presentation-10-20 minutes and discussion-5-10 minutes each):

- Oceanography (A.Trofimov/V. Lien)
- Primary production (NPP) (P.Dalpadado)
- Plankton (E. Bagøien/I. Prokopchuk)
- Fish recruitment (E. Eriksen/D. Prozorkevich)
- Pelagic fish (G.Skaret/(H. Gjøsæter /D.Prozorkevich)
- Demersal fish (B.Bogstad/ Yu. Kovalev)
- Benthos (L. Jørgensen/N.Strelkova/D.Zakharov)
- Fish trophic interactions (B.Bogstad/A.Dolgov)
- Non-commercial fish (E-JOhannesen/T. Prokhorova/E.Eriksen)
- Marine mammals N-Øien/(M. Skern-Mauritzen)
- Seabirds (P. Fauchald)
- Marine litter (BE.Grøsvik/L.Buhl-Mortensen/E.Eriksen)

General discussion about the changes and status of the ecosystem components

20:00 Dinner

March 10, Saturday (Radisson Blu)

09:00–12:00

Prepare relevant datasets that can be used to describe and analyse fluctuations and changes in the Barents Sea ecosystem (Tor a)

Presentation of new spatial dataset:

- Oceanography (V.Lien)
- Plankton (H.R. Skjoldal)
- 0-group fish (E. Eriksen)

Identify knowledge gaps for improvement of future integrated ecosystem assessments (ToR c)

12:00–13:00 Lunch

13:00–17:00 Practical work by groups

Perform the integrated analysis of multivariate datasets (R. Primicerio/H.R. Skjoldal/B.Husson/E. Bagøien/ / E. Eriksen H.Gjøsæter/ and other)

Prepare an annual report on the status and trends of the Barents Sea ecosystem

March 11, Sunday (Radisson Blu)

09:00–12:00

Produce recommendations to improve the monitoring of the Barents Sea ecosystem (ToR e)

The Barents Sea ecosystem survey (BESS) 2017

Which ecosystem components should the autumn (BESS) and the winter ecosystem survey cover?

Standardization of marine litter monitoring

12:00–13:00 Lunch

13:00–17:00 Continue practical work by groups

Prepare an annual report on the status and trends of the Barents Sea ecosystem

March 12, Monday (Radisson Blu)

09:00–12:00 Plenary

Explore the use of the ecosystem /multispecies models as an analytical tool in integrated ecosystem assessment for the Barents Sea (Tors d)

- IEA in ICES: approaches and experiences (Mette Skern-Mauritzen)
- Multivariate analyses (Raul Primicerio)
- Ecopath (Torstein Pedersen)
- STOCOBAR (A. Filin)
- Atlantis (M-Skern-Mauritzen)
- Beyond PCA (B. Planque)

12:00–13:00 Lunch

13:00–16:00

Continue practical work by groups

Describe research questions, analyse multivariate dataset and give current state of knowledge pertaining to these questions discuss

Prepare presentation to the Norwegian-Russian scientific meeting (March Meeting)

16:00–17:00 Plenary

Summing up the results of the meeting

Communication and documentation of the results

Future work, next meeting

Annex 4: New spatial time-series

Hydrography in the Barents Sea from autumn cruises 1970-2016 by TIBIA subareas

By Øystein Skagseth

Mean temperature and salinity in three depth layers: 4–25 m, 30–60 m, 99–201 m. from joint IMR-PINRO data.

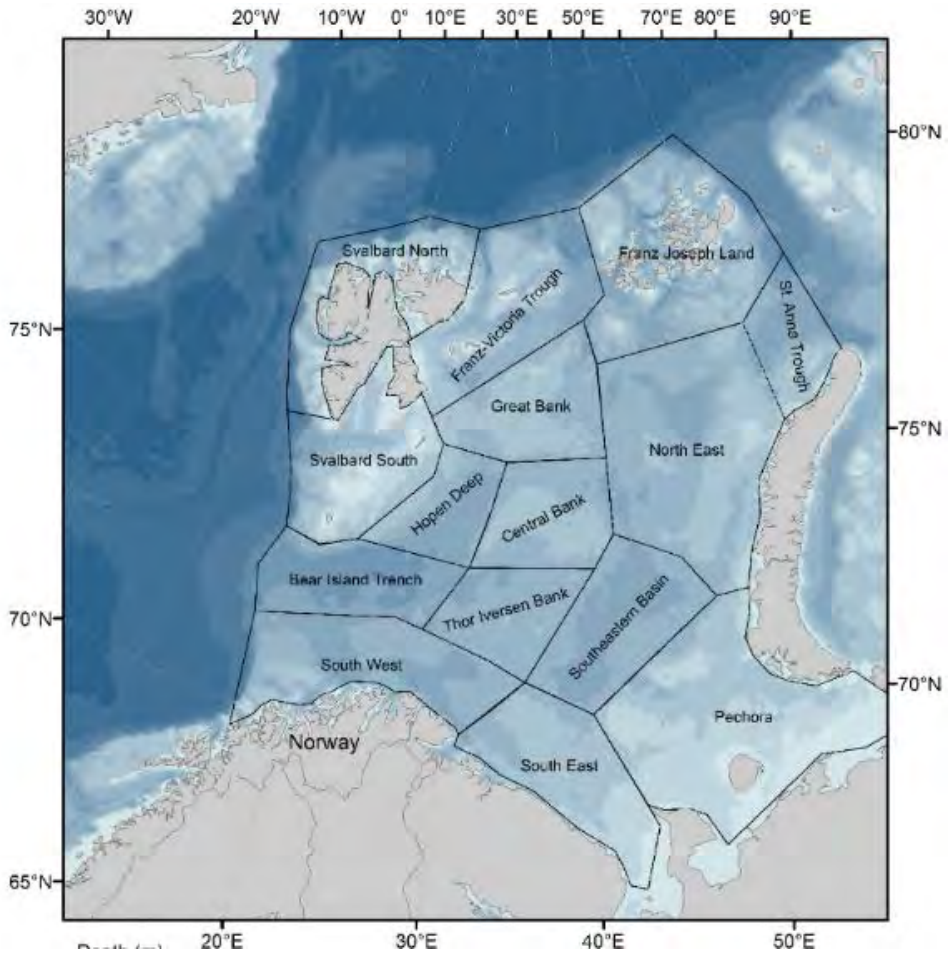

TIBIA subareas (polygons)

Mean temperature and salinity for the subareas.

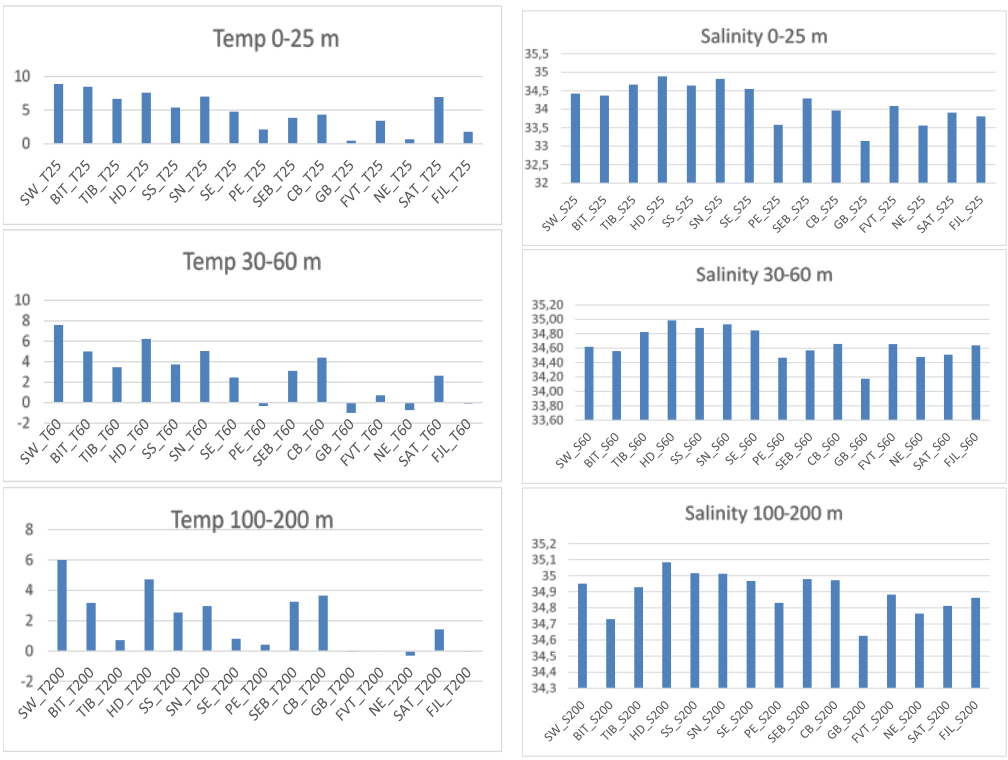

Great Bank and NorthEast are generally the coldest areas in deeper layers.

Pechora is cold in the 30–60 m layer (from ice formation in winter).

Thor Iversen Bank and SouthEast are surprisingly cold in the deep layer.

For TIB this reflects cold water from CB (and GB) that circulates E of CB.

Low salinity in SW due to NCC.

Bear Island Trench has relatively low salinity in 100–200 m; outflowing cold water from banks, in Bear Island Current

Relatively saline and cold dense water from ice formation over banks.

Lowest salinity over GB.

Time-series – temperature and salinity for each subarea.

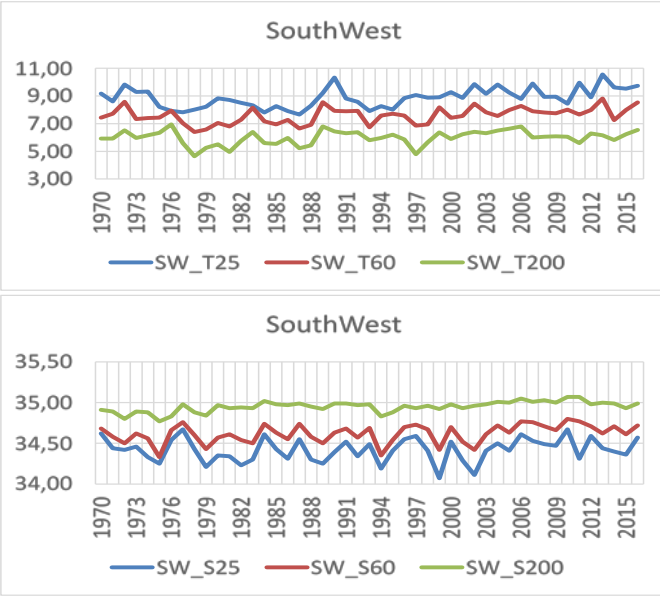

Low temperature and salinity in the cold period 1977–1981.

Low salinity in 1994.

Low temperature in 1997.

Local temperature max (100–200 m) in 2006, 2012, 2016.

Declining trend in salinity after 2010.

Saline and cooler water in deep-water layer. Low saline and warm water in upper 60 m caused by mixing of coastal water in upper layer.

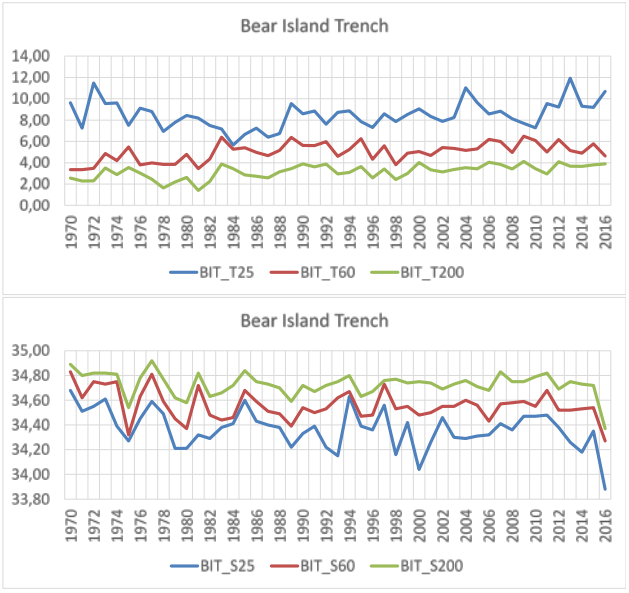

Low salinity in 1975, and again in 1979–1980 and 1982.

Salinity minima in 1995 and 2010.

Low temperature (2–4°C) and salinity (34.6–34.8) at 100–200 m show that this is not inflowing Atlantic water but a mixture also with outflowing modified water.

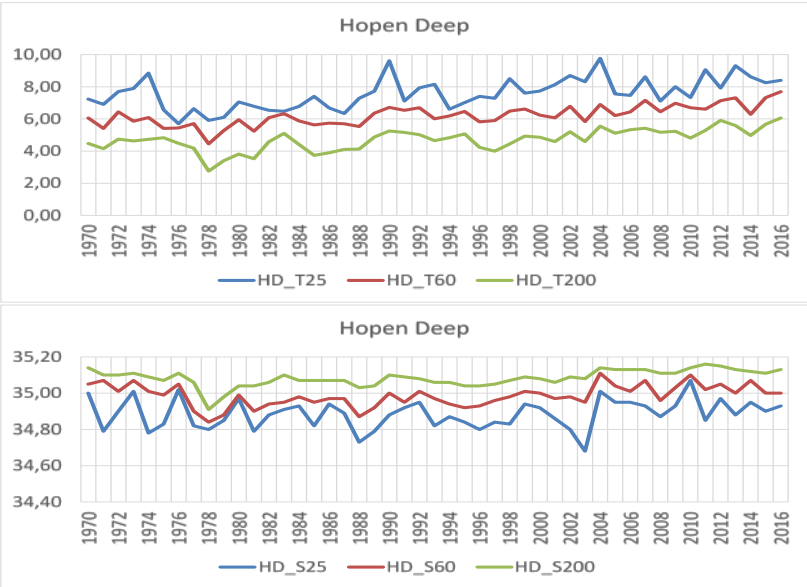

Temperature and salinity minimum in 1978 (100–200 m).

Temperature and salinity maxima in 1983 and 1990.

Temperature minimum in 1997.

Temperature maxima in 2012 and 2016.

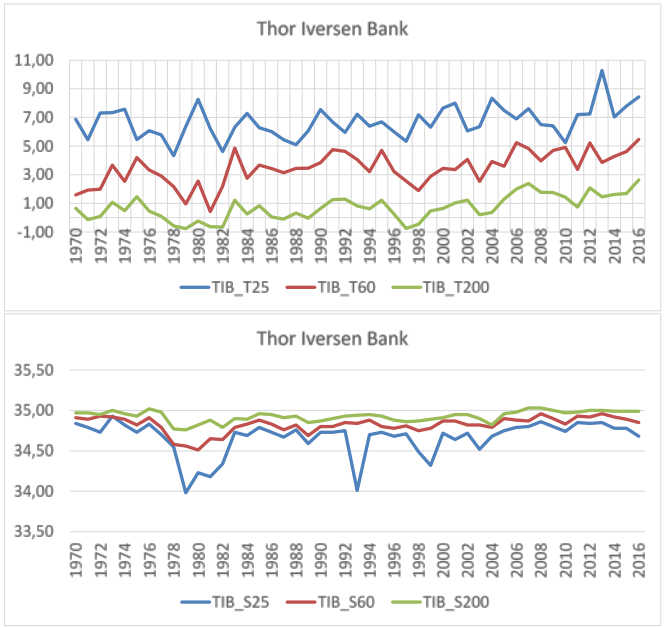

Temperature and salinity minima in the cold period 1978–1981.

Low temperature also in 1997.

Generally low temperature at 100–200 m, between -1°C and +1°C up to 2004.

Low salinity in surface layer in 1993.

Local temperature maxima in 2007, 2012, and 2016.

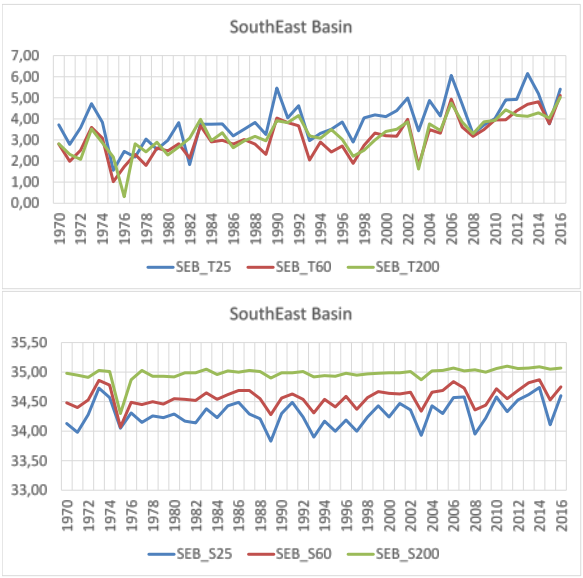

Generally small vertical differences in temperature despite strong salinity gradients. Temperature at 30–60 m and 100–200 m fluctuates in parallel.

There is a pronounced temperature minimum in 1975, and one year later (1976) in the 100–200 m layer. This is accompanied by a pronounced salinity minimum (34.3 at 100-200 m).

There are temperature maxima in 1983, 1990, 2002, 2006, 2012, and 2016.

Temperature minima in 1997, 2003, 2008, and 2015.

Salinity minima in 1989, 2003, 2008, and 2015. Increasing temperature trend in all depths.

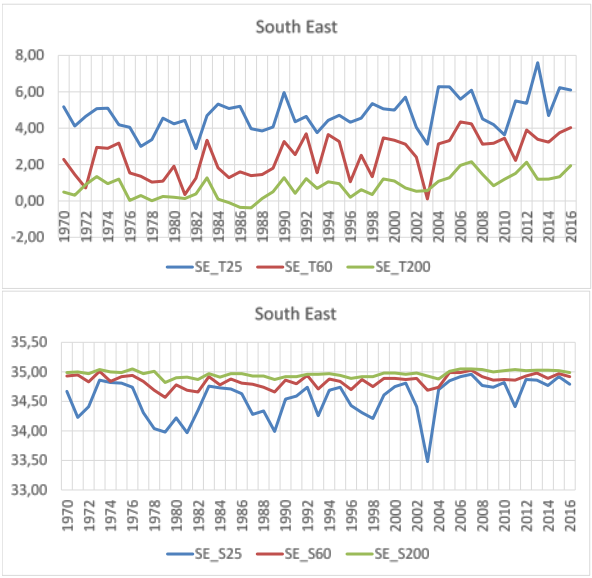

Low temperature at 100–200 m, 0–1°C up to 2004, increasing to 1–2°C after 2004 with local maxima in 2007, 2012, and 2016.

Temperature increases in 1983, 1990, and 2004.

Low salinity in cold period 1978–1981–1982.

Salinity minima in 1989, 1996, and 2003–2004.

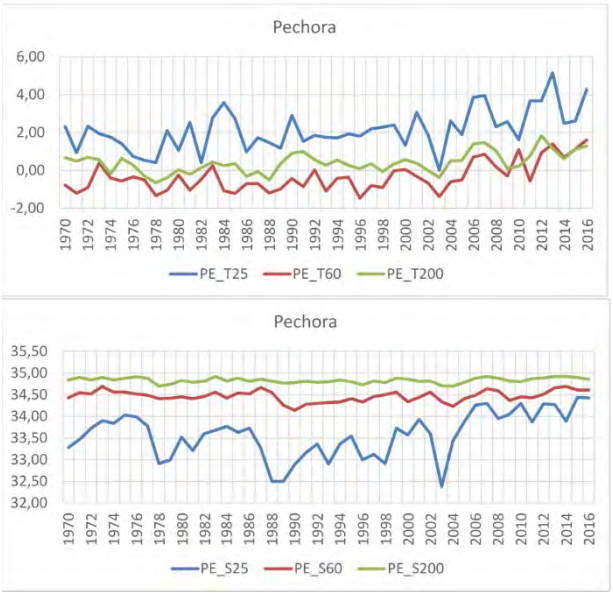

Generally low temperatures. Lowest in 30–60 m layer, reflecting ice formation in winter; <°C up to 2005, warmer after 2005.

Marked change in salinity before and after 2005; 32.5–34.0 before, 34.0–34.5 after.

Seems that temperature increased from 1970s to 2016

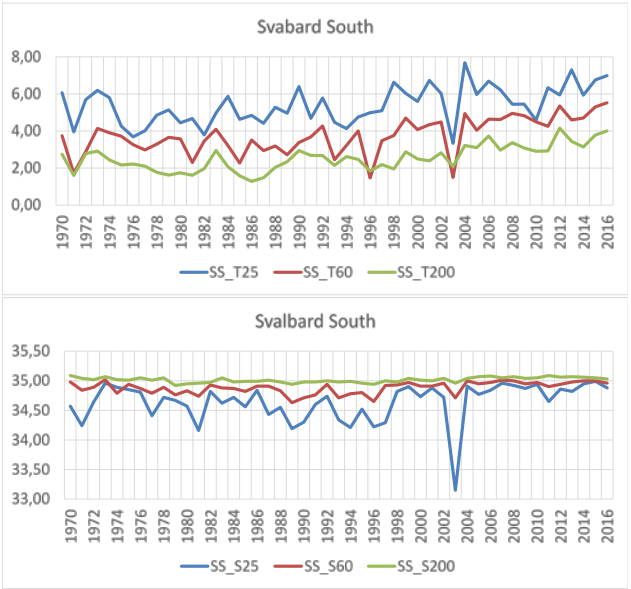

Low temperature in deep layer (100–200 m) in 1978–1982, 1986–1987 and 1996–1998.

Warming in 1983, 1990, 2006, 2012, and 2016.

Marked cooling, and low salinity, in 2003.

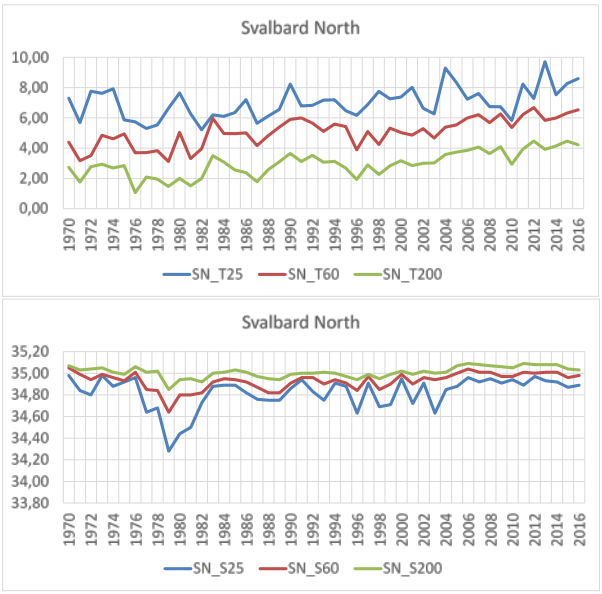

The Great Salinity Anomaly (GSA) is pronounced as temperature and salinity minima 1976–1981.

Pronounced warming in 1983.

Local temperature minima in 1987, 1996, and 2010.

Warming to local maxima in 1990, 2007, 2012.

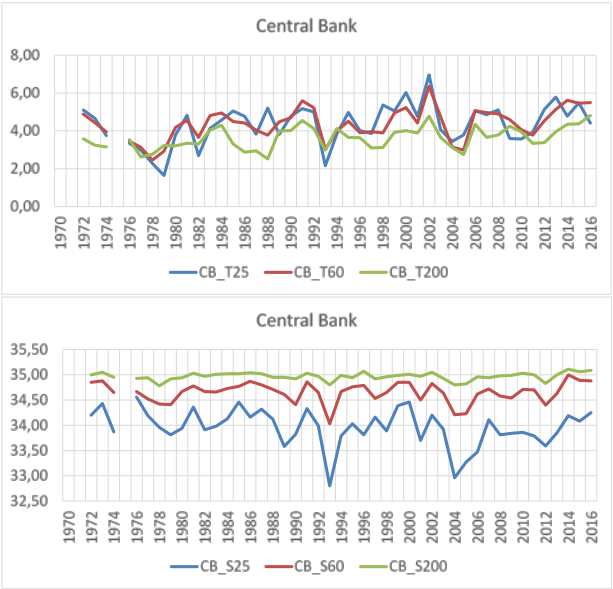

Little temperature difference, particularly in upper 60 m, despite strong salinity gradients.

Relatively warm, 4–6°C in upper 60 m, 3–4°C at 100–200 m.

Cold at the time of the GSA, late 1970s.

Warming 1983–1984, 1989–1991, local temperature maxima 1994, 2002, 2006, and 2016.

Cooling with reduced salinity in 1993, and 2004; some cooling also in 2010-11.

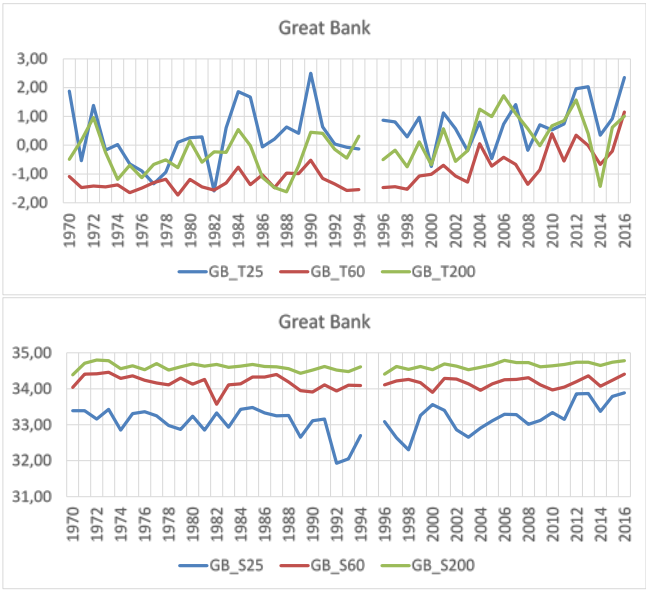

Coldest area overall.

Coldest at 30–60 m, reflecting Arctic water and ice formation in winter. Temp largely <-1°C up to 2003.

Cold periods 1974–1979, and 1986–1988.

Warming to maxima in 1984, 1990, 2004–2006, 2012, and 2016.

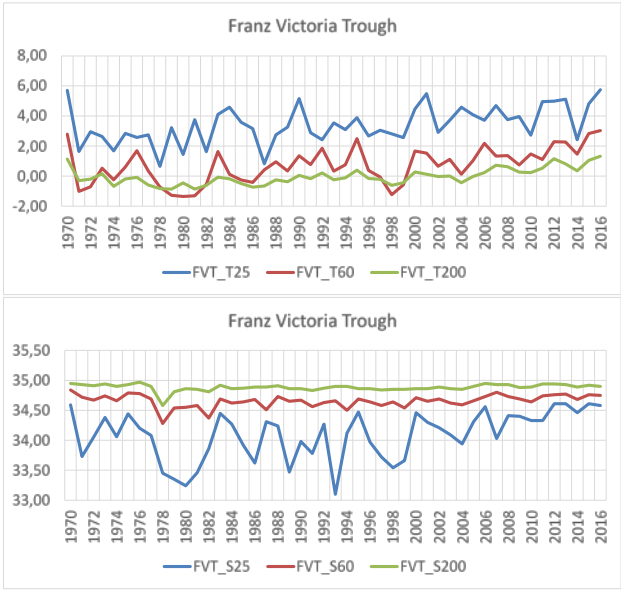

Cold deeper water, -1 to +1°C, with a warming trend.

Cold 1978–1981, 1998; local cooling in 2014.

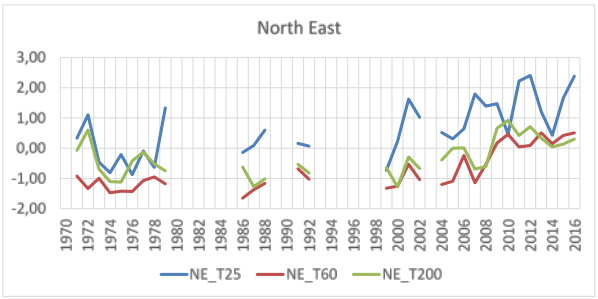

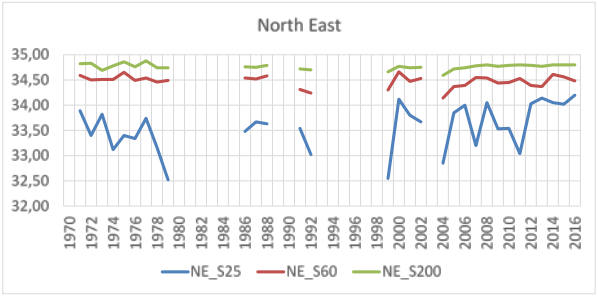

Many years of missing data, difficult to describe a trend

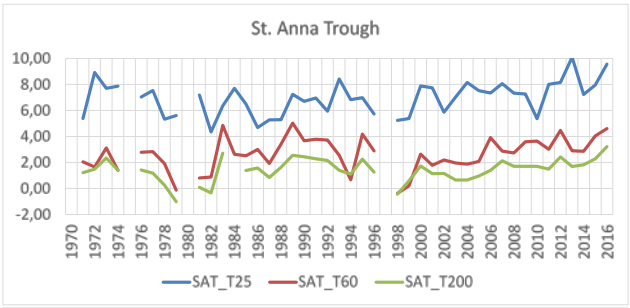

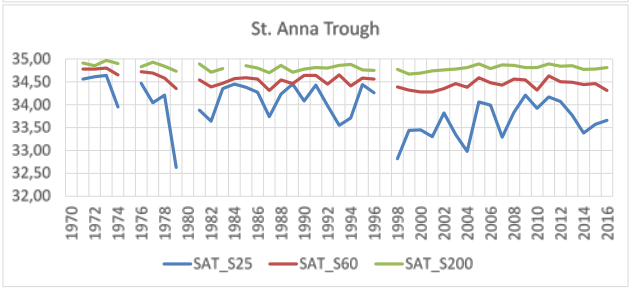

Surprisingly warm, 6-8°C in surface layer.

Cold around 1980 and 1998.

Lower salinity in surface layer after 1998.

Time-series for all polygons

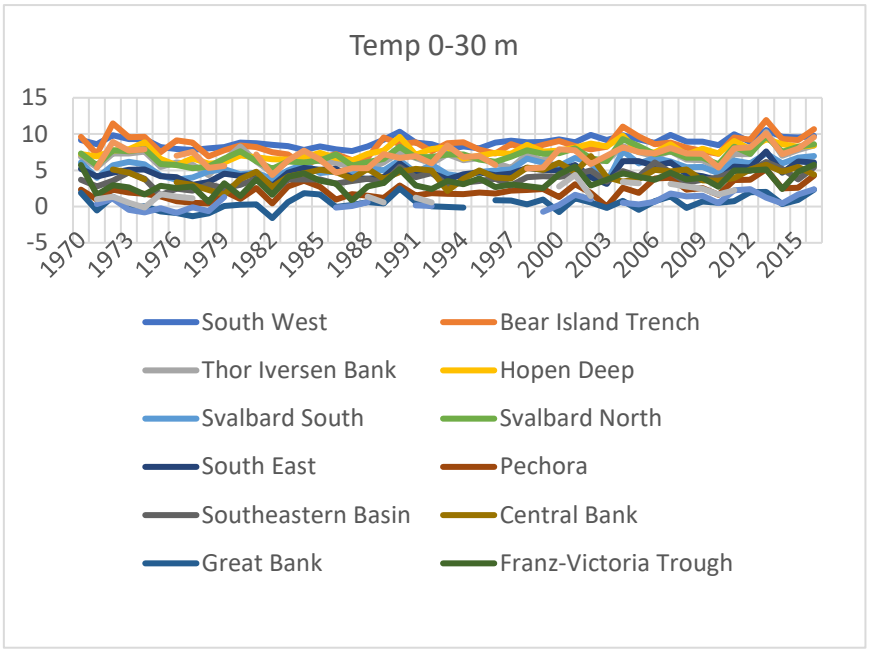

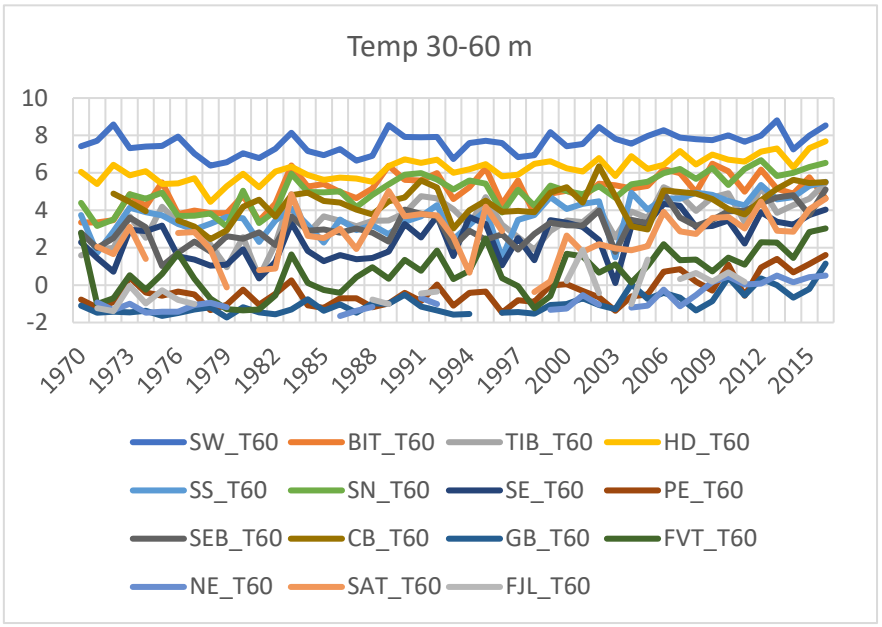

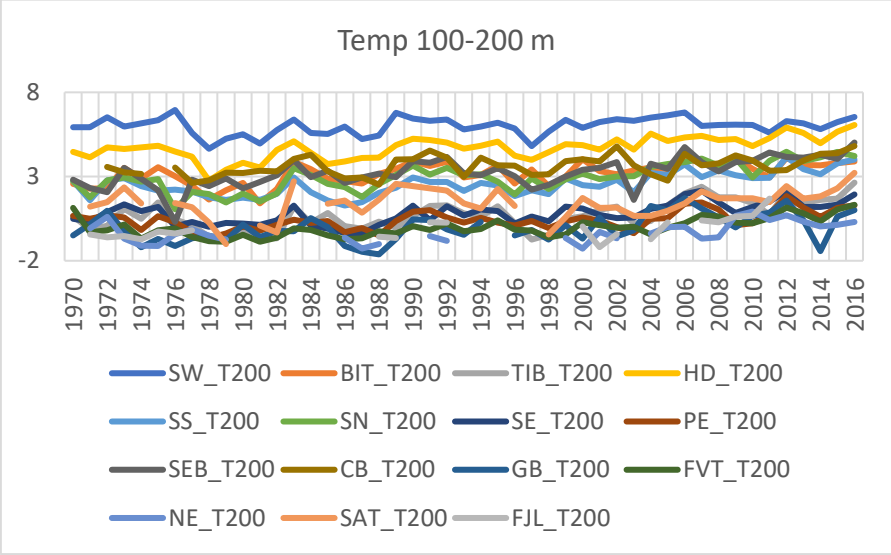

Temperature in 100–200 m layer forms three 'bundles' or groups:

- Lower group (coldest): TIB, SE, NE, GB, FVT, SAT, FJL – with more or less parallel ups and downs (calculate correlations).
- Middle group: BIT, SS, SN, CB, SEB
- Upper: SW and HD. Note the stronger warming of Hopen Deep compared to SW.

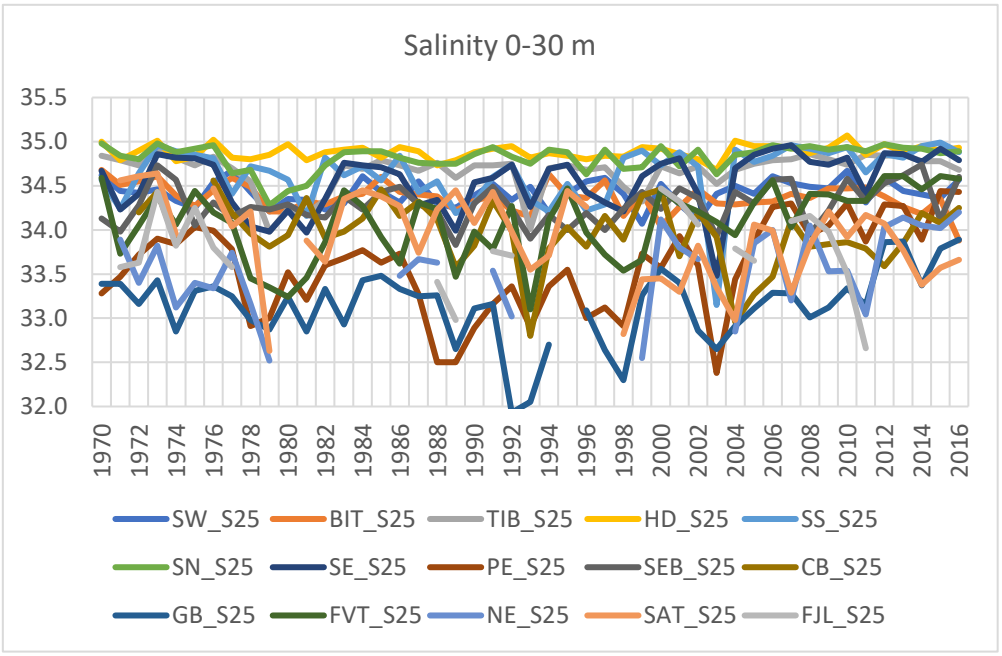

Low salinity is from meltwater. Note the increased salinity after about 2000.

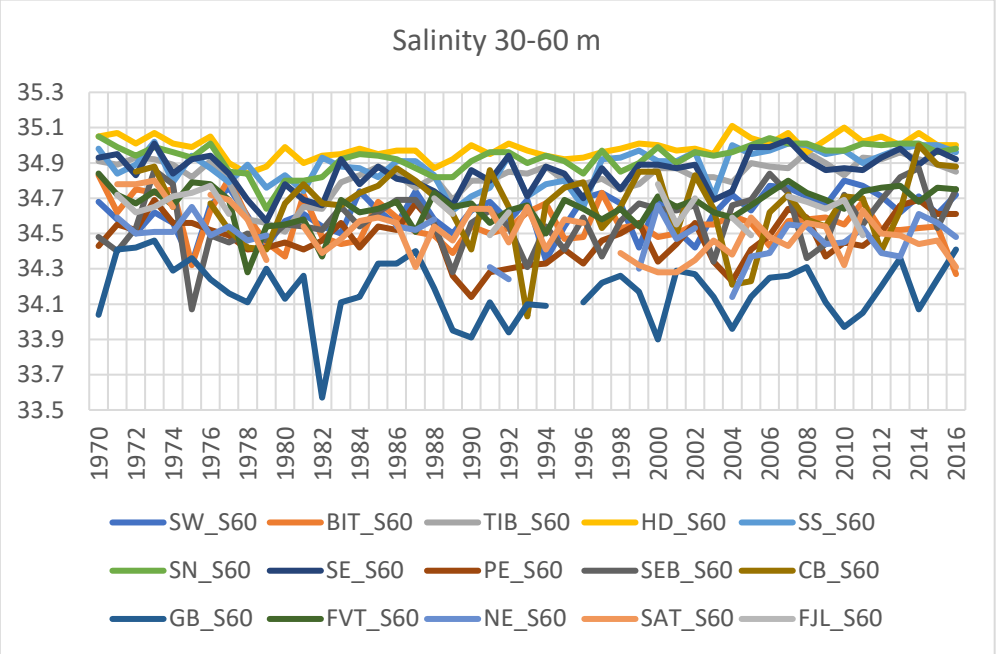

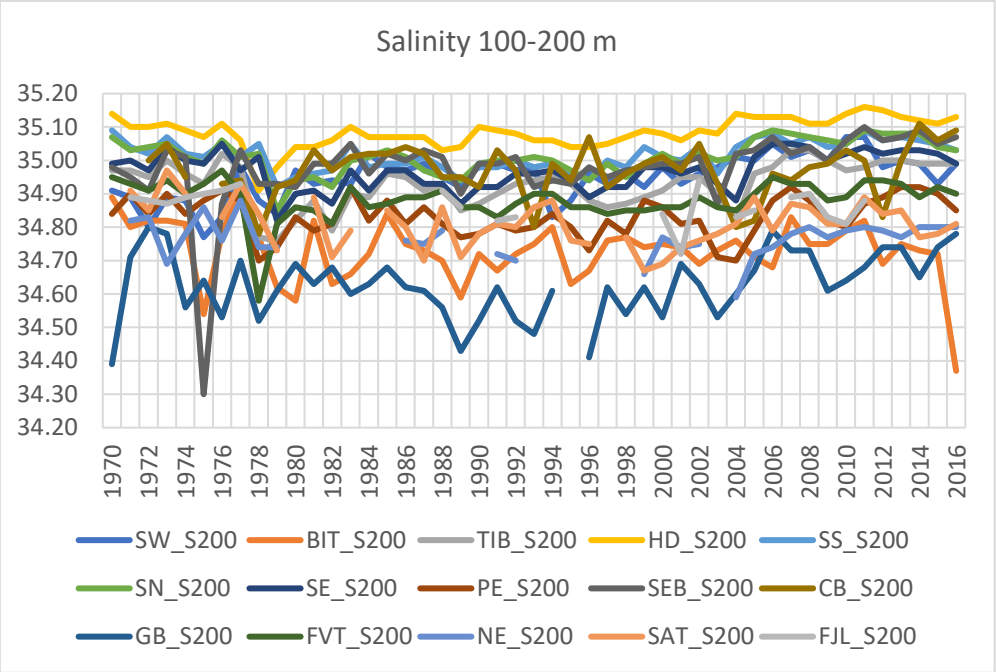

Oceanographic events:

2003 can be characterized as year of low temperature and salinity, mainly in the central and eastern parts. Low temperature was observed in CB, SS, SEB, SE, PE and low salinity i CB, HD, SS, SEB, SE.

Years of higher temperatures, mainly in the central and eastern parts, 1990 (SEB, SE, PE, FVT), 2004-2006 (SEB, SE, PE, BIT, HD) and 2013 (SEB, SE and PE).

New time-series of zooplankton biomass in the Barents Sea 1989–2016

By Hein Rune Skjoldal, Padmini Dalpadado, Johanna M. Aarflot, Espen Bagøien, Andrey Dolgov, Irina Prokopchuk, Magnus Reeves

Overview of data

IMR plankton investigations

Beginning in 1979 (with the project 'Summer feeding of capelin') and continuing during the Norwegian national PRO MARE program (1984–1988), IMR has conducted systematic investigations of zooplankton in the Barents Sea. During this period, the studies were mainly research addressing feeding conditions of capelin and other fish, and most data collection was carried out during spring and summer. Starting in 1987, zooplankton sampling was included as a monitoring component on the autumn surveys, which at that time was called multispecies surveys (combining 0-group fish and capelin acoustic surveys). The multispecies surveys later developed into the ecosystem surveys from 2003 (Eriksen *et al.,* 2017). These surveys were all the time coordinated joint surveys with PINRO, and we describe here the plankton studies on the Norwegian IMR vessels.

IMR has used a combination of two sampling gears during the surveys since the 1980s: a vertically hauled, simple plankton net (generally WP-2 net), and MOCNESS (1-m^2) which is a depth-stratified, multinet sampler. The vertical net was a Juday net in the first years (1979–1987), replaced with WP-2 net from 1988 onwards. The mesh size of the nets has commonly been 180 μm although courser nets (333 μm) were used on some cruises in the 1980s. Skjoldal *et al.* (1987) provided details on sampling gears used in the first years up to 1985. Dalpadado *et al.* (2003) provide more descriptions on methods for subsequent periods. Skjoldal (2017, unpublished manuscript) provides an overview of the IMR zooplankton investigations in the Barents Sea from 1979 to 2016.

IMR has used a standard method for determining dry weight biomass in three size fractions, introduced in 1983–1985. Each sample (rinsed from the net into the codend) is split in two halves; one is preserved with buffered formalin and stored for later taxonomic examination, the other half is sieved successively through three screens (with mesh sizes 2000, 1000, and 180 μm) (Melle *et al.,* 2004; Hassel *et al.,* 2017). The contents retained on each screen are rinsed quickly with freshwater (to remove adherent salt water) and transferred to preweighed aluminum vessels, and stored frozen. Back in the laboratory, the samples are dried and weighed to obtain dry weight biomass in three size fractions: >2 mm, 1–2 mm, and <1 mm. Note that these sizes denote the screen meshes and not the size of the organisms directly. This method was used in an ICES/GLOBEC workshop with an extensive comparison of various zooplankton sampling nets. The results showed that the method was robust and reproducible with relatively low variance generated by the splitting and sieving procedures (Skjoldal *et al.,* 2013).

PINRO plankton investigations

PINRO has a long history of plankton investigations in the Barents Sea (Orlova *et al.* 2011). From 1959 to 1992, PINRO carried out zooplankton sampling in spring and summer to describe feeding conditions of fish larvae along their drift routes from spawning areas into the western and southern Barents Sea (Kvile *et al.,* 2017). From 2001 (2003), a

joint sampling program for zooplankton has been operated by PINRO and IMR during the autumn ecosystem surveys in the Barents Sea.

PINRO uses a different method where the zooplankton biomass is determined as wet weight. In the laboratory, each sample is sieved using 180-μm mesh sieve to remove the preserved liquid, and washed with freshwater. To remove surplus liquid, the plankton sample is placed on filter paper, and subsequently weighed with an electronic balance with an accuracy of 0.1 mg. The data on wet weight biomass is then converted to dry weight biomass using conversion factor 0.2 (assuming 80% water content) and presented as g per m^{-2}.

Four datasets

We describe in this background document four different datasets. While each dataset can be used to describe consistent time-series, they are partially overlapping.

1. IMR WP2 dataset, 1989–2016. This dataset is based on vertical net hauls from near the bottom (generally within 10 m) to the surface. WP2 net with 180 μm mesh has been used as standard net, although Juday net (also with 180 μm mesh) was used on some of the cruises in 1989 and 1990.
2. IMR MOCNESS dataset, 1989–2016. This dataset is based on oblique hauls with MOCNESS plankton sampler from near the bottom (generally within 30 m) to the surface. MOCNESS has been used with 180 μm mesh nets from 1992, but was used with coarser nets (333 μm) in the first years, 1989–1991.
3. Joint IMR-PINRO dataset for vertical net hauls, 2001–2016. IMR has used WP2 net, while PINRO has used Juday net, both with 180 μm mesh.
4. Combined IMR-PINRO dataset for vertical net hauls, 1989–2016. This is a merged dataset of IMR sampling with WP2 (or Juday) net in 1989–2000 (dataset 1), and the joint IMR-PINRO dataset for 2001–2016 (dataset 3).

Table 1 provides a summary of the four datasets.

Table 1. Summary information of four datasets for zooplankton sampling on autumn surveys in the Barents Sea, 1989–2016

Data set No.	Institution	Sampling gear	Time period	No. of stations
1	IMR	WP2 – 56 cm diameter, 180 um	1989-2016	3903
2	IMR	MOCNESS – 1-m^2, 180 um (1992-2016), 333 um (1989-1991)	1989-2016	983
3	IMR-PINRO	WP2 (56 cm, 180 um), Juday (36 cm, 180 um)	2001-2016	3551
4	IMR-PINRO	WP2 (56 cm, 180 um), Juday (36 cm, 180 um)	1989-2016	5044

Sampling stations

The Barents Sea has been divided into 15 subareas or polygons (Figure 1). The division is based on topography and oceanography and is a modification (with some subdivisions) of the system used by Eriksen *et al.* (2017) in a summary analysis of pelagic biomass. The four western areas, South-West, Bear Island Trough, Hopen Deep, and Tor Iversen Bank, are areas covered mainly with Atlantic water and constitute the inflow

region of Atlantic water with the splitting of the current branches east through the Kola Section (south of the Central Bank) and north in the Hopen Deep (west of the Central Bank).

An overview of samples collected during the autumn surveys by IMR from 1989 to 2016 (datasets 1 and 2) in the various subareas is given in Table 2. Nearly 4000 sampling stations (3903) have been taken with WP-2 net, with an average of 139 stations per year (varying from 77 to 197). Nearly 1000 profiles (983) have been taken with MOCNESS during the same cruises, with an average of 35 MOCNESS samples each year. In two of the years, no MOCNESS samples were taken for technical reasons (2009 and 2016). The number of MOCNESS stations varied from 10 to 59 for the other years.

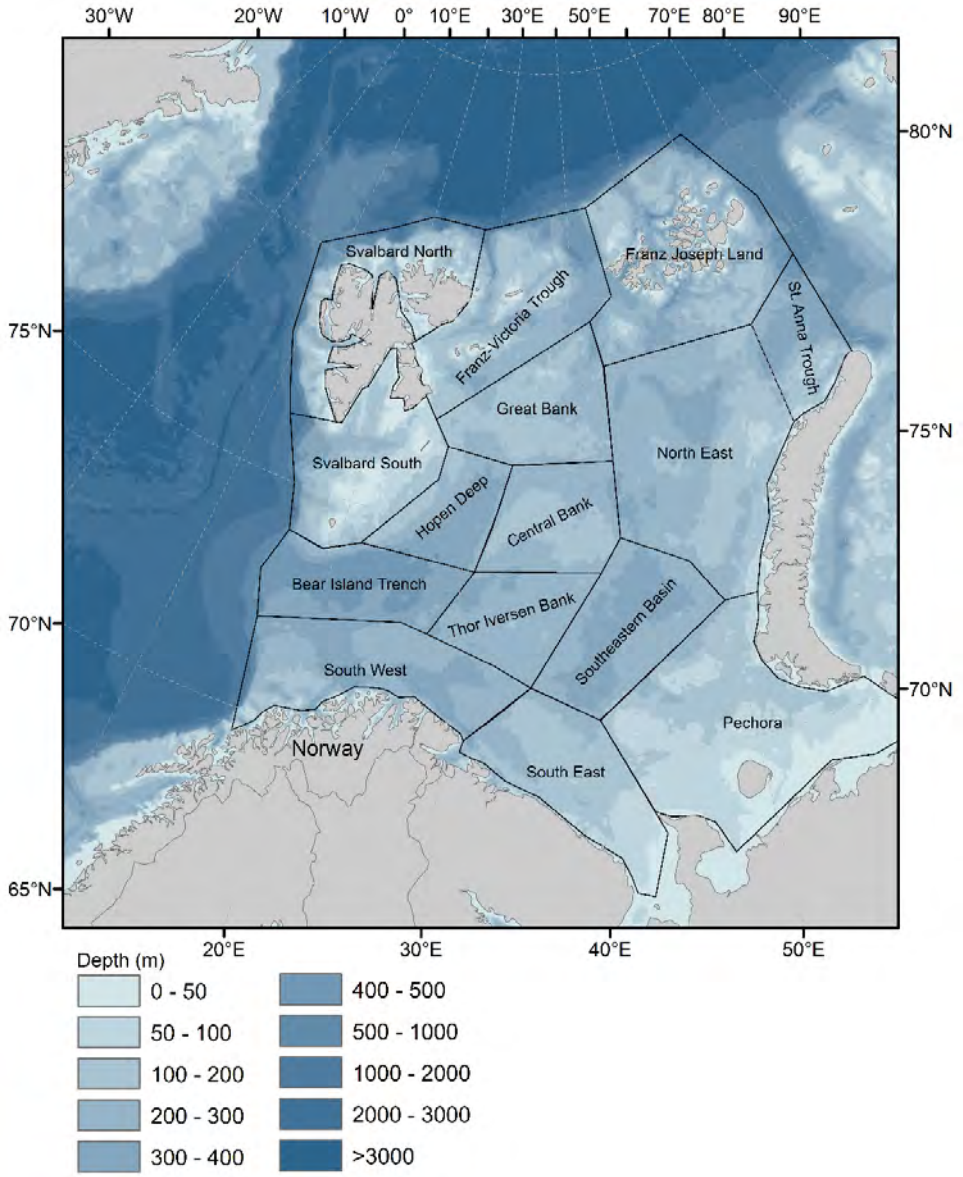

Figure 1. Map showing subdivision of the Barents Sea into 15 subareas (polygons) used to calculate mean biomass of zooplankton based on data from the autumn surveys.

Table 2. Number of sampling stations for zooplankton biomass collected with WP-2 net and MOC-NESS sampler by IMR for the years from 1989 to 2016 (datasets 1 and 2, see Table 1). Stations are given for 15 subareas of the Barents Sea shown in Figure 2. BIT – Bear Island Trench, TIB – Tor Iversen Bank, HD – Hopen Deep, SEB – Southeast Basin, SW – South-West, SE – South-East, PE – Pechora, CB – Central Bank, GB – Great Bank (Persey Elevation), SS – Svalbard South, SN – Svalbard North, FVT – Franz-Victoria Trough, NE – North-East, STA – St. Anna Trough, FJL – Franz Josef Land.

Year	BIT		TIB		HD		SEB		SW		SE		PE		CB		GB		SS		SN		FVT		NE		SAT		FJL		Total	
	WP2	MOC	WP2	MOC	WP2	MOC	WP2	MOC	WP2	MOC	WP2	MOC	WP2	MOC	WP2	MOC	WP2	MOC	WP2	MOC	WP2	MOC	WP2	MOC	WP2	MOC	WP2	MOC	WP2	MOC	WP2	MOC
1989	14	2	3	1	4	2	2		20		9	2	4		2		4	2	13	5			1		1						77	14
1990	14	6	13	4	3	2	12	1	17	4	15	1	2		9	1	4	4	4	2			3	2	6						102	27
1991	4	3	6	1	7	3	17	2	7	3	3		4		12	1	14	2	13	5			4	2	27	9	3	1	3	2	124	34
1992	12	3	10	1	9	3	16	2	33	5	5	1	13		6	2	12	4	15	1			4	1	23	6	2		2	1	162	30
1993	9	1	10	5	10	5	7	2	14	2	7	1	8		11	6	14	6	17	5			3		15	8					125	41
1994	16	4	13	7	15	3	15	7	19	2	7	7	6	2	16	7	10	3	26	8		3	2		17	6					162	59
1995	7	4	5	4	8	6	7	1	29	6	5	3	9	2	10	3	7	4	8	5		1			12	5					107	44
1996	5	5	12	7	6	5	10	3	11	6	11	2	19	5	5	3	5	1	10	4		2	2	2	14	7	1	2			111	54
1997	14	6	13	7	18	3	3	2	18	5		1			13	6	13	5	18	6		1	2	1	3	1					115	44
1998	24	3	21	7	24	7	14	4	22	3	1				16	6	20	4	40	5			4	3	11	2					197	44
1999	10	2	10	3	17	5	5	1	18	4					20	5	22	5	28	9			13	2	19	5					160	41
2000	16	4	14	5	18	10	5	4	16	10					21	6	13	3	20	6			3	4	6	3					132	55
2001	14	6	12	4	18	6	2	2	19	4					25	5	22	9	17	8		1	7	7	1					1	137	53
2002	15	4	12	4	15	10	1	1	19	3					16	8	17	5	17	6			13	5							125	46
2003	12	7	11	2	10	5	1		18	8	1				8	2	5	5	16	5		1	1		4	2					87	37
2004	24	4	12	5	16	5	3		29	4	1	1			14	4	25	8	7				18	4							149	35
2005	19	7	15	8	16	7	4		26	10					17	6	13	4	6	2		1	2	1	6	2			1		125	48
2006	22	8	18	5	12	3	5		34	11					19	5	21	6	8	1			6	3							145	42
2007	16	4	14	3	15	6			31	8					20	4	16	5	21	3		1	4	1	1						138	35
2008	11	1	10	4	8	4	4	1	19	3					20	2	15	3	6	2			2	1	1						96	21
2009	17		14		16		3		29		2				20		20		23		28		10		1						183	0
2010	21	4	16	4	14	4	2		30	4					18	1	20	5	28		11		19	3	1	1					180	26
2011	18	2	20		20	1	3		32	1					21	2	19	3	20	4	16		26	3	1						196	16
2012	22	4	14	2	17	1	3	1	30	2					20		19		25		12		26		1						189	10
2013	20	4	13	1	13	3	3	1	25	3					20	3	18	4	23	3	19	2	24	7	1						179	31
2014	11	9	7	5	11	4	1	2	14	13					16	4	16	2	14	6	26	3	1	1	1						118	49
2015	9	7	9	6	13	3	1	2	15	12					13	7	21	1	14	6	13	3	19		1						128	47
2016	16		4		14		3		24						20		18		20		17		18								154	0
Sum	412	114	331	105	367	116	152	39	618	136	67	19	65	9	428	99	423	103	475	107	142	19	237	53	174	57	6	3	6	4	3903	983

An overview of samples in the joint and combined IMR-PINRO datasets (No.3 and 4) collected with vertical net hauls during autumn cruises from 1989 to 2016 is given in Table 3. The joint dataset (No. 3) for 2001–2016 comprises 3551 sampling stations, with an average of 222 stations per year (ranging from a minimum of 87 stations in 2003 to a maximum of 285 stations in 2006). The combined dataset for 1989 to 2016 consists of 5125 sampling stations, with an average of 131 stations per year for the first part sampled by IMR in 1989–2000.

Table 3. Number of sampling stations for zooplankton biomass (total) for the combined IMR and joint IMR-PINRO datasets (no. 3 and 4). Samples collected with WP-2 net (IMR) and Juday net (PINRO) nets from 1989 to 2016. The sampling in 1989-2000 was carried out by IMR and is similar to the overview of stations for WP-2 in Table 1. The sampling from 2001 to 2016 is the joint IMR-PINRO sampling program. Stations are given for 15 subareas of the Barents Sea shown in Figure 2. BIT – Bear Island Trench, TIB – Tor Iversen Bank, HD – Hopen Deep, SEB – Southeast Basin, SW – South-West, SE – South-East, PE – Pechora, CB – Central Bank, GB – Great Bank (Persey Elevation), SS – Svalbard South, SN – Svalbard North, FVT – Franz-Victoria Trough, NE – North-East, STA – St. Anna Trough, FJL – Franz Josef Land.

Year	BIT	TIB	HD	SEB	SW	SE	PE	CB	GB	SS	SN	FVT	NE	SAT	FJL	Total
1989	14	3	4	2	20	9	4	2	4	13		1	1			77
1990	14	13	3	12	17	15	2	9	4	4		3	6			102
1991	4	6	7	17	7	3	4	12	14	13		4	27	3	3	124
1992	12	10	9	16	33	5	13	6	12	15		4	23	2	2	162
1993	9	10	10	7	14	7	8	11	14	17		3	15			125
1994	16	13	15	15	19	7	6	16	10	26		2	17			162
1995	7	5	8	7	29	5	9	10	7	8			12			107
1996	5	12	6	10	11	11	19	5	5	10		2	14	1		111
1997	14	13	18	3	18			13	13	18		2	3			115
1998	24	21	24	14	22	1		16	20	40		4	11			197
1999	10	10	17	5	18			20	22	26		13	19			160
2000	16	14	18	5	16			21	13	20		3	6			132
2001	14	12	18	2	19			25	22	17		7	1			137
2002	15	12	15	13	19		14	16	21	17		15	33	1	1	192
2003	12	11	10	1	18	1	16	8	5	16		1	4			103
2004	24	19	24	14	32	6		17	31	24	2	30	26	7	1	257
2005	19	15	16	4	26			17	13	6		2	6		1	125
2006	26	29	33	7	42	24		23	33	34		7	27			285
2007	16	14	19	11	31	11	11	20	17	25		12	22	6	8	223
2008	11	10	8	21	21	10	21	20	15	6		2	19	2	10	176
2009	17	14	16	13	29	16	4	20	21	23	28	14	20	8	5	248
2010	21	16	14	10	30	1	21	18	24	28	11	27	23	3	12	259
2011	18	20	20	14	32	10	23	21	22	20	16	32	25	1	5	279
2012	22	16	17	15	30	10	21	20	23	25	12	37	26		7	281
2013	20	15	13	14	25	10	19	20	22	23	19	35	26	3	12	276
2014	17	14	12	14	23	11	21	20	20	17	28	2	25		6	230
2015	16	17	16	15	27	9	19	20	26	20	16	24	27	3	6	261
2016	16	4	14	10	24	1	25	20	22	20	17	21	21		4	219
Sum	429	368	404	291	652	183	280	446	475	531	149	309	485	40	83	5125

The geographical distribution of all WP-2 and MOCNESS sampling stations taken by IMR over the whole period are shown in Figures 3 and 4. The sampling stations in the joint IMR-PINRO program (2002–2016) is shown in Figures 5. Maps of location of sampling stations for each year have been prepared and will be made available as later.

Most sampling by IMR has been in the Norwegian sector where there are a fair number of samples over the whole time-series for the SW, BIT, HD, TIB, CB, GB and SS subareas (Table 2, Figure 2). As can be seen from Figures 3 and 4, IMR has also collected a fair number of samples from the Russian sector; this was primarily during the 1990s with few samples taken after year 2000 (Table 2). The coverage of IMR sampling was relatively good in the North-East subarea, as well as in the South-East and Pechora subareas in the years up to 1996. For the latter two subareas, there are no samples from the years around 2000 (Table 3). The northeastern-most subareas (St. Anna Trough and Franz Josef Land) was only occasionally sampled before more regular sampling was done by PINRO from 2007. The Svalbard-North subarea was not sampled before 2009, except for two stations in 2004.

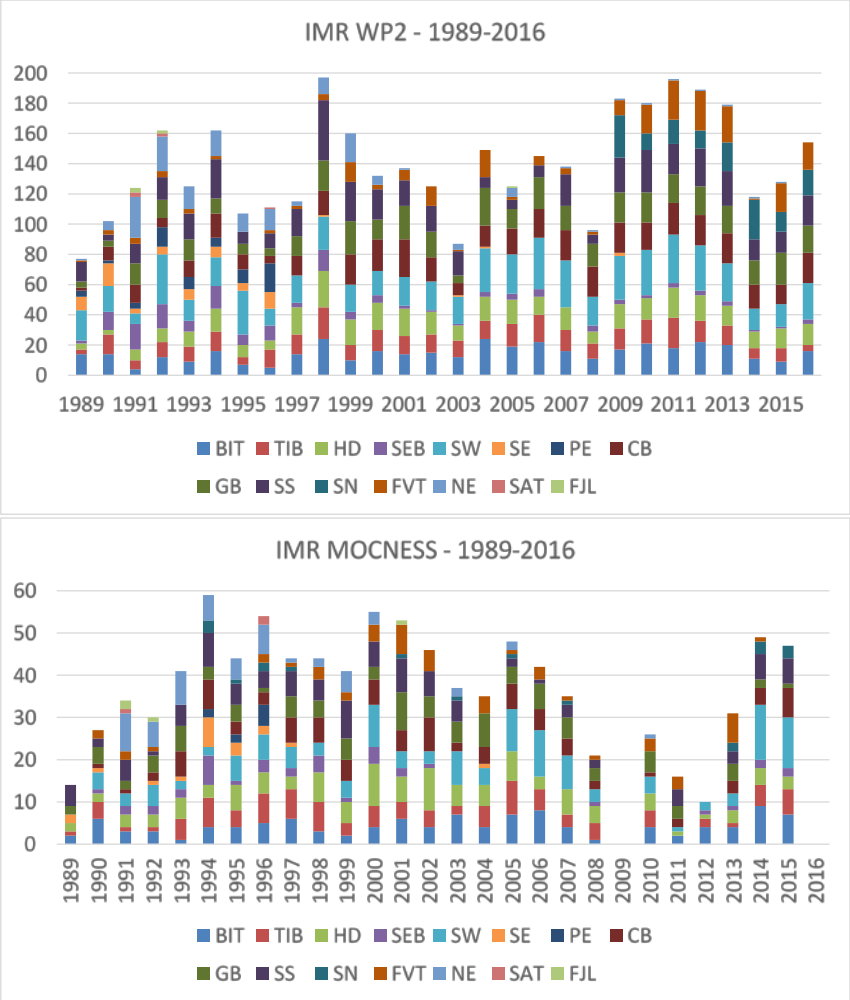

Figure 2. Number of sampling stations for zooplankton biomass taken with WP-2 net (upper) and MOCNESS (lower) for each year from 1989 (or 1987) to 2016. Number of stations are shown for 15 subareas; see Figure 1 and legend to Table 1.

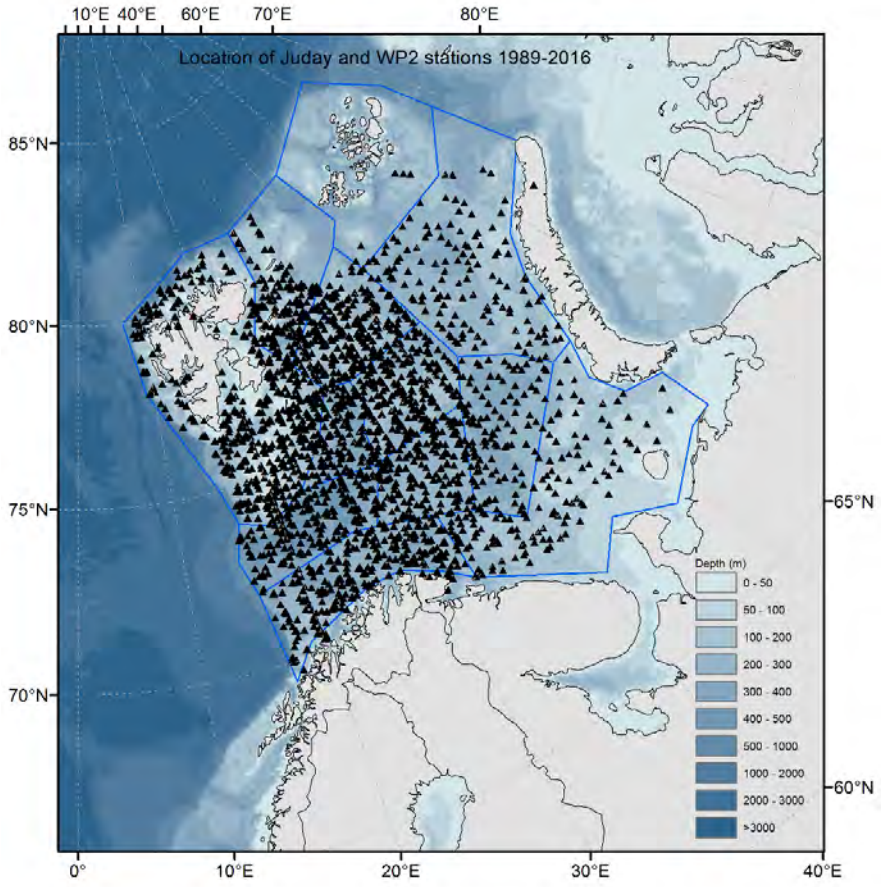

Figure 3. Map showing sampling stations taken by IMR for zooplankton biomass determination for samples obtained with WP-2 net, 1989–2016.

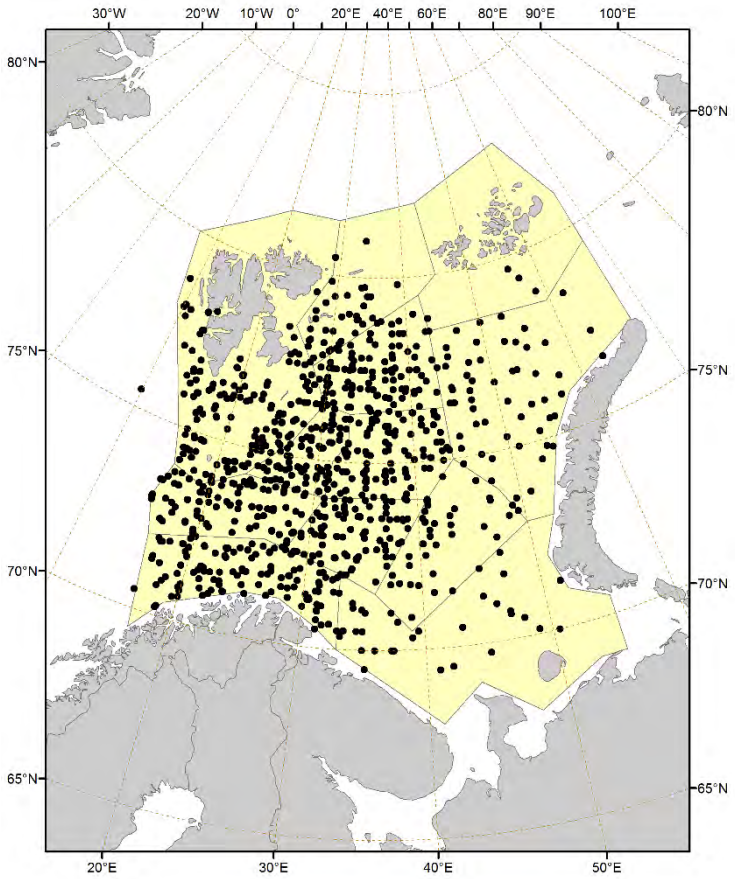

Figure 4. Map showing sampling stations taken by IMR for zooplankton biomass determination for samples obtained with MOCNESS, 1987-2016.

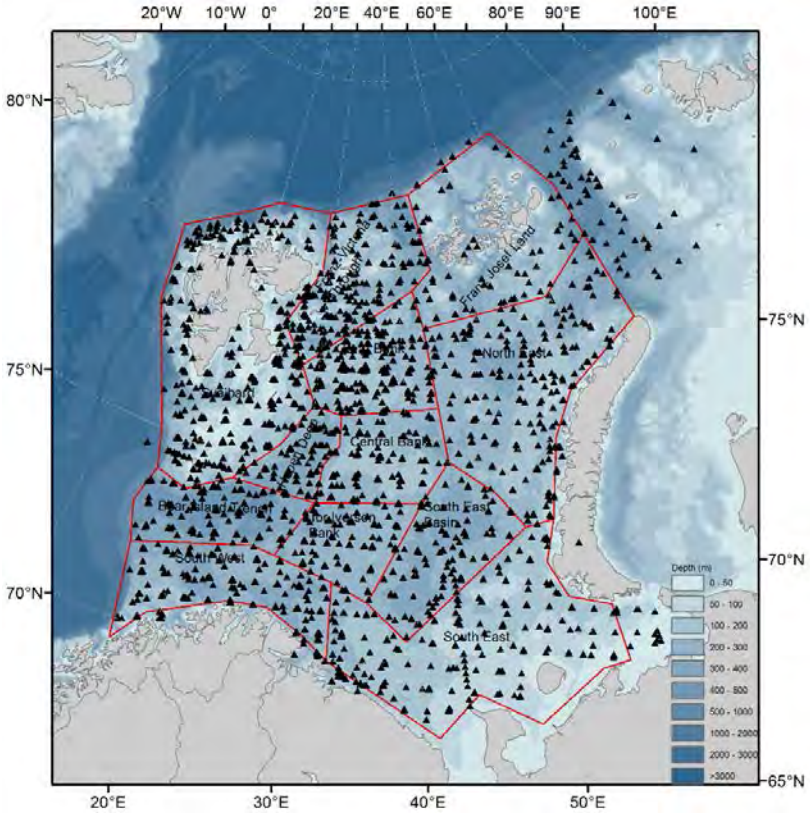

Figure 5. Map of zooplankton sampling stations in the Barents Sea by IMR and PINRO, 2002-2016.

Zooplankton biomass results
Mean biomass by subareas

General pattern

The biomass data from the autumn cruises have been gridded and mean values with statistics (standard deviation, SD and standard error, SE) for each subarea or polygon have been calculated for each year for WP-2 and MOCNESS separately (datasets 1 and 2 by IMR; Table 1).

The mean biomass for the subareas over the period 1989–2016 is shown in Figure 6 for 10 of the subareas covered by IMR. The mean biomass varied from about 5 to 11 g dw m^{-2}, with highest values over the deeper areas (Bear Island Trench, Southeast Basin, Franz-Victoria Trough) and lowest over the Central and Great Banks. The results for WP-2 and MOCNESS showed similar levels and trends among the subareas. Note that the temporal coverage is somewhat uneven, particularly for the North-East subarea where there were few samples in the latter part of the series (Table 2).

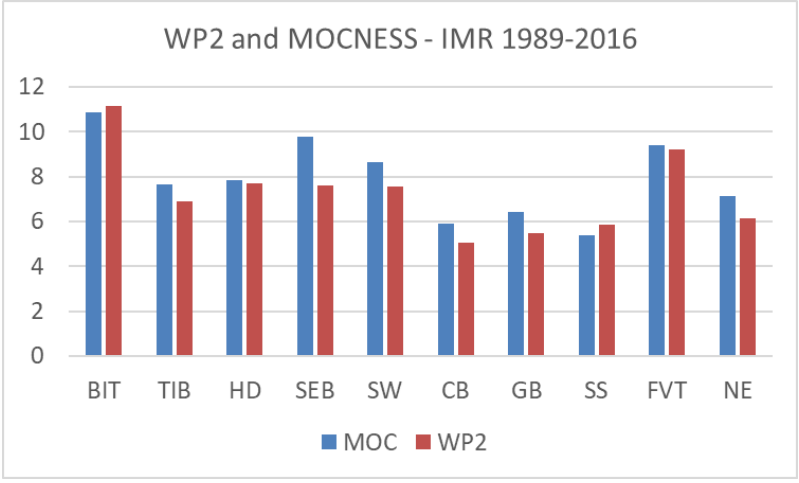

Figure 6. Mean total zooplankton biomass (g dry weight m^{-2}) for annual mean biomass values from autumn surveys for ten subareas of the Barents Sea, 1989–2016 (see Figure 1). Data obtained with WP-2 net and MOCNESS sampler. IMR surveys – datasets 1 and 2.

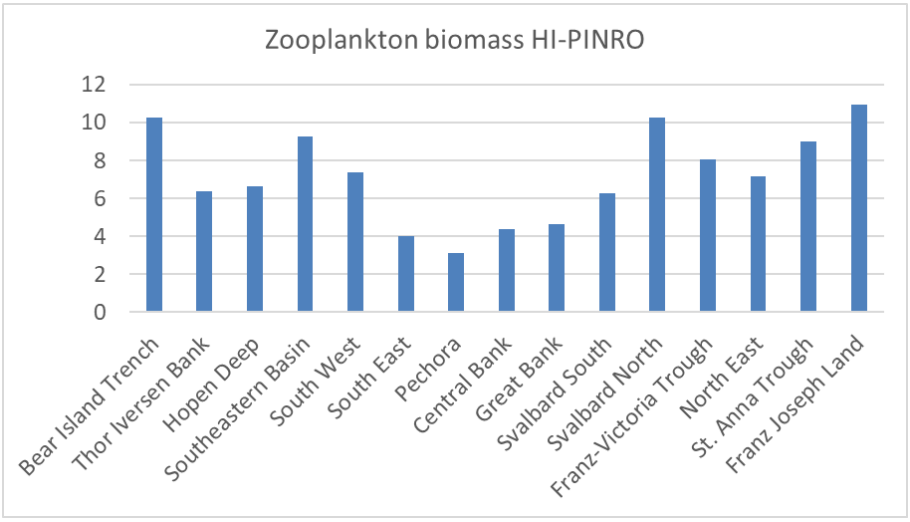

Figure 7. Mean total zooplankton biomass (g dry weight m^{-2}) for annual mean biomass values from autumn surveys for 15 subareas of the Barents Sea (see Figure 1). Data obtained with Juday and WP-2 nets. Joint IMR-PINRO surveys, 2001–2016 – dataset 3.

Data from the joint surveys (2001–2016; dataset 3) showed similar levels and trends for total zooplankton biomass, with subarea means varying from 3 to 11 g dw m^{-2} (Figure 7). Highest values were found in the deeper areas, while the lowest values occurred in the shallower areas including South-East and Pechora. The five northernmost subareas (Svalbard-North to Franz Josef Land) had generally higher mean biomass than southern and central subareas.

Size fractions

The results for three size fractions of biomass in the IMR datasets (#1 and 2) are shown in Figures 8 (WP-2) and 9 (MOCNESS) as absolute and relative values (percentage) for all 15 subareas. Note that the number of stations were low for northern subareas, e.g. only 3-6 stations for St. Anna Trough and Franz Josef Land (see Table 2).

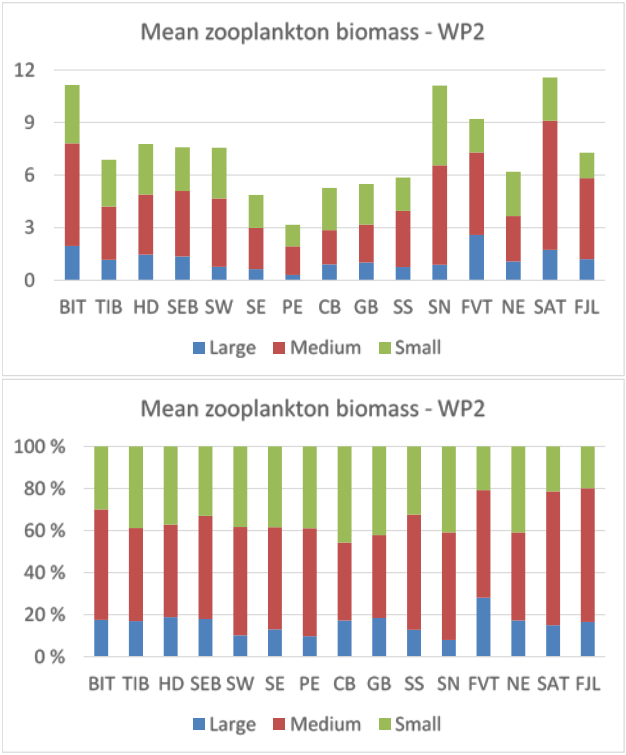

Figure 8. Mean biomass (g dry weight m^{-2}) of three size fractions (shown cumulatively) of zooplankton for 15 subareas of the Barents Sea over the period 1989–2016. Results obtained with WP-2 net by IMR (dataset 1). Note that the number of years and the number of samples are limited for several subareas (see Table 1). A and B (upper and lower panels) show the results in absolute and relative (%) units.

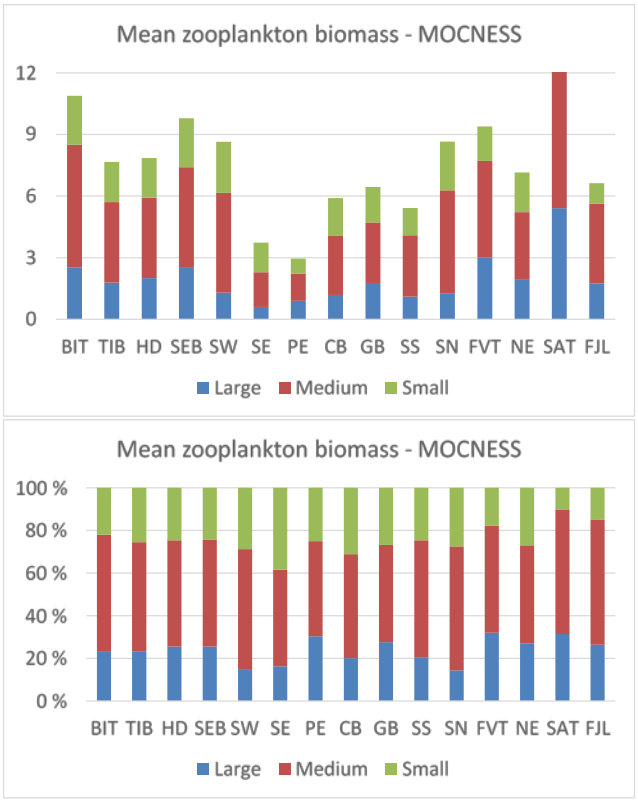

Figure 9. Mean biomass (g dry weight m^{-2}) of three size fractions (shown cumulatively) of zooplankton for 15 subareas of the Barents Sea over the period 1989–2016. Results obtained with MOCNESS plankton sampler by IMR (dataset # 2). Note that the number of years and the number of samples are limited for several subareas (see Table 1). A and B (upper and lower panels) show the results in absolute and relative (%) units. (Note that the column for SAT is cut; total value was 17.2 and small fraction 1.7 g dw m^{-2}).

Averaged over the two sampling gears, the large fraction (>2 mm) made up about 20%, the medium fraction (1–2 mm) about 50%, and the smallest fraction (<1 mm) about 30% of the total mesozooplankton biomass. MOCNESS collected consistently more of the large fraction (23.2% vs. 16.3%), and less of the small fraction (25.7% vs. 36.1%), compared to WP-2 (Figure 10).

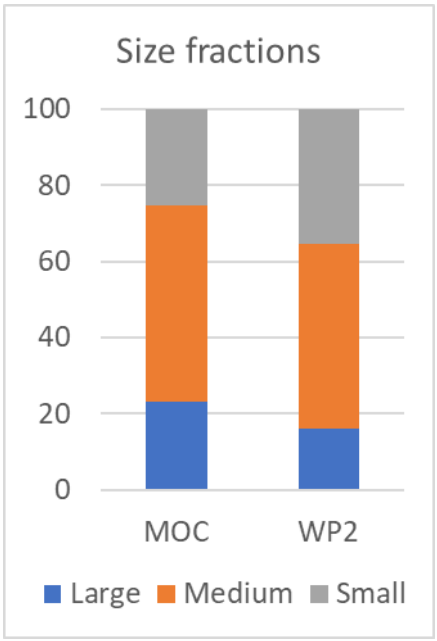

Figure 10. Mean relative distribution (%) of 3 size fractions of zooplankton biomass based on the mean values for 15 subareas of the Barents Sea for samples collected by WP-2 net and MOCNESS by IMR (1989–2016; datasets #1 and 2).

As can be seen from Figure 5, there is a good agreement between the WP-2 and MOCNESS results for the total biomass (Figure 11). The trendline A more detailed comparison of WP-2 and MOCNESS is carried out in a separate study (Skjoldal *et al.* manuscript 2017).

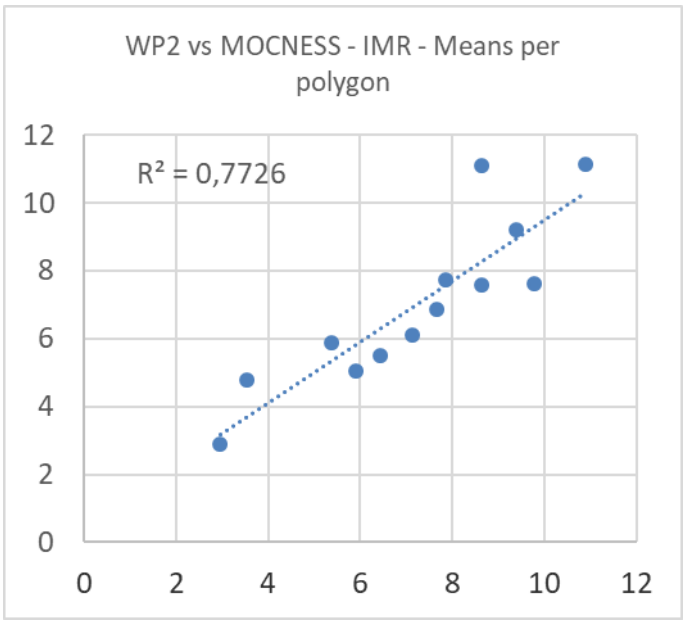

Figure 11. Mean total zooplankton biomass obtained with WP-2 net and MOCNESS plankton sampler for 13 subareas of the Barents Sea (excluding St. Anna Trough and Franz Josef Land with small number of stations).

Variability

A measure of variability of the data is the coefficient of variation (CV) which is the standard deviation divided by the mean value (CV = SD/mean). Two different CV values have been calculated for the mean values by subareas shown in Figures 6 and 7.

One (denoted CV1) is the average over the time-series of the annual CV values based on the SD for the individual stations, which are used to calculate the annual subarea mean. The other (denoted CV2) is based on the SD for the annual mean values for the subareas, averaged over the time-series.

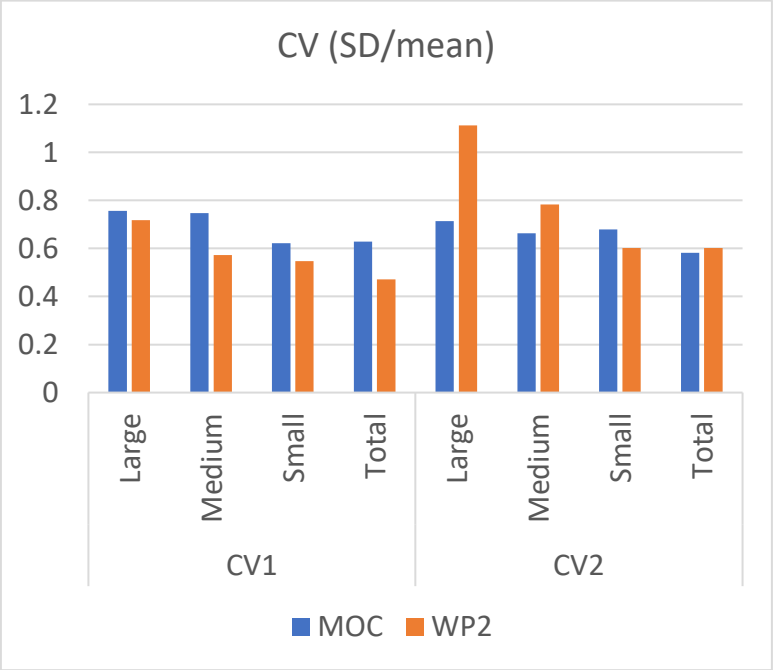

Figure 12. Coefficient of variation (CV = SD/mean) for the variability of the annual mean values for 13 of the 15 subareas (not including Franz Josef Land and St. Anna Trough with few observations). CV1 is based on the variability among the individual stations, which were used to calculate annual subarea means, while CV2 is based on the variability of the annual means over the time-series. Based on the data obtained with WP-2 and MOCNESS by IMR, 1989–2016 (datasets #1 and 2).

For the results obtained with WP-2 and MOCNESS by IMR (datasets #1 and 2, 1989–2016), both CV1 and CV2 generally declined from the largest to the smallest fraction, and the total (Figure 12). CV1 (reflecting variation among stations in a subarea within a year) tended to be somewhat lower for WP-2 than MOCNESS, being about 0.5 and 0.6 for the total biomass, respectively. CV2 (reflecting variation between years) tended to be somewhat higher for WP-2, with values of about 0.6 for total biomass for both gears.

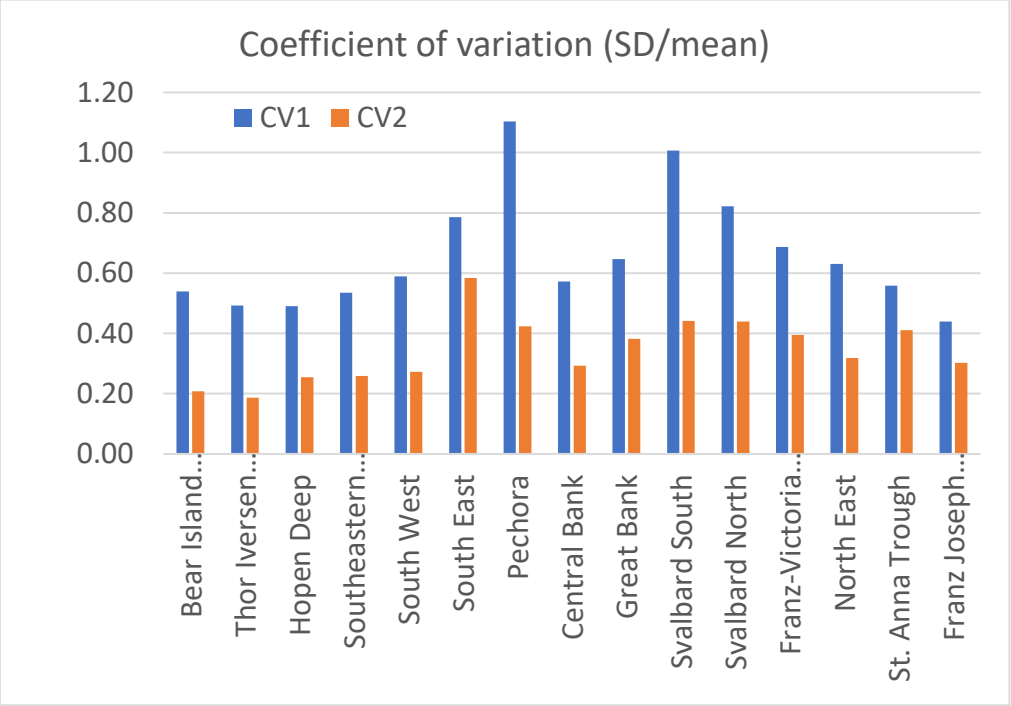

Figure 13. Coefficient of variation (CV = SD/mean) for the variability of the annual mean values for 15 subareas of the Barents Sea. See legend to Figure 11 and text for explanation of CV1 and CV2. Based on data obtained with Juday and WP-2 nets in the joint IMR-PINRO surveys, 2001–2016 (dataset #3).

The joint dataset (obtained with Juday and WP-2 nets, 2001–2016, by IMR and PINRO; dataset #3) had somewhat different variance characteristics. Expressed as mean values for the 15 subareas, CV1 (within-year, between-stations variation) tended to be higher than CV2 (between-years) (Figure 13). CV1 varied from about 0.4 to 1.1, with most values around 0.5–0.6. CV2 varied from about 0.2 to 0.6, with most values between 0.2 and 0.4. The lower values for CV2 may reflect the shorter time-series compared to the results in Figure 12. There is a tendency to higher variability of the southeastern (South-East and Pechora) and northwestern (Svalbard-South and -North) subareas compared to the rest (Figure 13).

A separate study of the statistical distributions and variance characteristics of the zooplankton biomass data is planned.

Time-series – datasets #1 and 3 (1989–2016)

A set of plots of time-series of total biomass and biomass in the three size fractions are shown for different subareas (not included). In these plots a measure of variability (+/- standard error, SE) for the annual means are included. The number of observations each year is given in Table 1. In general, where the number of observations are reasonably high (>10 stations), the error bands are relatively narrow, as can be seen from the figures in the Annex.

The temporal development of total zooplankton biomass is shown in Figure 14 for 9 of the 15 subareas for which there is reasonably coverage in the IMR sampling (see Table 2); these subareas are located in the southern and central parts of the Barents Sea. The total variation in these time-series is from about 1 to 23 g dw m^{-2}, with most values fluctuating between 5 and 10 g dw m^{-2}. There is a common pattern for most subareas, with low values around 1990, a pronounced peak in 1994, and lower and more stable, although variable values since about 1998 (Figure 14).

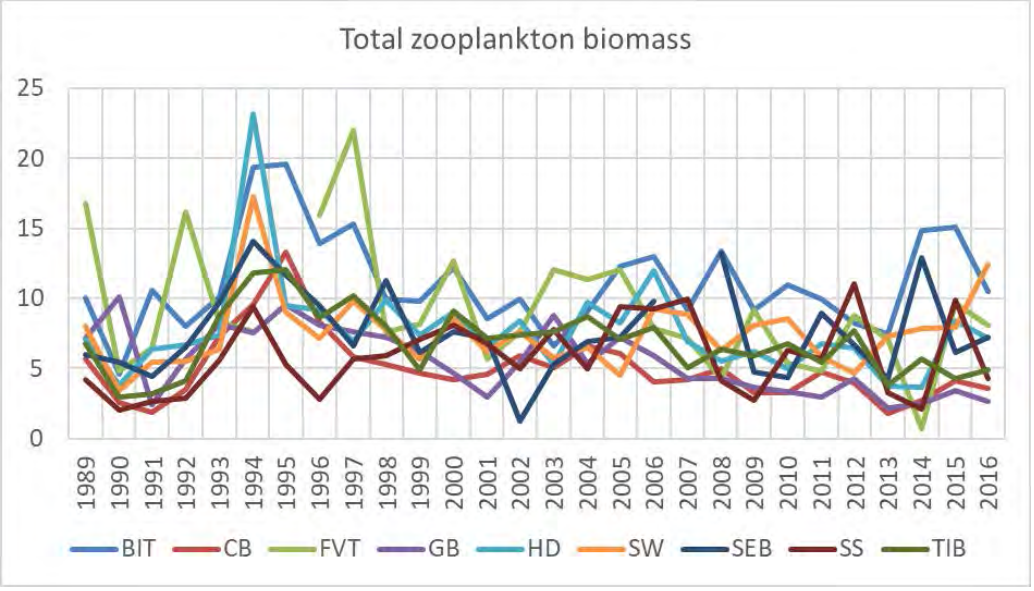

Figure 14. Time-series of total zooplankton biomass for 9 subareas of the Barents Sea. Results obtained with WP-2 net, 1989–2016 (IMR, dataset #1).

Southwestern Barents Sea

Time-series for 4 of these subareas located in the southwestern Barents Sea and influenced by inflowing Atlantic water, are shown in Figure 15. The peak in 1994 was prolonged with high values also in 1995 for the Bear Island Trough subarea. The peak was less pronounced for the Tor Iversen Bank area (south of the Central Bank), which is downstream from the Barents Sea opening in west. The values for the Bear Island Trench tended to be higher than the other areas, particularly after 2004 when biomass here was around 10–12 g dw m^{-2} compared to variations around 5–8 g dw m^{-2} for the other areas (Figure 8).

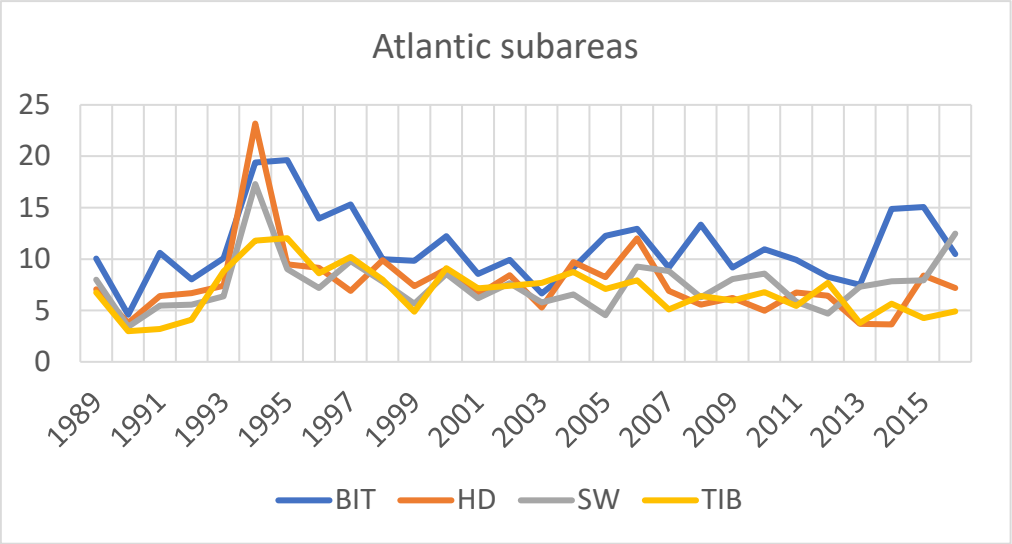

Figure 15. Time-series of total zooplankton biomass for 4 subareas in the inflow region of Atlantic water in the southwestern Barents Sea. Results obtained with WP-2 net, 1989–2016 (IMR, dataset #1).

Figure 16 shows the time-series for these 4 Atlantic subareas separately but including results for the three size fractions. The peak in biomass in 1994 was driven to a large extent by the smallest size fraction (<1 mm) along with an increase also in the middle

fraction (1–2 mm). *Calanus finmarchicus* falls predominantly into the middle fraction for older copepodites (CV and adults) and into the smallest fraction for the younger copepodites (CI-CIII) (IMR, unpublished results). The strong contribution by the smallest fraction (to a biomass level of about 10 g dw m^{-2} for the South-West, Bear Island Trench and Hopen Deep areas) suggests that zooplankton other than *Calanus* contributed to this peak. This could have been small copepods like *Pseudocalanus* and possibly other zooplankters. This requires further investigation and we can do this by analysing our stored and preserved samples.

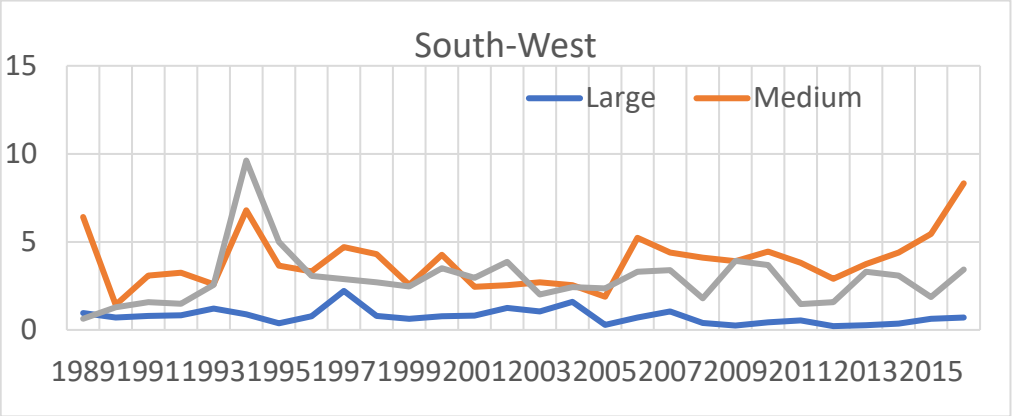

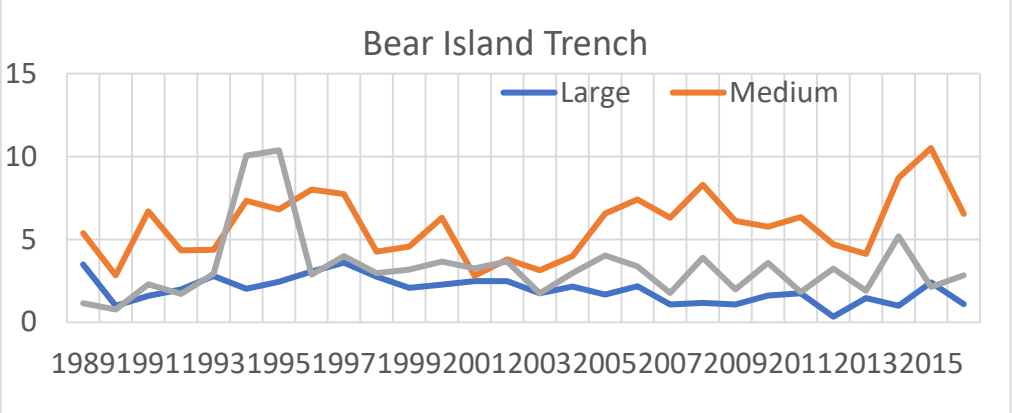

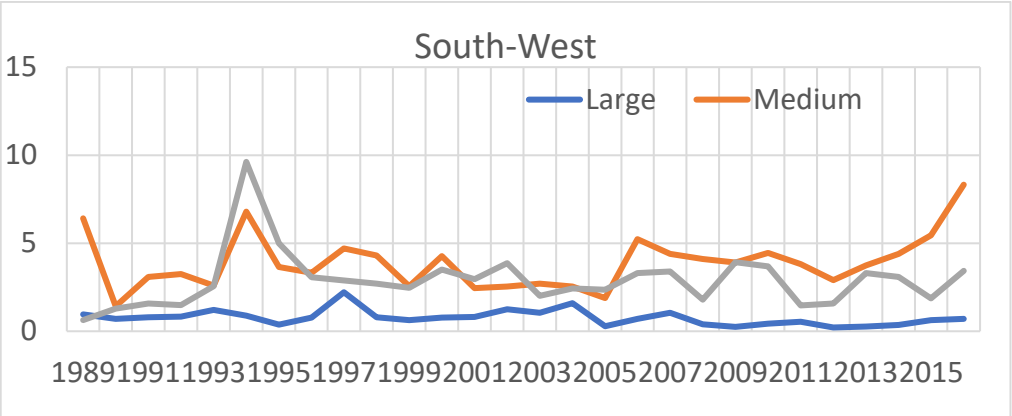

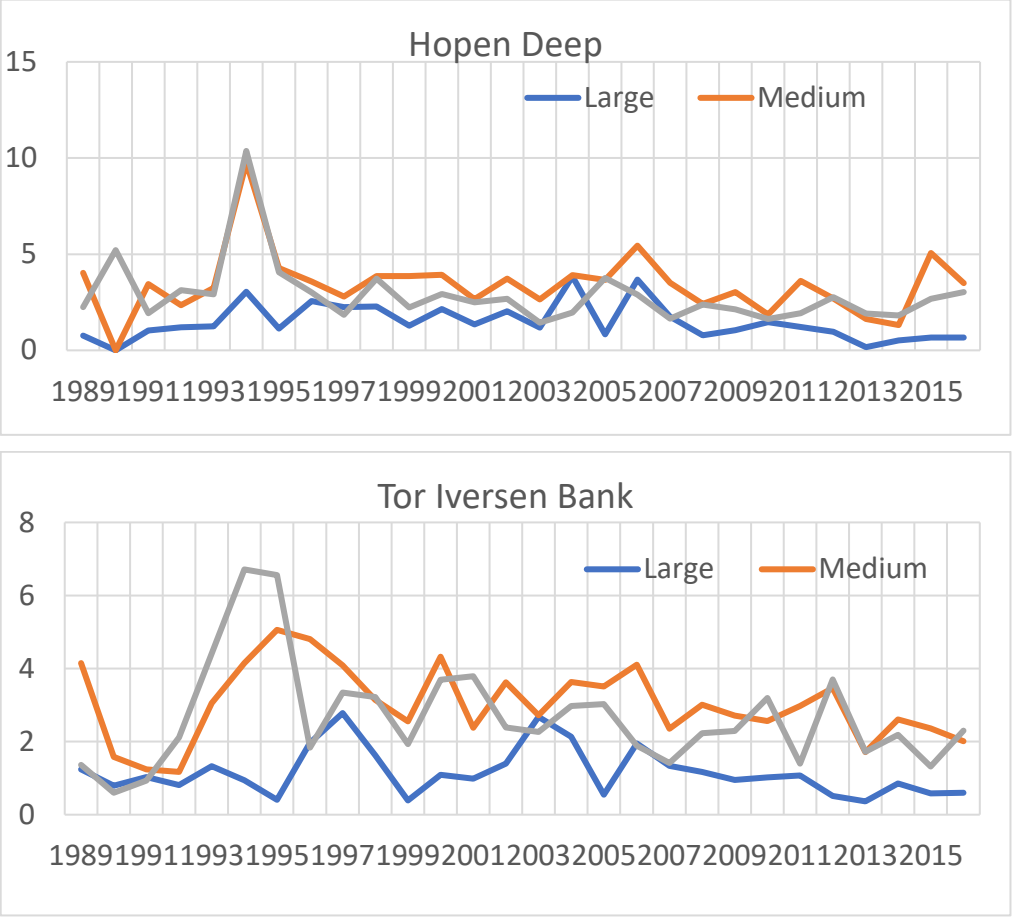

Figure 16. Time-series of zooplankton biomass in 3 size fractions (Large: > 2 mm, Medium: 1–2 mm, Small: <1 mm) in four Atlantic subareas in the southwestern Barents Sea. A) Bear Island Trench, B) South-West, C) Hopen Deep, D) Tor Iversen Bank. Results obtained with WP-2 net, 1989–2016 (IMR, dataset #1).

The peak biomass in 1994 was clearly an event that was recorded in all 4 subareas with inflowing Atlantic water. We will call this 'the 1994 peak biomass event', which appears to be largely an advective phenomenon associated with the Atlantic water. While the peak was most pronounced in the South-West and Hopen Deep subareas, it was broader with high values also in 1995 in the Bear Island Trench and Tor Iversen Bank subareas (Figure 16).

Another feature in these time-series is an increase in the medium size fraction (1–2 mm) after 2005 in the westernmost areas, South-West and Bear Island Trench (Figure 16 A, B). This may reflect an increased amount of *Calanus finmarchicus* in the inflowing Atlantic water, as suggested by a more detailed analysis in a separate study (Aarflot et al. 2017). The increase in the middle fraction was associated with a stable or increase in the total biomass for these two areas, whereas the total biomass tended to decrease in recent years for the two downstream areas (Hopen Deep and Tor Iversen Bank) (Figure 16 C and D). The largest size fraction (>2 mm) has shown a declining trend in recent years, most pronounced for the same two downstream areas.

Central Barents Sea

Figure 17 shows time-series for total biomass for the Central Bank and Great Bank subareas, while Figure 18 shows the time-series for these two areas including size fractions. The two time-series show large similarity, with a declining trend since the 1990s. The

1994 event is pronounced but shows a one-year delay with peak in 1995, resembling the broader peaks in 1994–1995 seen in the Bear Island Trench and Tor Iversen Bank (Figure 16 A and D). The Central and Great Banks are important feeding areas for capelin. There is a general inverse relationship between zooplankton biomass in these areas and the capelin stock, which peaked in 1989–1991, 1999–2000, and 2007–2012, which are periods when the zooplankton biomass was low. The declining trend to low values during the recent years may also reflect a decrease in the Arctic water mass in these areas; this needs to be examined in more detail.

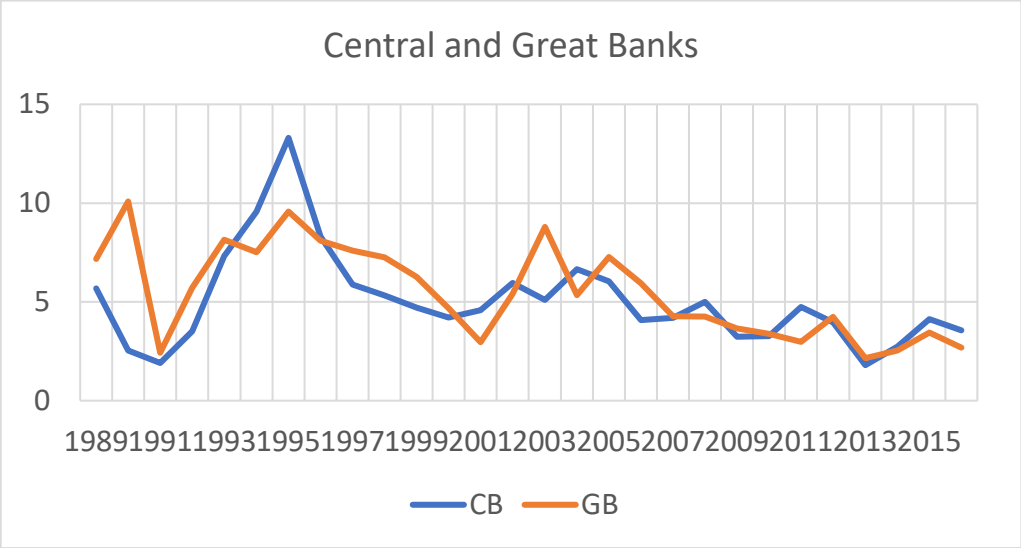

Figure 17. Time-series of total zooplankton biomass for the Central Bank and Great Bank subareas in the Barents Sea. Results obtained with WP-2 net, 1989–2016 (IMR, dataset #1).

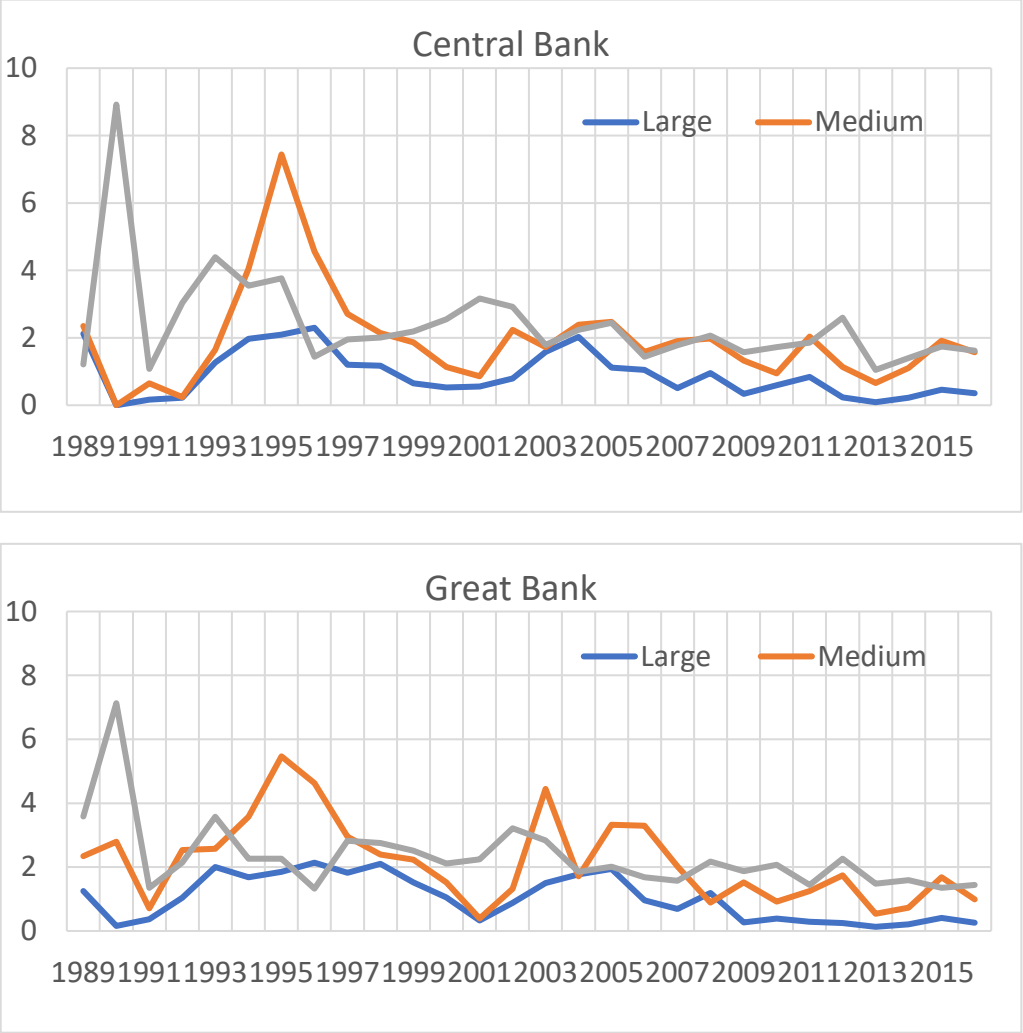

Figure 18. Time-series of zooplankton biomass in 3 size fractions (Large: > 2 mm, Medium: 1–2 mm, Small: <1 mm) in the Central Bank (A) and Great Bank (B) subareas in the Barents Sea. Results obtained with WP-2 net, 1989–2016 (IMR, dataset #1).

The '1994 event' was associated with an increase in the smallest size fraction (<1 mm) in 1993 followed by an increase in the mid-size fraction (1–2 mm), corresponding to *Calanus*, with a peak in 1995 for both areas (Figure 18). The largest size fraction also increased with a peak in 1996. There appears to be a pattern of decrease to low values for the largest size fraction at the times of peak in capelin stock, associated with an increase (relative) in the smallest fraction (Figure 18). This may reflect the predation impact from capelin on the zooplankton community, but this requires more analysis.

Prior to the 1994 peak, there was a pronounced peak of the smallest fraction in 1990 recorded in both subareas (Figure 18). This peak was associated with very low values for the large and medium fractions. (Note that we need to check whether this is partly an artefact due to variation in size fractionation procedure; see Skjoldal 2017, manuscript on IMR methods).

Southeastern Barents Sea

Time-series of biomass for the Tor Iversen Bank, South-East Basin, South-East, and Pechora subareas are shown in Figure 19. The biomass for these regions has shown a similar trend to that of subareas further west (Figure 15) with a pronounced increase from low values in 1990–1991 to a peak in 1994–1995, reflecting what we have called

the '1994 peak zooplankton event'. From similar levels around 7.5–10 g dw m^{-2} in the late 1990s, the subareas have shown somewhat different trends. The Tor Iversen Bank has shown a declining trend after 2006 (from about 7.5 to 5 g dw m^{-2}), whereas the biomass increased after 2005 in the South-East Basin. The South-East and Pechora subareas have been fluctuating at relatively low biomass values (about 2–6 g dw m^{-2}), with a recent decline to a low level in 2016 (about 1 g dw m^{-2}). The biomass in the South-East Basin has also declined in the two last years (to about 7.5 g dw m^{-2}).

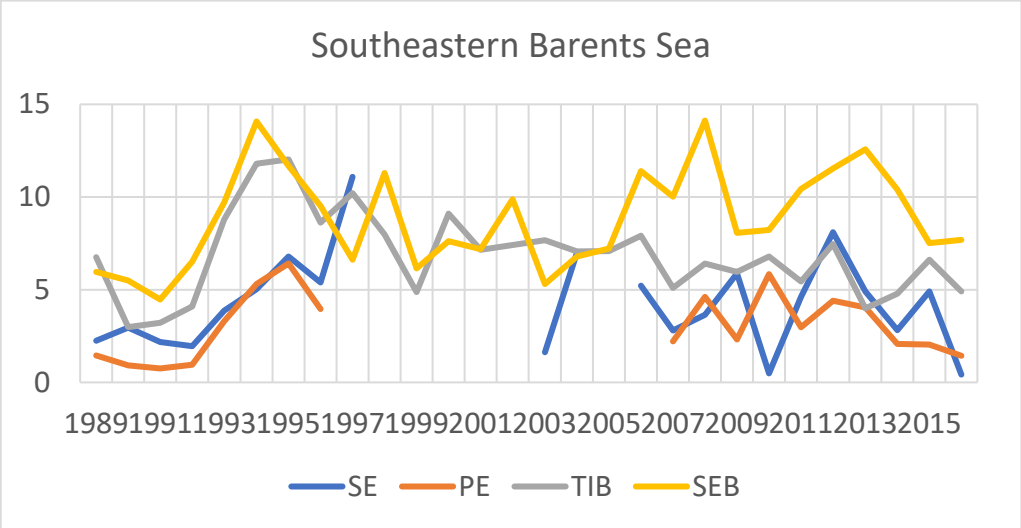

Figure 19. Time-series of total zooplankton biomass for four subareas in the southeastern Barents Sea. Results obtained with WP-2 and Juday nets, 1989–2016 (combined IMR and PINRO dataset #4).

Western Barents Sea

Time-series of total biomass for the Svalbard-South subarea is shown in Figure 20 along with the time-series for the adjacent subareas Bear Island Trench and Hopen Deep (included here for reference; shown previously in Figure 15). The Svalbard-South subarea show similar overall pattern to the other subareas, although the 1994 peak is considerably lower. From around year 2000, the biomass of the Svalbard-South subarea fluctuated more or less in parallel to, and at the same level (mostly 3–9 g dw m^{-2}) as the biomass in the Hopen Deep subarea.

The fluctuating biomass in the Svalbard-South subarea showed peaks in the medium fraction (at about 6–8 g dw m^{-2}) in 2007, 2012, and 2015 (Figure 21). The 1994 peak was driven mainly by the medium fraction and less by the small fraction, in contrast to the group of 'Atlantic' subareas in the southwestern Barents Sea (Figure 16).

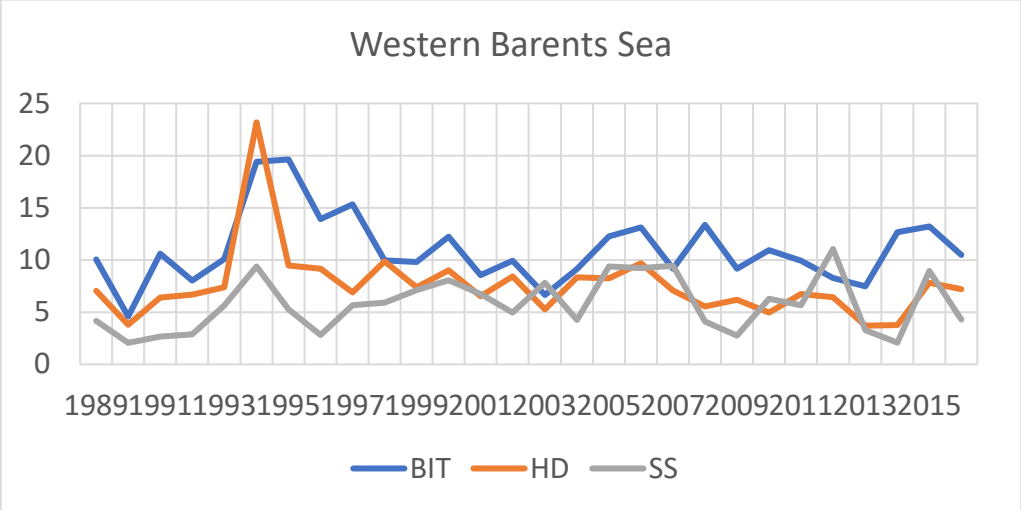

Figure 20. Time-series of total zooplankton biomass for three subareas in the western Barents Sea. Results obtained with WP-2 net, 1989-2016 (IMR, dataset #1).

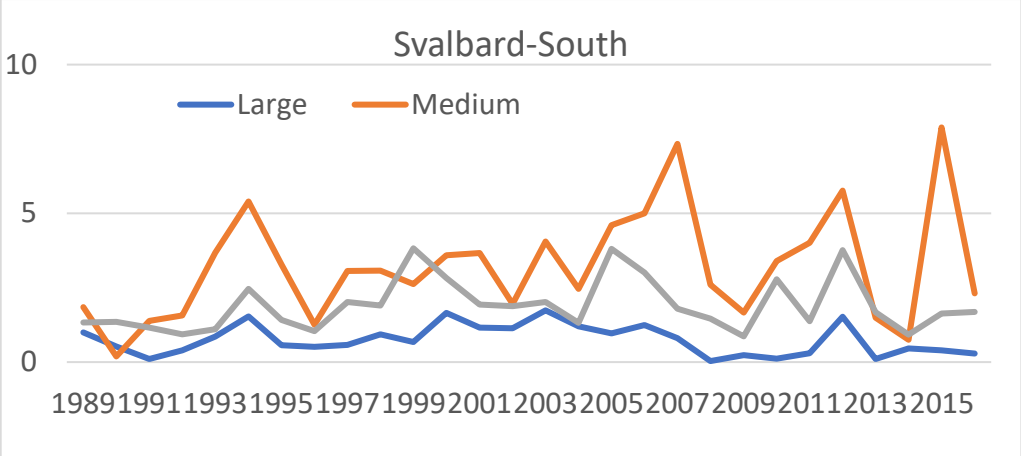

Figure 21. Time-series of zooplankton biomass in 3 size fractions (Large: > 2 mm, Medium: 1-2 mm, Small: <1 mm) in the Svalbard-South subarea in the Barents Sea. Results obtained with WP-2 net, 1989-2016 (IMR, dataset #1).

Northern Barents Sea

Time-series information of biomass changes for the five northern subareas of the Barents Sea (Svalbard-North, Franz-Victoria Trough, Franz Josef Land, St. Anna Trough, and North-East) are shown in Figure 22. The biomass in these northern areas has tended to be high, varying around 10 g dw m^{-2} with high mean values up to 15–20 g dw m^{-2}. These are time-series from the combined IMR-PINRO dataset #4, and there are substantial gaps and interruptions. There are no data from the Svalbard-North subarea before 2009, only some scattered data from Franz Josef Land before 2007, and limited data from a few years only for the St. Anna Trough (Table 3). It should be noted that variable spatial coverage between years (due to ice conditions and survey constraints) may have influenced the results, and caution is therefore necessary when interpreting the interannual variation and trends.

The biomass in the North-East subarea has been low the last two years of the time-series. Taken together, the data for Franz-Victoria Trough and North-East subareas indicate a declining trend since the late 1990s. However, this requires more careful examination (e.g. related to water mass properties). The biomass for the Svalbard-North subarea showed a peak of about 20 g dw m-2 in 2015 and was high also in 2016. The

biomass in the Franz Josef Land subarea has fluctuated around a relatively high level of 8-15 g dw m^{-2} (Figure 22).

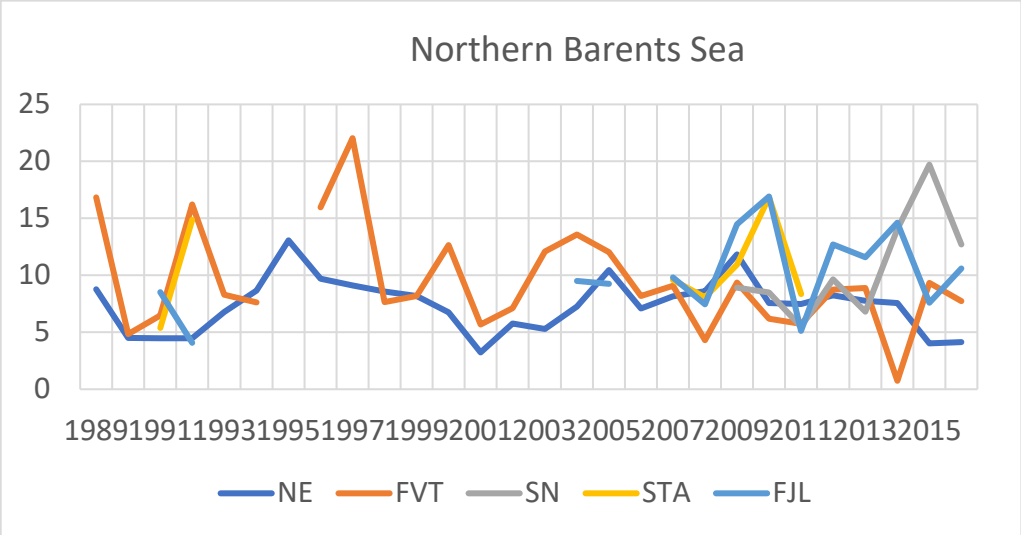

Figure 22. Time-series of total zooplankton biomass for five subareas in the northern Barents Sea. Results obtained with WP-2 and Juday nets, 1989–2016 (combined IMR and PINRO dataset #4).

Biomass in three size fractions are shown for 3 of the northern subareas in Figure 23. The biomass in the Franz-Victoria Trough subarea had usually a clear dominance of the medium fraction, with relatively low contribution by the small fraction (Figure 23 A). In the North-East subarea, in contrast, the small fraction has been relatively more important and the dominant fraction in the recent years (Figure 23 B; note that there are only single stations each year in 2007–2015, see Table 2). In the Svalbard-North subarea, sampled only since 2009, the small fraction contributed substantially to the peak in 2015, although the medium fraction ('*Calanus* fraction') was the most important (Figure 23 C).

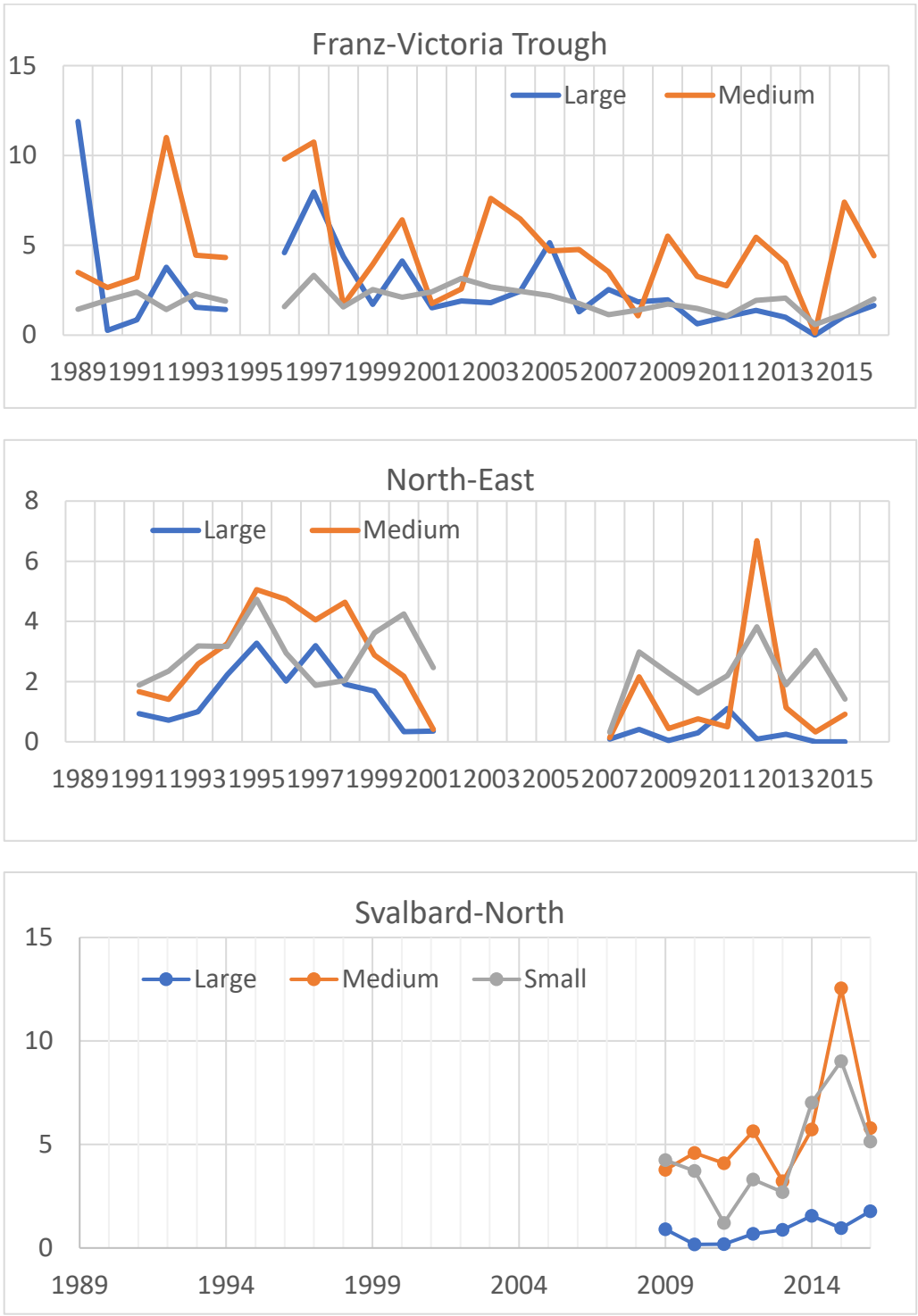

Figure 23. Time-series of zooplankton biomass in 3 size fractions (Large: > 2 mm, Medium: 1-2 mm, Small: <1 mm) in three subareas in the northern Barents Sea. A) Franz-Victoria Trough, B) North-East, and C) Svalbard-North. Results obtained with WP-2 net, 1989–2016 (IMR, dataset #1).

New spatial 0-group abundance indices in the Barents Sea for the period 1980–2017.

by Elena Eriksen[1], Hein Rune Skjoldal[1], Harald Gjøsæter[1], Dmitry Prozorkevich[2], Tatiana Prokhorova[2]

[1] – *Institute of Marine Research, Norway;* [2] – *Polar Research Institute of Marine Fisheries and Oceanography, Russia*

Overview of 0-group investigations and data collected

0-group fish investigations

A joint Norwegian-Russian 0-group fish trawl survey has been carried out annually in August-September between 1965 and 2003. The main goals of the 0-group survey have been to give an initial indication of year-class strength of the commercially important fish stocks and to map their spatial distribution in the Barents Sea (Eriksen and Prozorkevich, 2011). A small-meshed pelagic trawl ("Harstad") with 20 m x 20 m mouth opening has been used to cover the upper water layer (0–60 m) with the head-line at 0 m, 20 m, and 40 m (Anon, 2004; Eriksen *et al.,* 2009). At each depth level, the trawl is towed for 10 min at a speed of 3 knots (corresponding to a tow length of 0.5 nm or 0.93 km). Additional tows with the headline at 60 and 80 m are occasionally made when dense concentrations of 0-group fish are recorded deeper than 60 m on the echo-sounder.

Since 2004, the 0-group trawl survey and other four surveys have been part of a Barents Sea ecosystem survey (BESS), designed and jointly carried out by the Institute of Marine Research (IMR, Norway) and the Polar Research Institute of Marine Fisheries and Oceanography (PINRO, Russia). In addition to covering fish, zooplankton and oceanography, the survey includes sampling and observations of benthos, seabirds, marine mammals, and contaminants (Michalsen *et al.,* 2011; 2013; Eriksen and Gjøsæter, 2013). The timing of the BESS allows access by research vessels to most of or the whole Barents Sea, sea-ice being at its seasonal minimum. In August-September, migratory species such as capelin have reached their maximum northern distribution at the end of the summer feeding period. At this time, the juvenile 0-group fish of commercially and ecologically important species are sufficiently large to be caught by trawl, while 0-group demersal species such as cod and haddock have not yet settled to the bottom.

During the 0-group fish and BESS surveys, the pelagic trawl samples 0-group fish were sorted and identified to the species level. 100 specimens of each 0-group fish species were length measured, while pooled weight was obtained for species.

Sampling effort

During the period 1980–2016, more than 11 thousand pelagic station were taken in August–September with an average of 300 stations per year (Table 4).

Table 4. Number of sampling stations for 0-group fish (capelin, cod, haddock, herring, redfish, and polar cod) for the period 1980–2017.

Year	Total N of stations	Number of stations with					
		Capelin	Cod	Haddock	Herring	Redfish	Polar cod
1980	328	155	71	14	66	154	58
1981	297	191	72	6	36	106	88
1982	280	162	142	44	133	132	42
1983	279	190	196	117	144	137	62
1984	324	178	225	74	171	103	53
1985	292	84	220	56	110	100	70
1986	305	66	211	17	118	143	94
1987	288	57	116	7	78	121	44
1988	288	125	117	75	77	172	70
1989	425	271	189	125	113	182	65
1990	398	157	255	118	195	179	88
1991	408	173	249	127	187	96	91
1992	306	26	241	137	152	51	80
1993	273	39	201	87	110	47	62
1994	247	51	178	60	106	63	91
1995	247	45	178	64	103	69	14
1996	400	162	297	114	131	26	99
1997	269	157	193	106	109	47	69
1998	361	190	187	132	134	40	114
1999	230	149	89	87	77	19	91
2000	269	142	175	72	113	47	93
2001	278	130	101	58	126	10	51
2002	255	120	165	95	125	14	91
2003	277	145	136	97	105	17	89
2004	309	157	212	117	128	28	86
2005	318	128	178	74	128	40	122
2006	304	228	167	111	159	66	97
2007	304	162	156	74	120	95	67
2008	300	229	203	76	114	56	57
2009	332	157	252	121	166	96	73
2010	304	145	179	69	77	68	88
2011	309	192	224	84	127	58	82
2012	329	247	266	97	134	95	101
2013	304	172	271	93	159	41	45
2014	266	175	236	92	110	78	69
2015	298	209	219	81	137	94	70
2016	179	145	120	100	95	50	41
2017	228	154	203	83	141	43	37
Sum	11408	5665	7090	3161	4614	2983	2804

Spatial distribution

The Barents Sea has been divided into 15 subareas or polygons (Figure 24). The division is based on topography and oceanography and is a modification (with some subdivision) of the system used by Eriksen *et al.* (2017) in a summary analysis of pelagic biomass. The four western areas, South-West, Bear Island Trough, Hopen Deep and Tor Iversen Bank, are areas covered mainly with Atlantic water and constitute the inflow region of Atlantic water with the splitting of the current branches east through the Kola Section (south of the Central Bank) and north in the Hopen Deep (west of the Central Bank). The Central Bank subarea contains the Central Bank and the deeper areas between the Central Bank and Great Bank where Atlantic water from the Hopen Deep branch flows east on the way to the opening in northeast. The Central Bank has a clockwise circulation of water over it, and used to have Arctic conditions associated with ice freezing and formation of cold bottom water in winter. With warming, this is now changing. The Great Bank subarea (or the Persey Elevation) to the north is another major bank in the northern Barents Sea which is traditionally an important summer feeding area for the Barents Sea capelin stock. The Svalbard subarea is heterogenous with the Svalbard (or Spitsbergen) Bank and the Storfjord-system south of the archipelago along with the West Spitsbergen and North Svalbard shelf and slope areas. The Franz-Victoria Trough subarea lies between Svalbard and Franz Josef Land and includes the Franz-Victoria Trough leading into Olga Deep south of Kong Karls Land as

well as the shelf region around Kvitøya and Victoria Island. The Franz Josef Land subarea is the waters around the archipelago bounded by St. Anna Trough in the Kara Sea in east and a line along approximately 78.5°N in south.

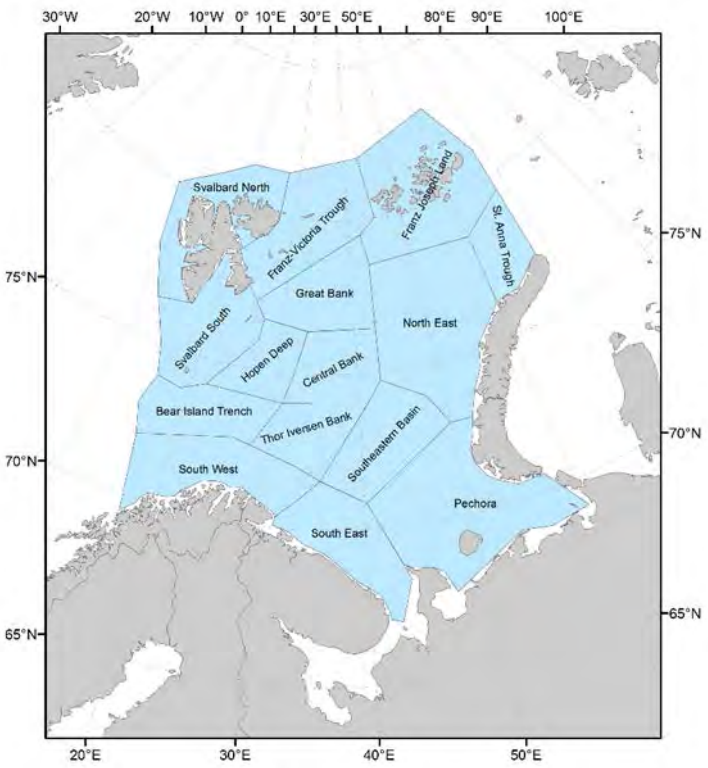

Figure 24. Map showing subdivision of the Barents Sea into 15 subareas (polygons) used to calculate mean densities of 0-group fish based on data from the Joint Norwegian-Russian 0-group fish survey (1980-2003) and the Joint Norwegian-Russian ecosystem survey (BESS).

The North-East subarea is the area east of the Great Bank and Central Bank and includes the North-Eastern Basin, Novaya Zemlya Bank, the sill region between Novaya Zemlya and Franz Josef Land, and the head of the St. Anna Trough leading into the northern Kara Sea. The South-East Basin includes the deep basin and the surrounding slopes to the east of the Central Bank and Thor Iversen Bank. The South-East subarea is comprised of the general shallow waters of the southeastern Barents Sea with the Murman Rise, North Kanin Bank, and Goose Bank, and the Pechora Sea.

Estimation of spatial indices

The 0-group station data are expressed as number per sq nm (= 3.43 km^2) and by using tow length, number of depth layers and capture area of trawl (width of 20 m) (Eriksen *et al.*, 2009). Small individuals pass through the coarser meshes in the front part of the trawl and the capture efficiency of the trawl differs between species and increases generally with fish length (Godø *et al.*, 1993; Hylen *et al.*, 1995). Therefore, correction factors based on empirical data for catchability (Hylen *et al.*, 1995; Mamylov, 2004) have been established and used in the annual calculations of abundance (Mamylov, 2004; Dingsør, 2005; Eriksen *et al.*, 2011a). Capture efficiencies for other 0-group fish such as polar cod, redfish, saithe, long rough dab and other have not been estimated. Number per sq nm corrected for capturing efficiency at each station were used to estimate mean abundance per each subarea, while fish length corrected for capturing efficiency at each station were used to estimate the mean fish length for subarea. To estimate the total abundance per subarea the mean abundance per subarea were multiplied with

covered area within subarea. The estimation of densities and abundance per subarea were done in MatLab R2017a (9.2 0.556344).

0-group fish abundance indices

Time-series for 0-group fish species were annually estimated after the 0-group fish surveys and the BESS (see above) and presented in the surveys reports (1980–2017) and since 2014, in the WGIBAR reports.

Time-series for 0-group most abundant and ecologically important species (capelin, cod, haddock, herring, redfish, and polar cod) are shown in Figure 25. During 1980s, low abundance indices were estimated for 0-group cod, herring, haddock and polar cod in 1980s, while high for capelin and redfish. Cod, herring and polar cod abundance increased in 1990s due to occurrence of strong year classes of cod (1995–1997), herring (1996–1998), polar cod (1991, 1994, 1996, and 1999), while abundance of capelin and redfish decreased. Abundance of all fish increased, except redfish during early 2000s, and decreased.

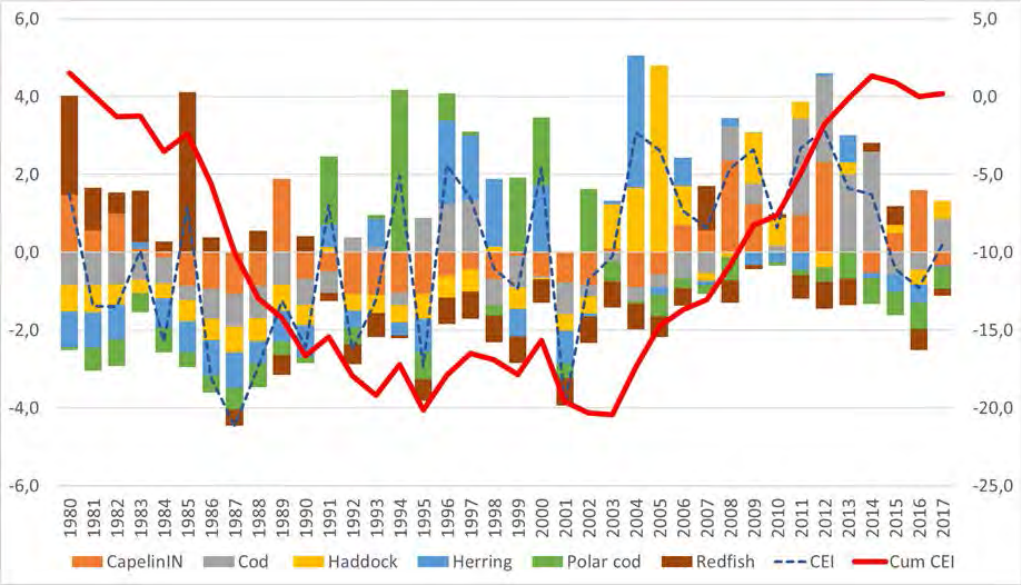

Figure 25. Anomalies of 0-group indices over the period 1980–2017. Red line indicated cumulative fluctuations.

Clustering of 0-group indices (capelin, cod, haddock, herring, redfish, and polar cod) over the period 1980–2017 is shown in Figure 26. The 38-year period could be divided in to three subperiods (1980–1993, 1995–2003, and 2005–2017) with two years as breakpoints (1994 and 2004).

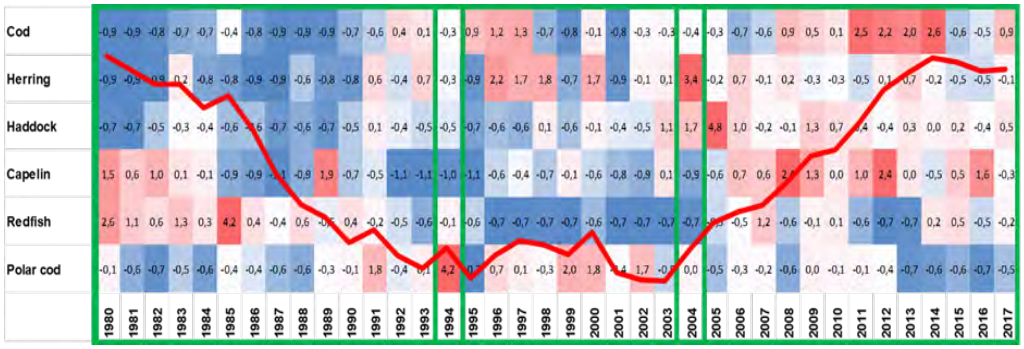

Figure 26. 0-group indices fluctuations. 0-roup indices centered by mean and standard deviation ((x-mean)/StDev) and low indices shown by blue colors, while high 0-group indices shown by red colors. Classic clustering of 0-group indices (capelin, cod, haddock, herring, redfish and polar cod) over the period 1980–2017. Red line indicated cumulative fluctuations.

In first subperiod (1980–1993), the system dominated by strong years redfish and some years classes of capelin. At the beginning of second subperiod (1995–2003), abundance of all fish decreased or were low and some strong years classes of cod, herring and polar cod occurred, while capelin and redfish continued to decrease. The last period (2005–2017), could be characterized as period of good fish recruitment for most of fish.

Spatial 0-group fish abundance indices

The mean fish abundance over the study period was low during 1980s and twice higher during last three decades (9*e9 and 16-18*e9 ind., correspondently).

The mean abundance for the subareas over the 1980–2017 is shown in Figure 27. The mean abundance varied from 631 million ind. to 36*e9 individuals, and were high in the western and eastern areas and low in the northern areas (St. Anna Through and Franz-Viktoria Trough). The high long-term mean (1980–2017) fish abundance in the Pechora and Northeast, influenced by high decadal mean abundance during 1990s and early 2000s, which dominated by strong year classes of polar cod (see below). During 2000s, the mean fish abundance was high in the west central areas (South West, Bear Island Trench, Thor Iversen Bank, Central Bank, and Svalbard North) and dominated by strong year classes of herring, capelin, and cod (see below).

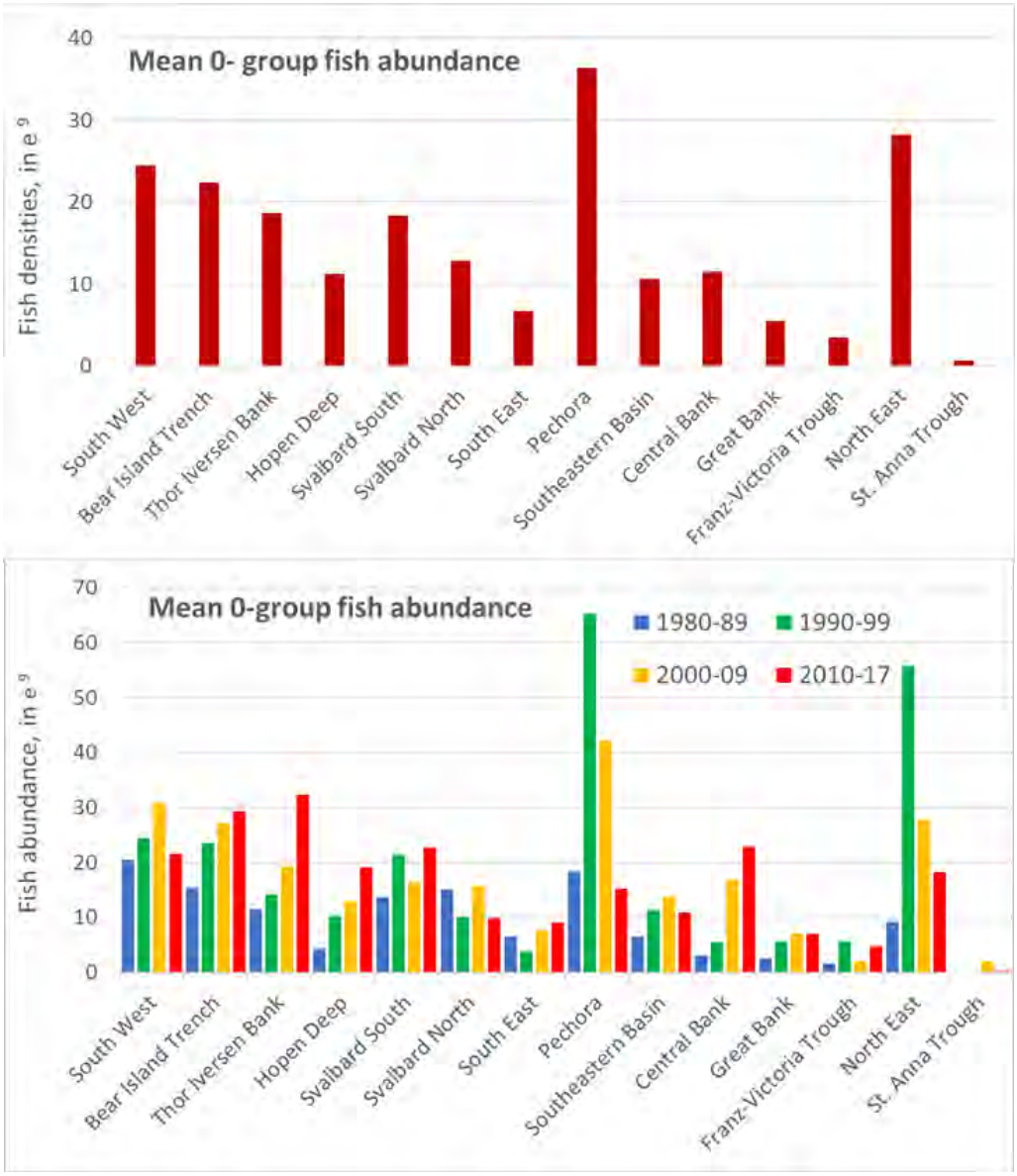

Figure 27. Mean 0-group fish abundance for the whole period 1980–2016 (above) and by decades (below) 1980–1989, 1990–1999, 2000–2009, 2010, 16 for subregions in the Barents Sea.

In the western areas (the South West, Bear Island Bank, and Thor Iversen Bank), the mean abundance of 0-group fish was highest in late 1990s and moderate in early 1980s and 2000s, and dominated by strong year classes of herring (late 1990s and early 2004 in the South West) and capelin (1980s and 2000s), and cod (mid-1990s and 2000s, Figure 28).

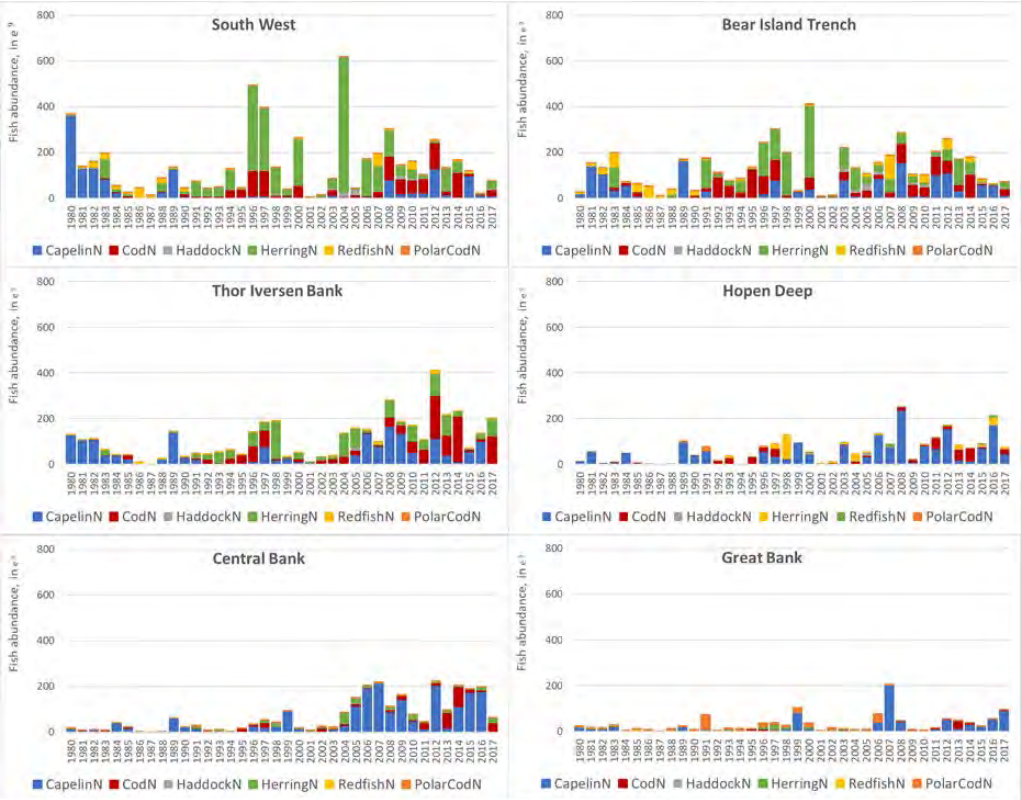

Figure 28. Annual mean biomass of 0-group fish (capelin, cod, haddock, herring, redfish and polar cod) in the South West, Bear Island Bank, Thor Iversen Bank, Hopen Deep, Central Bank and Great Bank in the period 1980–2016.

In the central areas (Hopen Deep, Central bank and Great Bank), the mean abundance of 0-group fish was lower than in western areas (Figure 29). Relatively high fish abundance was in 2000s and dominated by strong year classes of polar cod (1990s, Great Bank), capelin (2000s), and cod (late 2000s).

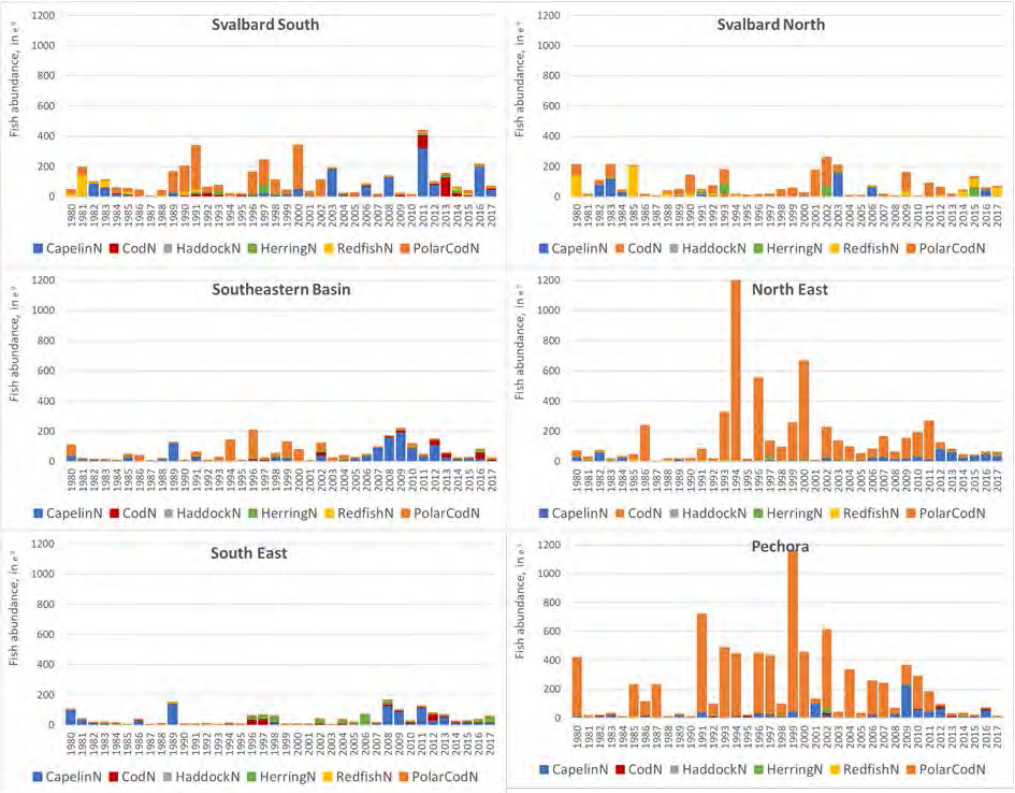

Figure 29. Annual mean biomass of 0-group fish (capelin, cod, haddock, herring, redfish and polar cod) in Svalbard South, Svalbard North, Southeastern Basin, North East, South East and Pechora in the period 1980-2016.

In the Svalbard South and Svalbard North areas, the mean abundance of 0-group fish was lower than in the western areas, but higher than central areas (Figure 30). 0-group fish abundance in the Svalbard's areas dominated by polar cod in 1990s and capelin in 2000s. Abundance of 0-group fish in the Franz-Victoria Trough and St. Anna Trough were low and thus not shown in the Figure 6. The eastern areas, Southeastern Basin, Pechora and North East, dominated by polar cod during whole period and capelin in 2000s, while in South East, capelin and herring were mainly abundant.

Mean fish length per subarea

During the 0-group survey and the BESS, 0-group fish (capelin, cod, haddock, herring, redfish, and polar cod) were length measured (Table 5). Number of fish per station were estimated considering capture efficiency (Dingsør, 2005; Eriksen *et al.*, 2009) and after the mean fish length were estimated (Dingsør, 2005). Mean fish length per station were used to estimate mean fish length for each subarea.

Table 5. Number of sampling stations with 0-group fish (capelin, cod, haddock, herring, redfish and polar cod) length measurement for the period 1980-2016 measurement.

Year	Total N of stations	Number of stations with length measurement of					
		Capelin	Cod	Haddock	Herring	Redfish	Polar cod
1980	328	155	71	66	14	154	58
1981	297	192	72	37	6	106	88
1982	280	161	142	132	44	132	42
1983	279	190	196	144	117	135	61
1984	324	178	225	171	74	103	53
1985	292	84	220	110	56	100	70
1986	305	66	211	118	17	143	94
1987	288	57	116	78	7	121	44
1988	288	125	117	77	75	172	172
1989	425	271	189	113	125	182	65
1990	398	157	255	195	118	179	88
1991	408	173	249	186	127	96	91
1992	306	26	241	152	137	51	80
1993	273	39	201	110	87	47	62
1994	247	51	178	106	60	63	91
1995	247	45	178	103	64	69	14
1996	400	162	297	131	114	26	99
1997	269	157	193	109	106	47	69
1998	361	190	187	134	132	40	114
1999	230	149	89	77	87	19	91
2000	269	141	175	113	72	47	93
2001	278	130	101	126	58	10	51
2002	255	118	165	125	95	14	91
2003	277	140	133	105	95	17	82
2004	309	157	212	128	117	28	86
2005	318	128	178	128	74	40	122
2006	304	228	167	159	111	66	97
2007	304	162	156	120	74	95	67
2008	300	229	202	114	76	56	57
2009	332	157	252	166	121	96	73
2010	304	145	179	77	69	68	88
2011	309	192	224	127	84	58	82
2012	329	247	266	134	97	95	101
2013	304	172	271	159	93	41	45
2014	266	175	235	110	92	78	69
2015	298	209	219	137	81	94	70
2016	179	146	121	96	101	51	41
2017	228	154	203	141	82	43	37
Sum	11408	5658	7086	4614	3159	2982	2898

Fish length varied between species, and haddock were largest, while redfish and polar cod were smallest among the 0-group fish (Figure 7). The large haddock (with average fish length of 7.5–8.4 cm) were found in BIT, HD, CB, GB, NE. The large cod (with average fish length of 7–7.4 cm) were found in BIT, TIB, HD, SE, SEB, CB, GB. The large capelin (with average fish length of 5–5.7 cm) was observed in CB, GB, FJL, NE. the large herring (with average fish length of 6–6.4 cm) were distributed in SW, BIT, TIB, FJL.

A statistically significant increasing trend of fish length was observed for cod and haddock, indicating that fish length was generally smaller in 1980s and fish length increased with years and were largest during recent years. Cod fish length were correlated with haddock and herring, while polar cod were correlated with fish length of all studied fish species.

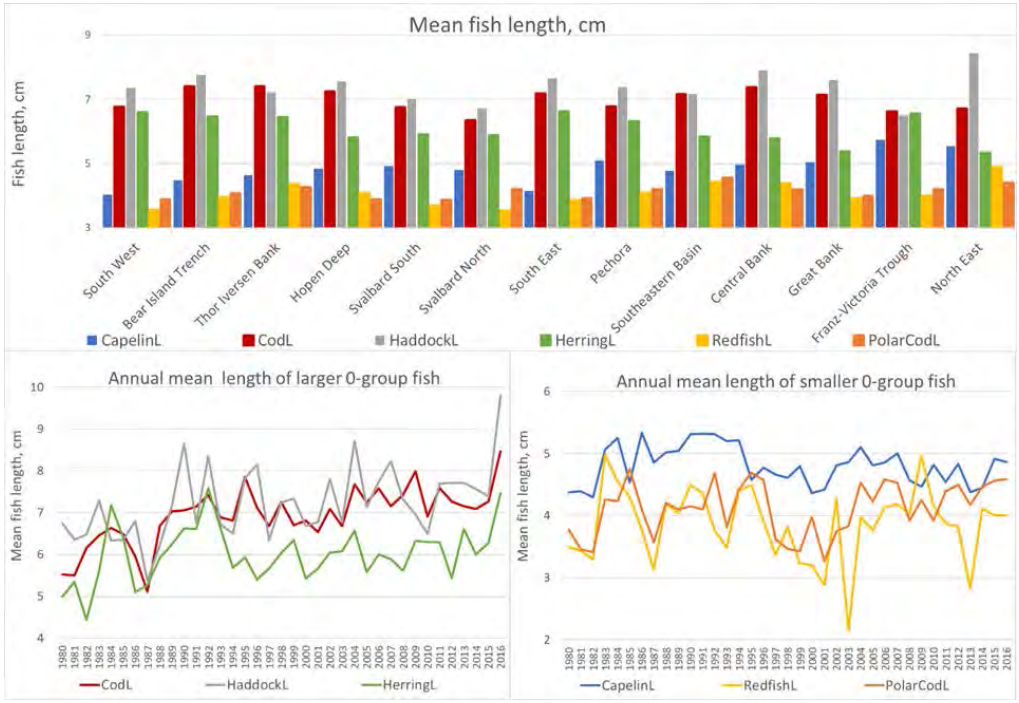

Figure 30. Annual mean length for capelin, cod, haddock, herring, redfish, and polar cod for 13 subareas (above) and mean fish length of larger (below, left) and smaller (below, right) 0-group fish.

Dissemination for the results

These new spatial time-series will be published in peer reviewed articles, where fish recruitment will be linked to the feeding (plankton biomass and distribution) and environmental (currents and water temperature) conditions to understand better fish recruitment and factors influencing the recruitment success.

List of fish species recorded at the ecosystem survey 2004–2017.

by E. Johannessen1 and T.Prokhorova2

[1] – *Institute of Marine Research, Norway;* [2] – *Polar Research Institute of Marine Fisheries and Oceanography, Russia*

A few other species has been recorded but we judge them to be misidentifications and do not show them here. The last indicates which species are included in the maps over the distribution of zoogeographic groups found at the ecosystem survey 2004–2017 and shown in this report.

Order	Family	Scientific_name	Author	English	Andriashev	Mecklenbu	WGIBAR
Myxiniformes	Myxinidae	Myxine glutinosa	Linnaeus, 1758	Hagfish	B	B	zoogeogr
Petromyzontiformes	Petromyzontidae	Petromyzon marinus1	Linnaeus, 1758	Sea lamprey	SB		
Petromyzontiformes	Petromyzontidae	Lethenteron camtschaticum	(Tilesius, 1811)	Arctic Lamprey	MB		zoogeogr
Squaliformes	Dalatiidae	Etmopterus spinax	(Linnaeus, 1758)	Velvet belly	WD		zoogeogr
Squaliformes	Dalatiidae	Somniosus microcephalus	(Bloch & Schneider 1	Greenland shark	MB	AB	zoogeogr
Rajiformes	Arhynchobatidae	Bathyraja spinicauda	(Jensen, 1914)	Spinetail ray	MB	AB	zoogeogr
Rajiformes	Rajidae	Amblyraja hyperborea	(Collett, 1879)	Arctic skate	A	A	zoogeogr
Rajiformes	Rajidae	Amblyraja radiata	(Donovan, 1808)	Thorny skate	MB	AB	zoogeogr
Rajiformes	Rajidae	Rajella lintea	(Fries, 1838)	Sailray	B	MB	zoogeogr
Rajiformes	Rajidae	Rajella fyllae	(Lütken, 1887)	Round ray	MB	B	zoogeogr
Chimaeriformes	Chimaeridae	Chimaera monstrosa	Linnaeus, 1758	Rabbit fish	B		zoogeogr
Anguilliformes	Synaphobranchidae	Diastobranchis capensis	Barnard 1923	Basketwork eel	WD[2]	WD	zoogeogr
Clupeiformes	Clupeidae	Clupea harengus harengus	Linnaeus, 1758	Atlantic herring	MB	MB	
Clupeiformes	Clupeidae	Clupea pallasii suworowi	Rabinerson 1927	Kanin herring	AB[3]	AB	
Osmeriformes	Argentinidae	Argentina silus	(Ascanius, 1775)	Greater argentine	B	B	zoogeogr
Osmeriformes	Microstomatidae	Nansenia groenlandica	(Reinhardt, 1840)	Large-eyed argentine	SB	WD	zoogeogr
Osmeriformes	Osmeridae	Mallotus villosus	(Müller, 1776)	Capelin	MB	AB	
Osmeriformes	Osmeridae	Osmerus mordax dentex	Steindachner, 1870	Rainbow smelt	AB		zoogeogr
Salmoniformes	Salmonidae	Salmo salar	Linnaeus, 1758	Atlantic salmon	MB		zoogeogr
Stomiiformes	Sternoptychidae	Argyropelecus hemigymnus	Cocco, 1829	Half-naked hatchet fish	WD	WD	
Stomiiformes	Sternoptychidae	Maurolicus muelleri	(Gmelin, 1789)	Pearlside	B	MB	zoogeogr
Aulopiformes	Paralepididae	Arctozenus risso	(Bonaparte, 1840)	White barracudina	WD	WD	zoogeogr
Myctophiformes	Myctophidae	Benthosema glaciale	(Reinhardt, 1837)	Glacier lanternfish	MB	AB	zoogeogr
Myctophiformes	Myctophidae	Lampanyctus macdonaldi	(Goode & Bean, 1896	Rakery beaconlamp	WD	WD	zoogeogr
Myctophiformes	Myctophidae	Notoscopelus kroyeri	(Malm, 1861)	Kroyers lanternfish	MB	MB	zoogeogr
Gadiformes	Macrouridae	Coelorinchus labiatus	(Köhler 1896)	Spearsnouted grenadier		B	zoogeogr
Gadiformes	Macrouridae	Coryphaenoides rupestris	Gunnerus 1765	Roundnose grenadier	WD	B	zoogeogr
Gadiformes	Macrouridae	Macrourus berglax	Lacepede, 1801	Roughhead grenadier	B	MB	zoogeogr
Gadiformes	Gadidae	Arctogadus glacialis	(Peters, 1874)	Arctic cod	A	A	zoogeogr
Gadiformes	Gadidae	Boreogadus saida	(Lepechin, 1774)	Polar cod	A	A	
Gadiformes	Gadidae	Eleginus nawaga	(Koelreuter, 1770)	Atlantic navaga	A	A	
Gadiformes	Gadidae	Gadiculus argenteus	Guichenot, 1850	Silvery pout	SB		zoogeogr
Gadiformes	Gadidae	Gadus morhua	Linnaeus, 1758	Atlantic cod	MB	MB	
Gadiformes	Gadidae	Melanogrammus aeglefinus	(Linnaeus, 1758)	Haddock	MB	MB	
Gadiformes	Gadidae	Merlangius merlangus	(Linnaeus, 1758)	Whiting	SB	B	zoogeogr
Gadiformes	Gadidae	Micromesistius poutassou	(Risso, 1826)	Blue whiting	MB	MB	
Gadiformes	Gadidae	Pollachius pollachius	(Linnaeus, 1758)	Pollack	B		zoogeogr
Gadiformes	Gadidae	Pollachius virens	(Linnaeus, 1758)	Saithe	MB	B	
Gadiformes	Gadidae	Trisopterus esmarkii	(Nilsson, 1855)	Norway pout	B	B	
Gadiformes	Lotidae	Brosme brosme	(Ascanius, 1772)	Tusk	MB	B	zoogeogr
Gadiformes	Lotidae	Enchelyopus cimbrius	(Linnaeus, 1766)	Fourbeard rockling	B	B	zoogeogr
Gadiformes	Lotidae	Gaidropsarus argentatus	(Reinhardt, 1838)	Arctic threebearded rocl	A	AB	zoogeogr
Gadiformes	Lotidae	Molva molva	(Linnaeus, 1758)	Ling	B	B	zoogeogr
Gadiformes	Merlucciidae	Merluccius merluccius	(Linnaeus, 1758)	European hake	SB		zoogeogr
Gadiformes	Phycidae	Phycis blennoides	(Brünnich, 1768)	Greater forkbeard	SB	B	zoogeogr
Lophiiformes	Lophiidae	Lophius piscatorius	Linnaeus, 1758	Anglerfish	SB	B	zoogeogr
Beloniformes	Belonidae	Belone belone1	(Linnaeus, 1761)	Garfish	B	B	
Lampriformes	Trachipteridae	Trachipterus arcticus1	(Brünnich, 1771)	Dealfish	WD	B	

Gasterosteiformes	Gasterosteidae	Gasterosteus aculeatus	Linnaeus, 1758	Three-spined stickleback	MB		zoogeogr
Gasterosteiformes	Gasterosteidae	Pungitius pungitius	(Linnaeus, 1758)	Ninespine stickleback	MB[3]		zoogeogr
Syngnathiformes	Syngnathidae	Entelurus aequoreus	(Linnaeus, 1758)	Snake pipefish	B	B	zoogeogr
Scorpaeniformes	Sebastidae	Sebastes mentella	Travin 1951	Deepwater redfish	MB	MB	
Scorpaeniformes	Sebastidae	Sebastes norvegicus	(Ascanius, 1772)	Golden redfish	MB	MB	
Scorpaeniformes	Sebastidae	Sebastes viviparus	Kröyer, 1844	Norway redfish	B	B	
Scorpaeniformes	Triglidae	Eutrigla gurnardus1	(Linnaeus, 1758)	Grey gurnard	SB		
Scorpaeniformes	Cottidae	Artediellus atlanticus	Jordan & Evermann,	Atlantic hookear sculpin	MB	AB	zoogeogr
Scorpaeniformes	Cottidae	Artediellus scaber	Knipowitsch, 1907	Rough hookear sculpin	A	A	zoogeogr
Scorpaeniformes	Cottidae	Gymnocanthus tricuspis	(Reinhardt, 1830)	Arctic staghorn sculpin	MA	A	zoogeogr
Scorpaeniformes	Cottidae	Icelus spp[2]	Krøyer, 1845				zoogeogr
Scorpaeniformes	Cottidae	Icelus bicornis	(Reinhardt, 1840)	Twohorn sculpin	MA	MA	zoogeogr
Scorpaeniformes	Cottidae	Icelus spatula	Gilbert & Burke, 1912	Spatulate sculpin	AB	AB	zoogeogr
Scorpaeniformes	Cottidae	Myoxocephalus scorpius	(Linnaeus, 1758)	Shorthorn sculpin	MB	AB	zoogeogr
Scorpaeniformes	Cottidae	Myoxocephalus sp.[3]	Tilesius, 1811	Daddy sculpins			zoogeogr
Scorpaeniformes	Cottidae	Triglops murrayi	Günther, 1888	Moustache sculpin	B	AB	zoogeogr
Scorpaeniformes	Cottidae	Triglops nybelini	Jensen, 1944	Bigeye sculpin	A	A	zoogeogr
Scorpaeniformes	Cottidae	Triglops pingelii	Reinhardt, 1937	Ribbed sculpin	AB	AB	zoogeogr
Scorpaeniformes	Psychrolutidae	Cottunculus microps	Collett, 1875	Polar sculpin	MA	AB	zoogeogr
Scorpaeniformes	Psychrolutidae	Cottunculus sadko	Essipov, 1937	Sadko sculpin	A		zoogeogr
Scorpaeniformes	Agonidae	Agonus cataphractus	Linnaeus, 1758)	Hooknose	B	B	zoogeogr
Scorpaeniformes	Agonidae	Leptagonus decagonus	(Bloch & Schneider, 1	Atlantic poacher	AB	AB	zoogeogr
Scorpaeniformes	Agonidae	Aspidophoroides olrikii	(Lütken, 1876)	Arctic alligatorfish	A	MA	zoogeogr
Scorpaeniformes	Cyclopteridae	Cyclopterus lumpus	Linnaeus, 1758	Lumpsucker	MB	MB	zoogeogr
Scorpaeniformes	Cyclopteridae	Eumicrotremus derjugini	Popov, 1926	Leatherfin lumpsucker	A	A	zoogeogr
Scorpaeniformes	Cyclopteridae	Eumicrotremus spinosus	(Fabricius, 1776)	Atlantic spiny lumpsucker	MA	MA	zoogeogr
Scorpaeniformes	Liparidae	Careproctus spp4	Krøyer, 1862				zoogeogr
Scorpaeniformes	Liparidae	Careproctus micropus	(Günther, 1887)	Smalleye tadpole	A	A	zoogeogr
Scorpaeniformes	Liparidae	Careproctus ranula	(Goode and Bean, 18	Scotian snailfish	A		zoogeogr
Scorpaeniformes	Liparidae	Careproctus rienhardti	(Krøyer, 1862)	Sea tadpole	A	A	zoogeogr
Scorpaeniformes	Liparidae	Liparis fabricii	Kröyer, 1847	Gelantinous snailfish	A	A	zoogeogr
Scorpaeniformes	Liparidae	Liparis bathyarcticus	Bean, 1881	Variegated snailfish	MA	MA	zoogeogr
Scorpaeniformes	Liparidae	Liparis liparis	(Linnaeus, 1766)	Striped seasnail	B	B	zoogeogr
Scorpaeniformes	Liparidae	Liparis montagui	(Donovan, 1805)	Montagu's sea snail	B	B	zoogeogr
Scorpaeniformes	Liparidae	Liparis tunicatus	Reinhardt, 1837	Kelp snailfish	A	A	zoogeogr
Scorpaeniformes	Liparidae	Paraliparis bathybius	(Collett, 1879)	Black seasnail	A	A	zoogeogr
Scorpaeniformes	Liparidae	Rhodichthys regina	Collett, 1879	Threadfin seasnail	A	A	zoogeogr
Perciformes	Carangidae	Trachurus trachurus1	(Linnaeus, 1758)	Atlantic horse mackerel		WD	
Perciformes	Centrolophidae	Schedophilus medusophagu	(Cocco, 1839)	Cornish blackfish			
Perciformes	Zoarcidae[8]	Lycenchelys kolthoffi	Jensen 1903	Checkered wolf eel	A	A	zoogeogr
Perciformes	Zoarcidae[8]	Lycenchelys muraena	(Collett, 1878)	Moray wolf eel	A	A	zoogeogr
Perciformes	Zoarcidae[8]	Lycenchelys sarsii	(Collett, 1871)	Sars' wolf eel	B	B	zoogeogr
Perciformes	Zoarcidae[8]	Lycodes adolfi	Nielsen and Fosså, 1	Adolf's eelpout	A	A	zoogeogr
Perciformes	Zoarcidae[8]	Lycodes esmarkii	Collett, 1875	Esmark's eelpout	MB	MB	zoogeogr
Perciformes	Zoarcidae[8]	Lycodes eudipleurostictus	Jensen, 1901	Doubleline eelpout	A	A	zoogeogr
Perciformes	Zoarcidae[8]	Lycodes frigidus	Collett, 1878	Glacial eelpout	A	A	zoogeogr
Perciformes	Zoarcidae[8]	Lycodes gracilis	Sars, 1867	Vahl's eelpout	MB	MB	zoogeogr
Perciformes	Zoarcidae[8]	Lycodes luetkenii	Collett 1880	Lutken's eelpout	A	A	zoogeogr
Perciformes	Zoarcidae[8]	Lycodes paamiuti	Møller 2001	Paamiut eelpout	A[3]	A	zoogeogr
Perciformes	Zoarcidae[8]	Lycodes pallidus	Collett, 1878	Pale eelpout	A	A	zoogeogr
Perciformes	Zoarcidae[8]	Lycodes polaris	(Sabine, 1824)	Canadian eelpout	A	A	zoogeogr
Perciformes	Zoarcidae[8]	Lycodes reticulatus	Reinhardt, 1935	Arctic eelpout	A	A	zoogeogr
Perciformes	Zoarcidae[8]	Lycodes rossi	Malmgren, 1864	Threespot eelpout	A	A	zoogeogr
Perciformes	Zoarcidae[8]	Lycodes seminudus	Reinhardt, 1837	Halfnaked eelpout	A	A	zoogeogr
Perciformes	Zoarcidae[8]	Lycodes squamiventer	Jensen, 1904	Scalebelly eelpout	A	A	zoogeogr
Perciformes	Zoarcidae[8]	Lycodonus flagellicauda	(Jensen, 1901)	Clue tail eelspout	A	A	zoogeogr
Perciformes	Zoarcidae[8]	Gymnelus spp.5	Reinhardt, 1834				zoogeogr
Perciformes	Stichaeidae	Anisarchus medius	(Reinhardt, 1837)	Stout eelblenny	B	AB	zoogeogr
Perciformes	Stichaeidae	Leptoclinus maculatus	(Fries, 1838)	Daubed shanny	MB	AB	zoogeogr
Perciformes	Stichaeidae	Lumpenus fabricii	Reinhardt, 1836	Slender eelblenny	MA	AB	zoogeogr
Perciformes	Stichaeidae	Lumpenus lampretaeformis	(Walbaum, 1792)	Snakeblenny	MB	MB	zoogeogr
Perciformes	Anarhichadidae	Anarhichas denticulatus	Kröyer, 1845	Northern wolffish	MB	AB	
Perciformes	Anarhichadidae	Anarhichas lupus	Linnaeus, 1758	Atlantic wolffish	MB	MB	
Perciformes	Anarhichadidae	Anarhichas minor	Olafsen, 1772	Spotted wolffish	MB	MB	
Perciformes	Ammodytidae	Ammodytes marinus6	Raitt, 1934	Lesser sandeel	MB	MB	zoogeogr
Perciformes	Scombridae	Scomber scombrus	Linnaeus, 1758	Atlantic mackerel	SB	B	

Pleuronectiformes	Pleuronectidae	Glyptocephalus cynoglossu	(Linnaeus, 1758)	Witch flounder	MB	B	zoogeogr
Pleuronectiformes	Pleuronectidae	Hippoglossoides platessoide	(Fabricius, 1780)	Long rough dab	MB	AB	
Pleuronectiformes	Pleuronectidae	Hippoglossus hippoglossus	(Linnaeus, 1758)	Atlantic halibut	MB	MB	zoogeogr
Pleuronectiformes	Pleuronectidae	Limanda limanda	(Linnaeus, 1758)	Dab	MB	MB	zoogeogr
Pleuronectiformes	Pleuronectidae	Microstomus kitt	(Walbaum, 1792)	Lemon sole	B	B	zoogeogr
Pleuronectiformes	Pleuronectidae	Liopsetta glacialis	(Pallas, 1776)	Arctic flounder	MA	AB	zoogeogr
Pleuronectiformes	Pleuronectidae	Pleuronectes platessa	Linnaeus, 1758	European plaice	MB	B	
Pleuronectiformes	Pleuronectidae	Reinhardtius hippoglossoide	(Walbaum, 1792)	Greenland halibut	MA	AB	
Pleuronectiformes	Scophthalmidae	Lepidorhombus whiffiagonis	(Walbaum, 1792)	Megrim			zoogeogr
Pleuronectiformes	Scophthalmidae	Zeugopterus norvegicus	(Günther, 1862)	Norwegian topknot	B		zoogeogr

Notes:

[1] only caught in pelagic trawls;

[2] difficult to determine to species level;

[3] species found in the eastern Barents Sea that needs to be identified and verication in the Barents Sea;

[4] the genus is under revision (Chernova, 2006), since 2007 only recorded to genus level on Norwegian boats, Russian boats determined to the species level, using taxonomy before Chernova, 2006, three species *C. reinhardtii, C. microps, C. ranula;*

[5] this genus is under taxonomic revision;

[6] difficult to determine to species level, all recordings in this familiy has been pooled with *Ammodytes marinus*.

Annex 5: The state and trends of the Barents Sea ecosystem in 2017

Contributing Authors (Alphabetic):

Espen Bagøien[1], Alexander Benzik[2], Bjarte Bogstad[1], Padmini Dalpadado[1], Anatoly Chetyrkin[2], Andrey Dolgov[2], Elena Eriksen[1], Anatoly Filin[2], Harald Gjøsæter[1], Elvar H. Hallfredsson[1], Randi Ingvaldsen[1], Per Fauchald[4], Edda Johannesen[1], Lis Lindal Jørgensen[1], Stuart Larsen[1], Vidar Lien[1], Anna Mikhina[2], Alexey Karsakov[2], Roman Klepikovskiy[2], Yuri Kovalev[2], Tor Knutsen[1], Margaret Mary McBride[1], Valentina Nesterova[1], Raul Primicerio[3], Tatiana Prokhorova[2], Irina Prokopchuk[2], Dmitri Prozorkevich[2], Jon Rønning[1], Øystein Skagseth[1], Georg Skaret[1], Hein Rune Skjoldal[1], Natalia Strelkova[2], Alexey Russkikh[2], Alexander Trofimov[2], Denis Zakharov[2]

[1]Intitute of Marine Research (IMR), Norway

[2]Knipovich Institute of Polar Research of Marine Fisheries and Oceanography (PINRO), Russia

[3] The Arctic University of Norway, Norway

[4]The Norwegian Institute for Nature Research (NINA), Norway

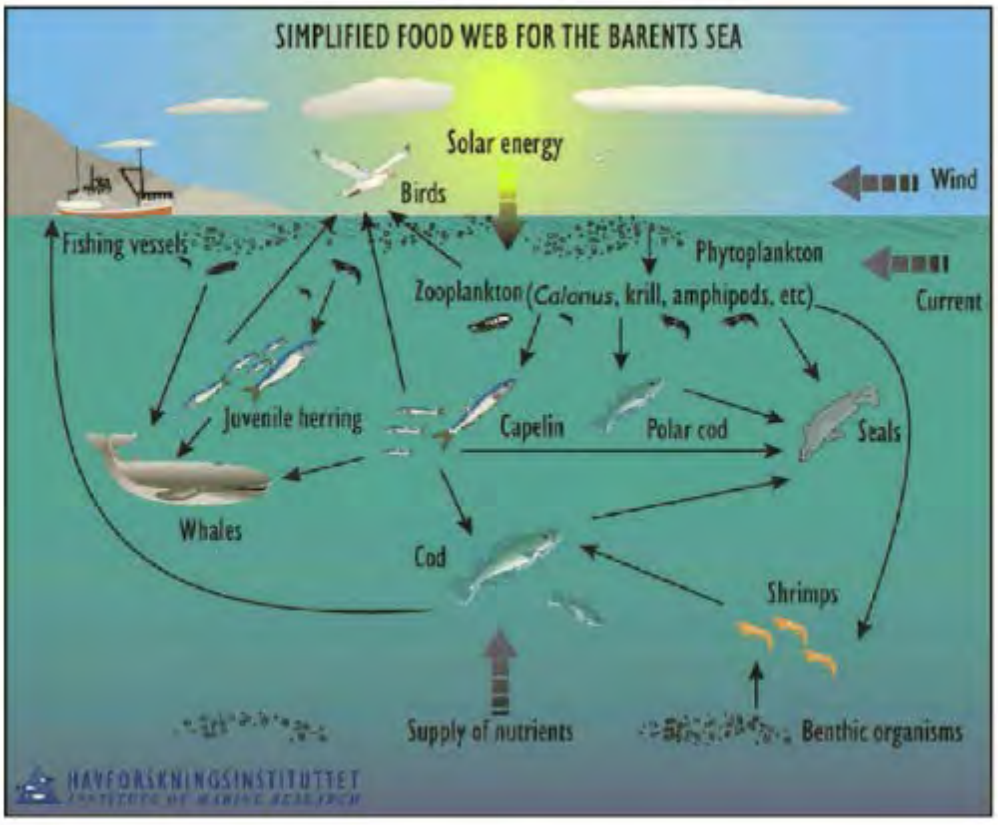

Contents

1 Summary

Since the 1980s, the Barents Sea has gone from a situation with high fishing pressure, cold conditions and low demersal fish stock levels, to the current situation with high levels of demersal fish stocks, reduced fishing pressure and warm conditions. The current situation is unprecedented, and the Barents Sea appears to be changing rapidly. The main points for 2017 are:

- The air and water temperatures remained higher than average and typical of warm years, yet lower than temperature in 2016. In autumn, the area covered by Atlantic waters (>3°C) was large than in 2016; areas covered by Arctic and cold bottom waters (<0°C) were small but larger than in 2016. Ice coverage was much lower than normal, but higher than in 2016; the lowest value (1%) was observed in September.
- Spatially integrated net primary production has increased over the years. A noteworthy increase is observed in the eastern regions where sea ice coverage has diminished over the years. An increase in ice-free areas, and length of the growing season, provide improved habitat for phytoplankton growth.
- Mesozooplankton biomass during autumn was higher than in autumn 2016 in the eastern Barents Sea and on the Central Bank, but lower on the Great Bank. Zooplankton biomasses in the Central Bank and Great Bank subareas have shown declining trends since the peak in 1995. An increasing trend in krill biomass has been observed during the last decades – and the level in 2017 was above the long-term average. Amphipods are still considered to be at a low level - although some large catches were made north and east of Svalbard. Jellyfish biomass was at third highest level since 1980.
- The capelin stock has recovered after a mini-collapse in 2015–2016, and the biomass of young herring is the highest since 2005. Polar cod and blue whiting biomass is low. Cod and haddock biomass have decreased in recent years following a peak around 2013, but is still above the long-term mean. The 2016 and 2017 year classes of haddock seem strong and could be of the same order of magnitude as the strong 2004–2006 year classes. *Sebastes mentella*, Greenland halibut and long rough dab biomass is stable at or above the long-term mean.
- Assessments of the benthos biomass in 2017 were very high but this most likely related with overestimation of the biomass due to the technical causes during the benthic monitoring like in 2012. The distribution area of the invasive snow crab was larger than in previous years, and for the first time recorded northeast of Svalbard. The shrimp, *Pandalus borealis*, population was within the long-term mean and stable.
- The summer abundance of minke whales in the Barents Sea is now about 50 000 animals and has been quite stable or increasing over the period. The sighting rate from the 2017 survey is the highest recorded which may confirm the apparent increasing trend at present. In 2017, 1518 individuals of nine species of marine mammals were observed during the BESS, August-October 2017 and an additional 46 individuals were not identified to species level.
- A large-scale monitoring of marine litter performed in the joint Norwegian–Russian ecosystem monitoring surveys in the period from 2010 to 2017.
- During the time-series, plastic dominated number of observations with marine litter, as 72% of surface observations, 94% of pelagic trawls, and 86% of bottom trawls contained plastic. In 2017, marine litter on the surface (floating) and taken by trawls dominated by plastic. Wood was registered in the

28.4% of stations, while textile, paper, rubber and metal was observed occasionally.

2 Temporal development

2.1 Subareas of the Barents Sea

The Barents Sea has been divided into 15 subareas or polygons (Figure 2.1.1). The division is based on topography and oceanography and is a modification (with some subdivision) of the system used by Eriksen *et al.* (2017) in a summary analysis of pelagic biomass. The four western areas, South-West, Bear Island Trough, Hopen Deep and Tor Iversen Bank, are areas covered mainly with Atlantic water and constitute the inflow region of Atlantic water with the splitting of the current branches east through the Kola Section (south of the Central Bank) and north in the Hopen Deep (west of the Central Bank).

A new time-series for the oceanographic conditions (temperature and salinity (1980–2017), mesozooplankton (1989–2017) and 0-group fish (six fish species, 1980–2017) were estimated based on new subareas for the Barents Sea. Description of data used, methods and results are presented as working document in Annex 4 in the WGIBAR Report 2018.

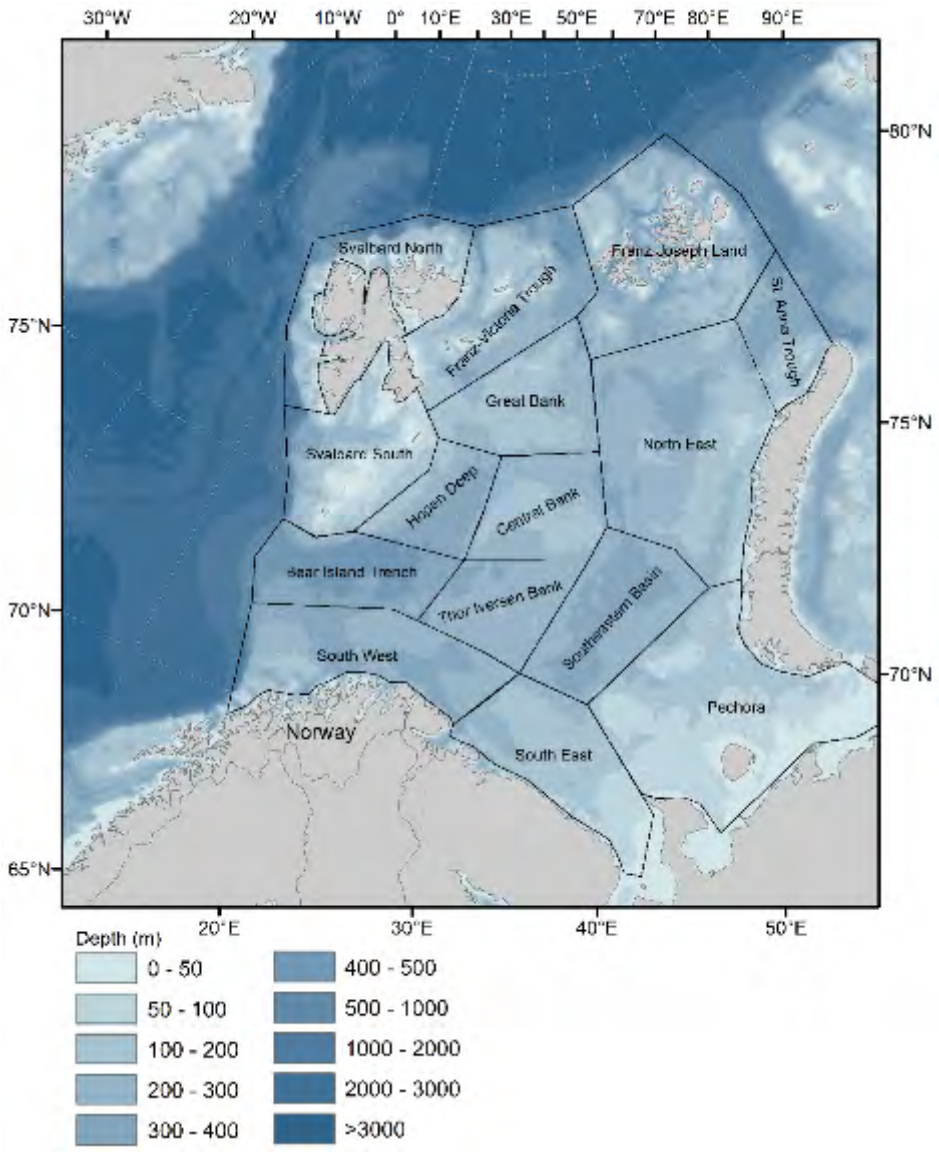

Figure 2.1.1. Map showing subdivision of the Barents Sea into 15 subareas (regions) used to calculate mean values and time-trends data from Barents Sea surveys.

2.2 Trend Analysis

Abiotic variables

Figure 2.2.1 clearly shows the warming of the Barents Sea during the period 1979–2017. Temperature related variables, such as temperature itself, the area occupied by Atlantic Water (T>3°C) and Mixed Water (0<T°C>3), and the ice area at minimum and maximum sea-ice extent all show a clear trend towards warmer conditions. The variables connected to the dynamics, i.e. the flow of Atlantic Water (e.g. BSO – the inflow of Atlantic Water to the Barents Sea) and the atmospheric forcing represented by the NAO does not show any clear trend. These results corroborate the findings that, while both the temperature and volume transport of the Atlantic Water into the Barents Sea contribute to the oceanic heat transport into the Barents Sea, they (temperature and volume transport) vary on different time-scales. While the volume transport fluctuates from year-to-year and even shorter time-scales, the temperature shows a clear signal of multidecadal variability, i.e. climate variability of addition to an underlying trend induced by climate change

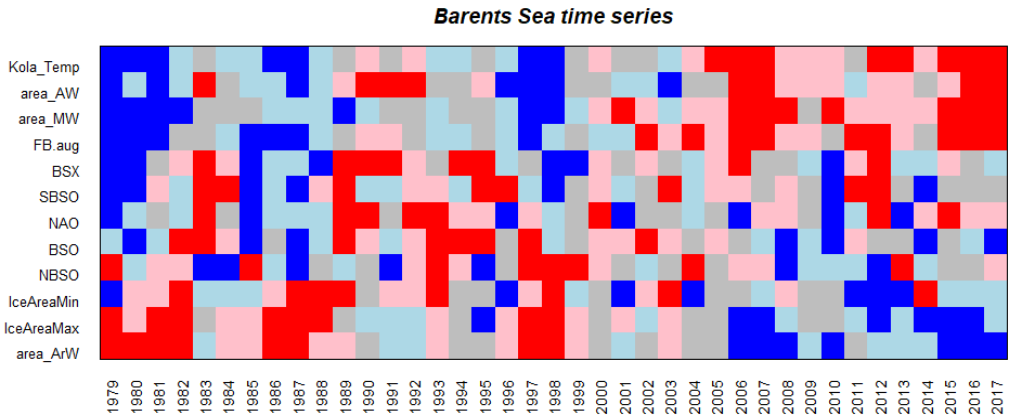

Figure 2.2.1. Time-series of annual means of abiotic variables in the Barents Sea sorted by trend. Blue means value below the 1979–2017 average and red means above the 1979–2017 average.

The eastern Barents Sea has experienced the largest warming trend over the last 47 years, with considerably less warming along the boundaries (Figure 2.2.2). There is, however, a slightly different geographical pattern at different depth intervals, with the warming trend being skewed towards the south with depth. Here, one should note that the upper-layer is more in contact with the atmosphere and, thus, governed by the air-sea fluxes, whereas the deepest depth interval, i.e. 100–200 m, is more strongly dictated by advection of Atlantic Water. Furthermore, there is considerable interannual variability superimposed onto the underlying, multidecadal trend.

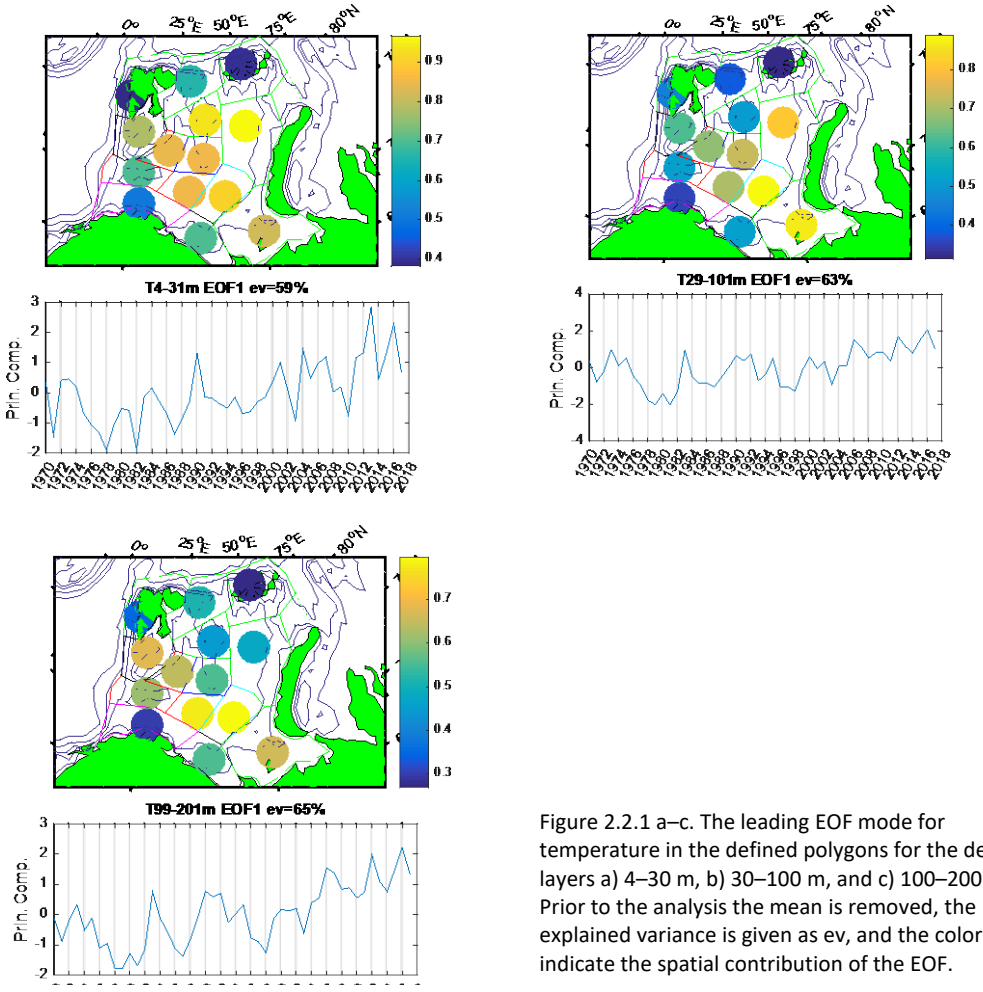

Figure 2.2.1 a–c. The leading EOF mode for temperature in the defined polygons for the depth layers a) 4–30 m, b) 30–100 m, and c) 100–200 m. Prior to the analysis the mean is removed, the explained variance is given as ev, and the colorbar indicate the spatial contribution of the EOF.

The largest trend in salinity is found along the boundary areas in the northeastern parts in the upper-layer (4–30 m), and in the northwestern parts in the below the mixed-layer depth, with only small trends being found in the interior parts of the Barents Sea (Figure 2.2.2). As opposed to temperature, there is not a strong overall trend in salinity over the 47-year period investigated. However, there is considerable interannual variability also in the average salinity.

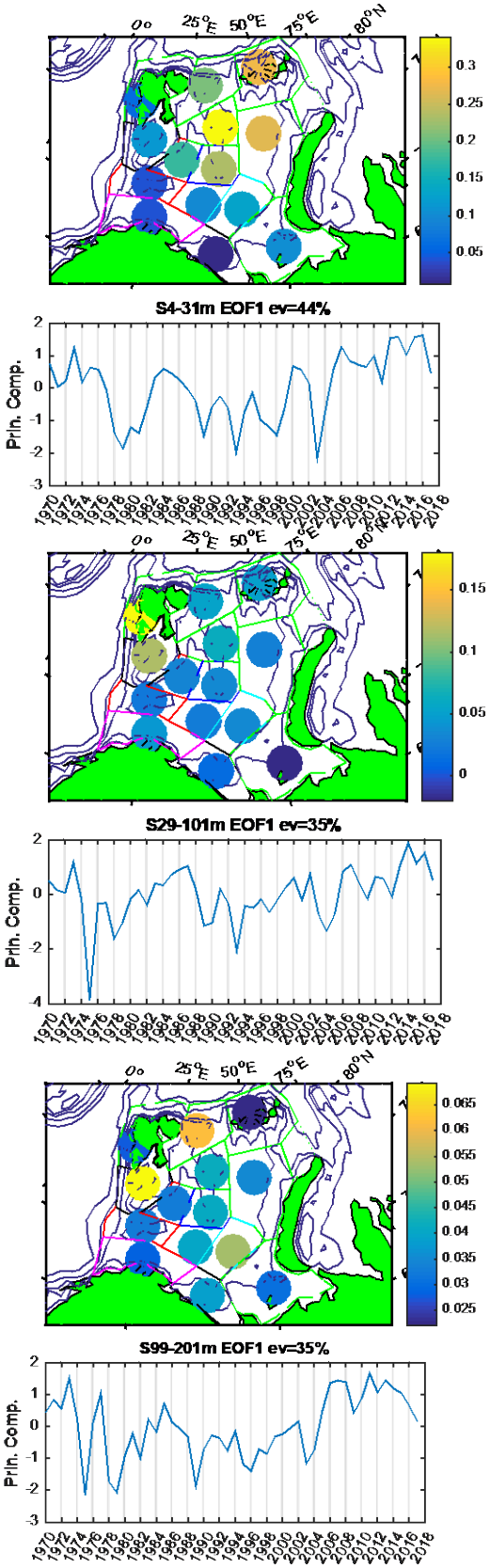

Figure 2.2.2 a–c. The leading EOF mode for salinity in the defined polygons for the depth layers a) 4–30 m, b) 30–100 m, and c) 100–200 m. Prior to the analysis the mean is removed, the explained variance is given as ev, and the colorbar indicate the spatial contribution of the EOF.

Overall, the temperature and salinity averaged over the whole Barents Sea and at different depth levels were lower in 2017 than in 2016, albeit above long-term average values (Figure 2.2.3), which is in line with the future expectations stated in last year's report.

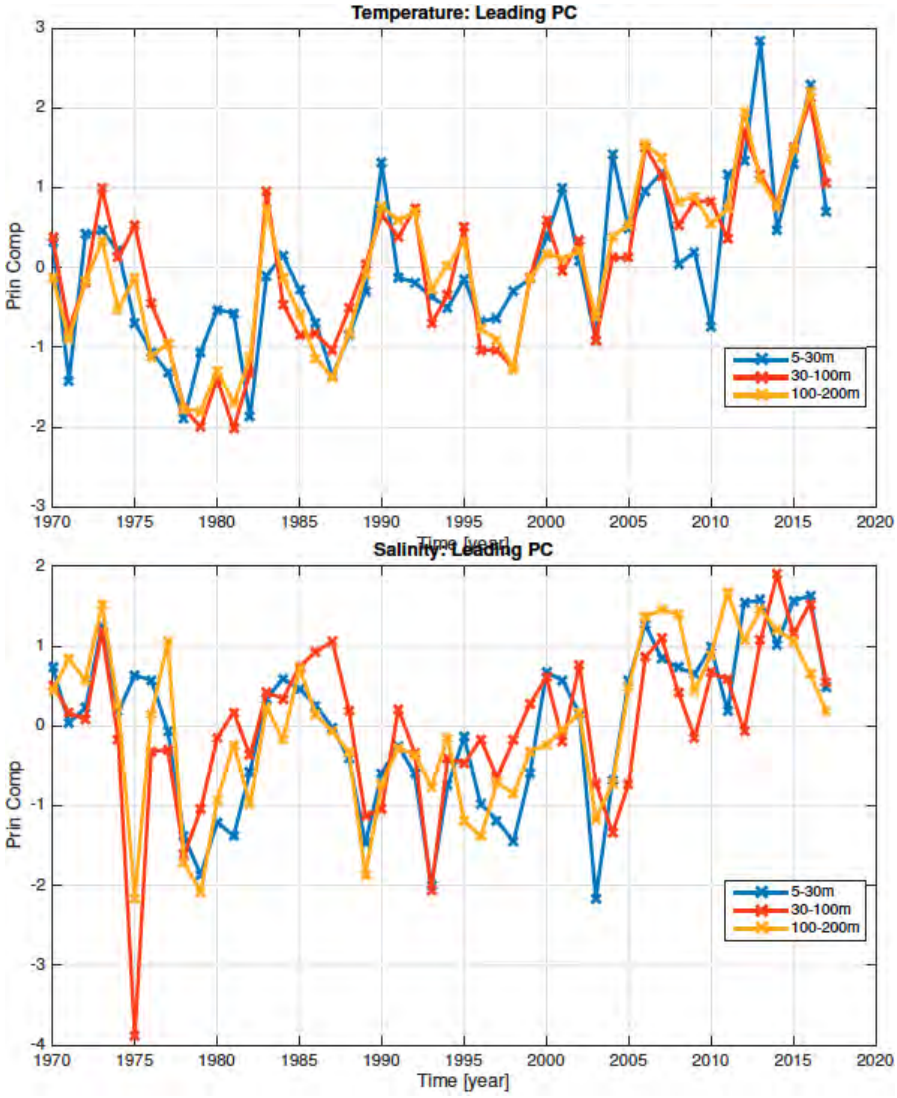

Figure 2.2.3. The leading EOF principal components for a) temperature and b) salinity. See fig caption 2 and 3 for details. The scale of the y-axis is in degC but should be multiplied with the spatial loading.

Zooplankton and 0-group fish

Figure 2.2.4 clearly shows increasing of macroplankton (krill and jellyfish) and capelin, cod and haddock recruitment during the period 1980–2017. However, plankton (M-medium size), and saithe recruitment does not show any clear trend. Polar cod, arctic species, and plankton Large and small size fraction showed opposite trend, there were at high level during 1990s, and decreased in recent decades.

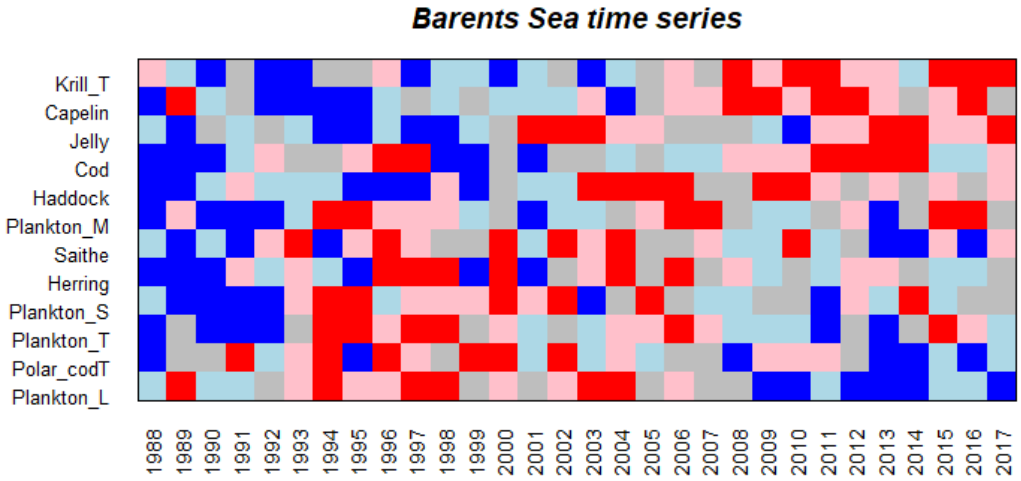

Figure 2.2.4. Time-series of zooplankton and 0-group fish amount in the Barents Sea sorted by trend. Blue means value below the 1980–2017 average and red means above the 1980–2017 average.

Fish variables

Figure 2.2.5 shows increasing trend of cod, haddock, Greenland halibut and lumpfish biomass during the period 1980–2017. Recruitment to the fisheries exploited stocks (age 3) for cod and haddock in addition to spawning stocks biomass does not show any clear trend. Decrease of haddock weight (age 5) since 2008 occurred most likely due to occurrence of very strong 2005 year class. Herring biomass decreased since 2007 due to strong 2004 year class moved to the Norwegian Sea and since that, no strong year classes occurred.

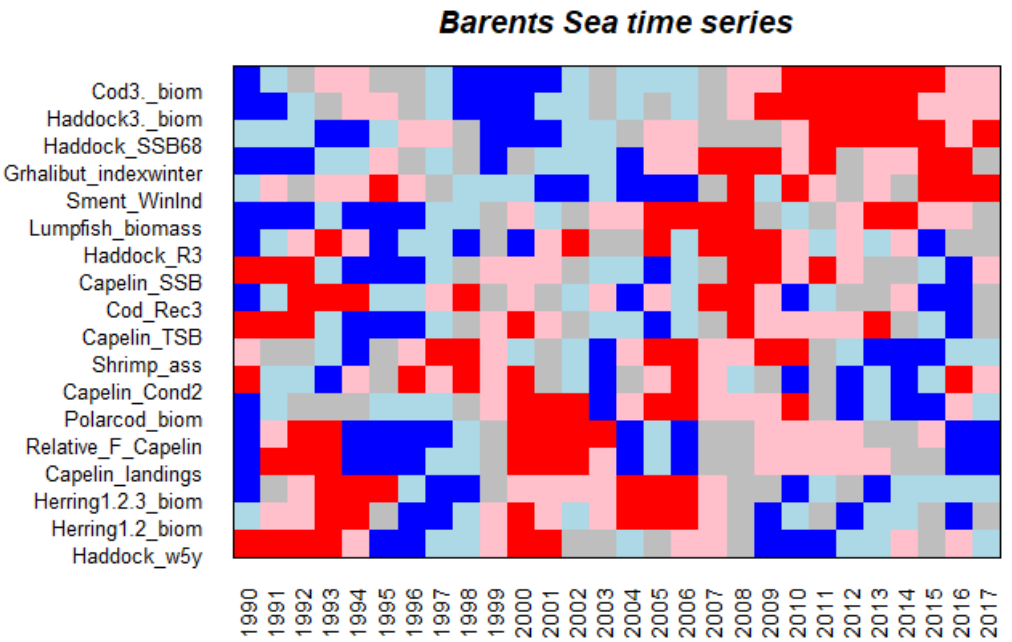

Figure 2.2.5. Time-series of fish biomass (both recruited at age 3, spawning and stock) and landings in the Barents Sea sorted by trend. Blue means value below the 1980–2017 average and red means above the 1980–2017 average.

3 Current state of the Barents Sea ecosystem components

3.1 Meteorological and oceanographic conditions

The Barents Sea is a shelf sea of the Arctic Ocean. Being a transition area between the North Atlantic and the Arctic Basin, it plays a key role in water exchange between them. Atlantic waters enter the Arctic Basin through the Barents Sea and the Fram Strait (Figure 3.1.1). Variations in volume flux, temperature and salinity of Atlantic waters affect hydrographic conditions in both the Barents Sea and the Arctic Ocean and are related to large-scale atmospheric pressure systems.

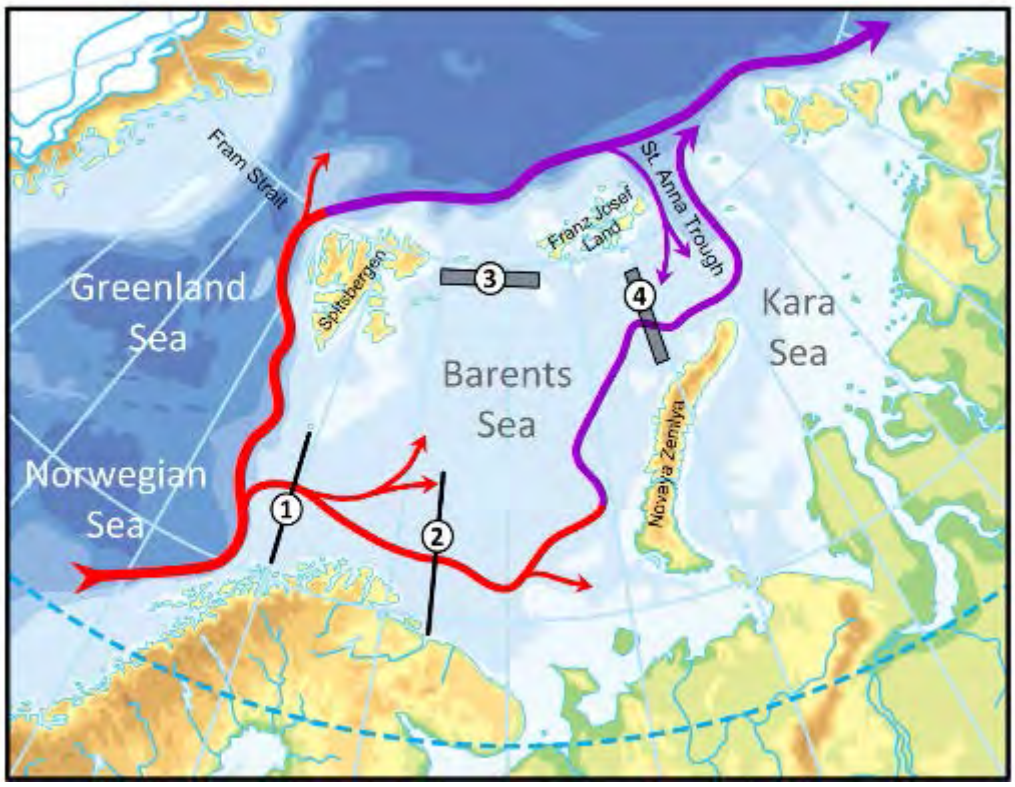

Figure 3.1.1. The main paths of Atlantic waters in the Barents Sea as well as Fugløya–Bear Island Section (1), Kola Section (2) and boxes in the northwestern (3) and northeastern (4) Barents Sea.

Air pressure, wind and air temperature

In 2017, winter (December–March) NAO index was 0.89 that was slightly less than in 2016 (1.00). Over the Barents Sea, westerly winds prevailed in January–March 2017 and easterly winds – during the rest of the year. The number of days with winds more than 15 m/s was larger than usual most of the year. It was close to normal only in April, July and October in the western part of the sea, in March, July and October in the central part and in July in the eastern part. In 2017, overall, the storm activity in the central and eastern Barents Sea was a record high since 1981.

Air temperature (http://nomad2.ncep.noaa.gov) averaged over the western (70–76°N, 15–35°E) and eastern (69–77°N, 35–55°E) Barents Sea showed that positive air temperature anomalies prevailed over the sea during most of 2017 (Figure 3.1.2). Higher positive anomalies (>5.0°C) were found in the eastern part in January, February, March and December. Significant negative anomalies (–1.7°C in the west and –1.2°C in the east) were only observed in May (see Figure 3.1.2).

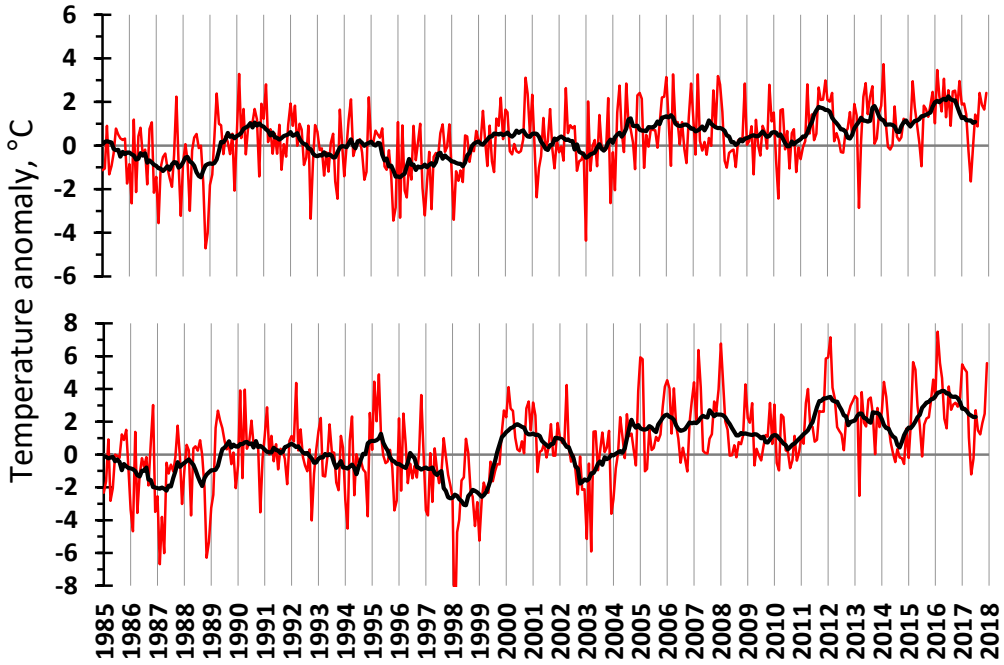

Figure 3.1.2. Air temperature anomalies in the western (upper) and eastern (lower) Barents Sea in 1985–2017. The red line shows monthly values, the black one – 11-month running means.

Ice conditions

Ice conditions in the Barents Sea in 2017 developed as in low-ice years. In January–March, the ice coverage (expressed as a percentage of the sea area) was 20–23% lower than normal (Figure 3.1.3). However, it was higher than in 2016 from February to the end of the year. The seasonal maximum of ice coverage was, as usual, in April, and it was 17% lower than normal. Ice melting started intensively only in June. In summer, the ice coverage was 6–15% lower than normal but 4–17% higher than in the previous year. In September, ice was only observed between islands of the Franz Josef Land Archipelago and east of the Spitsbergen Archipelago; the ice coverage was 1% that was 6% lower than normal. Freezing started in the northern Barents Sea in October (more intensively in the third decade); the monthly mean ice coverage was 6% that was 9% lower than normal but 4% higher than in the previous year. In November and December, the ice coverage was 18–23% lower than normal. Overall, the 2017 annual mean ice coverage of the Barents Sea was 15% lower than normal but 7% higher than in 2016.

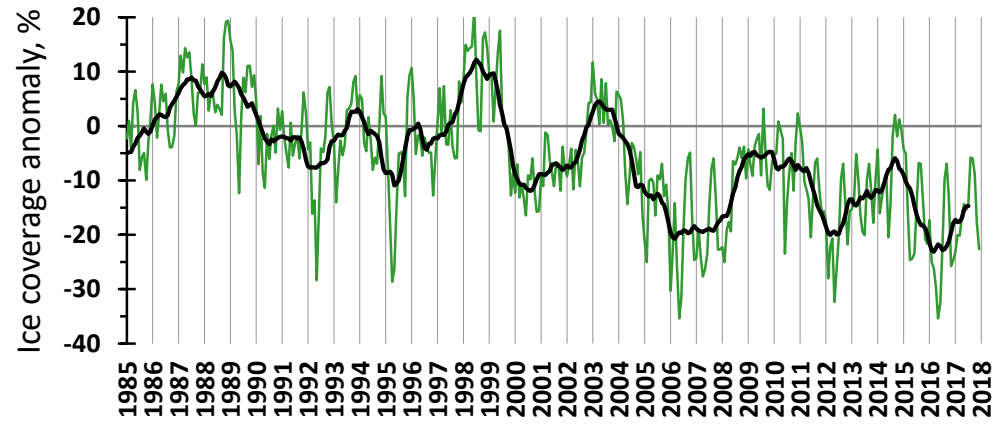

Figure 3.1.3. Ice coverage anomalies in the Barents Sea in 1985–2017. The green line shows monthly values, the black one – 11-month running means.

Currents and transports

The volume flux into the Barents Sea varies with periods of several years, and was significantly lower during 1997–2002 than during 2003–2006. In 2006, the volume flux was at a maximum during winter and very low during fall. After 2006, the inflow has been relatively low. Throughout 2016, other than during the winter months, the inflow of Atlantic Water was somewhat lower than the long-term average (Figure 3.1.4), whereas in early 2017 the inflow was close to or slightly above the long-term average. The dataseries currently stops in March 2017, thus no information about summer, fall and early winter 2017 is yet available.

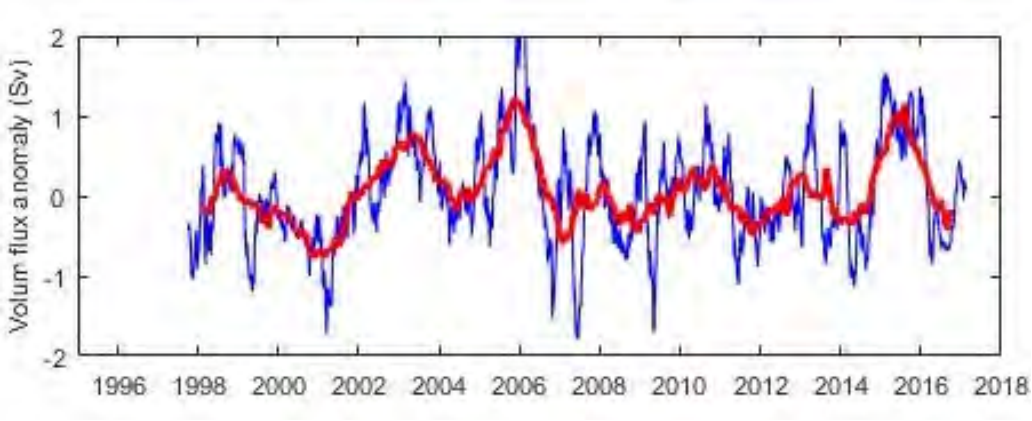

Figure 3.1.4. Volume flux anomalies through the Fugløya–Bear Island Section.

Complementing the observed volume flux, numerical modelling suggests that the volume flux into the Barents Sea through the BSO was below average throughout 2017, except for the months January and March (Figure 3.1.5). Indeed, during February and May-September the inflow through the BSO was about 1 Sv or more, translating to one standard deviation, or more, below the seasonal average. Similarly, the eastward flow through the BSX, i.e. into the norther Kara Sea, was below average during the same period, although to a lesser extent in summer (July-August). In June, however, the volume flux was 2 standard deviations below average in both BSO and BSX. In the SBSO, which feeds into the Kara Gate, volume flux was generally close to average, except for the months February, April, and September. The NBSO, i.e. the openings between Svalbard and Franz Josef Land providing a direct link between the Barents Sea and the Polar Basin, showed opposite behavior to the other three openings, with a generally neutral to positive (i.e. northward) anomaly in volume flux throughout 2017. However, June stands out with the positive anomaly exceeding 2 standard deviations.

Note that the model has been found to be accurate for annual mean and standard deviation of the volume transports, while modelled monthly averages are usually weakly, yet statistically significantly correlated with observations (Lien *et al.*, 2013, 2016).

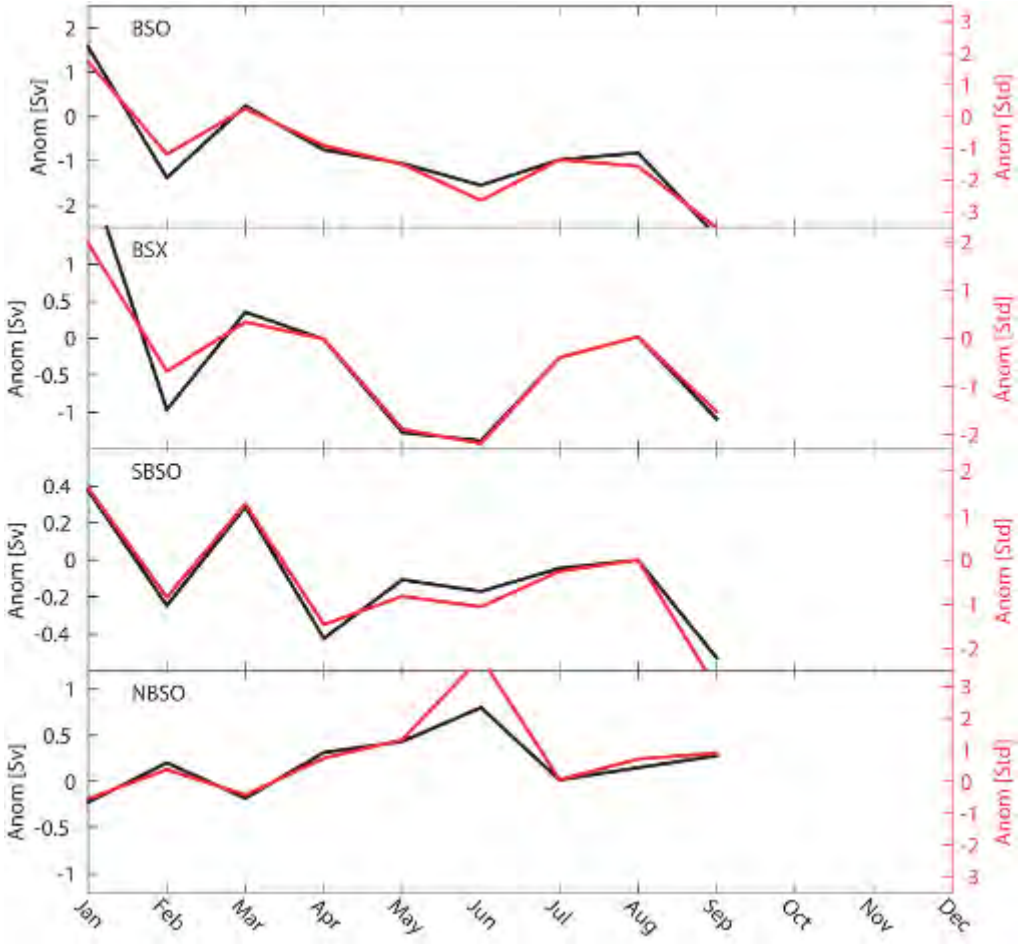

Figure 3.1.5. Modelled volume flux anomalies in 2017 relative to average and standard deviation during the period 1961–1990.

Temperature and salinity in standard sections and northern boundary regions

Fugløya–Bear Island Section covers the inflow of Atlantic and Coastal water masses from the Norwegian Sea to the Barents Sea, while the Kola Section covers the same waters in the southern Barents Sea. Note a difference in the calculation of the temperatures in these sections; in Fugløya–Bear Island Section temperature is averaged over the 50–200 m depth layer while in the Kola Section temperature is averaged from 0 to 200 m depth.

In 2017, the temperature of Atlantic Water flowing into the Barents Sea through Fugløya–Bear Island Section (50–200 m) was 0.7°C above the long-term average in March and October and 0.4°C above the long-term mean in summer and early autumn (Figure 3.1.6). On average, the 2017 temperature was slightly lower than that in 2016 (Figure 3.1.6).

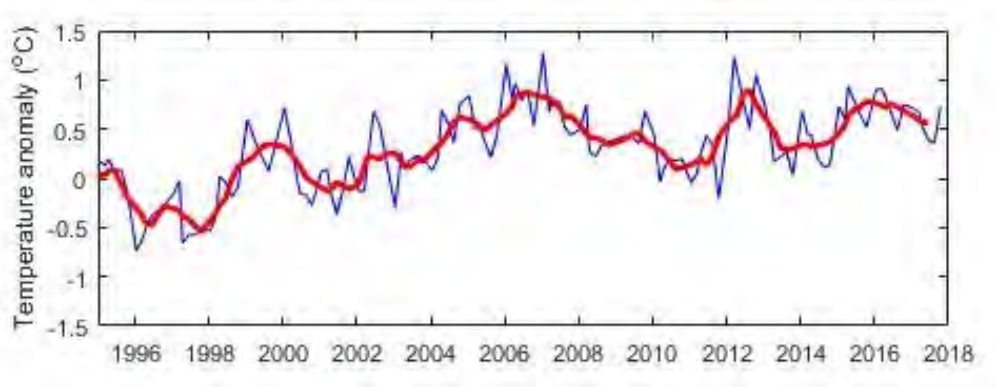

Figure 3.1.6. Temperature anomalies in the 50–200 m layer in the Fugløya–Bear Island Section.

Compared to the first half of 2016, when record high positive temperature anomalies (1.2–1.5°C) were observed in the Kola Section, in the second half of 2017 they decreased significantly (Figure 3.1.7). During most of the 2017 observation period, Atlantic waters in the 0–200 m layer were 0.8–0.9°C warmer than average. Temperature anomalies in coastal waters were decreasing from June (0.8°C) to October (0.2°C). Thus, by October, the temperature of the coastal water was close to average. In November–December, seasonal cooling rates of waters in the Kola Section were much lower than average (by 0.6°C per month). As a result, by December, positive temperature anomalies in the 0–200 m layer exceeded 1.0°C in all parts of the section this was typical of anomalously warm years (Figure 3.1.7).

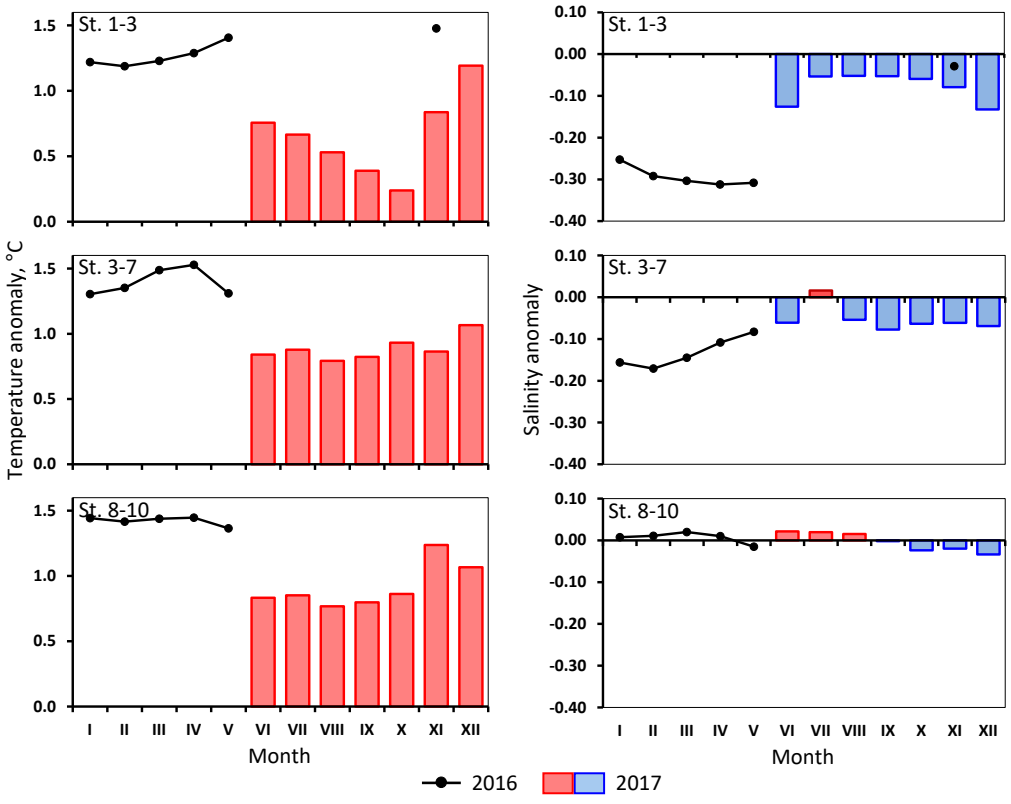

Figure 3.1.7. Monthly mean temperature (left) and salinity (right) anomalies in the 0–200 m layer in the Kola Section in 2016 and 2017. St. 1–3 – Coastal waters, St. 3–7 – Murmansk Current, St. 8–10 – Central branch of the North Cape Current.

In 2017, the salinity of the coastal and Atlantic waters (the Murmansk Current) in the Kola Section was 0.05–0.13 lower than normal (Figure 3.1.7). The salinity of Atlantic waters in outer part of the section (the Central branch of the North Cape Current) was close to average.

In the northern Barents Sea (NW) there was temperature decrease in 2017 compared with the two years preceding, with the temperature anomaly decreasing from 0.95°C in 2015 and 0.78°C in 2016 to 0.19°C in 2017. In the northeastern Barents Sea, the temperature increased, with a temperature anomaly of 1.08°C in 2017 compared with 0.70°C in 2015.

Spatial variation in temperature and salinity (surface, 100 m and bottom)

Sea surface temperature (SST) (http://iridl.ldeo.columbia.edu) averaged over the southwestern (71–74°N, 20–40°E) and southeastern (69–73°N, 42–55°E) Barents Sea showed positive anomalies prevailing in both areas during 2017 (Figure 3.1.8). In January–March, they exceeded 1.0°C and were the largest since 1981. In spring and early summer, anomalies decreased to 0.5°C in the southwest and to 0.3°C in the southeast. In July, they increased abruptly. In July and August, the anomalies in 2017 were observed in the southwestern part of the sea were the highest since 1981; the largest anomalies in 2017 were observed in the southeastern part. In autumn, positive anomalies were relatively high (0.7–1.5°C).

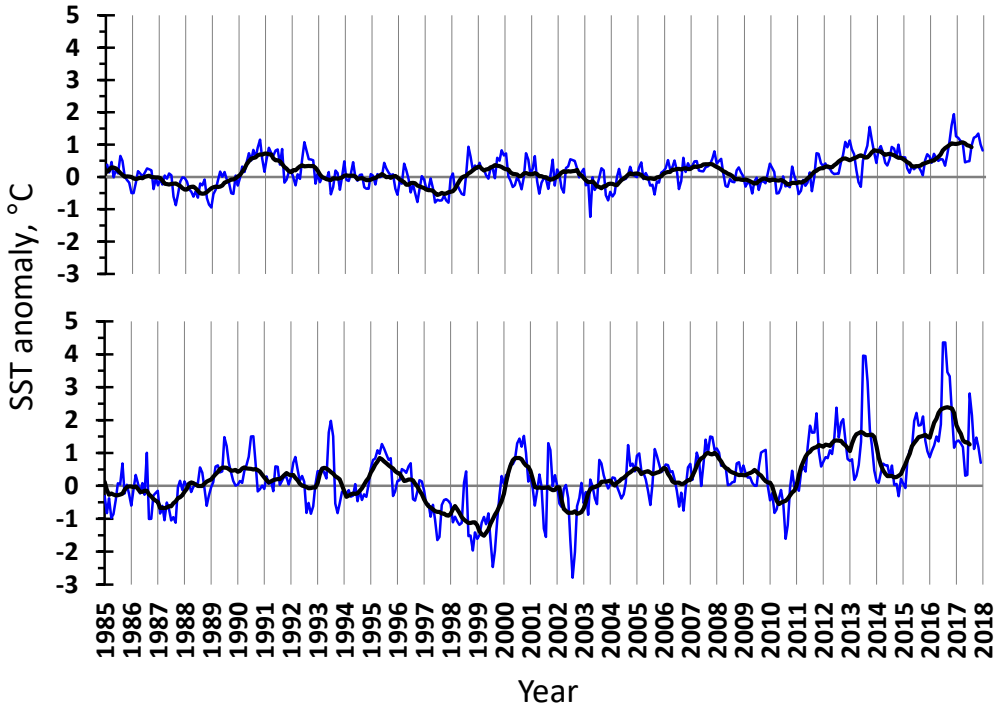

Figure 3.1.8. Sea surface temperature anomalies in the western (upper) and eastern (lower) Barents Sea in 1985–2017. The blue line shows monthly values, the black one – 11-month running means.

During August–October 2017, the joint Norwegian-Russian ecosystem survey was carried out in the Barents Sea. Surface temperature was on average 1.1°C higher than the long-term mean (1931–2010) in most of the Barents Sea (five sixths of the surveyed area) (Figure 3.1.9). The largest positive anomalies (>2.0°C) were observed west of Bear Island, west and south of Spitsbergen Archipelago and in the southeastern part of the sea. Negative anomalies were observed in the southwestern and northernmost Barents

Sea as well as north of Spitsbergen Archipelago. Compared to 2016, surface temperature was lower (by 1.0°C on average) in most of the Barents Sea (five sixths of the surveyed area), especially in the northern and eastern parts. Surface waters were on average 0.4°C warmer than in 2016 only in the western Barents Sea, especially in the areas where the largest positive anomalies were observed in 2017.

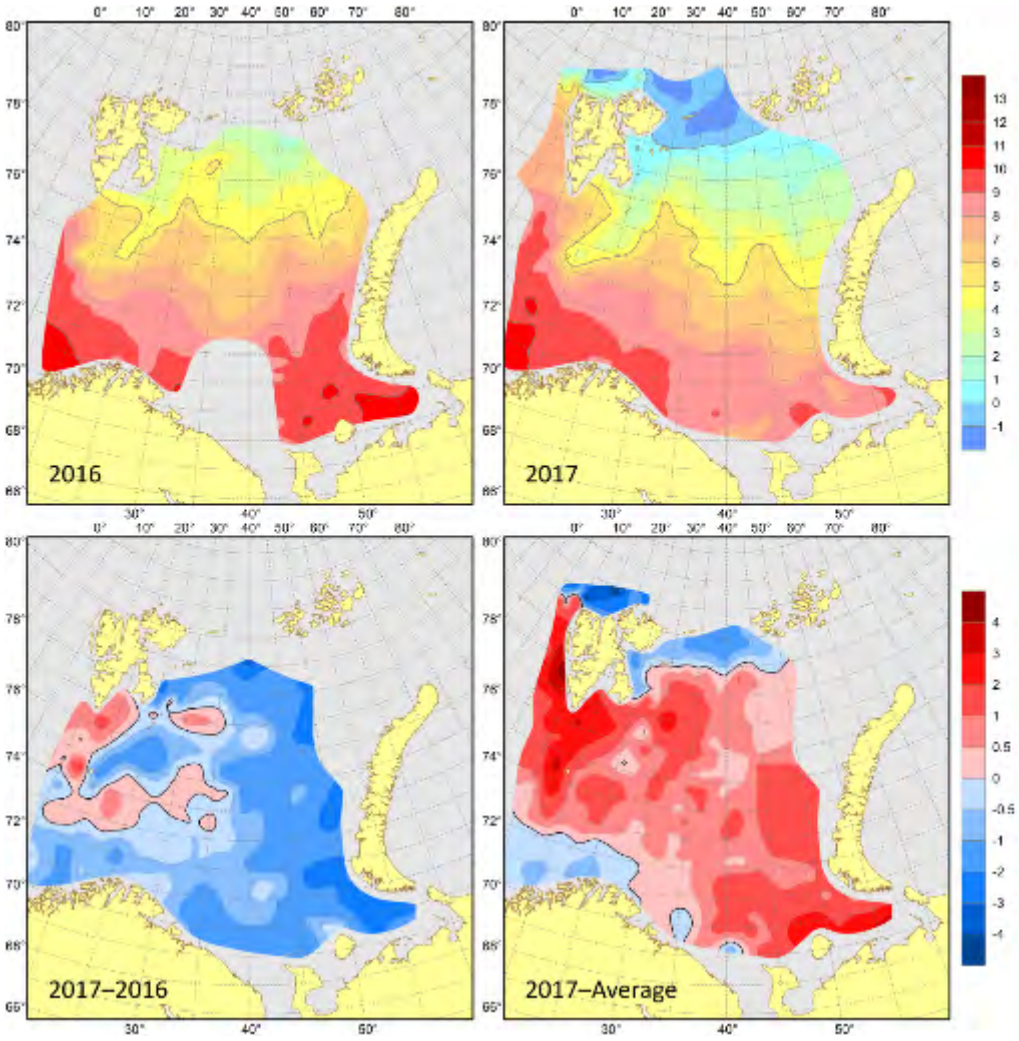

Figure 3.1.9. Surface temperatures (°C) in August–October 2016 (upper left) and 2017 (upper right), their differences between 2017 and 2016 (lower left, °C) and anomalies in August–October 2017 (lower right, °C).

As usual, Arctic waters were mainly found in the 50–100 m layer north of 77°N and dominated at 50 m depth. The temperatures at depths of 50 and 100 m were higher than the long-term mean (on average, by 1.0 and 0.8°C respectively) in most of the Barents Sea (Figure 3.1.10). Negative anomalies were mainly observed in the northern part of the sea and north of the Spitsbergen Archipelago. Compared to 2016, the 50 m temperature was lower (on average, by 1.1°C) in most of the sea (six sevenths of the surveyed area) and the 100m temperature was lower (on average, by 0.7°C) almost all over the Barents Sea. Positive differences in 50 m temperature between 2017 and 2016 took place only in some small areas located in the central and western Barents Sea.

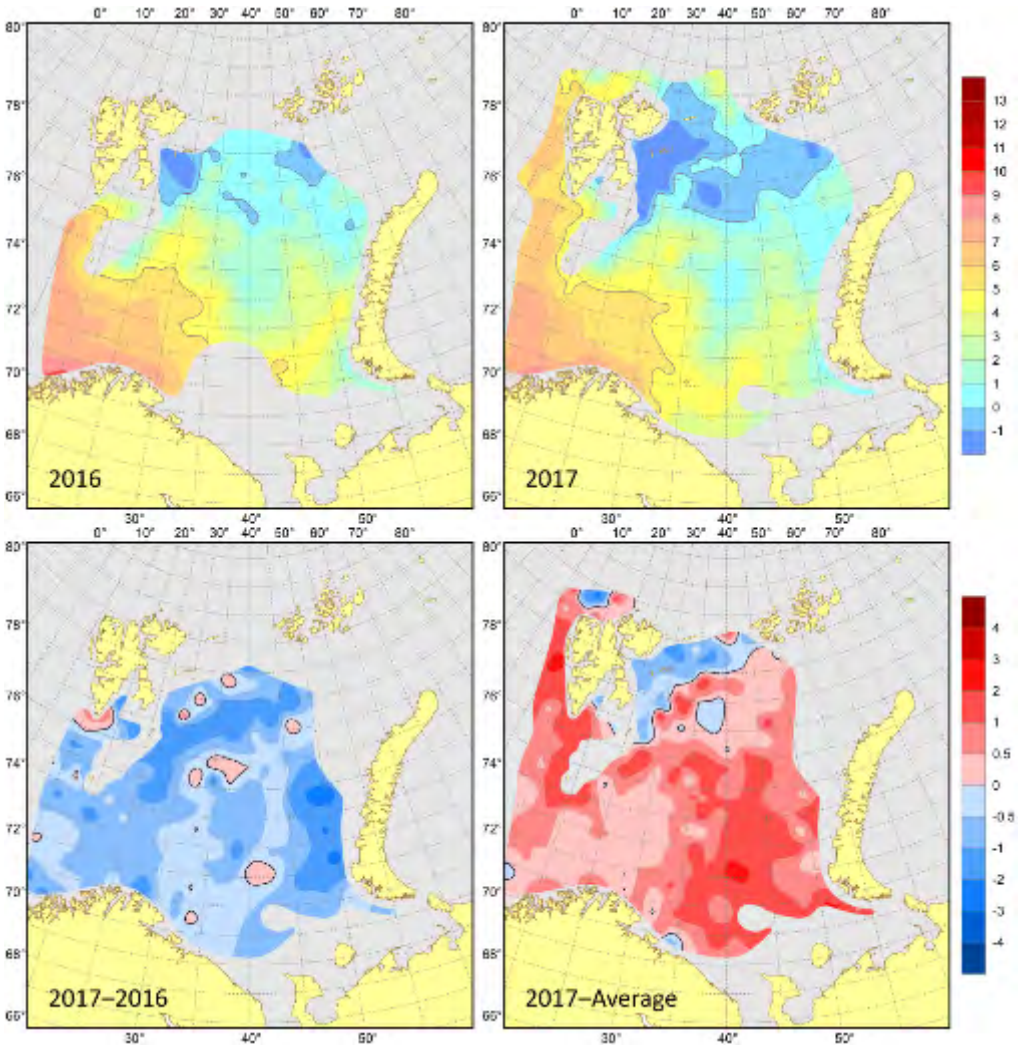

Figure 3.1.10. 100 m depth temperatures (°C) in August–October 2016 (upper left) and 2017 (upper right), their differences between 2017 and 2016 (lower left, °C) and anomalies in August–October 2017 (lower right, °C).

Bottom temperature was in general 1.1°C above average in most of the Barents Sea (Figure 3.1.11). Negative anomalies (–1.0°C on average) were only observed in the northern sea and north of Spitsbergen Archipelago. Compared to 2016, bottom temperature was on average 0.8°C lower in most of the Barents Sea. Bottom waters were slightly warmer (on average, by 0.2°C) than in 2016 only in the Eastern Basin and in a small area east of Great Bank. In August–October 2017, the area occupied by water with temperatures below zero was larger than in the previous year and it was mainly located east of Spitsbergen Archipelago. Lowest bottom temperatures (below –1°C) were observed between Great Bank and Spitsbergen Archipelago.

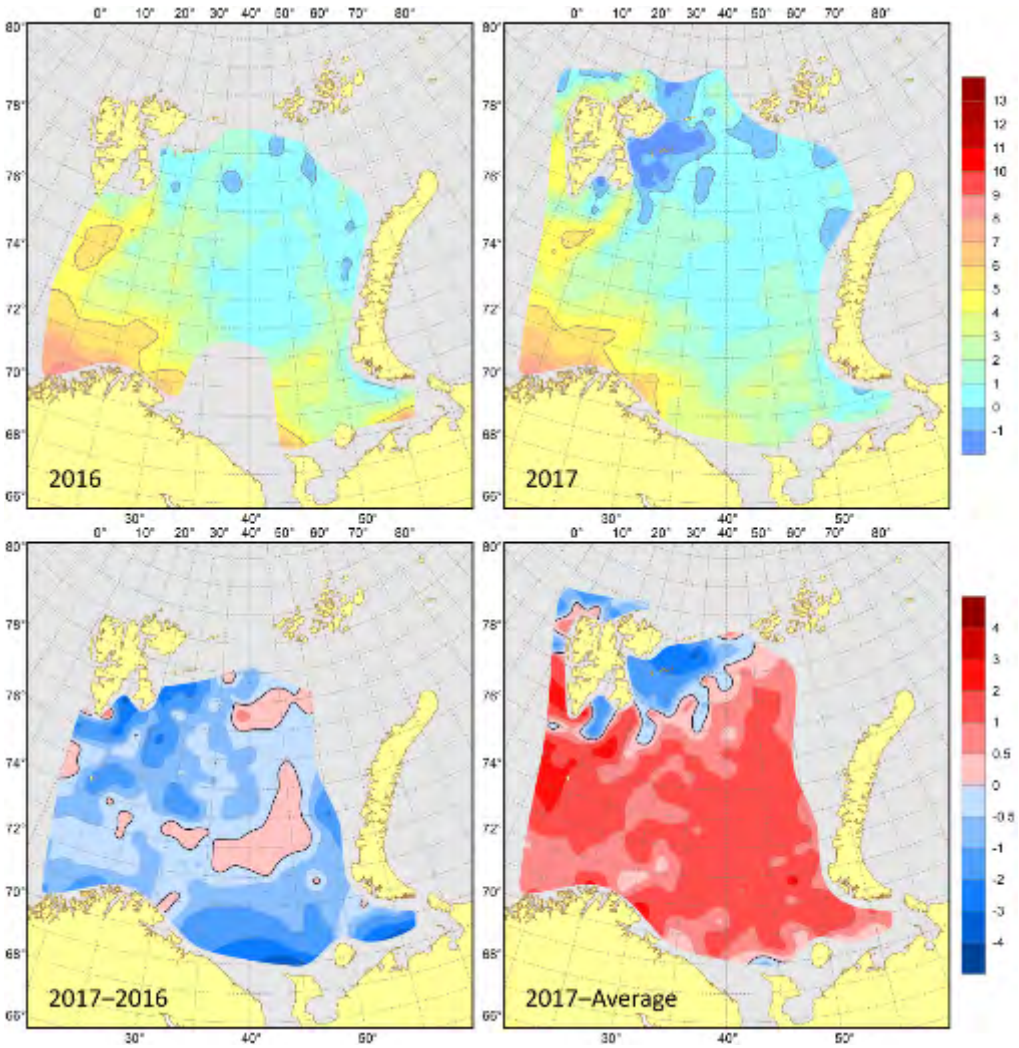

Figure 3.1.11. Bottom temperatures (°C) in August–October 2016 (upper left) and 2017 (upper right), their differences between 2017 and 2016 (lower left, °C) and anomalies in August–October 2017 (lower right, °C).

Surface salinity was on average 0.3 higher than the long-term mean (1931–2010) in most of the Barents Sea (two thirds of the surveyed area) with the largest positive anomalies (>0.8) west of Spitsbergen Archipelago as well as in the southeastern and northeastern sea (Figure 3.1.12). Negative anomalies (–0.3 on average) were mainly observed in southern and northern parts of the sea with largest values north of Kanin Peninsula and north of Spitsbergen Archipelago. In August–October 2017, surface waters were on average 0.3 fresher than in 2016 in 75% of the surveyed area with largest negative differences in the northern (North of 77°N) and southeastern (along Southern Island of the Novaya Zemlya Archipelago and north of Kanin Peninsula) parts of the Barents Sea. Small positive differences in salinity between 2017 and 2016 (0.1 on average) were observed in central and western parts of the sea as well as north of Kolguev Island.

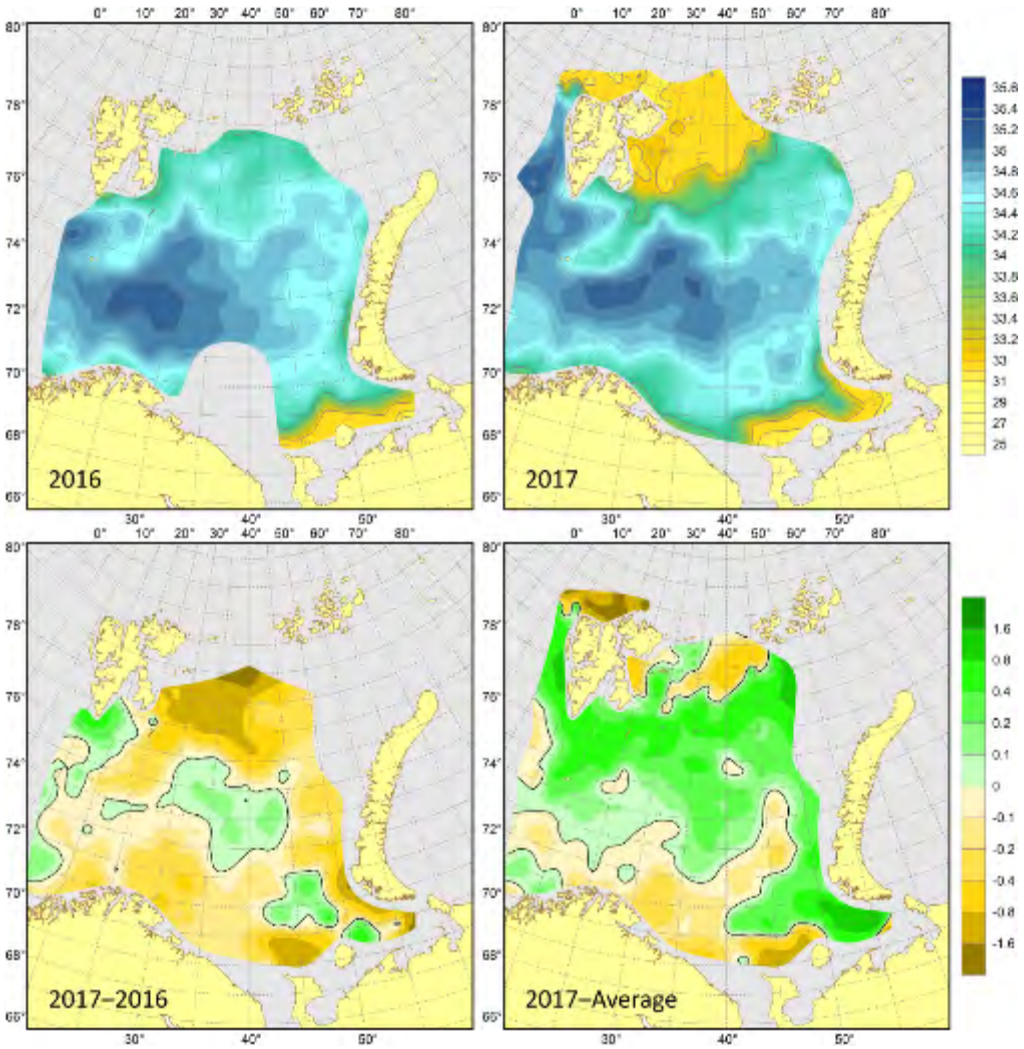

Figure 3.1.12. Surface salinities in August–October 2016 (upper left) and 2017 (upper right), their differences between 2017 and 2016 (lower left) and anomalies in August–October 2017 (lower right).

Salinity at 100 m was close to average in general (Figure 3.1.13). Small negative anomalies (on average –0.1) were mainly observed in the southern Barents Sea and north of Spitsbergen Archipelago. Small positive anomalies (on average 0.1) were found in the northwestern Barents Sea, especially east of Spitsbergen Archipelago. Compared to 2016, salinity at 100 m was lowest in most of the Barents Sea in 2017. The positive differences in salinity between 2017 and 2016 were mainly found in northwestern and southeastern parts of the sea, as well as in coastal waters in south-westernmost part of the surveyed area.

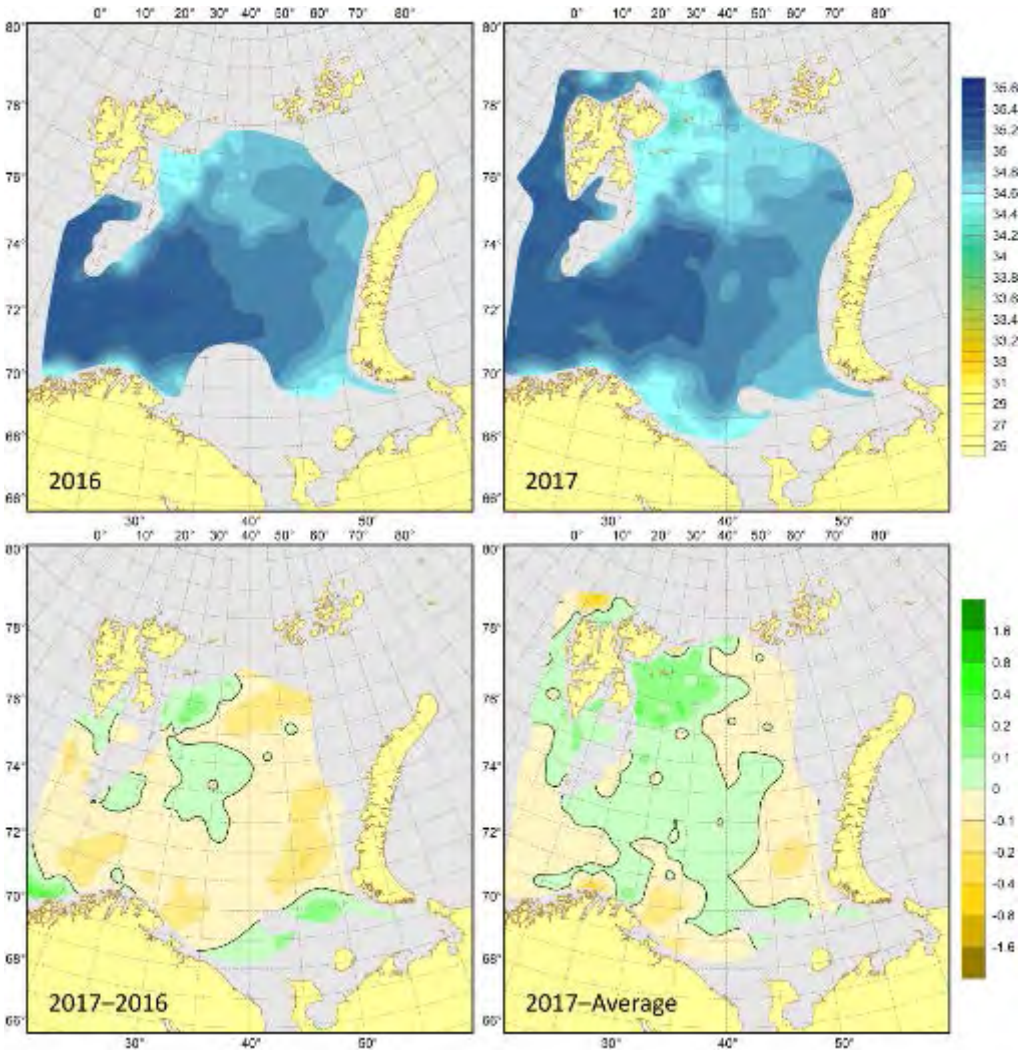

Figure 3.1.13. 100 m salinities in August–October 2016 (upper left) and 2017 (upper right), their differences between 2017 and 2016 (lower left) and anomalies in August–October 2017 (lower right).

Bottom salinity was close to both the average and that observed in 2016 in most of the Barents Sea (Figure 3.1.14). Significant anomalies were mainly found in shallow waters: negative – in southeasternmost Barents Sea and east of Spitsbergen Archipelago, positive – over Spitsbergen Bank and north of Kolguev Island.

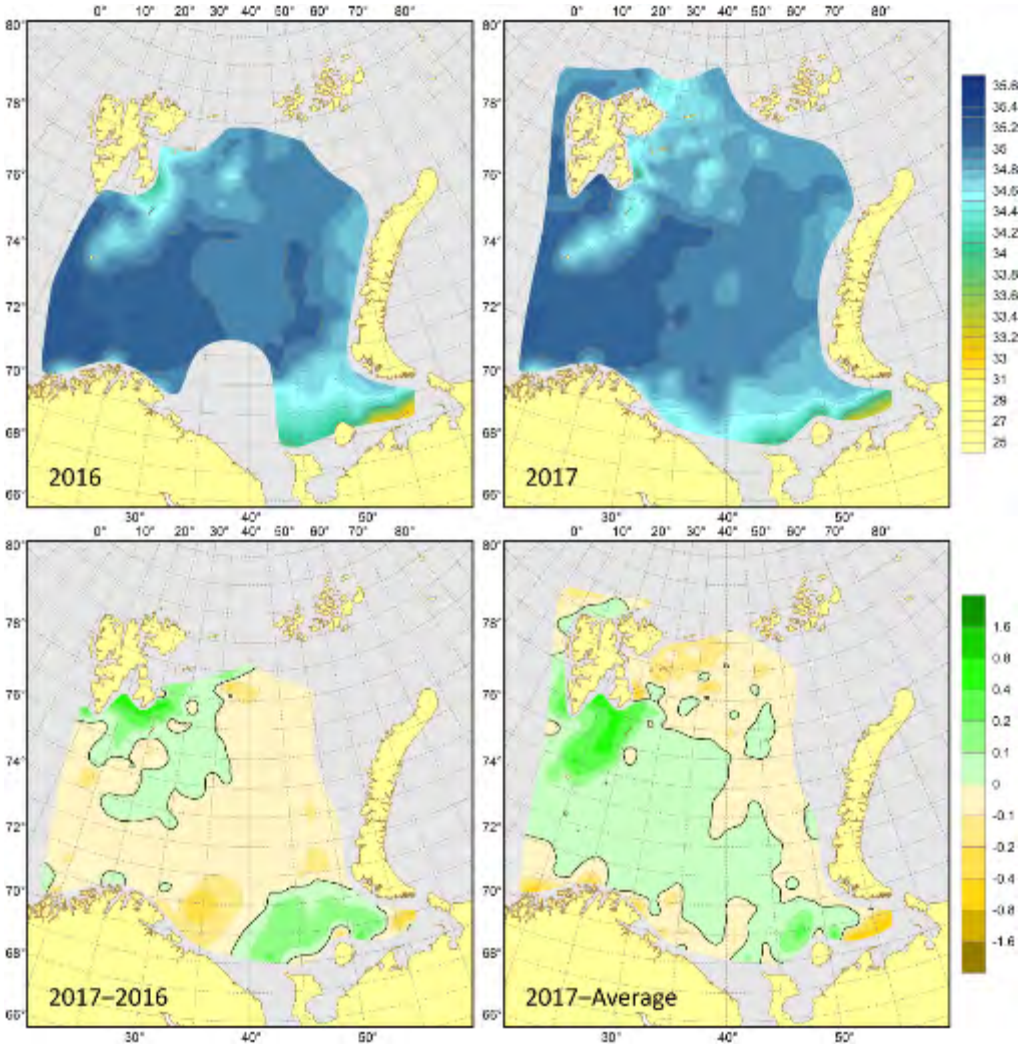

Figure 3.1.14. Bottom salinities in August–October 2016 (upper left) and 2017 (upper right), their differences between 2017 and 2016 (lower left) and anomalies in August–October 2017 (lower right).

Area of water masses

In August–October 2017, at 50, 100 m, and near the bottom, the area covered by warm water (above 4, 3, and 1°C respectively) was smaller (by 7, 11, and 10% respectively) than in 2016, when it was the record largest recorded (Figure 3.1.15). In contrast, the area covered by cold water (below 0°C) was larger (by 9, 10, and 4% respectively) in 2017 compared to 2016, when it was smallest on record (Figure 3.1.15). Since 2000, the area covered by cold bottom water was largest in 2003 and relatively small in 2007, 2008, 2012, 2016, and 2017. In 2016, the area covered by cold bottom water was the lowest since 1965 – the year when the joint autumn surveys started.

In recent decades, the area of Atlantic and mixed waters has increased, whereas that of Arctic waters has decreased (Figure 3.1.16). In August–October 2017, the area covered by Atlantic waters remained large, but decreased relative to 2016, when it was the largest since 1965. The area covered by Arctic waters was remained small in 2017, but increased relative to 2016, when it was the smallest since 1965.

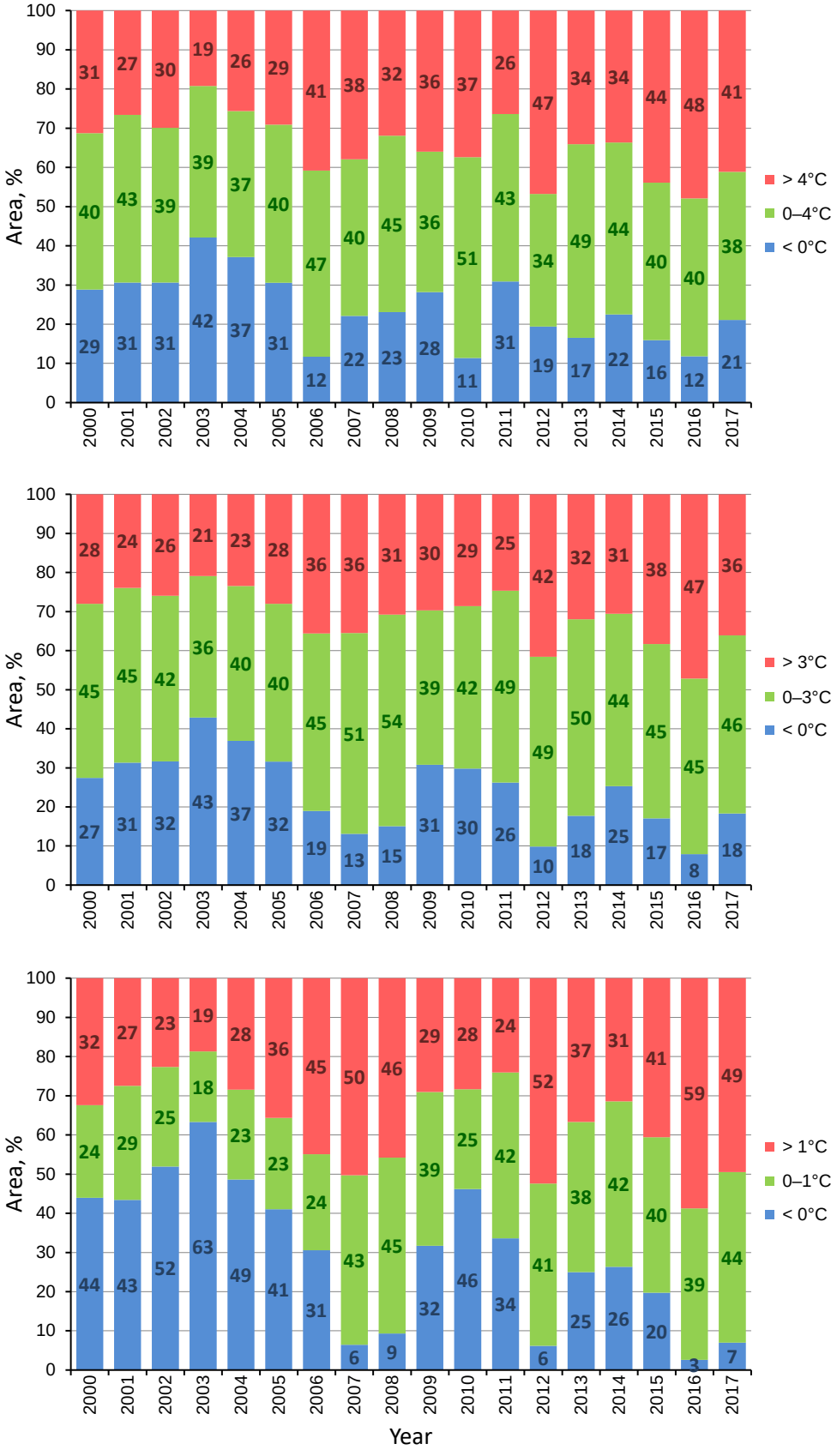

Figure 3.1.15. Areas covered by water with different temperatures at 50 m (upper panel), 100 m (middle panel) and near the bottom (lower panel) in the Barents Sea (71–79°N, 25–55°E) in August–September 2000–2017.

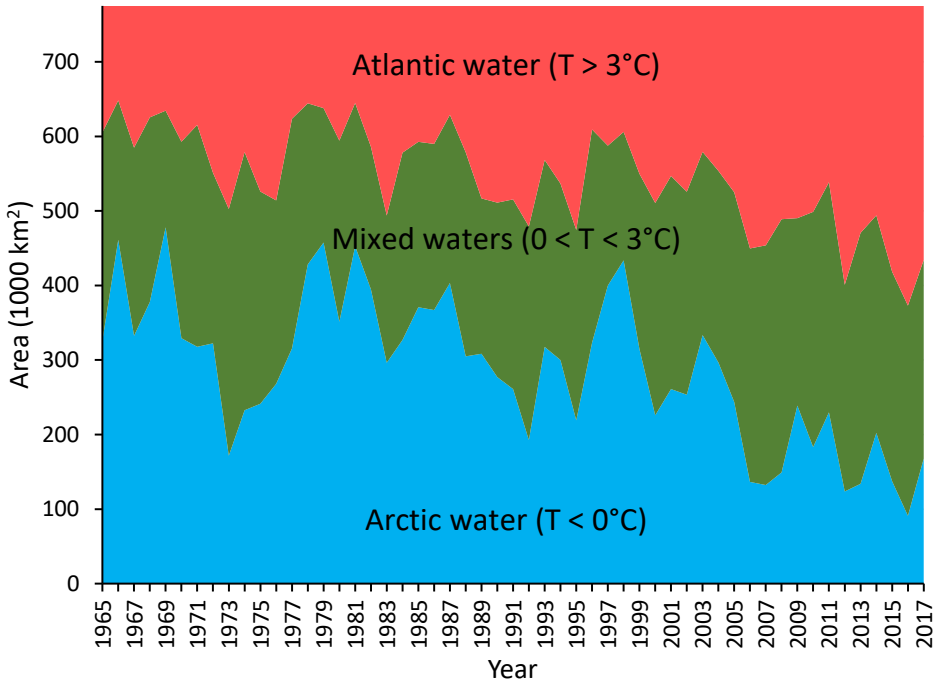

Figure 3.1.16. Area of water masses in the Barents Sea (71–79°N, 25–55°E) in August–September 1965–2017 (based on 50–100 m averaged temperature).

3.2 Phytoplankton and primary production

Phytoplankton development in the Barents Sea is typical for a high latitude region with pronounced maximum biomass and productivity during spring. During winter and early spring (January-March), both phytoplankton biomass and productivity are relatively low. Spring bloom is initiated during mid-April to mid-May and may vary strongly from year-to-year. Bloom duration is typically about 3-4 weeks and is followed by a reduction in phytoplankton biomass mainly due to nutrient exhaustion and grazing by zooplankton. Later in autumn when the increasing winds start to mix the upper layer and bring nutrients to the surface, a short autumn bloom can be observed. However, the timing of phytoplankton development can vary geographically. Spring bloom in the Atlantic water domain (without sea ice) is thermocline-driven; whereas in the Arctic domain (with seasonal sea ice), stability from ice-melt determines the bloom (Skjoldal and Rey 1989; Hunt *et al.*, 2012). Thus, spring bloom at the ice edge can sometimes take place earlier than in the southern regions of the Barents Sea due to early stratification from ice melting.

Phytoplankton samples from the 2017 BESS survey collected at of 10 m depth by CTD casts at 21 stations (Table 3.2.1), were analysed for taxonomy and abundance. In addition, water samples taken at 50 m depth at four of these stations were also analysed. All samples were fixed in Lugol's solution and analysed using the Utermöhl sedimentation method.

Dominant genera sampled were Cryptophyceae, Dinophyceae, Bacillariophyceae, and unidentified flagellates (Table 3.2.1). East of Svalbard, where satellite imaging suggested that chlorophyll-a concentrations relatively low (not shown), unidentified flagellate species tended to dominate. It should be noted that these waters were sampled later than waters to the south; this, may account for observed the taxonomic differences.

Table 3.2.1Summary of the cell abundances for the main phytoplankton genera and ciliates (x 1000 cell l-1) identified.

				10 metre sample cell concentrations (×1000 cell l^{-1})								
Station	lat.	long.	dd-mm-yy	U.flag	Monader	Cryptophyceae	Dinophyta	Diatom	Dictyophyceae	Haptophyta	Phaeocystis	Ciliate
371	70.2348	18.4422	22-08-17	47.5	0.0	52.9	8.5	198.2	0.0	0.0	0.0	20.0
378	71.1683	25.1083	25-08-17	18.4	0.0	9.7	7.2	159.5	0.0	0.0	0.0	2.5
400	72.3162	24.7593	31-08-17	81.0	0.0	224.6	146.7	186.5	0.0	0.0	0.0	1.6
415	72.4922	16.7937	04-09-17	116.6	0.0	543.2	6.4	93.6	0.0	0.0	0.0	7.9
425	74.1758	15.3028	07-09-17	278.6	0.0	179.3	9.7	15.8	0.0	0.0	0.0	1.0
427	74.5030	18.4957	08-09-17	15.7	0.0	0.0	0.6	5.0	0.0	0.0	0.0	0.2
444	76.3935	12.6855	10-09-17	216.0	0.0	104.8	5.2	110.4	15.2	15.1	0.0	2.6
456	77.0162	35.4797	17-09-17	17.8	0.0	36.7	2.8	12.1	6.6	4.0	0.0	0.1
462	76.9575	23.7290	18-09-17	10.8	0.0	108.0	26.6	98.1	0.4	0.0	0.0	2.6
470	77.6350	30.2868	20-09-17	23.8	0.0	2.2	0.7	73.6	0.0	0.0	0.0	0.8
495	78.5237	30.2805	25-09-17	0.0	145.8	3.2	0.4	0.2	0.0	0.0	0.0	0.5
504	78.7013	24.2017	27-09-17	33.5	0.0	0.0	0.4	4.3	2.6	2.5	0.0	0.3
513	80.4965	33.9960	29-09-17	1.1	0.0	0.3	0.4	0.0	0.0	0.0	0.0	0.2
519	78.7535	34.0123	29-09-17	70.2	0.0	2.2	0.1	0.2	0.0	0.0	0.0	0.4
521	77.9995	34.0027	30-09-17	37.8	0.0	6.5	0.9	127.4	0.0	0.0	0.0	1.2
524	76.5008	31.2180	30-09-17	37.8	0.0	3.2	1.4	0.9	0.9	0.8	0.0	0.6
526	75.4977	31.2188	01-10-17	141.5	0.0	4.3	0.3	0.2	0.0	0.0	0.0	0.3
529	74.2540	31.2175	01-10-17	0.0	123.1	0.0	1.6	7.7	0.0	0.0	0.0	0.8
533	73.2513	31.2207	01-10-17	104.8	0.0	9.7	0.9	8.5	0.0	0.0	0.0	0.5
540	71.5033	31.2200	02-10-17	204.1	0.0	37.8	6.3	3.1	0.0	0.0	0.0	0.6
543	70.7507	31.2158	02-10-17	34.6	0.0	14.0	10.6	5.0	0.4	0.0	0.0	0.5
				10 metre sample cell concentrations (×1000 cell l^{-1})								
Station	lat.	long.	dd-mm-yy	U.flag	Monader	Cryptophyceae	Dinophyta	Diatom	Dictyophyceae	Haptophyta	Phaeocystis	Ciliate
533	73.2513	31.2207	01-10-17	49.7	0.0	0.0	0.1	4.2	0.0	0.0	0.0	0.4
526	75.4977	31.2188	01-10-17	71.3	0.0	7.6	1.0	0.0	2.3	2.2	0.0	0.2
470	77.6350	30.2868	20-09-17	55.1	0.0	4.3	0.2	2.4	0.0	0.0	0.0	0.4
513	80.4965	33.9960	29-09-17	141.5	0.0	2.2	0.1	0.2	0.0	0.0	0.0	0.2

Nutrient and chlorophyll samples were collected from various depths at roughly 170 CTD stations. The nutrient samples (20 ml) were preserved with chloroform (200 µl), and kept at about 4°C until chemical analysis was conducted on shore at IMR. Chlorophyll-samples were collected by filtering 263 ml of seawater through glassfibre filters, which were frozen at about -18°C followed by extraction of pigments in acetone with subsequent fluorometric analysis at the IMR laboratory. All samples are currently being analysed to determine concentrations of nitrate, nitrite, silicate, and phosphate, along with chlorophyll and phaeopigments.

Satellite data

Daily Net Primary Production (NPP) and Open Water Area (OWA) were calculated from satellite data as described in detail in Arrigo and Van Dijken (2015). Satellite-derived surface Chl *a* (Sat Chl *a*, Level 3, 8 days binned) was based on SeaWiFS & MODIS/Aqua sensors; SeaWiFS was used from 1998–2002, and MODIS/Aqua from 2003–2017. Data were updated using NASA's latest reprocessing - version R2018.0. Note that results presented in the 2018 WGIBAR Report (Annex 4) are updated in the current report. This work was done in collaboration with Professor Kevin Arrigo and Gert van Dijken from Stanford University, USA.

Validation of satellite data

The Barents Sea model from Arrigo *et al.* (2008) gives reasonable results that compare well with at sea field measurements. Some previous work done to validate of satellite chl data using *in situ* data showed significant correlation between the two variables (Dalpadado *et al.*, 2014; 2018 WGIBAR Report (Annex 4)). New production (NP) estimates using nitrogen consumption (seasonal draw-down of nitrate in the water column) for the Fugløya-Bjørnøya (FB) and Vardø-Nord (VN) sections from March to June were comparable to satellite NPP values (Rey *et al.*, in prep).

Exploring spatial data– Polygon division

When exploring spatial data, Barents Sea was divided into 15 polygons (Figure 2.2.1). See 2018 WGIBAR Report (Annex 4) working document on zooplankton for more details. Chl *a* (mg m-3), Mean Production (g C m-2 day-1), Integrated NPP (Tg C day-1),

Open Water Area (km2), and Sea surface temperature (SST-degree Celsius) were calculated for each of the polygons on a yearly basis. Values for the South East and Pechora polygons were recalculated excluding regions most influenced by river inflow.

Sea Surface Temperature (SST)

There was an increasing trend in the mean SST in the Barents Sea during 1998–2017 (Figure 3.2.1). As expected, the surface temperature was highest in the regions influenced by the warm Atlantic Current (South West, Bear Island Trench, Thor Iversen Bank and South East). The northern most polygons (St. Anna Trough, Franz Joseph Land), influenced by the Arctic waters had the lowest SST. Polygons in the east such as the Pechora and Southeastern Basin showed a sharp increase in SST during the study period.

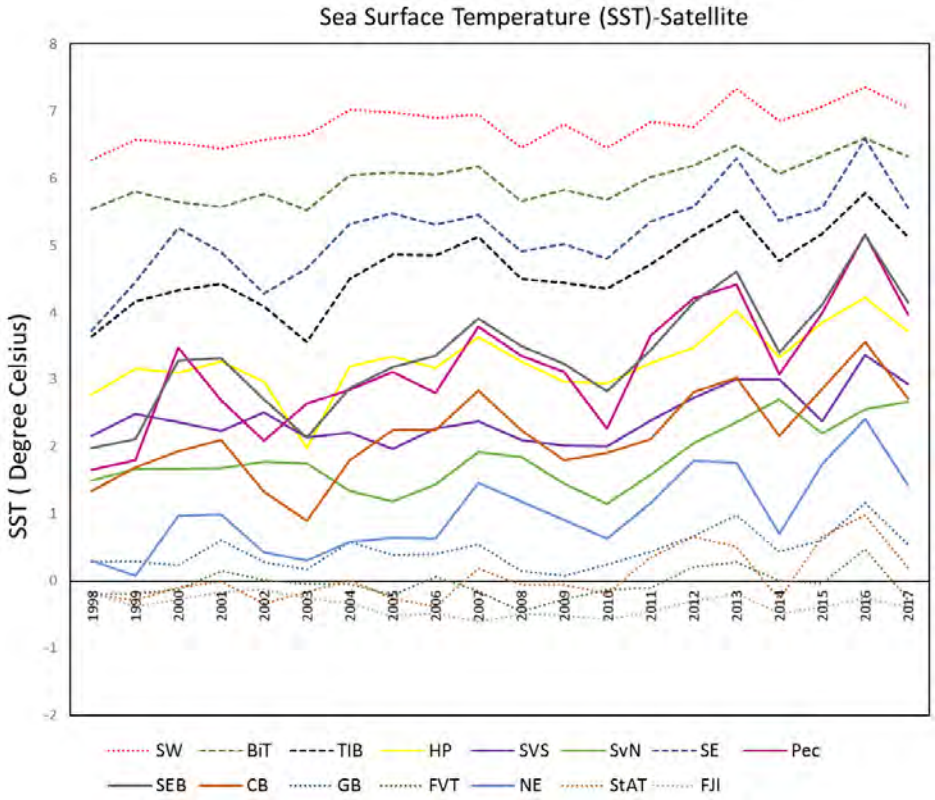

Figure 3.2.1. Interannual variability of Sea Surface Temperature for the different polygons. South West (SW), Bear Island Trench (BIT), Thor Iversen Bank (TIB), Hopen Deep (HP), Svalbard South (SvS), Svalbard North (SvN), South East (SE), Pechora (Pec), Southeastern Basin (SEB), Central Bank (CB), Great Bank (GB), Franz-Victoria Trough (FVT), North East (NE), St. Anna Trough (StAT), Franz Joseph Land (FJI)

Spatial distribution patterns of Chlorophyll a

As remote sensing data provide good spatial and temporal coverage, we use these data to explore interannual variability of chlorophyll spatial distributions. Satellite data from the Barents Sea during 1998–2017 showed that there is large year-to-year variability and that the highest chlorophyll concentrations in general are observed in May (not shown). Comparison of Chlorophyll *a* distribution patterns from a cold year (1998) and a warm year (2016) with less ice, shows the north- and eastward expansion of distribution with earlier blooming and higher concentrations in eastern regions (Figure 3.2.2).

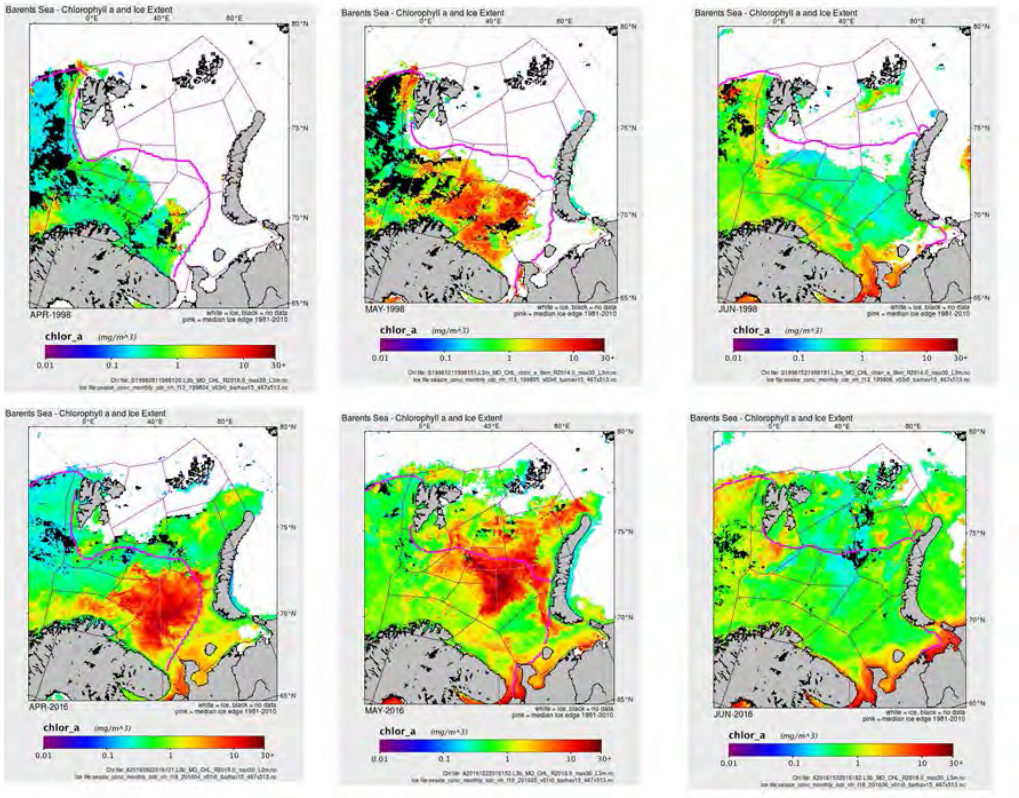

Figure 3.2.2. Spatial distribution patterns of Chlorophyll *a* for 1998 (cold year; upper panels) vs. 2016 (warm year; lower panels) for April, May, and June. White areas are ice covered. The pink lines show the climatological (1981–2010) position of the ice edge.

Seasonal dynamics of Chl *a* concentration

We have explored seasonal dynamics of Chl *a* concentration per polygon during the years 1998–2017. Seasonal development of phytoplankton in the Barents Sea is typical for a high latitude region with a marked spring bloom. There is a large interannual variability of magnitude of the spring bloom over time (not shown). From March to June phytoplankton production in the Barents Sea is mostly based on winter nitrate. The autumn bloom is generally characterized with a smaller peak occurring around August/September, coinciding with autumn replenishment of nitrate due to deepening of the upper mixed layer. Chlorophyll *a* decreases gradually towards November, returning to very low-level winter conditions.

Examples of seasonal dynamics of Chl concentrations in two polygons from southern Barents Sea are shown in Figures. 3.2.3 and 3.2.4. Spring bloom Chl *a* concentration was higher and occurred somewhat earlier during the recent warm year (2016) than in colder years, such as 1998. During 2017, spring bloom was not apparent as a peak in either of the two regions, with much lower spring Chl concentrations than in 2016 and also lower than the long-term mean.

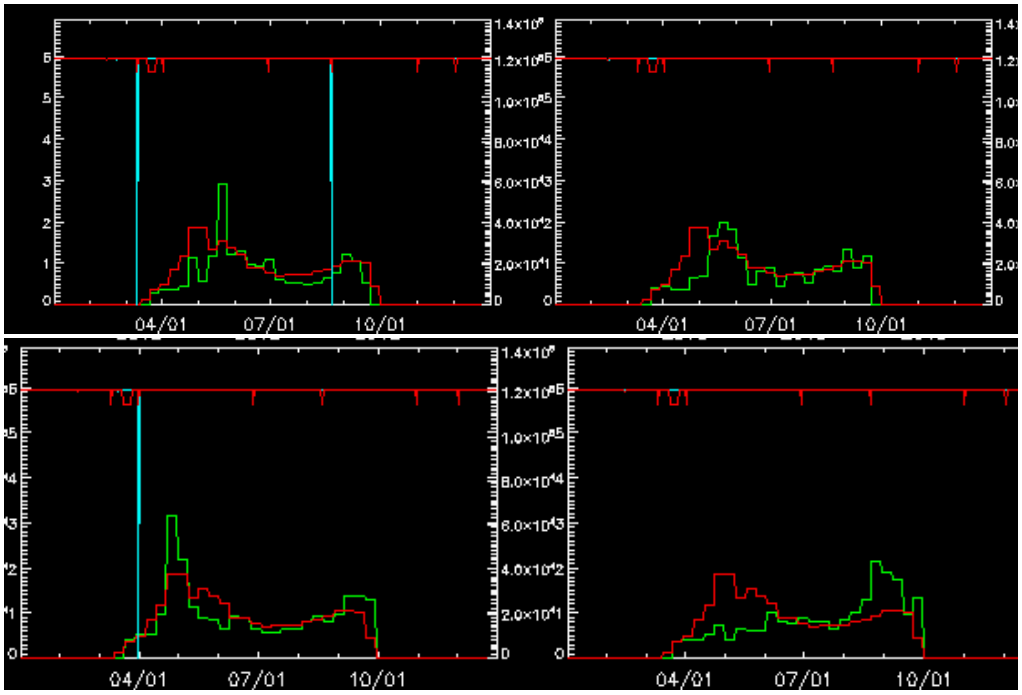

Figure 3.2.3. Seasonal dynamics of Chl *a* concentration (green curve) in the South West polygon for four selected years. Upper panels = years 1998 (left) and 1999 (right); Lower panels = 2016 and 2017. The area of open water (blue line) is shown on the top (note that this line is mostly hidden by the red line). Climatology of open water (red line on the top) and Chlorophyll *a* (red line at the bottom) is shown averaged for the period 1998–2017. The x-axis is time from January to December, with dates of 1 April, 1 July, and 1 October indicated. Scale of Chlorophyll *a* axis is to the left (mg Chl *a* m-3), while the scale for area of open water (104 km²) is shown to the right.

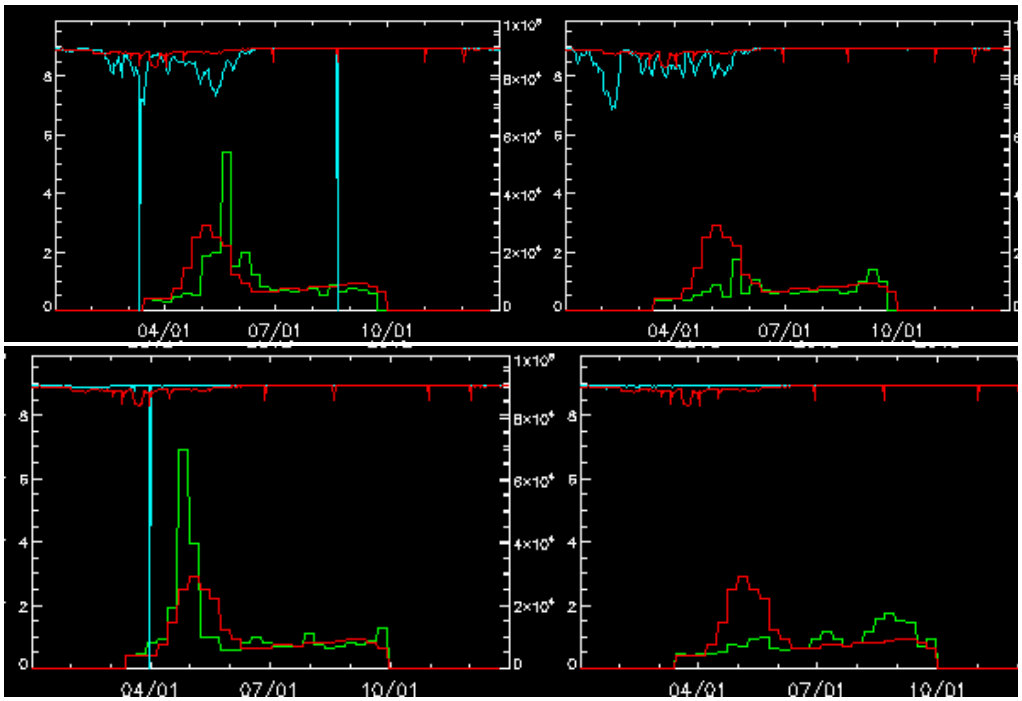

Figure 3.2.4. Seasonal dynamics of Chl *a* concentration (green curve) in the South East polygon for the years 1998 and 1999 (upper left and right), and 2016 and 2017 (lower left and right. See legend to Figure 4 for explanation of lines and scales.

Net Primary Production (NPP)

Remote sensing NPP data were explored using the polygon areas shown in Figure 3.2.1.

Satellite based NPP in the entire Barents Sea showed significant interannual variability during the period 1998–2017. However, the general trend shows that NPP has increased significantly (p=0.006) over time (Figure 3.2.5). This increase is mainly due to reduced ice coverage, leading to larger ice-free areas and a longer growth period (Figure 3.2.8; see Dalpadado *et al*., 2014; Arrigo and Van Dijken, 2011; 2015). Furthermore, mean production per unit area has in general also increased over time. Our results show that mean daily production rate (mg C m-2 day-1) averaged over time (combining all polygons), has increased from an average of 163 mg C m-2 day-1 for the years 1998–2009, to an average of 186 mg C m-2 day-1 for 2010-2017. The NPP in the eastern regions (North East and Pechora polygons) have increased significantly (p<0.01) during the study period (Figure 3.2.6). The NPP in the northern polygons, have also shown an increasing trend over the years (Figure 3.2.7). The production values here are low, however, compared to the southern and eastern regions. The NPP in the South West polygon showed large interannual variability, but no marked trend of increase (not shown).

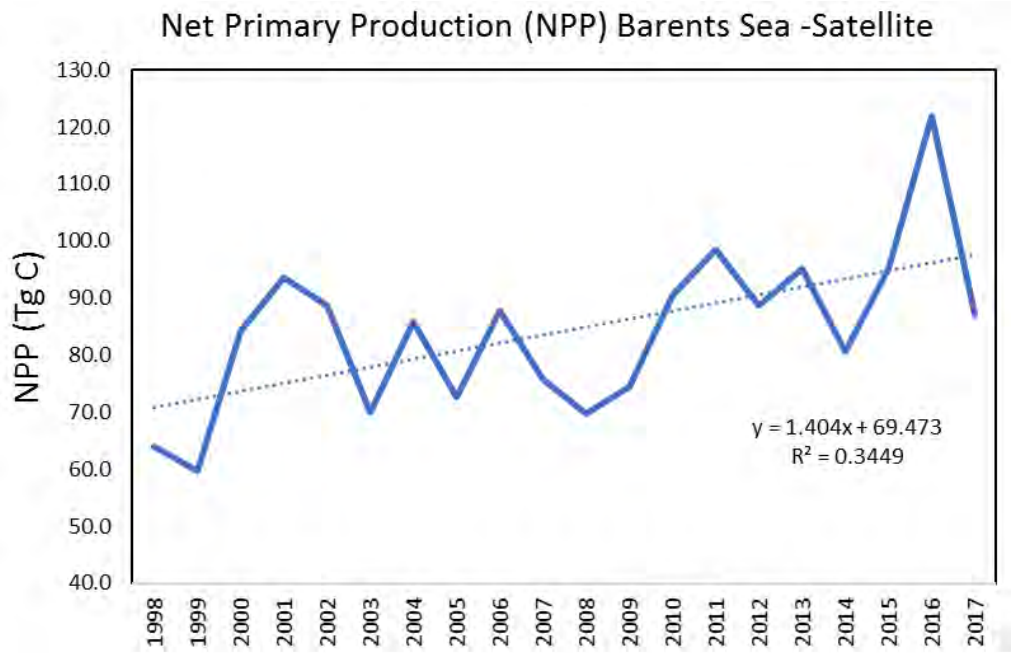

Figure 3.2.5. Annual net primary production (NPP- satellite based) in the Barents Sea.

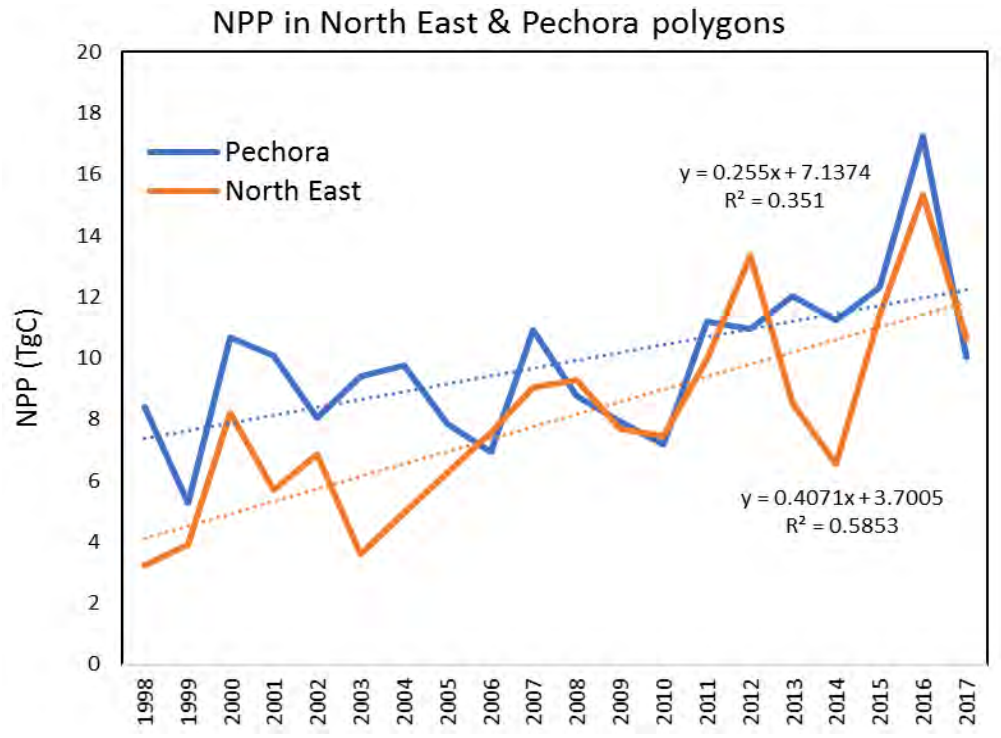

Figure 3.2.6. Annual net primary production (NPP- satellite based) in the North East and Pechora polygons.

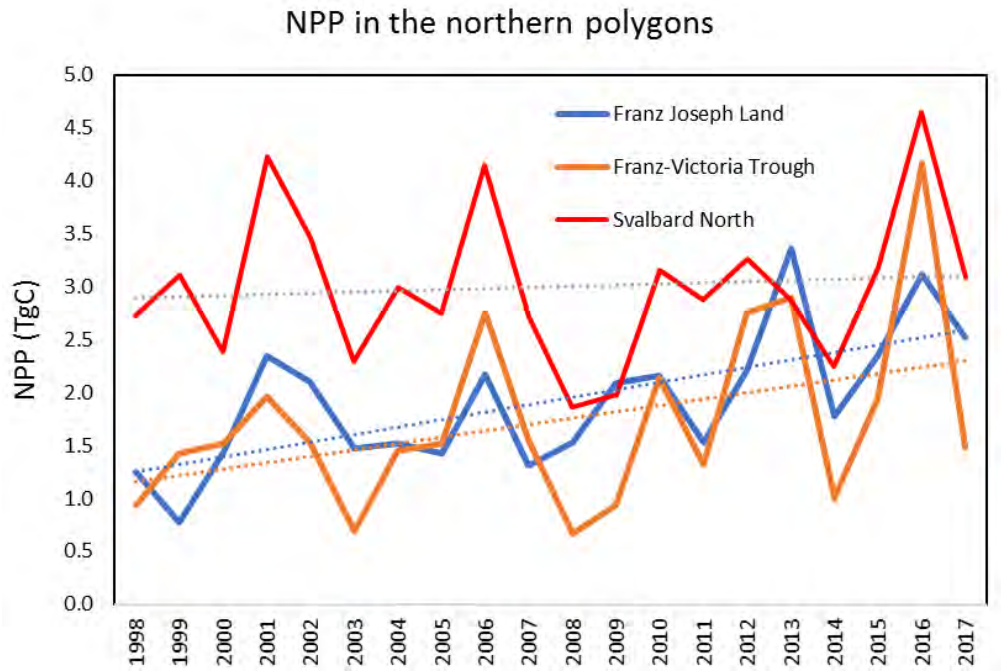

Figure 3.2.7. Annual net primary production (NPP- satellite based) in 3 northern polygons.

Open Water Area (OWA)

The concentration of sea ice in the Arctic has dropped by ca. 9% per decade since 1978 and has been accompanied with reduced sea-ice thickness and duration (Arrigo and Van Dijken, 2015). Due to the reduction of sea ice, the OWA (maximum ice-free waters in late summer or autumn) in the Barents Sea has increased significantly over time, likely leading to higher NPP in the region. Satellite based Open Water Area (OWA) estimates confirm this (Figure 3.2.8-upper; $p<0.01$). The increase is most pronounced in North East and South East polygons (Figure 3.2.8-lower).

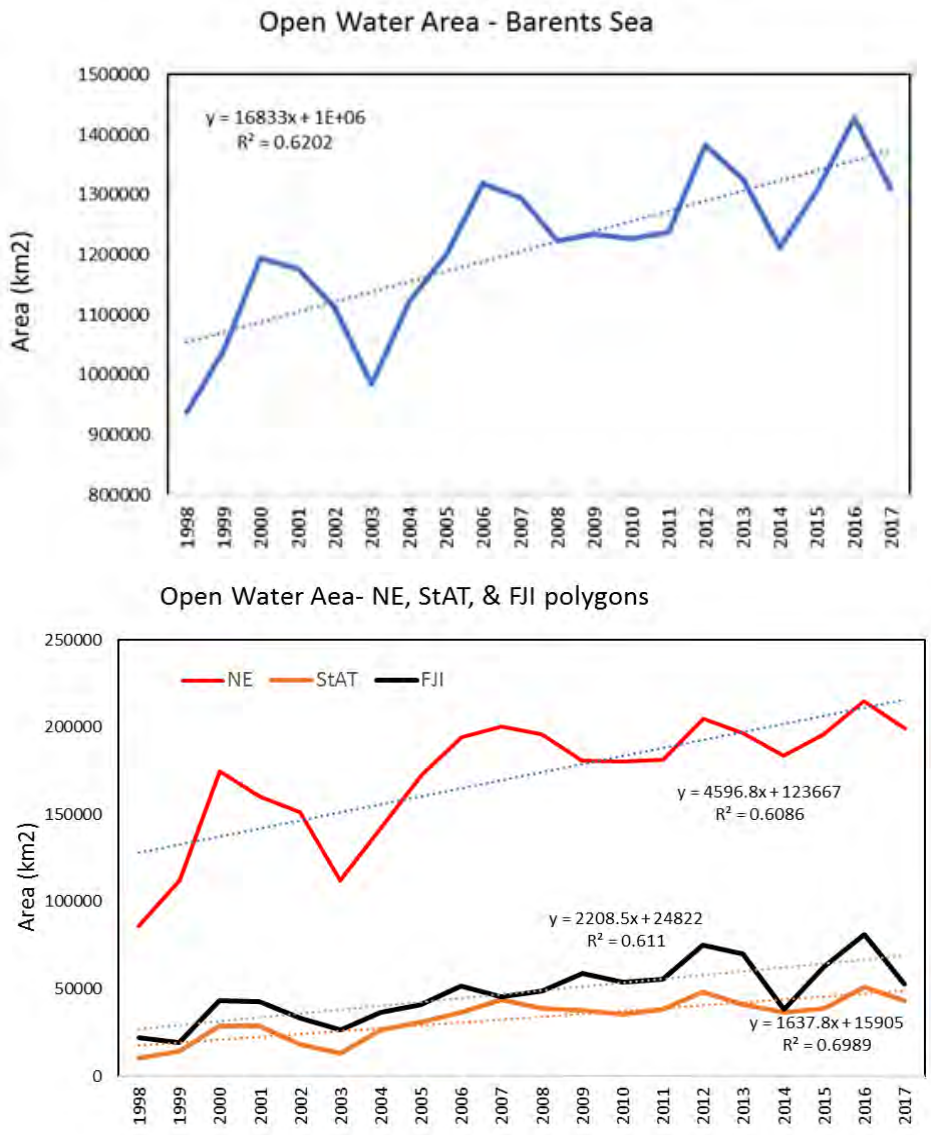

Figure 3.2.8. Open water area for the whole Barents Sea (upper) and for northern and eastern polygons (lower; North East (NE), St. Anna Trough (StAT), Franz Joseph Land (FJI)).

There was a significant relationship between increasing satellite-based NPP and increasing OWA (Figure 3.2.9). In addition, NPP was also related to increasing chlorophyll *a* concentration (Figure 3.2.9). The increasing trend in NPP shown in Figure 3.2.5 is, therefore, a reflection of an increase in both OWA and average biomass of phytoplankton (Chlorophyll *a*). The highest NPP value (122 Tg C) was observed in 2016, the year with lowest ice coverage since 1951.

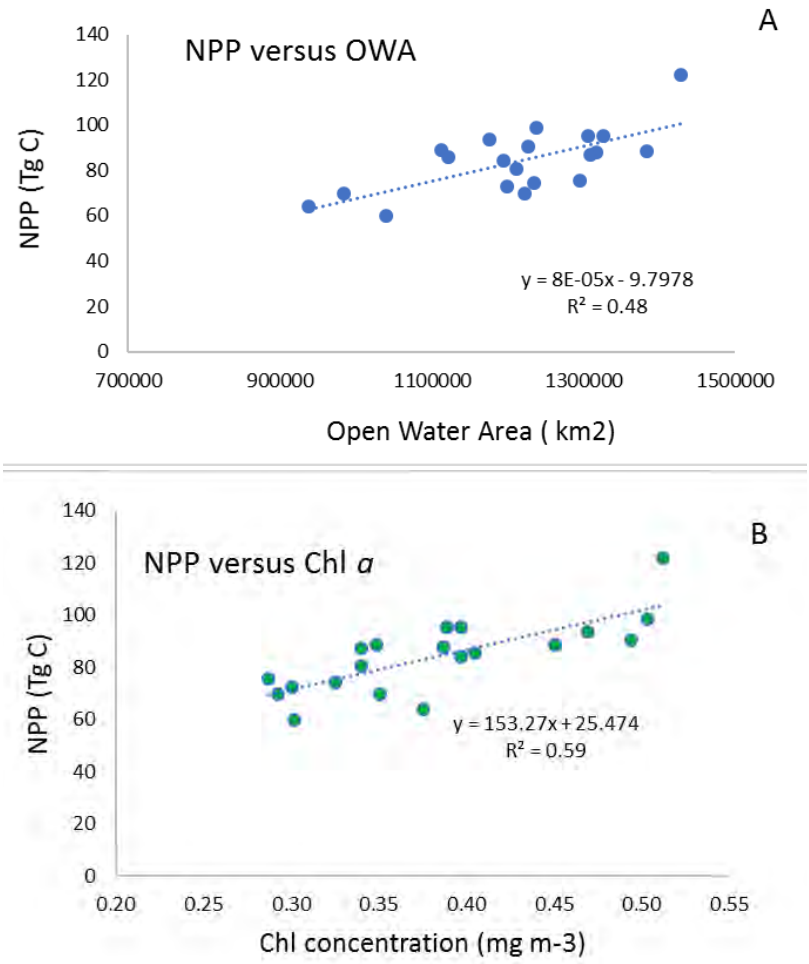

Figure 3.2.9. A) Relationship between satellite derived Net Primary Production (NPP) and and Open Water Area (OWA), and B) NPP and Chlrophyll *a* (Chl *a*)

Spring and Fall Bloom dynamics

Seasonal development of phytoplankton in the Barents Sea is typical for a high latitude region with a marked spring bloom usually peaking in May and an autumn bloom in August (Table 3.2.2.; Figures. 3.2.3 and 3.2.4). Peak Chlorophyll *a* concentration in spring is much higher (ca. 3.0 mg m^{-3}) than in autumn (<1 mg m^{-3}). The internannual variability of Chlorophyll concentration was much higher in spring (CV=27%) compared to autumn (10%).

Table.3.2.2. Spring and Fall Chlorophyll concentrations, and peak day averaged over all 15 polygons and years (1998-2017).

	Spring Bloom peak Chl	Fall Bloom peak Chl	Spring Bloom peak day	Fall Bloom peak day
	mg m-3	mg m-3	Day of the year	Day of the year
Average	3.20	0.84	145	239
SD	0.86	0.08	9	5
CV %	27	10	6	2

Spring bloom start day was defined in two ways; as a threshold level Chl concentration (0.5 mg m-3); and a fraction (0.3) of maximum chlrophyll level. Both definitions show that spring bloom has started earlier over time (shown only for the latter definition, Figure 3.2.10). Year-to-year variability of spring bloom start day was observed throughout the study period. A decrease in start-day number was observed though not significant (p=0.087), when using the threshold level of 0.5 mg m-3 Chl concentration. However, a significant (p=0.006) decrease was observed when using spring bloom start day, defined as the day with a fraction (0.3) of maximum chlrophyll level; the start day in 1998 was day 127 compared to day 106 in 2017, indicating that the date of spring bloom may have advanced by ca. 3 weeks in some years.

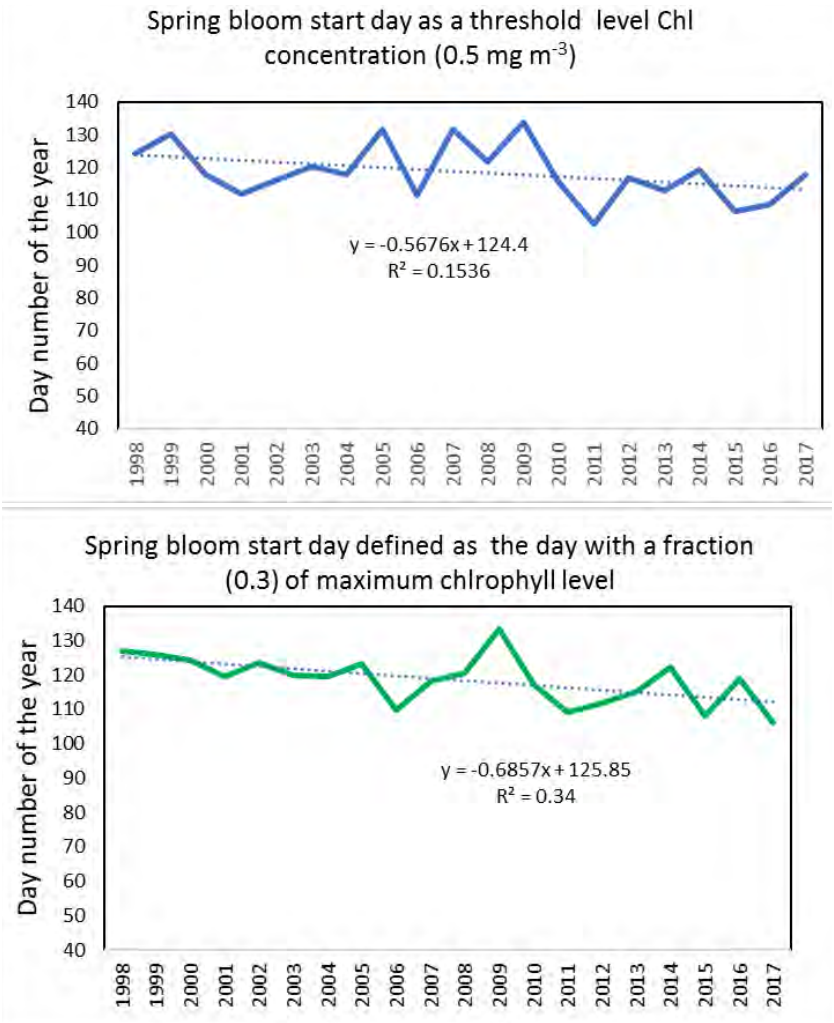

Figure 3.2.10. Spring bloom start day in the Barents Sea defined as the day as a threshold level of Chl *a* concentration of 0.5 mg m-3 (upper panel) and as the day with a fraction (0.3) of maximum chlorophyll level (lower panel).

Key points

1. Validations performed on *in situ* observations and satellite data for the Barents Sea, show that the model by Arrigo *et al.* (2008) gives reasonable results that compare well with observed measurements (Dalpadado *et al.*, 2014; Rey *et al.* (in prep), and ongoing TIBIA work).

2. Sea surface temperature in all polygons show an increasing trend over the 20-year study period. The increase in temperature conditions, and decrease in sea ice cover,

have led to large ice-free areas especially in the north and east, hence higher integrated phytoplankton production in the Barents Sea.

3. Spatially integrated NPP has increased over the years in most polygon regions. A noteworthy increase is observed in the eastern regions (North East and South East polygons), where sea ice coverage has diminished over the years.

4. There is a significant relationship between Chlorophyll *a*, OWA (ice-free area), and integrated net primary NPP. The increase in ice-free area provides improved habitat for phytoplankton growth as the growing season (number of days with open water) has increased.

5. Our investigations reveal that major part of the annual production has taken place by day 200 of the year. Published work also show that nearly half of the annual production occurs during the spring bloom and is fueled by winter nutrients.

6. Estimated start day of the spring bloom has decreased over the years, showing a general trend of 2–3 weeks earlier bloom over the 1998–2017 period.

3.3 Zooplankton

Mesozooplankton biomasses

Mesozooplankton plays a key role in the Barents Sea ecosystem by transferring energy from primary producers to animals higher in the foodweb. Geographic distribution patterns of total mesozooplankton biomass show similarities over time, although some interannual variability is apparent. Challenges in covering the same area each year are inherent in such large-scale monitoring programs, and interannual variation in ice cover is one of several reasons for this. This implies that estimates of average zooplankton biomasses for different years might not be directly comparable. In 2017, relatively high biomass (>10 g m^{-2}) was observed in the Bear Island Trench (southwestern region), north of Svalbard/Spitsbergen; south of Franz Josef Land, and in large parts of the easterly survey-region including the Southeastern Basin. Relatively low biomass (<3 g m^{-2}) was observed: in the westernmost area bordering the Norwegian Sea; in regions both south and east of Svalbard/Spitsbergen, and in the southeastern corner of the survey area (Figure 3.3.1). Relative to 2016, the most notable difference in 2017 was enhanced biomass in easterly parts of the Barents Sea. However, a large area just north of the Kola Peninsula was not covered in 2016, which complicates comparison.

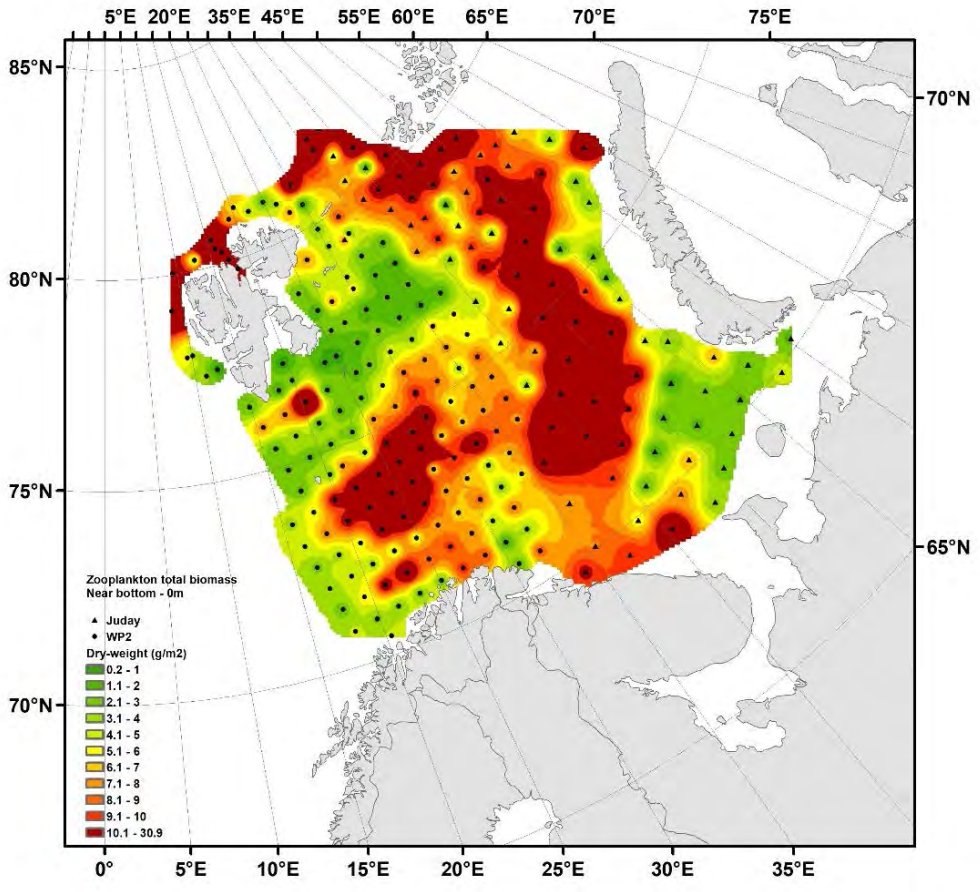

Figure 3.3.1. Distribution of total zooplankton biomass (dry weight, g m-2) from near bottom - 0 m in autumn 2017. Data based on 247 samples obtained during the joint Norwegian-Russian (IMR-PINRO) ecosystem survey in late August – mid-October. Interpolation made in ArcGIS v.10.3, module Spatial Analyst, using inverse data weighting (default settings).

In the Norwegian sector of the Barents Sea, mesozooplankton biomass was size-fractionated (180–1000 μm, 1000–2000 μm, and >2000 μm) before weighing. For the smallest size-fraction, estimated average biomass was similar to average biomass the last 20 years (1987–2017). For the intermediate size-fraction, 2017 average biomass was slightly lower than the average level over the last 20 years (Figure 3.3.2). For the largest size-fraction, the average values have shown a decreasing trend during the ca. last 13 years; in 2017 biomass for the largest size-fraction was well below the average level over the last 20 years. Based only on Norwegian data, which represent the longest time-series, average zooplankton biomass combined all size-fractions in August-October 2017 was 6.4 g dry-weight m^{-2} in the western-central Barents Sea, this estimate is lower than in 2016 (7.7 g dry-weight m^{-2}), and somewhat lower than the average for the last 20 years (7.0 g dry-weight m^{-2}). The reduction in average total biomass from 2016 was mainly due to decreased biomass in the mid-size fraction (1000–2000 μm).

Combined Russian and Norwegian data (247 stations in total) covering the entire Barents Sea provided an estimated average zooplankton biomass of 7.2 (SD 5.7) g dry-weight m^{-2} in 2017. This estimate is not directly comparable with that for 2016 (6.6 g m^{-2}), since areas covered these two years differed. In the Russian sector, average biomass in 2017 was 8.6 g dry weight m^{-2}, not directly comparable to 2016 estimate (3.9 g dry-weight m^{-2}) due to the above-mentioned incomplete 2016 coverage in the southern region.

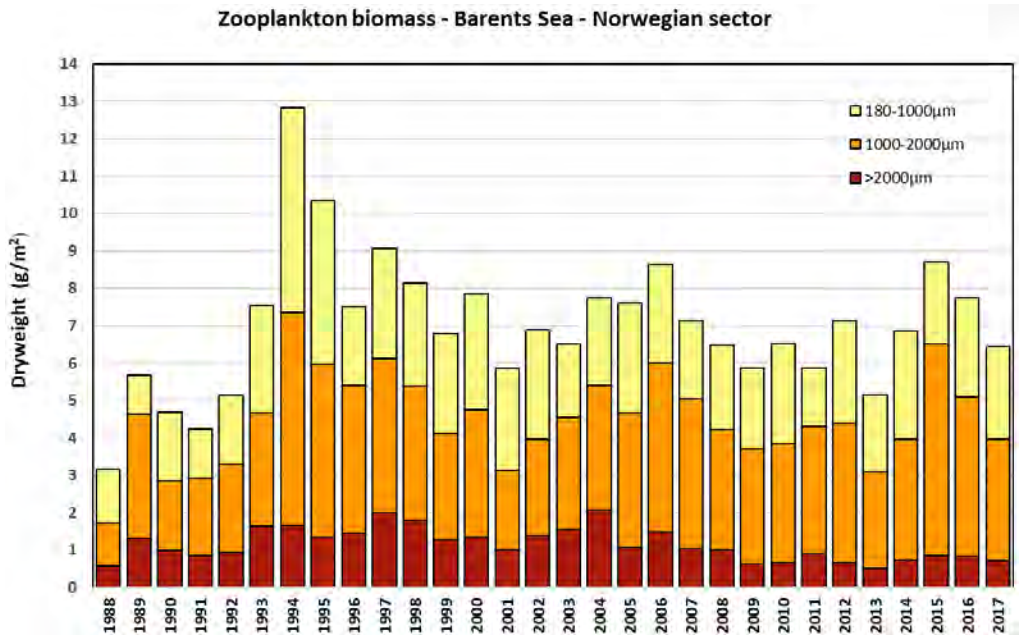

Figure 3.3.2. Time-series of mean zooplankton biomass from bottom – 0 m (dry-weight, g m-2) for the western and central Barents Sea (Norwegian sector) of the autumn ecosystem-survey, 1988–2017. Data are shown for the three size-fractions; 0.18–1 mm (yellow), 1–2 mm (orange), >2 mm (red) based on wet-sieving.

Zooplankton biomass can vary considerably between years and appears to be controlled largely by predation pressure, e.g. from capelin, although the yearly predation impact is expected to vary between regions. Capelin stock size was relatively high during 2008-2013; thus, exerting high predation pressure on zooplankton. In 2014, the capelin stock-size decreased, and in 2015 and 2016 the stock declined further to very low levels; this likely easing pressure on their zooplankton prey. However, the 2017 estimate suggests a marked increase in capelin stock-size; this likely increasing pressure on their zooplankton prey. Predation from other planktivorous species (herring, polar cod and blue whiting) and pelagic juveniles of demersal fish (cod, haddock, saithe, and redfish) can also affect the state of the plankton in the Barents Sea. In addition, processes such as advective transport of plankton from the Norwegian Sea into the Barents Sea, primary production (see section above), and local production of zooplankton likely contribute to variability of zooplankton biomass. It should be noted that methodological factors, such as differing spatial surveillance areas, also contribute to the reported variability between years. For a more direct comparison of interannual trends, that is less influenced by variable spatial coverages, we refer to the time-series of biomass estimates for specific subareas of the Barents Sea (see highlights in the section below, more detailed information in 2018 WGIBAR Report, Annex 4).

Mesozooplankton biomass in subareas of the Barents Sea

The 2017 IMR zooplankton biomass estimates have been calculated as mean values for each of 9 subareas (polygons). A 1989–2016 time-series biomass estimates for these subareas described in a background document (2018 WGIBAR Report, Annex 4). Time-series of estimates for four Atlantic water subareas, Central Bank, and Great Bank are shown in Figure 3.3.3, and are updated with 2017results.

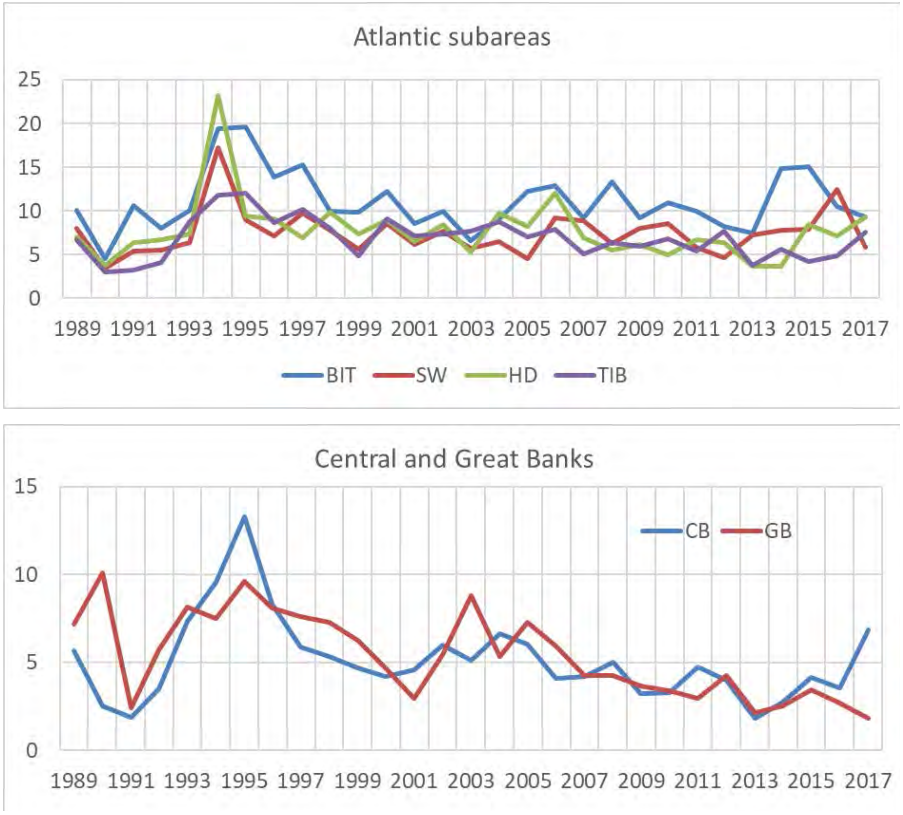

Figure 3.3.3. Time-series of mean zooplankton biomass (g dw m-2) for stations within subareas of the Barents Sea (see WGIBAR 2018 report, Annex 4) based on autumn surveys in the years from 1989 to 2017. Upper panel – four subareas in the southwestern Barents Sea covered mainly with Atlantic water: Bear Island Trench (BIT), South-West (SW), Hopen Deep (HD), and Thor Iversen Bank (TIB). Lower panel – two subareas in the central Barents Sea with colder and partly Arctic water conditions: Central Bank (CB), and Great Bank (GB). The results presented in these figures represent the total biomass as collected with WP2.

Biomass estimates in the 'Atlantic' subareas have fluctuated between 5 to 10 g dw m^{-2} since about year 2000, with generally higher values for the Bear Island Trench. Biomass in the three other subareas has tended to increase since 2012–2013, while biomass in the Bear Island Trench has decreased since 2015. It should be noted that sampling variance is high, with coefficient of variation (CV = SD/mean) of about 0.5 for mean values per subarea (see WGIBAR 2018 report, Annex 4). This translates into confidence intervals (95%) of ±20-25% around the mean for *n* observations of 16–25 (which is a typical number of stations within a subarea).

Biomass estimates at Central Bank and Great Bank have shown declining trends since the 1990s to minima in 2013 (Figure 3.3.3 Lower). Biomass at Central Bank has subsequently increased after this, the 2017 estimate was relatively high (about 7 g dw m^{-2}). In contrast, biomass at Great Bank was very low in 2017 (about 2 g dw m^{-2}).

Figure 3.3.4 shows a comparison of the long-term mean values (1989–2016) for each of the subareas along with the values for 2017. The biomass values for 2017 are in most cases close to the long-term mean, with a lower value for the Great Bank, as already pointed out, and lower values also for the Svalbard-South and Franz-Victoria Trough subareas.

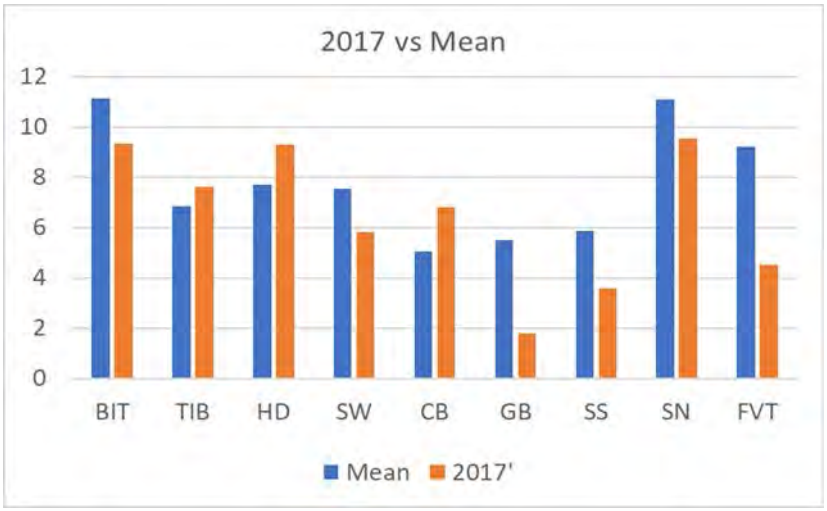

Figure 3.3.4. Mean zooplankton biomass (g dw m^{-2}) for nine subareas of the Barents Sea, comparing long-term means for the 1989–2016 period with mean values for the stations collected in 2017. SS – Svalbard-South, SN – Svalbard-North, FVT – Franz-Victoria Trough. for other abbreviations, see legends to Figures 3.3.3. and 3.3.

Mesozooplankton species-composition

Russian investigations along the Kola section in early June 2017 showed that copepods were the dominant zooplankton group at that time, comprising on average 75% in abundance and 72% in biomass; *Calanus finmarchicus* was the dominant species. The mean abundance of *C. finmarchicus* in 2017 was 159 761 ind. m^{-2}, less than half of the last years mean value (395 941 ind. m^{-2}), and comparable to that in 2013 (133 814 ind. m^{-2}), and somewhat lower than the long-term mean (Figure 3.3.5). The abundance of *C. finmarchicus* in the southern part of the section was lower than in the northern part, and the highest values, as in 2016, were observed at 72°00′ and 73°30′N. In the *C. finmarchicus* population, individuals of all stages were present, but while CI-CIV stages dominated at most stations, the portion of the young individuals CI-CII stages was higher at the northern stations.

In contrast to 2016, when *C. glacialis* was not found in the plankton samples along the Kola section, the 2017 mean abundance of this species was 15.8 ind. m^{-2}. This value was slightly lower than in 2015 (18.6 ind. m^{-2}) as well as the long-term mean (Figure 3.3.5). *C. glacialis* was found only north of 72°00′ N. In the *C. glacialis* population, individuals of stages CIV-V were observed, with a dominance of CV copepodites.

Abundance of the arctic *C. hyperboreus* in 2017 was higher than in 2016 (112.6 and 77.2 ind. m^{-2}, respectively) and very close to the long-term mean (111.3 ind. m^{-2}) (Figure 3.3.5). The highest abundance of *C. hyperboreus* was found north of 72°00′ N. Copepodites CIV-CV of *C. hyperboreus* represented its population.

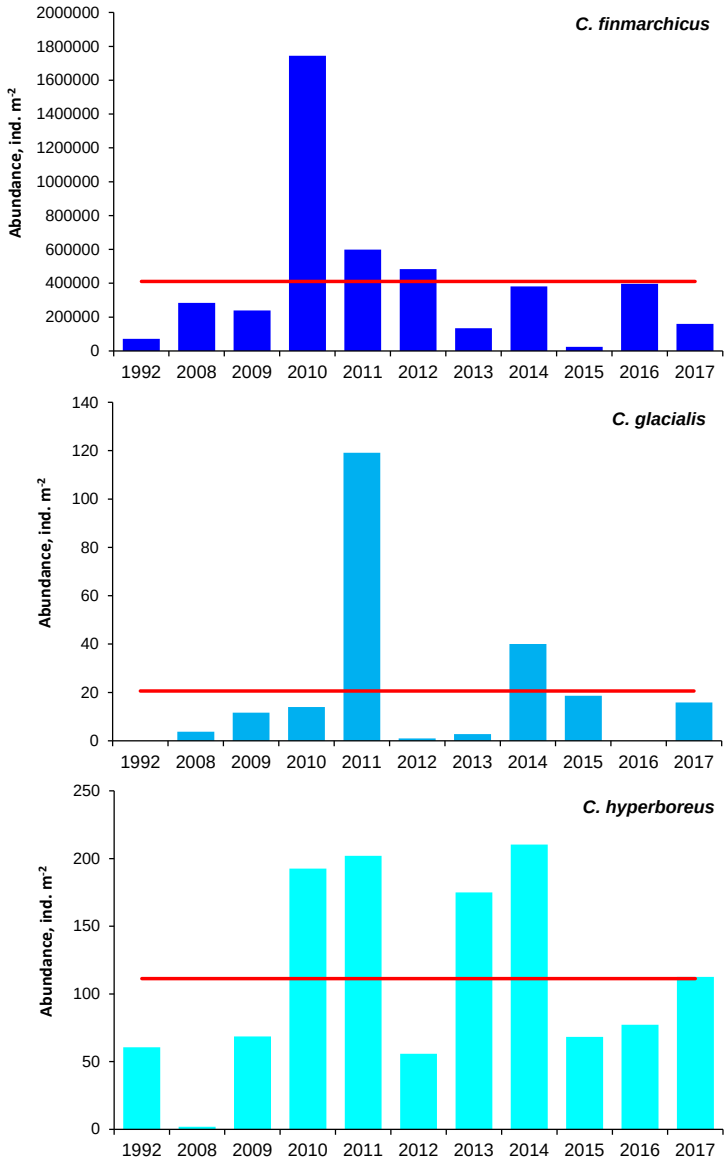

Figure 3.3.5. Abundances (ind. m^{-2}) of *C. finmarchicus*, *C. hyperboreus* and *C. glacialis* along the Kola section in May/June in 1992 and 2008–2017. Red lines show the long-term mean values.

Russian (PINRO) investigations of mesozooplankton during the 2016 BEES survey (August-September) showed that copepods dominated both abundance and biomass. Copepods comprised on average 88% of total zooplankton numbers and 75% of total zooplankton biomass (Figures. 3.3.6 and 3.3.7). Total zooplankton abundance and biomass in the southern Barents Sea (south of ca. 75°N) were both considerably higher than in the northern Barents Sea (north of ca. 75°N): averaging 2056 ind. m^{-3} and 1263 ind. m^{-3} and 145.8 ind. m^{-3} and 102.0 mg m^{-3}, respectively.

In northern Barents Sea, copepods (87%) were the most abundant zooplankton group, while heteropods (9.8%) were less numerous. Estimates of total zooplankton biomass, indicated that copepods represented the most important group (71%), while chaetognaths and heteropods comprised 12% and 11% respectively. Increase in total zooplankton abundance and biomass were observed relative to 2015; primarily due to more copepods, chaetognaths and heteropods. In the northern Barents Sea, the small copepods *Oithona similis* and *Pseudocalanus minutus* were numerous; comprising 60% and 26% of total copepod abundance. While, the larger species *Calanus finmarchicus*, *C. glacialis*,

and *Metridia longa* represented 7.5%, 5.7%, and 1.1% of total copepod abundance, respectively (Figure 3.3.6). Total copepod biomass consisted mainly of *C. glacialis* (45%), *C. finmarchicus* (20%), *M. longa* (12%), *P. minutus* (11%), and *C. hyperboreus* (8%). Relative to 2015, the 2016 observed abundance of most copepods had increased: particularly *C. finmarchicus* (by a factor 2.6) and *C. glacialis* (by a factor 1.8); while abundance of *P. minutus* decreased slightly. Increased biomass of *C. finmarchicus* and *O. similis* was also observed in 2016 relative to 2015, while biomass of *C. glacialis*, *M. longa*, and *C. hyperboreus* remained at the same level.

In the southern Barents Sea, copepods also dominated both abundance and biomass (90% and 79%, respectively). Among copepods, the small species *O. similis* and *P. minutus* were most abundant (66% and 23% of total copepod abundance, respectively); while larger species *C. finmarchicus* and *M. longa* contributed 10.3% and 1.2%, respectively (Figure 3.3.6). However, in copepod biomass, *C. finmarchicus* (71%), *M. longa* (12.7%), and *P. minutus* (11.7%) were the dominant species (Figure 3.3.7). In 2016, both abundance and biomass of *O. similis* were at the same level as in 2015, but relative to 2014, these parameters increased by factors of 2.3 and 2.4, respectively. Abundance and biomass of *P. minutus* and *C. finmarchicus* in the southern Barents Sea in 2016 increased (by factors of 2.3 and 2.2 and 1.9 and 2.6, respectively) relative to 2015. In 2016, abundance and biomass of *M. longa* had increased only by factors 1.1 and 1.2, relative to 2015.

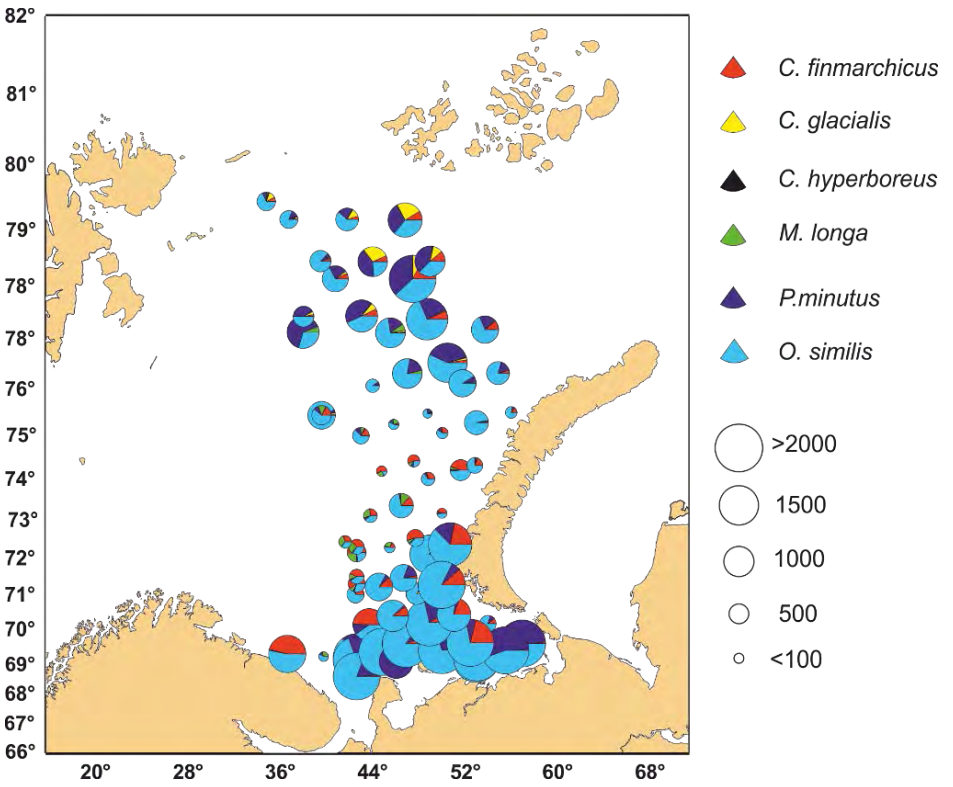

Figure 3.3.6. Abundance (ind. m^{-3}) of the most numerous copepod species (bottom-0 m) in the Barents Sea (based on the PINRO samples from the PINRO/IMR ecosystem survey in August-September 2016).

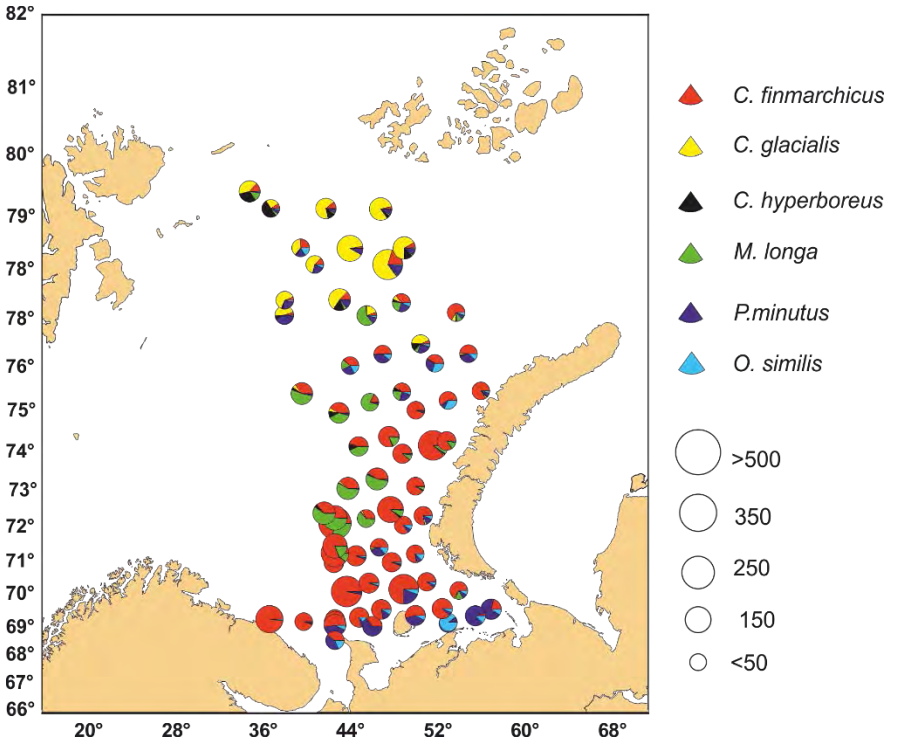

Figure 3.3.7. Biomass (mg wet-weight m^{-3}) of the most numerous copepod species (bottom-0 m) in the Barents Sea (based on the PINRO samples from the PINRO/IMR ecosystem survey in August-September 2016).

Fugløya-Bear Island (FB) transect, located at the western entrance to the Barents Sea, is typically monitored by IMR 5-6 timer per year, covering different seasons. Up to eight stations with fixed positions are sampled during each coverage, though the number may vary depending on weather conditions. Zooplankton samples taken during the 1995–2017 period from four locations representing different water masses (Coastal, Atlantic, and mixed Atlantic/Arctic), have been analysed taxonomically. Annual averages (sum of all copepodite stages I-VI) of the species *C. finmarchicus, C. glacialis and C. hyperboreus* are shown in Figure 3.3.8 for the period 2007–2017. *C. finmarchicus*, is by far the most common of the three species, and displays large interannual variations in abundance. *C. finmarchicus* tends to be most abundant at the station located at 73°30'N; high abundances was recorded during 2010 along most of the transect except at the northernmost position (74°00'N). Following very low abundances at all stations in 2013, *C. finmarchicus* has been abundant along the transect during the last 4 years (2014–2017).

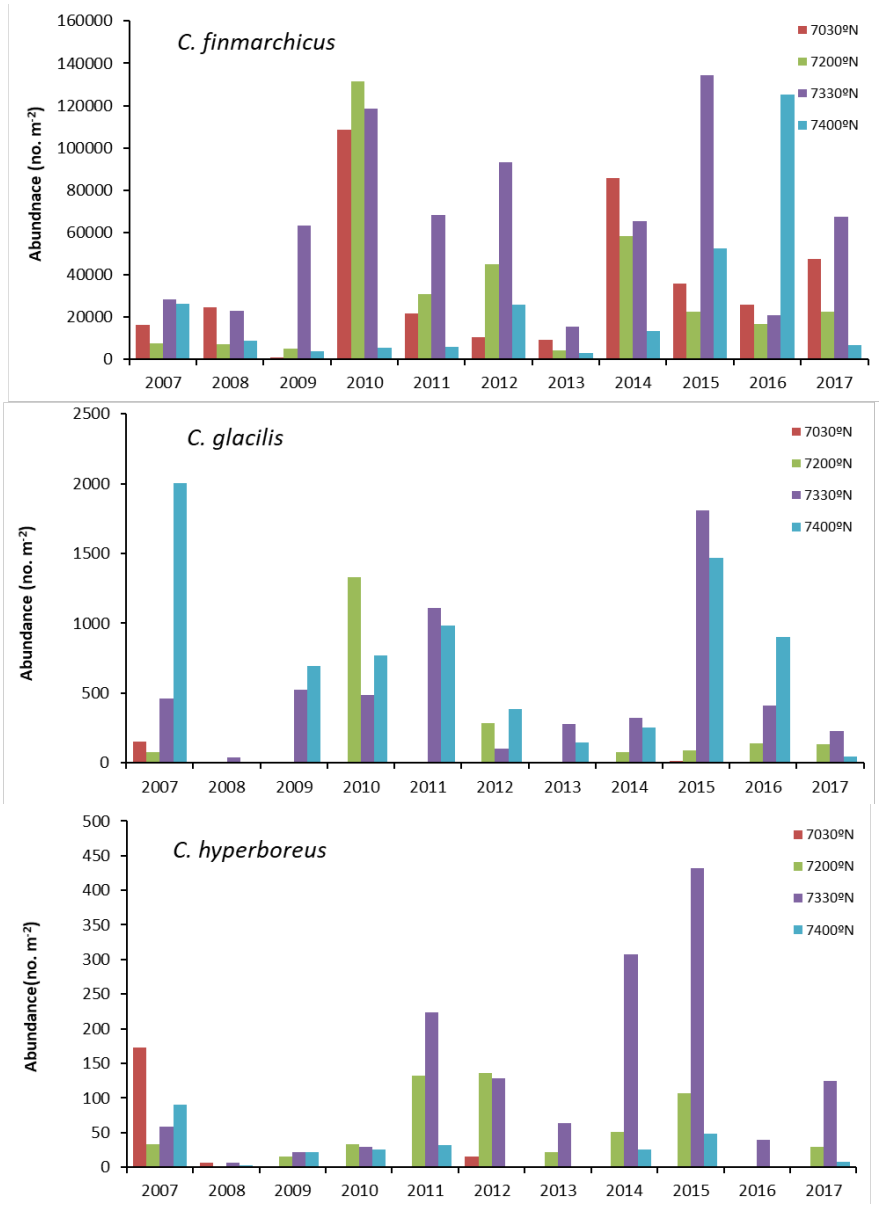

Figure 3.3.8. Abundance of *Calanus finmarchicus*, *C. glacialis* and *C. hyperboreus* along the Fugløya-Bjørnøya transect during 2007–2017. Note that only a portion of the time-series is shown in this figure. The bars represent the annual averages of the 5–6 coverages per year (except for 4 and 3 coverages in 2012 and 2013, respectively). Each station is shown separately.

As expected, *C. glacialis* was most abundant at the two northern-most stations (Figure 3.3.8), where Atlantic and Arctic waters mix. Abundance of this species also showed large interannual variations. Numbers of *C. glacialis* along FB transect seem to have decreased in later years of the time-series (1995–1998), with very low abundances recorded in 2005, 2008, during 2012-2014, and in 2017 (data for years before 2007 not shown in Figure 3.3.8). Abundance of the largest species, *C. hyperboreus*, along the FB transect has generally been low relative to *C. finmarchicus* and *C. glacialis* throughout the study period. Few individuals of this species were recorded during 2008-2010 and in 2016. (Figure 3.3.8). The FB time-series for *C. hyperboreus* shows a strong year-to-year variability of abundance. Still, abundances during 2008–2017 tended to be lower than during 1995–2007 (data before 2007 not shown in Figure 3.3.8).

Calanus helgolandicus, a more southerly species that spawns during autumn, has been observed regularly at the Fugløya – Bear Island transect, particularly during the period

from December to February (Dalpadado *et al.*, 2012). This species is similar in appearance to *C. finmarchicus*. In recent years, it has been observed more frequently in the North Sea as well as in the southern parts of the Norwegian Sea (Svinøy transect). Since taxonomic separation of *C. finmarchicus* and *C. helgolandicus* is time-consuming, limited numbers of individuals of the later stages up to 40 copepodites of stage V females were examined in each sample to establish the species-proportions. During winter, the ratio of *C. helgolandicus* to *C. finmarchicus* along the Fugløya – Bear Island transect has been observed to increase. At this time of the year *C. finmarchicus* is normally overwintering in deeper waters. Our FB time-series provides no evidence of an increase in the relative proportion nor absolute abundance of *C. helgolandicus* over the years at the entrance to the Barents Sea.

Macroplankton biomasses and distribution

Krill

Krill (euphausiids) represent the most important group of macrozooplankton in the Barents Sea, followed by hyperiid amphipods. Krill play a significant role in the Barents Sea ecosystem, facilitating transport of energy between different trophic levels. There are mainly four species of krill in the Barents Sea; *Thysanoessa inermis* associated with Atlantic water in the western and central Barents Sea, *Thysanoessa raschii* found mainly in shallow waters in the southeastern Barents Sea, while *Meganytiphanes norvegica* and *Thysanoessa longicaudata* are associated with the inflowing Atlantic water, particularly during warm periods. *Meganytiphanes norvegica* is the largest species reaching a maximum length of about 4.5 cm, while *T. inermis* and *T. raschii* reach lengths of about 3 cm and *T. longicaudata* is the smallest species – not exceeding 1.8 cm.

Winter distribution and biomass

Euphausiids were collected in the Barents Sea during the PINRO winter survey (November-December 2017) with the trawl-attached plankton net. Note, that results from only one cruise are presented here, covering the southern part of the Barents Sea; these data are not quite comparable with the previous years. Preliminary results indicate that in 2017, the trend of increasing euphausiid abundance continued, at least in the southern Barents Sea. Compared to 2015 (no sampling in 2016), mean euphausiid abundance in the southern Barents Sea in 2017 increased by a factor of 1.7 — from 803 to 1338 ind. 1000 m^{-3}. The main increase in euphausiid abundance was observed in central (from 266 to 535 ind. 1000 m^{-3}) and coastal areas (from 616 to 2290 ind. 1000 m^{-3}) of the Barents Sea. Euphausiid abundance in the eastern Barents Sea decreased in 2017 relative to 2015 by a factor of 2.3 (from 2695 to 1159 ind. 1000 m^{-3}). Euphausiid concentrations were formed mainly by local species (*T. inermis* and*T. raschii*) as well as Atlantic species (*M. norvegica* and *T. longicaudata*). The proportion of Atlantic species decreased in 2017 relative to 2015, but remained at a quite high level.

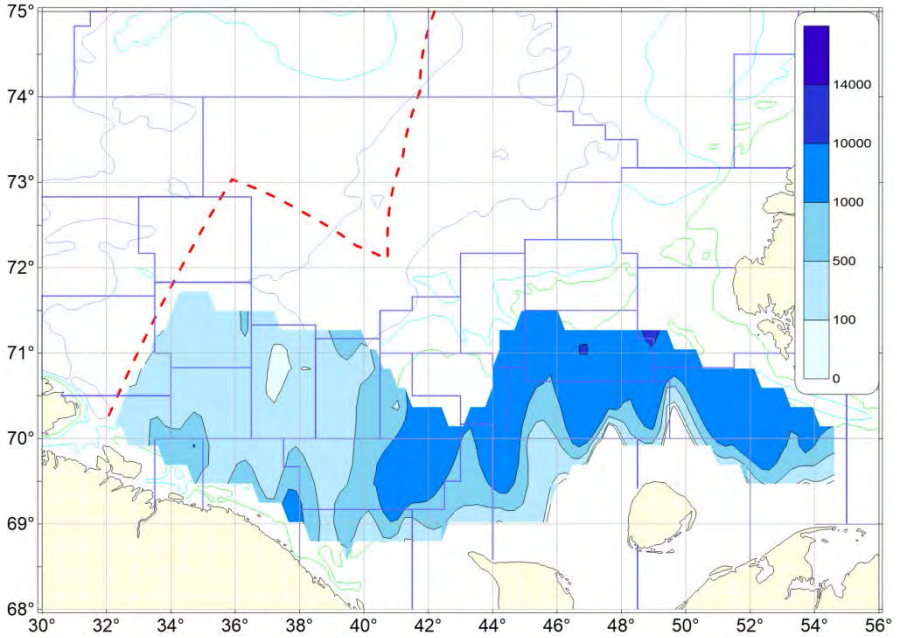

Figure 3.3.9. Distribution of euphausiids (ind. 1000 m^{-3}) in the near-bottom layer of the Barents Sea based on data from the Russian winter survey during November-December 2017.

Summer-autumn distribution and biomass

The following information on krill is based on the joint Norwegian-Russian Barents Sea Ecosystem survey conducted during autumn 2017. Euphausiids (krill) caught by standard pelagic trawl were identified to species level at 92% of all stations. Some parts of the northeastern Barents Sea were not covered in 2017, in contrast to most previous years.

Krill were widely distributed in the Barents Sea in 2017 (Figure 3.3.10), with very low abundances in the southeast. Biomass values in the upper 60 m are presented in wet weight grammes per square meter (g m^{-2}). The center of distribution varies between years. In 2013, largest catches were made mostly in the central area. In 2014, largest catches were made in the western area. In 2015, largest catches were made in the south and southeast of Svalbard/Spitsbergen. Whereas in 2016 and 2017, a wider distribution pattern was observed. The mean night-catch in 2017 (15.35 g/m^2) was higher than the long-term mean (7.7 g/m^2), and the highest observed since 2012. Note that areas covered may vary between the years.

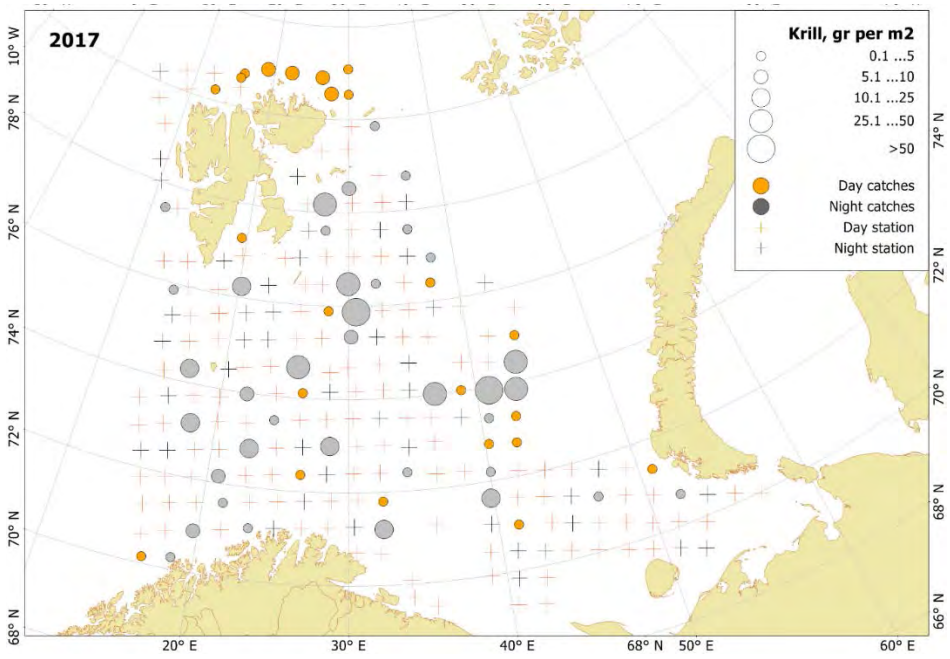

Figure 3.3.10. Krill distribution based on pelagic trawl stations covering the upper water layers (0-60 m) in the Barents Sea in August-October 2017.

The number of night stations in 2017 was approximately half that of day stations. During night, most krill migrate to upper layers of the water column to feed, and are therefore more available to the trawl. Larger catches (>50 gm^{-2}) were observed in the central area.

Based on euphausiid species identification in 2017, *Meganyctiphanes norvegica* and *Thysanoessa inermis* were widely observed in the Barents Sea. *M. norvegica* was mostly restricted to Atlantic waters in the south, with a few additional catches in west and north of Svalbard/Spitsbergen, in areas influenced by the north-flowing West Spitsbergen Current. Some samples from additional pelagic stations also showed occurrence of *M. norvegica* off southeastern Franz Josef Land and between Svalbard/Spitsbergen, and Franz Josef Land (up to 79-79˚N and 40-50˚E) (not shown in Figure 3.3.11). In contrast, *T. inermis* was mainly found in the central and northern Barents Sea, with a few additional catches of low abundance in the southeastern region. Two catches with *Thysanoessa longicaudata* were made in the northern area, and one catch with *Thysanoessa raschii* was made in the eastern area (Figure 3.3.11). Smaller *T. longicaudata* and juvenile euphausiids are not sampled representatively by the pelagic trawl due to escapement through the mesh.

In 2017, total krill biomass was estimated to be approximately 16 million tonnes wet-weight. This is higher than in 2016 and above the long-term (1980–2017) mean (9.0 million tonnes). The 2017 value is high considering heavy predation by capelin and other planktivorous fish during summer season.

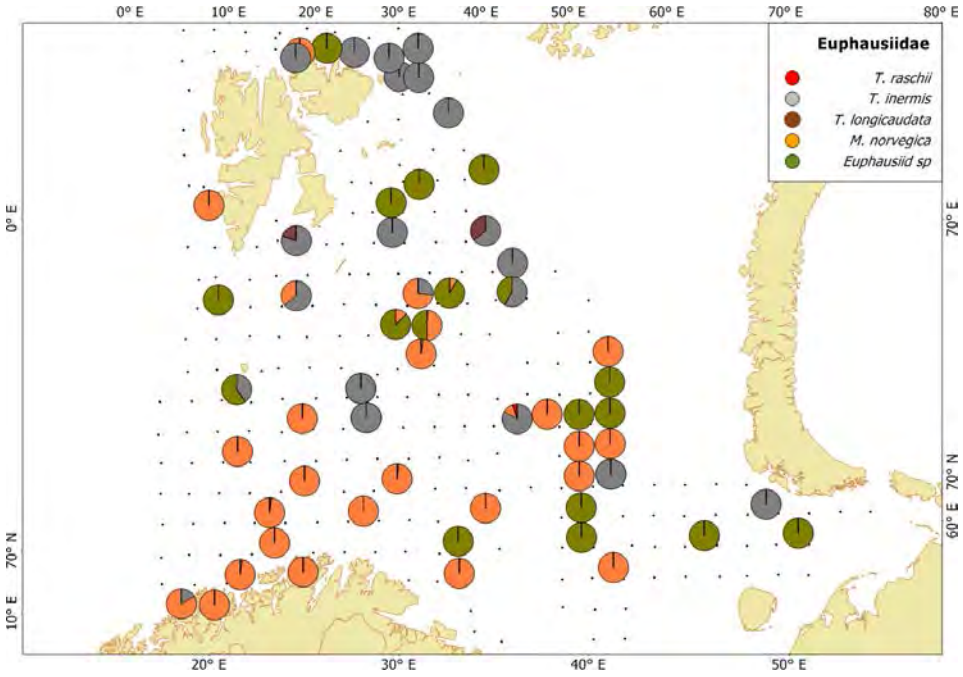

Figure 3.3.11. Krill species distributions based on trawl stations both day and night, covering the upper water layers (0-60 m) of the Barents Sea in August-October 2017. The proportions are based on wet-weights.

Amphipods

Information on amphipods (mainly Hyperiids) presented here is based the BEES survey in autumn 2017. In 2017, amphipods were observed in the northern Barents Sea (Figure 3.3.12) close to Svalbard/Spitsbergen region. In 2012 and 2013, amphipods were absent from the pelagic trawl catches, while in 2014 some limited catches were made north of Svalbard/Spitsbergen. During 2015–2017, several large catches were made east of Svalbard/Spitsbergen.

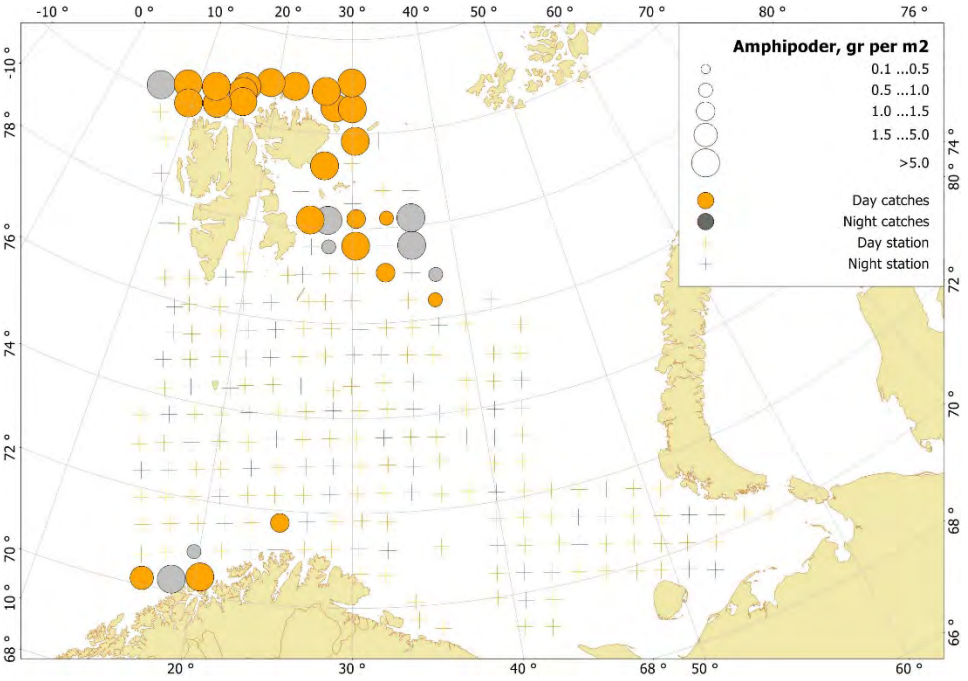

Figure 3.3.12. Amphipods distribution, based on trawl stations covering the upper water layers (0–60 m), in the Barents Sea in August-October 2017.

In 2017, the largest catches were made north and east of Svalbard/Spitsbergen, and were mostly represented by the Arctic species *Themisto libellula* (Figure 3.3.13). In 2017, daytime catches were generally larger than night-time catches. Smaller amphipods such as *T. abyssorum* were not sampled representatively using pelagic trawls. Estimated 2017 amphipod biomass in the upper 60 m was 30 thousand tonnes for the area covered. Catches in 2017 were substantially lower than in 2015 and 2016.

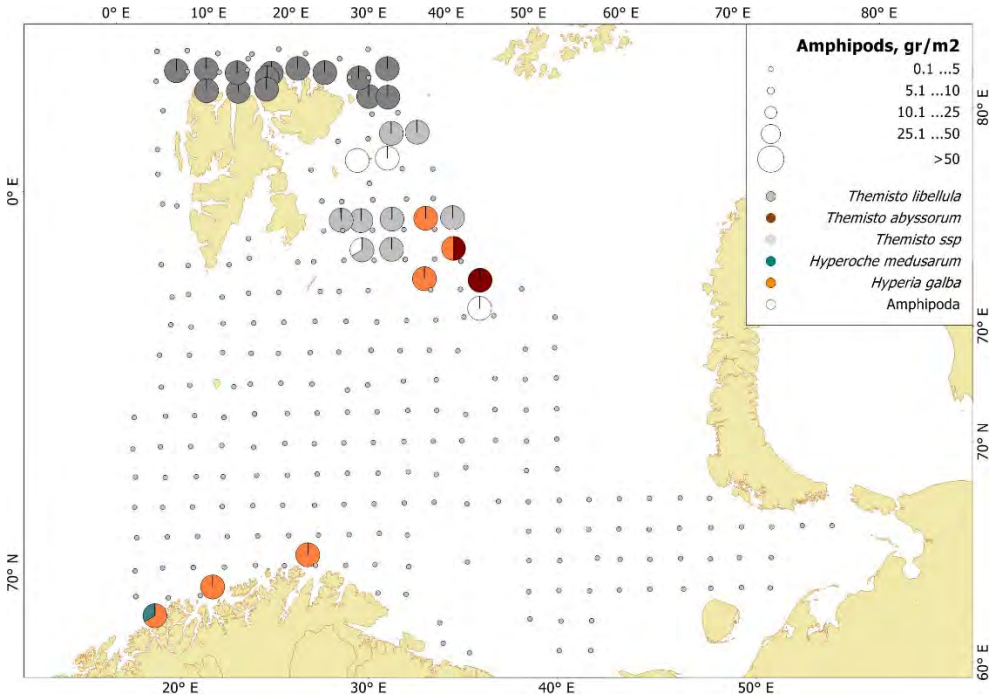

Figure 3.3.13. Amphipods species distribution, based on pelagic trawl stations covering the upper water layers (0–60 m), in the Barents Sea in August-October 2017. Figure by E. Eriksen

Jellyfish

Geographic distributions and estimated abundance biomass of gelatinous zooplankton presented in this report are based on data collected during the Joint Norwegian-Russian Barents Sea Ecosystem Survey conducted in autumn 2017, using the standard pelagic trawl for the 0–60 m depth-stratum. Gelatinous zooplankton was sorted from all trawl catches, identified to the lowest possible taxonomic level, and recorded as total wet weight per taxon.

Trawling is a harsh sampling method for gelatinous zooplankton, and data presented here should be considered semi-quantitative. The trawl used does not sample the entire water column, the filtered volume of water is not known, and small and fragile species may pass through the trawl mesh and are easily destroyed in the codend. The trawl likely has a higher catchability for large, robust scyphozoans (P*eriphylla periphylla*, *Cyanea capillata*) than for the smaller *Aurelia aurita.* Catchability may be even lower for fragile taxa such as ctenophores and small medusa. Nevertheless, we consider the error in catchability is constant for each taxon, allowing taxon-specific comparisons between years and stations.

In August-October 2017, lion's mane jellyfish (*Cyanea capillata*; Scyphozoa) was the most common jellyfish species, both with respect to weight and occurrence (average catch of 15 tonnes per sq nmi), and was widely distributed in the entire survey area (Figure 3.3.14). Catch per station was higher than in 2015–2016, and ranged between

155 kg and 224 tonnes per sq nm. Large catches (>10 tonnes per sq nmi) were taken at half of the stations; a higher frequency than observed during the previous two years.

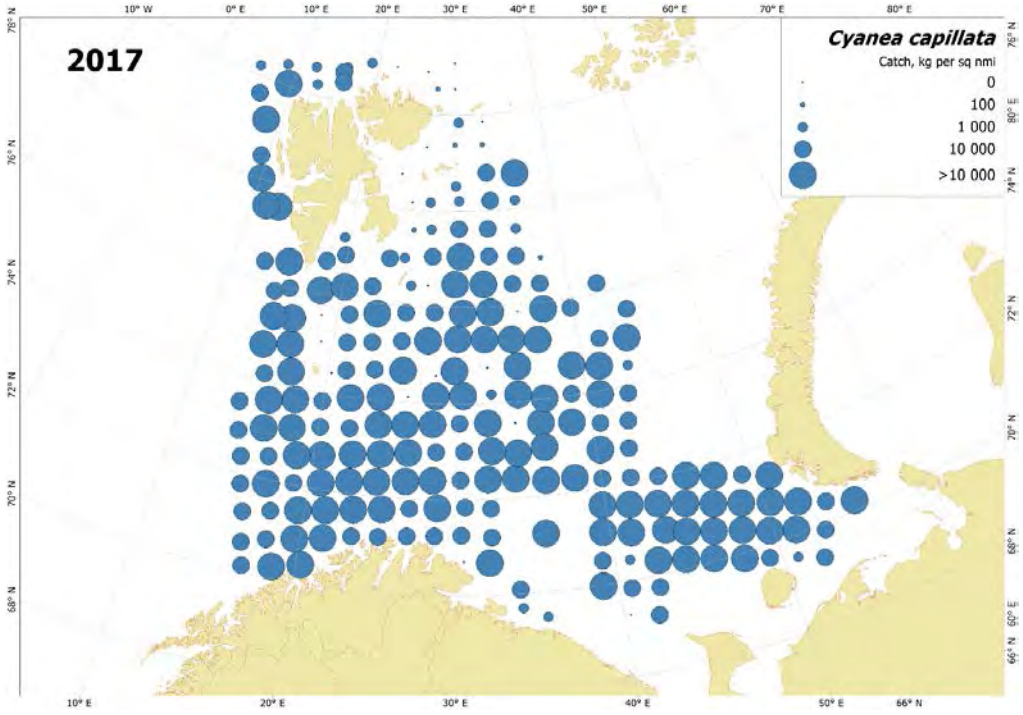

Figure 3.3.14. Distribution and catch (wet weight; kg per sq nmi) of *Cyanea capillata* in the Barents Sea, August-October 2017. Catches both day and night from standard pelagic trawl 0–60 m depth.

Cyanea capillata was observed throughout the entire Barents Sea, with the highest concentrations (>15 tonnes per sq nmi) in the central area, the southeastern area, and along the western Svalbard coast. Blue stinging jellyfish (*Cyanea lamarckii*; Scyphozoa) which-usually occurs mainly outside the Barents Sea have, most likely, been transported into the Barents Sea by Atlantic waters from the Norwegian Sea and Norwegian coast. The first observation of *C. lamarckii* in the Barents Sea was recorded during the 2014 BESS survey. In 2017, *C. lamarckii* distribution was similar to that in 2016 (Figure 3.3.15). *C. lamarckii* was recorded at 21 stations (~9% of standard pelagic trawl stations) in western and southwestern regions of the Barents Sea. Single specimens were observed in pelagic catches, with the average catch being 0.04 kg per nmi. Single specimens of the helmet jelly *Periphylla periphylla,* a deep-water jellyfish, were caught at two stations in the western Barents Sea in 2017 (Figure 3.3.15). Distribution of the helmet jelly in 2017 was similar to that in 2016. Only standard pelagic trawl stations are reported here, however, helmet jellies were caught by bottom trawl. Other species are not presented in this report due to technical challenges.

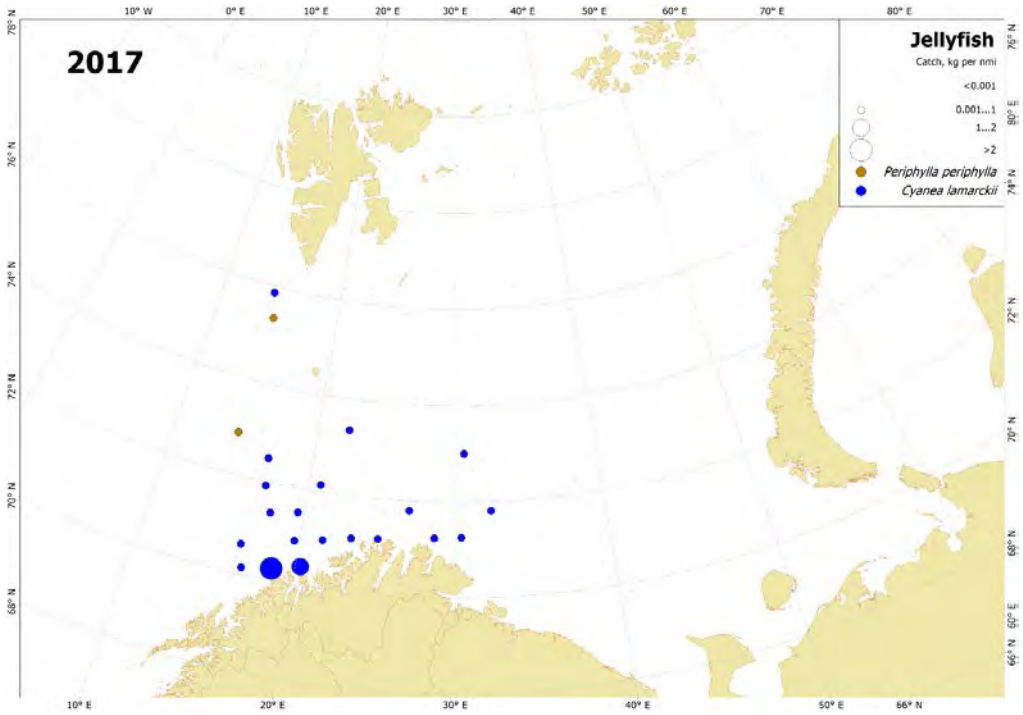

Figure 3.3.15. Distribution and catches (wet weight; kg per nmi) of *Cyanea lamarckii* and *Periphylla periphylla* in the Barents Sea, August-October 2017. Catches both day and night from standard pelagic trawl in the upper 0–60 m layer.

Total biomass of *C. capillata* in upper layers of the water column (0–60 m) of the Barents Sea during August-October 2017 was estimated to be 4.6 million tonnes (Figure 3.3.16). This is the third highest estimate so far, and much higher than the estimated long-term mean for 1980–2017 (1.3 million tonnes). Interannual variation in estimated total biomass of gelatinous zooplankton (dominated by *C. capillata*) based on data from Barents Sea Ecosystem Surveys (1980–2017) is considerable, with peaks also observed in 2001 and 2014 (5 million tonnes); the lowest estimate was in 1997 (0.02 million tonnes).

3.4 Benthos and shellfish

Benthos

Benthos is an essential component of the marine ecosystems. It can be stable in time, characterizing the local situation, and is useful to explain ecosystem dynamics in retrospect. It is also dynamic and shows pulses of new species distribution, such as the snow crab and the king crab, and changes in migrating benthic species (predatory and scavenger species such as sea stars, amphipods and snails with or without sea anemones). The changes in community structure and composition reflect natural and anthropogenic factors. There are more than 3000 species of benthic invertebrates registered in the Barents Sea (Sirenko, 2001), but here we only present the megafaunal component of the benthos collected by trawl and registered (species, abundance and biomass) during the BESS survey. This includes mainly large bodied animals with long lifespans. This includes mainly large-bodied animals with long lifespans. This investigation was initiated in 2005 - only a short timeline relative to investigations related to plankton and fish. Accordingly, interpretation of long-term trends for megabenthic data must be pursued with caution.

Benthos collection. Benthos, collected with the standard demersal trawl gear during the BESS, have been registered annually by benthic taxonomic specialists since 2005 onboard Russian vessels; annual surveys have been conducted during 2007–2013 and 2015–2016 onboard Norwegian vessels. Species identification has been to the lowest possible taxonomic level. In cases where there no specialist was available onboard (2007–2008 in northern Barents Sea in the Norwegian sector), the benthos has only been identified to major benthic group. Work is ongoing between IMR and PINRO specialists to standardize and improve species identification, as well as the catchability of benthos between different trawls and vessels. Several articles have been published based on the resulting high-resolution taxonomic data (Anisimova *et al.*, 2011; Jørgensen *et al.*, 2015a; Jørgensen *et al.*, 2015b).

Megafauna description. The distribution of large benthos groups shows that Porifera (mainly the *Geodia* group) dominate biomass in the west, while Echinodermata (mainly brittlestars) dominate in the east. In the Northeast, Cnidaria (soft corals, such as the sea pen *Umbellula encrinus*, and sea anemones) dominates along with Echinodermata, while Crustacea dominates along with the Echinodermata in the Southeast (Figure 3.4.1).

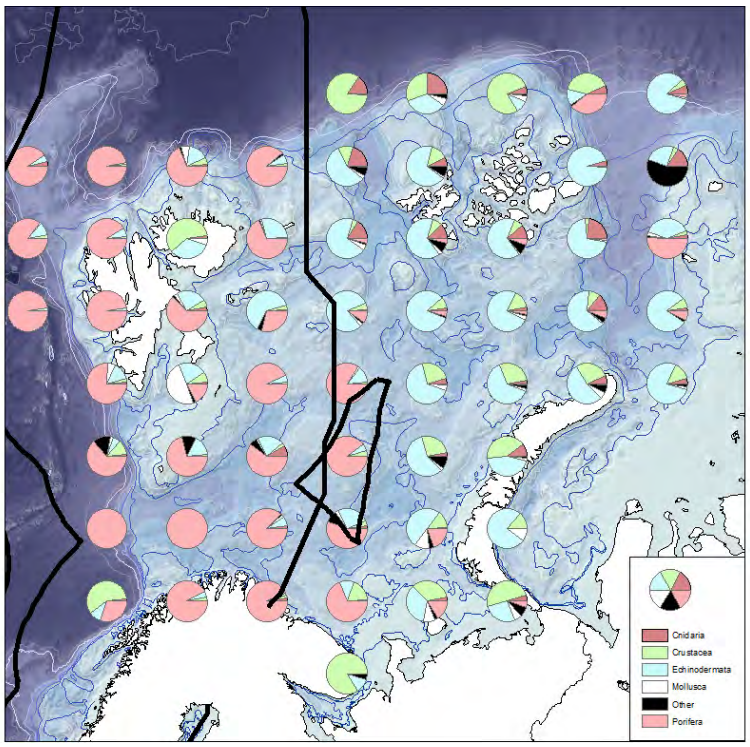

Figure 3.4.1 The main benthos group distribution (in biomass). The data are the integrated mean for the period 2009–2014.

Statistical analyses of monitoring data show that there are four distinct zones of benthos in the Barents Sea (Jørgensen *et al.*, 2015a, Figure 3.4.2). These four zones are characterized with temperate species in the southwestern zone, cold-water species in the eastern zone, arctic species in the northern and northeastern zone, and an area in the eastern Barents Sea where the snow crab, a new non-indigenous large benthic species, are expanding. The period with warmer water entering the Barents Sea has led to migration eastwards and northwards of temperate species and groups (Jørgensen *et al.*,

2015a). The retreating ice front opens for new areas for human impact as well as imposing changes in the planktonic production and annual cycles, with possible impact on the benthic zones.

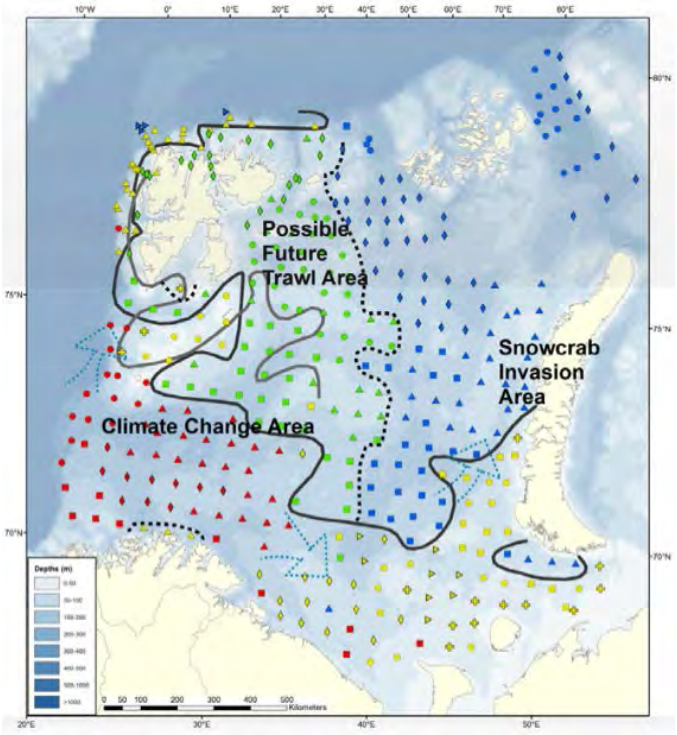

Figure 3.4.2. The baseline map of the Barents Sea mega-benthic zones in 2011, based on fauna similarity (see Jørgensen *et al.*, 2015a for methodology, results and discussion) with the northern (green and blue) and southern (yellow and red) region where the black full line is illustrating the "benthic polar front" in 2011. The grey full line is the approximately oceanographic Polar Front. Dotted line: Is partly illustrating a west-east division. Red: South West subregion (SW) Yellow: Southeast, banks and Svalbard coast (SEW). Green: North West and Svalbard fjords (NW). Blue: North East (NE). Source: IMR.

The status of the megabenthos in 2017 and possible trends.

Interannual fluctuation of the megafaunal biomass

The relatively short monitoring time-series for distribution of benthos (g/nml trawling) shows relative stable large-scale patterns, with high biomass particularly in the Southwest; biomass is also stable in the Northeast, but more variable. In central Barents Sea, biomass has a high level of spatial and temporal variability (Figure 3.4.3) which is difficult to characterize due to the relatively short data time-series.

The eastern part of the Barents Sea has the largest fluctuations in biomass, but non-standardized trawl technicalities may influence some of these fluctuations.

The most problematic years of benthic monitoring to estimate total biomass were: 2005 and 2014 due to reduced research area in Norwegian waters; 2012 and probably 2017 when biomass was overestimated in the Russian zone due to the technical issues with vessels; and 2014, 2015, and 2016 when the Loop Hole area was not sampled because of a commercial snow crab fishery. In addition, in 2016 benthos received low sampling priority in the Norwegian zone causing possible inconsistencies.

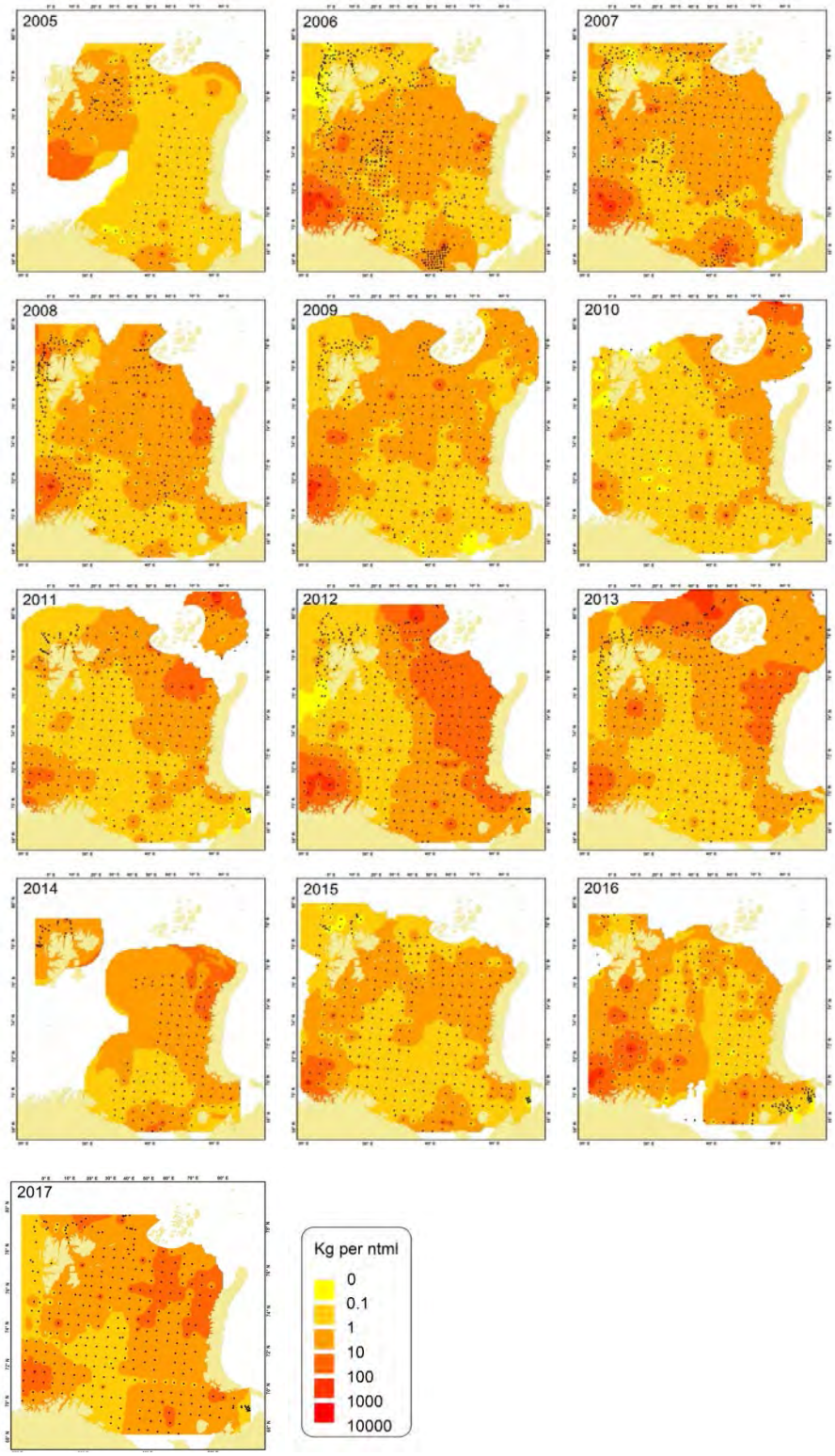

Figure 3.4.3. Distribution of the megabenthos biomass (excluding *Pandalus borealis*) in the Barents Sea from 2005 to 2017.

To estimate long-term dynamics of the benthos, interannual changes of the mean biomass were calculated for the total Barents Sea, then separated into the four sectors "NE", "NW", "SW", and "SE" before being analysed.

The total Barents Sea. Estimates of annual mean biomass for the total Barents Sea fluctuated during the 2006–2017 period (Figure 3.4.4.). However, the short time-series of observations, combined with years without full benthic coverage (2014), and years with technical changes in the Campelen trawl — affecting the catchability of benthic organisms (2012) — limit the ability to draw firm conclusions.

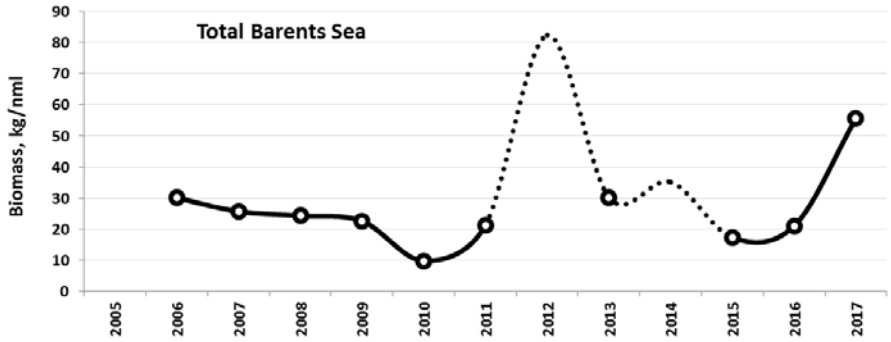

Figure 3.4.4. Interannually dynamics of mean biomass of the megabenthos (without *Pandalus borealis*) for the total Barents Sea during 2005–2017. The total Barents Sea are defined within 15–62°E, 68–80°N, but excludes W. Svalbard (NW of 76.5°N and 16.5°E). Catches >1 t are also excluded. Dotted line (2012 and 2014) means missing coverage.

However, deviations from the 2006–2017 interannual average (biomass anomalies) were lowest in 2010 and 2015–2016 (Figure 3.4.5.). These decreases may be explained by observed temperature minimum 6–7 years earlier. This hypothesis is supported by previous investigations documenting response of the macrobenthos to hydrological fluctuations in the Barents Sea (Blacker, 1957a, b; Nesis, 1960; Lubina *et al.*, 2011, 2016; Denisenko, 2013). But, longer time-series of observations are required to confirm the existence of a correlation between megabenthic biomass and short-time climatic fluctuations.

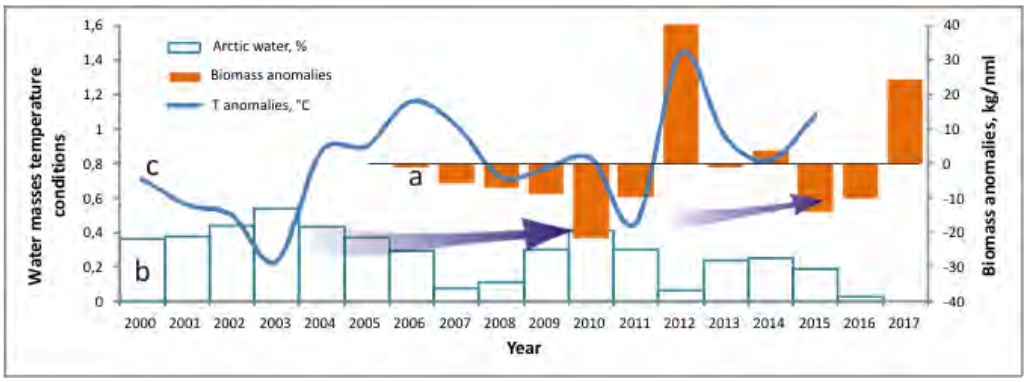

Figure 3.4.5. Temporal biomass fluctuations and oceanographic features of the Barents Sea. a) Megafauna biomass deviation from the interannual average level (2006–2017), b) area of the bottom covered by arctic water (part of the total) (WGIBAR report 2017, Figure 3.1.17) and c) the temperature anomalies in the Kola sections (http://www.pinro.ru)

The year 2010 had the largest negative anomaly for megabenthos biomass. This corresponds to the coldest year (2003), and with a delay of 7 years — reported to be the benthic response time. The second largest negative anomaly (2015–2016) was less dramatic, and can be correlated with decreasing water mass temperatures observed during 2010–2011.

Northwest (NW) and Southwest (SW). During most of the long-term monitoring period, the SW region had higher biomass than the NW region, although sponge catches >1T in the SW were excluded. Mean biomass of the NW, SW, and the total Barents Sea was lowest in 2010 (Figure 3.4.6). Subsequently, all three values increased until 2013. The 2014 value is unknown due to missing coverage, but mean biomass increased between 2015 and 2017 to the highest measured (48 kg/nml) for the SW Barents Sea; and a value comparable to the max year (2009) in the NW (33 kg/nml). Long-term variation in mean biomass of the NW, SW, and total Barents Sea shows strong correlations. This may indicate that the western Barents Sea is driven by factors similar to those driving the total Barents Sea.

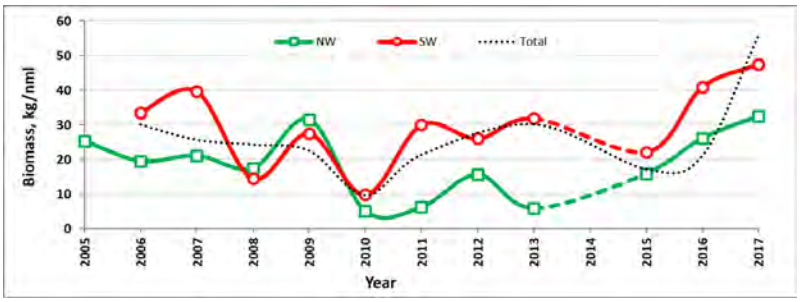

Figure 3.4.6. The interannually mean biomass fluctuation of the SW (red),) and NW (green) sectors of the Barents Sea in the 2005–2017. The dotted line is the total Barents Sea mean biomass (see also fig y3). Biomass of *Pandalus borealis* and all catches more than 1T are excluded NW=74-80°N 15-40°E but excluding all stations W and N of Svalbard, SW=65-74°N and 10-40°E. All stations west and north of Svalbard and all sponge catch >1T excluded.

Southeast (SE) and Northeast (NE). During the entire monitoring period (other than 2006) mean biomass of the megabenthos in the SE region was below that of the total Barents Sea (Figure 3.4.7). This might be explained by: 1) the high level of commercial trawling in this area; and 2) hydrological features of the Pechora Sea area (brackish water from Pechora River run-off). The first possible explanation becomes more plausible considering the high benthic biomass observed in the NE, where there is no trawling activity (Ljubin *et al.*, 2011).

Figure 3.4.7. The interannually mean biomass fluctuation of the SE (red line with yellow circles) and NE (blue with and purple without snow-crab biomass). The dotted line is the Barents Sea mean biomass (see also Figure y3). NE=74-80°N and 40-62°E, SE=65-74°N and 40-62°E.

The highest biomass (catch >1T excluded) in the Barents Sea was recorded in the NE. In most of the years monitored, biomass in the NE was above the mean for the total Barents Sea (Figure 3.4.7). But, following 2013, mean biomass decreased (Figure 3.4.3), to a record low (<20 kg/n.ml) in 2016, and below the total Barents Sea mean. In 2017,

however, record high biomass was observed in the NE (116 kg/nml); the highest value recorded both with and without snow crab biomass.

Since 2013, benthos biomass has decreased. This could be explained by both: overlap with the maximum distribution of snow crab (see below), and; increasing bottom temperatures (chapter 3.1). But the strong increase of benthos biomass in 2017 the NE could be an effect of the trawl-sampling.

State of selected benthic species

Snow crab

The snow crab (*Chionoecetes opilio*) is a non-indigenous species in the Barents Sea; first recorded in 1996 in the Goose Bank area. Of the several theories explaining the appearance of snow crab in the Barents Sea, introduction via ballast water is the most popular; this believed to have occurred during the 1997–1993 period (Strelkova, 2016).

Regular annual monitoring of the snow crab population began with the Barents Sea the Ecosystem Survey in 2004. This survey is, currently, the most important source of information on population status.

Assessments of snow crab dynamics based on ecosystem survey data (Table 3.4.1 and Figures 3.4.8 and 3.4.9) indicate that in the Barents Sea the snow crab population is still developing.

Table 3.4.1 Characteristics of the snow crab catches during ecosystem surveys of 2005-2017

Year	Total number of station	Number of station with snow crab	Total numbers, ind.	Total biomass, kg	Mean abundance, ind./nml	Mean biomass, kg/nml
2005	649	10	14	2.5	1	0.3
2006	550	28	68	11	3	0.5
2007	608	55	133	18	3	0.4
2008	452	76	668	69	11	1.2
2009	387	61	276	36	6	0.8
2010	331	56	437	22	10	0.5
2011	401	78	6 219	154	99	2.4
2012	455	116	37 072	1 169	395	12.6
2013	493	131	20 357	1 205	210	12.7
2014	304	78	12 871	658	206	10.5
2015	335	89	4 245	378	57	5.2
2016	317	84	2 156	137	26	1.9
2017	376	159	25 878	1422	147	10.0

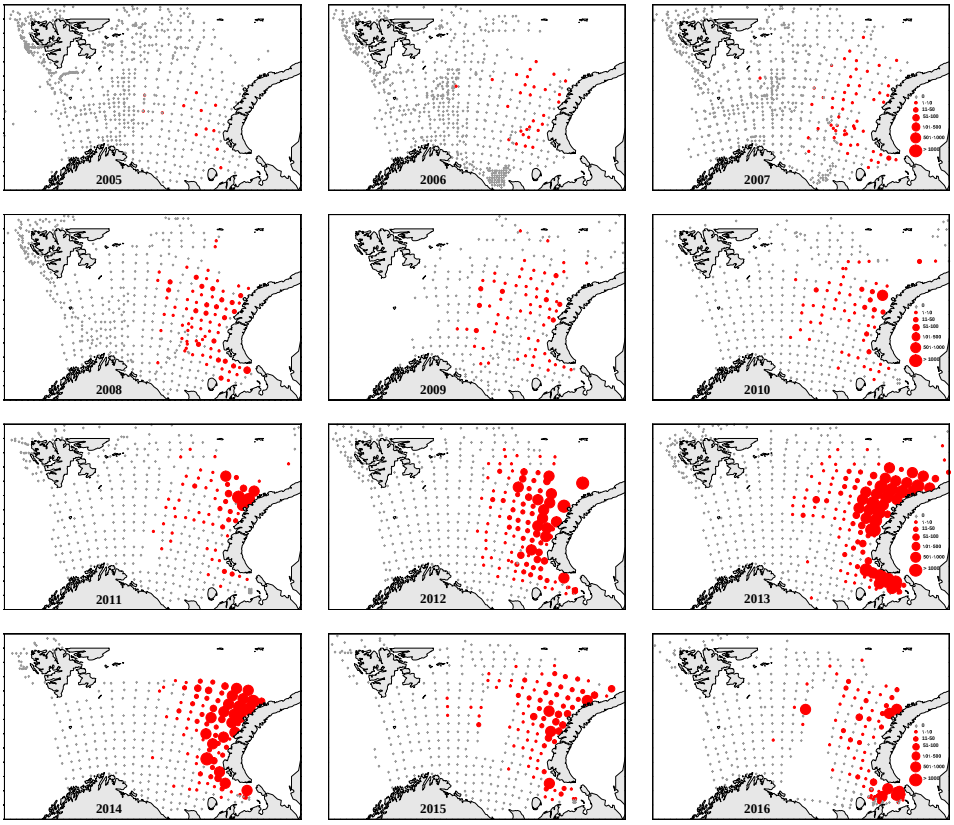

Figure 3.4.8. Dynamics of the snow crab population in the Barents Sea, in number of individuals in 2005–2016 (according to ecosystem data).

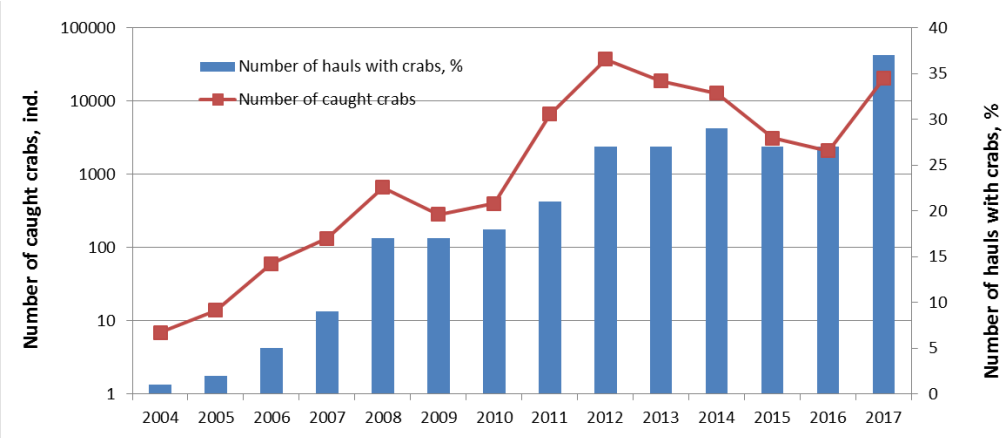

Figure 3.4.9. The dynamic of the snow crab population in the Barents Sea given as the total number of crabs (blue bars) and the number of trawl hauls with crabs (red line) during the Ecosystem Survey 2004–2017.

In 2017, as in previous years, the densest aggregations of snow crabs (more than 1000 ind/nml) were concentrated in the central part of the Barents Sea in the Loop Hole area and near Novaya Zemlya archipelago within the Russian Economic Zone. In 2017, the snow crab was for the first time recorded at Svalbard. One record was made in Storfjord at 162 m depth (two immature males with 47 mm and 48 mm carapace widths); the other was northwest of Svalbard archipelago at 506 m depth (one juvenile male with a 14 mm carapace width) (Figure 3.4.10.).

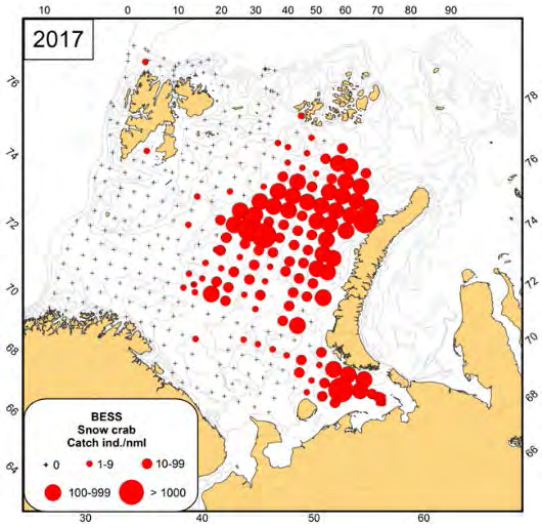

Figure 3.4.10. Distribution of the snow crab (*Chionoecetes opilio*) in the Barents Sea in August-October 2017 as observed by the Ecosystem Survey.

Studies of snow crab population size structure indicate that abundant generations appear periodically, and that this affects the overall population dynamics in the Barents Sea. During the ecosystem survey period, abundant generations were recorded in 2009, 2012, and 2015–2016 (Figure 3.4.11) (Bakanev and Pavlov, 2016).

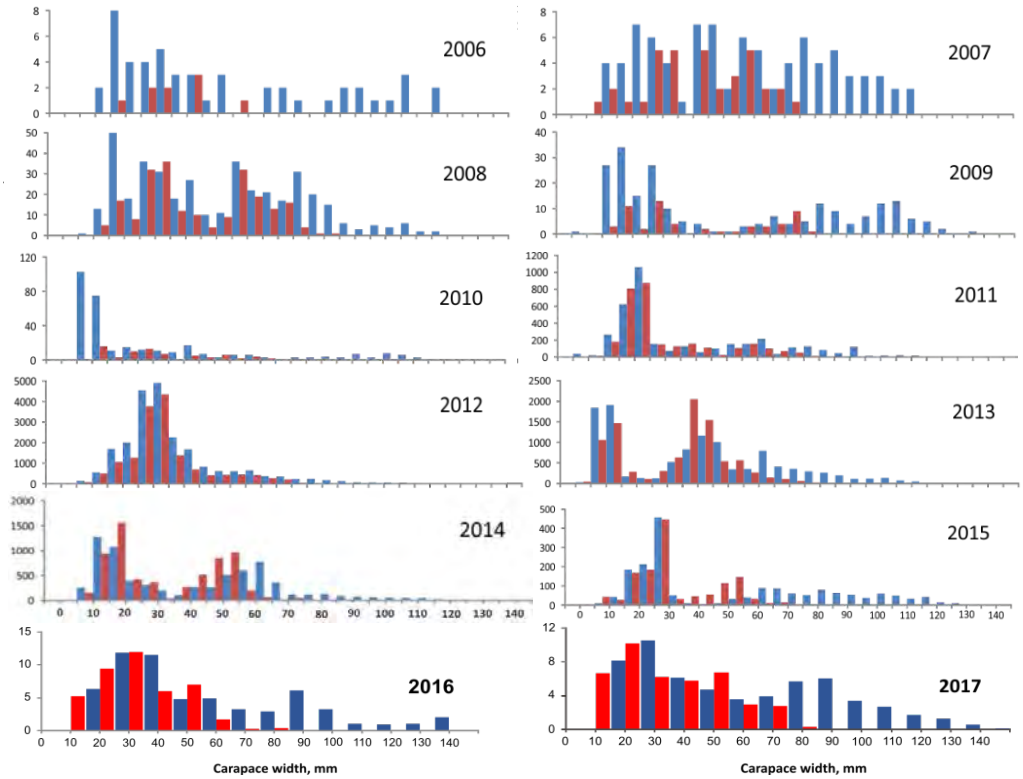

Figure 3.4.11. The sex and size structure of the snow crab population from 2006–2017 (Bakanev and Pavlov, 2016, with editions). On vertical axes: 2006–2015 – number of individuals; 2016–2017 – abundance, %.

Since 2003, snow crabs in the eastern part of the Barents Sea, have been recorded with bottom fish species (cod, haddock, catfish, American dub, and starry ray) in their stomachs.

In recent years, snow crabs have become one of the most important prey species for cod. In 2011–2012 it made up about 2% of the cod stomachs examined, in 2013–2014 it made up 4–7%, and in 2015–2016 it made up 5–6%. All size categories of snow crab (up to 120 mm carapace width) were eaten by cod. Cod feeding on snow crabs was most intensive (up to a quarter of total stomach content) during autumn at Novaya Zemlya, Great Bank, Central Banks.

Northern shrimp

Northern shrimp (*Pandalus borealis*) is common and widely distributed in the Barents Sea. During the 2017 BESS survey, it was recorded at 281 of the 376 trawl stations; shrimp biomass varied from several grammes to 439.8 kg per nautical mile, with an average catch of 13.8±1.7 kg/nml. The densest concentrations of shrimp were registered in central Barents Sea, around Spitsbergen, and in Franz Victoria Trough (Figure 3.4.12). In 2017, the northern shrimp biomass index (method of squares) was 314.2 thousand tons; 1.5% higher than in 2016, and 8% lower than the average index value.

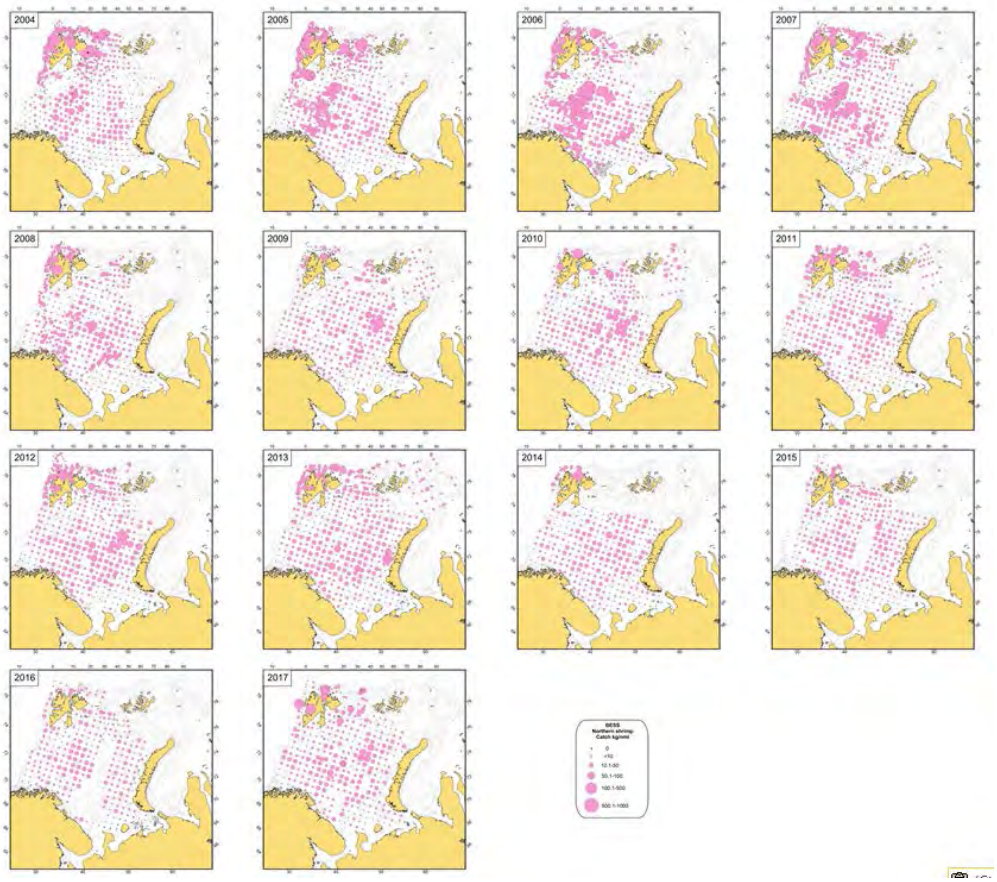

Figure 3.4.12. Distribution of the Northern shrimp (*Pandalus borealis*) in the Barents Sea, August–October 2004–2017

During the 2006–2007 BESS surveys, average catches of the shrimp varied from 4 to 11 kg (Figure 3.4.13), all stayed stable around the average level, regardless of the fishery. The increase of biomass in 2017 may be connected with the investigations in Franz Victoria Trough with dense biomasses of shrimp.

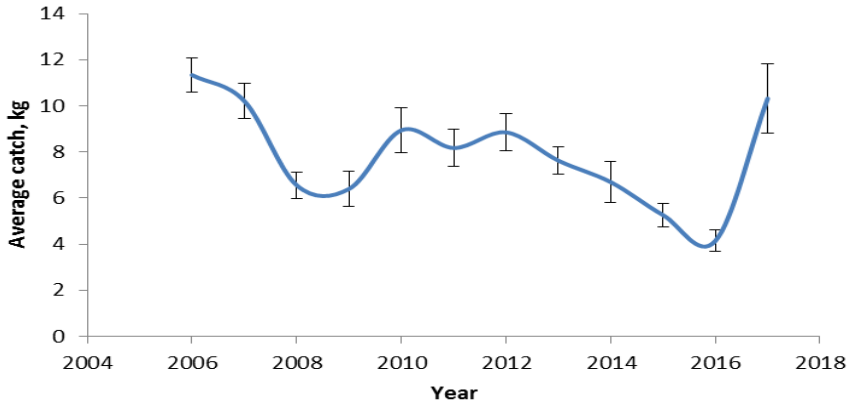

Figure 3.4.13. Average catches of the Northern shrimp (*Pandalus borealis*) in the Barents Sea during ecosystem surveys 2006-2017

Biological analyses of the northern shrimp population in the eastern part of the survey area were conducted in 2017 by Russian scientists. Similar to 2016, the bulk of the population consisted of younger individuals: males of 12–27 mm carapace length; and females of 17–30 mm carapace length (Figure 3.4.14).

In the western survey area, as in the eastern part of the Barents Sea, smaller shrimp (males 11–23 mm carapace length, and females 18–28 mm carapace length) were most abundant; comprising up 64% of catches (Figure 3.4.15)

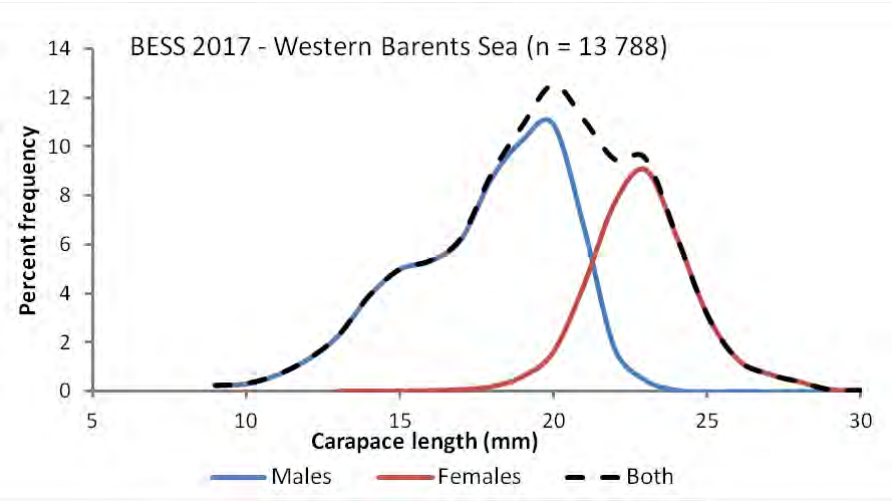

Figure 3.4.15. Size and sex structure of catches of the Northern shrimp (*Pandalus borealis*) in the western Barents Sea, August–October 2017

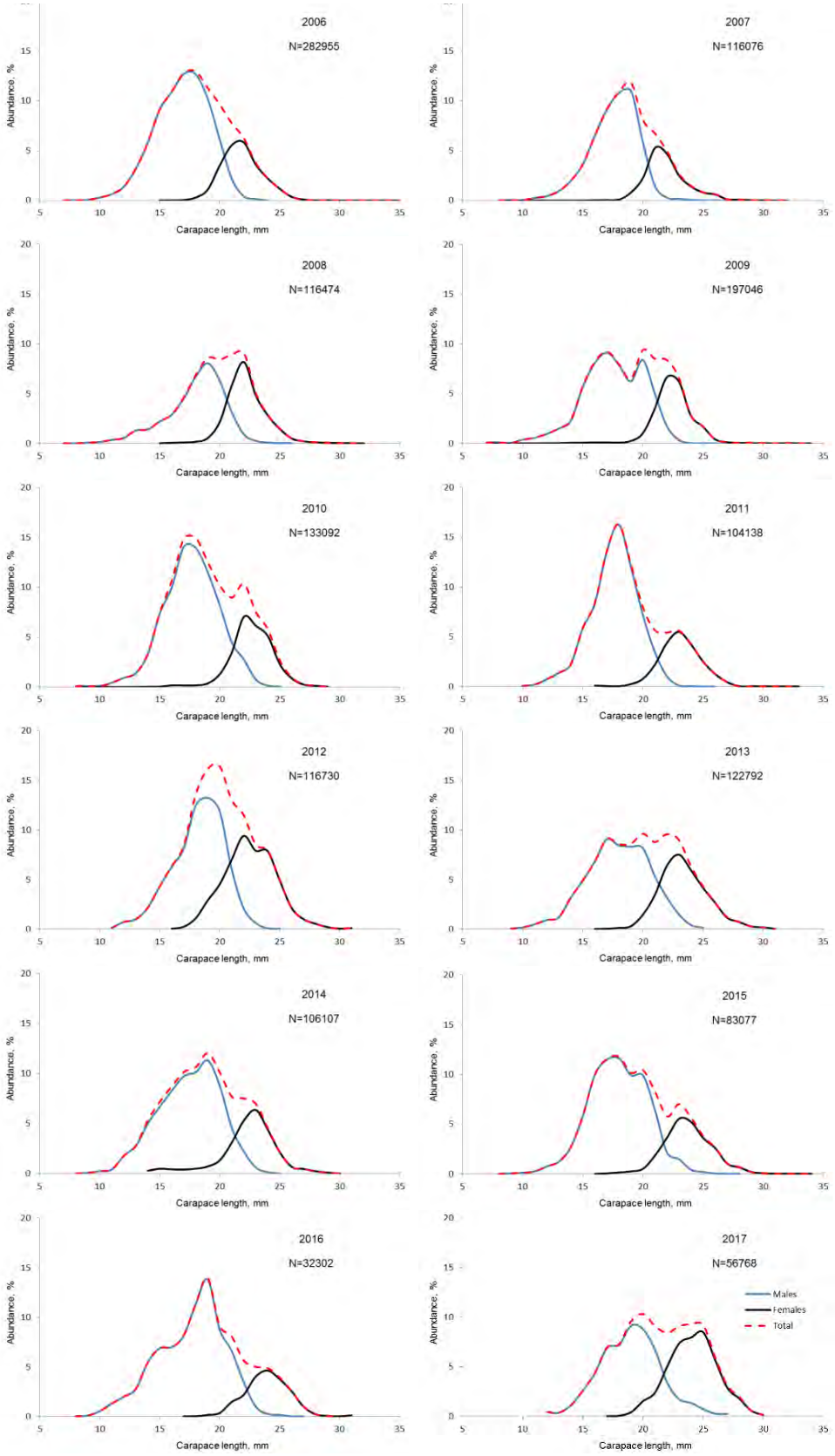

Figure 3.4.14. Size and sex structure of catches of the Northern shrimp (*Pandalus borealis*) in the eastern Barents Sea, August–October 2006–2017

3.5 Pelagic fish

Total biomass

Zero group fish are important consumers on plankton and are prey of other predators, and, therefore, are important for transfer of energy between trophic levels in the ecosystem. Estimated total biomass of 0-group fish species (cod, haddock, herring, capelin, polar cod, and redfish) was 1.92 million tonnes during August–September 2017; slightly above the long-term mean of 1.76 million tonnes (Figure 3.5.1). Biomass was dominated by cod and haddock, and mostly distributed in central and northern-central parts of the Barents Sea.

Capelin, polar cod, young herring, and blue whiting constitute the bulk of pelagic fish biomass in the Barents Sea. Note that the acoustic target strength for blue whiting has been changed recently, and the time-series has been recalculated. Total biomass of the main pelagic species (age 1 and older fish) in the Barents Sea in 1986–2017 has fluctuated between 0.5 and 9 million tonnes; mainly driven by fluctuations of the capelin stock. In 2017, cumulative biomass of capelin, herring, polar cod, and blue whiting was close to the long-term mean (Figure 3.5.2).

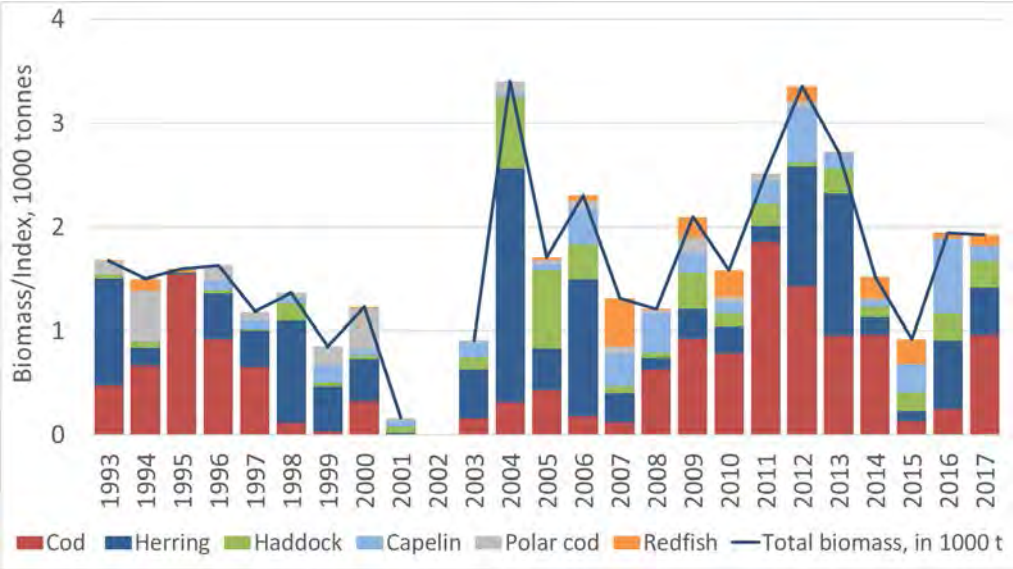

Figure 3.5.1. Biomass of 0-group fish species in the Barents Sea, August–October 1993–2017.

Capelin, young herring, and polar cod constitute the bulk of pelagic fish biomass in the Barents Sea. In some years (e.g. 2004–2007 and 2015–2016), blue whiting (*Micromesistius poutassou*) also have had relatively high biomass in the western Barents Sea (east of the continental slope). Total biomass of the main pelagic species during 1986–2017 has fluctuated between 0.5 and 9 million tonnes; mainly driven by fluctuations in the capelin stock. In 2017, the cumulative biomass of capelin, herring, polar cod, and blue whiting was close to the long-term mean (Figure 3.5.2).

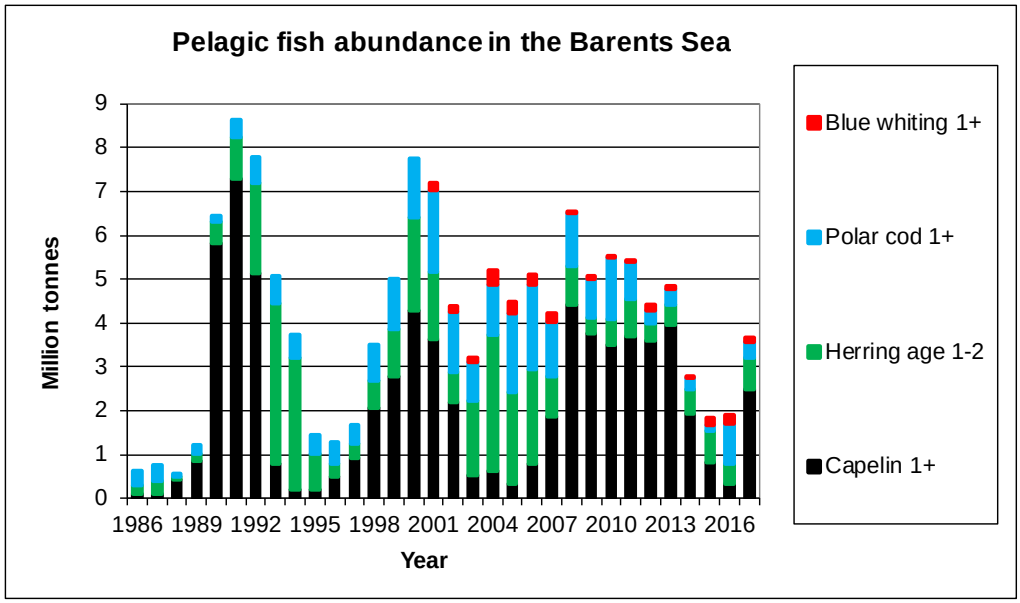

Figure 3.5.2 Biomass of main pelagic fish species (excluding 0-group stage) in the Barents Sea, August-October 1986–2017.

Capelin

Young of the year

As in 2016, 0-group capelin was distributed widely in the Barents Sea with dense concentrations in north-central Barents Sea. High densities of 0-group capelin were observed in the southeastern Barents Sea. This survey area was not completely covered; therefore, the 0-group abundance index is underestimated. Average fish length was 5.4 cm, close to the 2016 estimate, and larger than the long-term mean (1980–2017). The relatively large size of 0-group capelin likely indicates suitable living conditions during summer, and increases the likelihood of survival through winter. Capelin length varied from 2 to 7.4 cm; however, the length of most (85%) individuals was between 4.0 and 6.4 cm. The abundance index of 0-group capelin in 2017 was below the long-term mean (Figure 3.5.3).

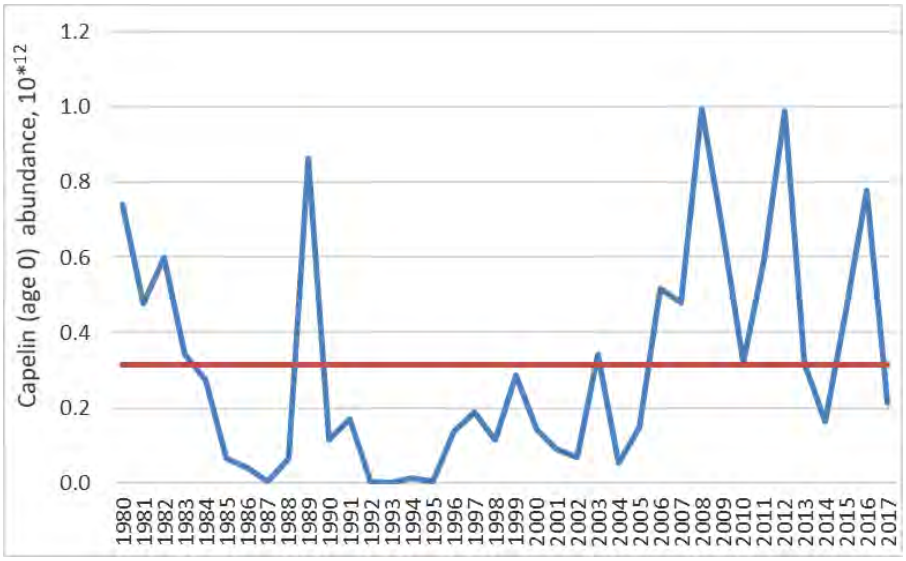

Figure 3.5.3. 0-group capelin abundance, corrected for trawl efficiency, in the Barents Sea 1980–2017. Orange line shows long-term mean for the period 1980–2017, while blue line indicate 0-group abundance fluctuation.

Adult capelin

The total adult capelin stock is estimated to be approximately 2.5 million tonnes; close to the long-term mean level (2.9 million tonnes); and 7.5 times higher than the 2016 estimate. About 69% (1.72 million tonnes) of the 2017 stock is above 14.0 cm in length, therefore considered to be maturing (Figure 3.5.4).

Age 2 capelin (2015 year class) dominated stock composition (45%); the 2014 year class (age 3) made up 8% of the stock. Recruitment-at-age 1 (2016 year class) was estimated at 86 billion individuals, which is below the average level. Older aged individuals (4+) were rare. (Figure 3.5.5)

In light of 2017 survey results, the survey results from 2016 become questionable. In 2017, the 2015 year class was estimated to be 4 times as abundant (Figure 3.5.5), and the 2014 year class twice as abundant as was estimated in 2016. This indicates a significant underestimation of the capelin stock based on 2016 survey data, or a major overestimation in 2017. The 2017 survey was considered an improvement over that in 2016, in terms of both: synopticity between the various ships taking part; and density of coverage in the main area of distribution. Consequently, it is considered more likely that the stock was underestimated in 2016 than that it was overestimated in 2017.

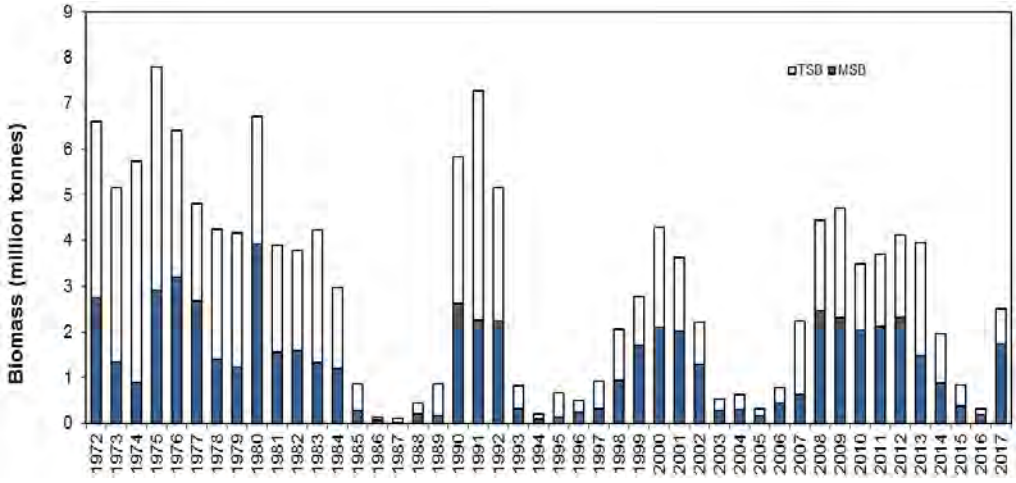

Figure 3.5.4. Capelin age1+ biomass by acoustic survey data in 1972–2017. Maturing stock (MSB) and total (TSB).

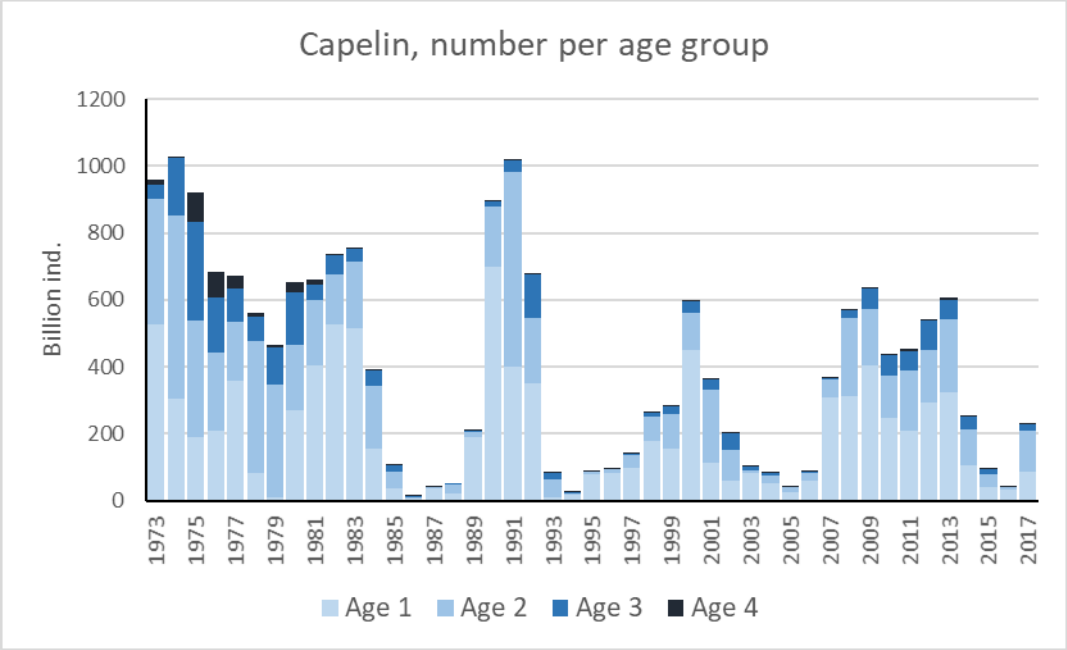

Figure 3.5.5. The capelin stock age composition (age 1-4) during 1972–2017. (Note: age 5 and older was removed due to negligible numbers in the total stock.)

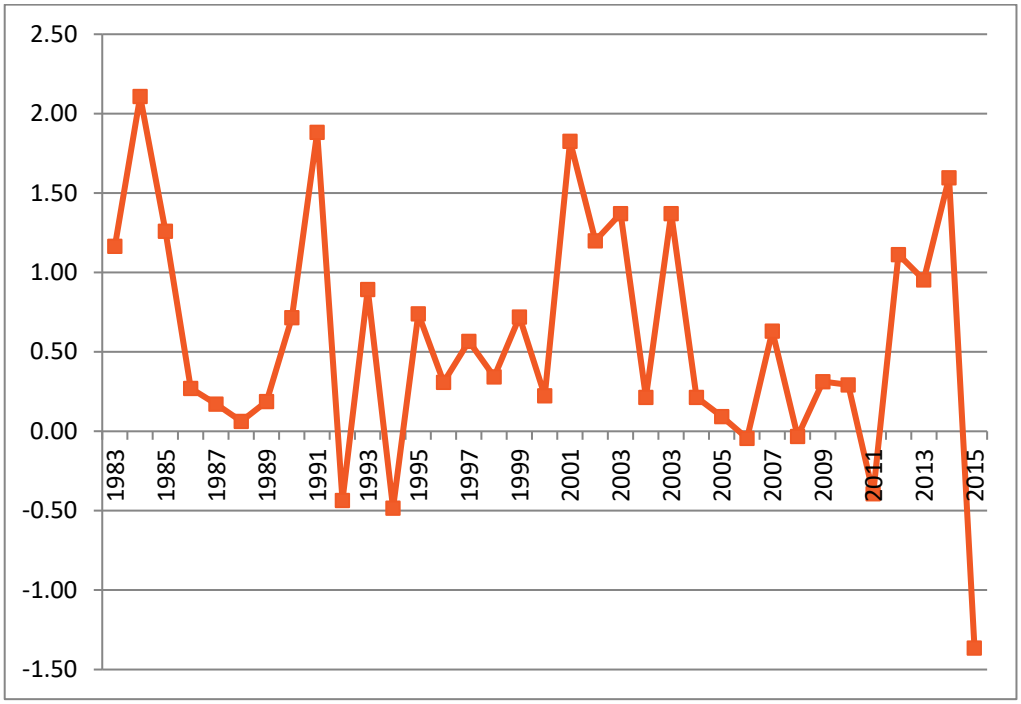

Figure 3.5.6. Natural mortality of age 1-2 capelin, as estimated from the acoustic surveys (x-axis shows cohorts not years).

Underestimation of the capelin stock in 2016 is being investigated. Among the reasons suggested are: misidentification of acoustic recordings; and that the survey was carried out in the opposite direction in 2016; north–south whereas south-north is standard. Measures have been taken avoid this situation in future surveys. It should be noted that in 2017 the main capelin area was covered with cruise tracks twice as dense as normal. In addition, acoustic and trawl data from 2016 will be further examined; this work is to be presented at the Russian-Norwegian Symposium in June 2018.

The geographic distribution of capelin density in 2017 is shown in Figure 3.5.7. The distribution was much wider than in 2016, and almost as extensive as in 2013; the year with widest observed capelin distribution. Capelin schools were recorded up to 81°30N between Svalbard and Franz Josef Land. The majority of capelin was found southeast of the King Karls Land. Mature capelin were also observed in small numbers in the bottom layer at a significant proportion of the survey area. Young capelin (1-year-olds) were mainly observed in the western part of survey area.

Average length of capelin in 2017 was 12.8 cm; average weight was 11.03 g. Compared to 2016, average fish weight for ages 2 and 3 (the main age groups in the stock) decreased slightly, remaining above the average level. For ages 1 and 4, the increasing trend in weight at age continued, as discussed in the interactions section.

Dynamics of changes in average weight-at-age reflect the capelin feeding conditions during the summer-autumn period. These conditions are determined not only by the stock size, but also by the state of the plankton community in the Barents Sea. It can assumed that in 2017 the food base for capelin (number and species composition of zooplankton) was favorable.

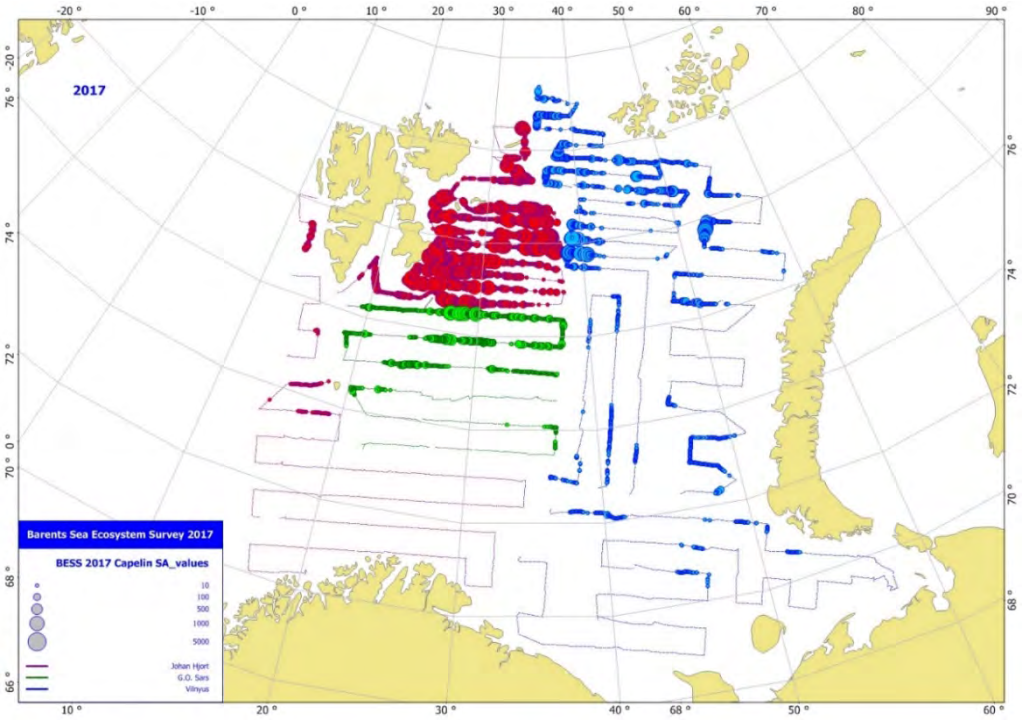

Figure 3.5.7. Estimated total acoustic density distribution of capelin, August–October 2017. Circle sizes corresponding to SA values per nautical mile.

Herring

Young of the year

In 2017, 0-group herring were more widely distributed than in previous years, and were observed in central, northern, and southeastern areas, and west of Svalbard/Spitsbergen. The densest concentrations of herring were found in the central Barents Sea, and close to the Finnmark coast (northern Norway). The length of 0-group herring varied between 4.0 and 11.4 cm; most (93%) were 6.0–8.9 cm long. In 2017, the mean length of 0-group herring was 7.4 cm; close to the long-term mean (7.1 cm). The 2017 year class was close to the long-term mean, and can be characterized as average (Figure 3.5.8).

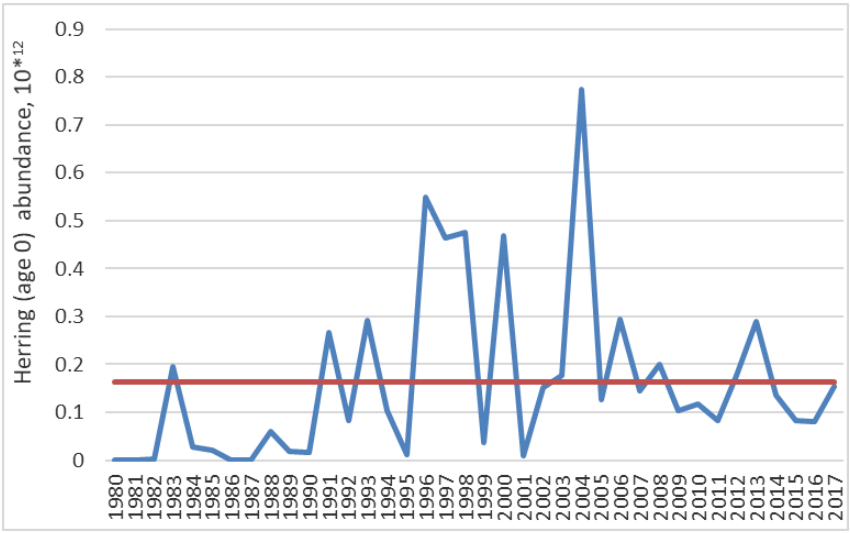

Figure 3.5.8. 0-group herring abundance, corrected for trawl efficiency, in the Barents Sea 1980–2017. Orange line shows long-term mean for the period 1980–2017, while the blue line indicates 0-group abundance fluctuation.

Herring age 1-2

Figure 3.5.9 shows the biomass of age 1 and 2 herring in the Barents Sea. During 2013–2017, abundance of young herring sampled during the ecosystem survey has been relatively stable. Biomass of young herring in 2017 was the highest since 2005, and well above the long-term average. Abundance of 1-year-olds in 2017 was close to the estimate for the 2004 year class, which turned out to be very strong (35 vs. 46 billion individuals). Figure 3.5.8 shows biomass of age 1 and 2 herring in the Barents Sea, calculated based on the last ICES assessment for age 2+ and assuming M=0.9 for age 1.

Figure 3.5.10 shows herring distribution in 2017 with highest amounts in the southern Barents Sea.

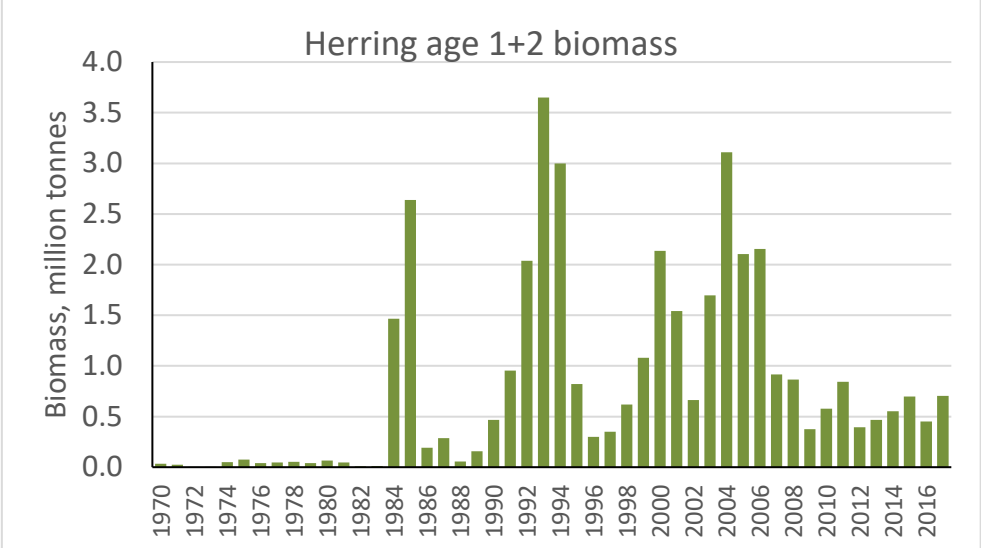

Figure 3.5.9. Age 1 and 2 NSS herring biomass in the Barents Sea – based on WGWIDE VPA estimates (ICES 2017b).

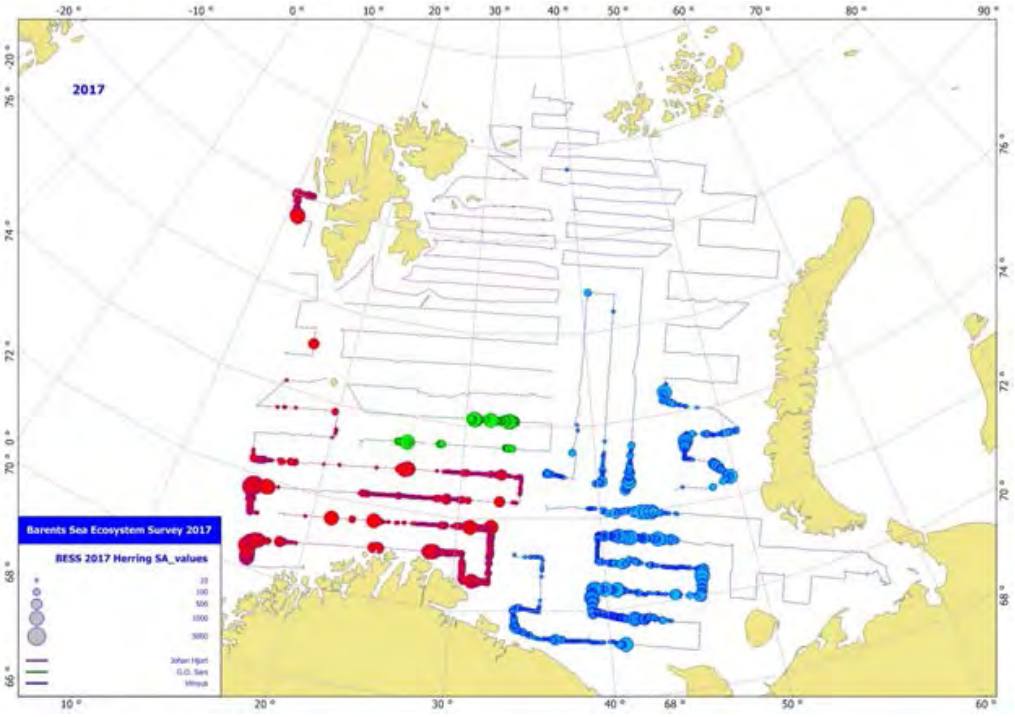

Figure 3.5.10. Estimated total density distribution of herring, August-October 2017. Circle sizes corresponding to SA values per nautical mile.

Polar cod

Polar cod is a true Arctic species with a circumpolar distribution. Traditionally, the world's largest population of this species has been found in the Barents Sea.

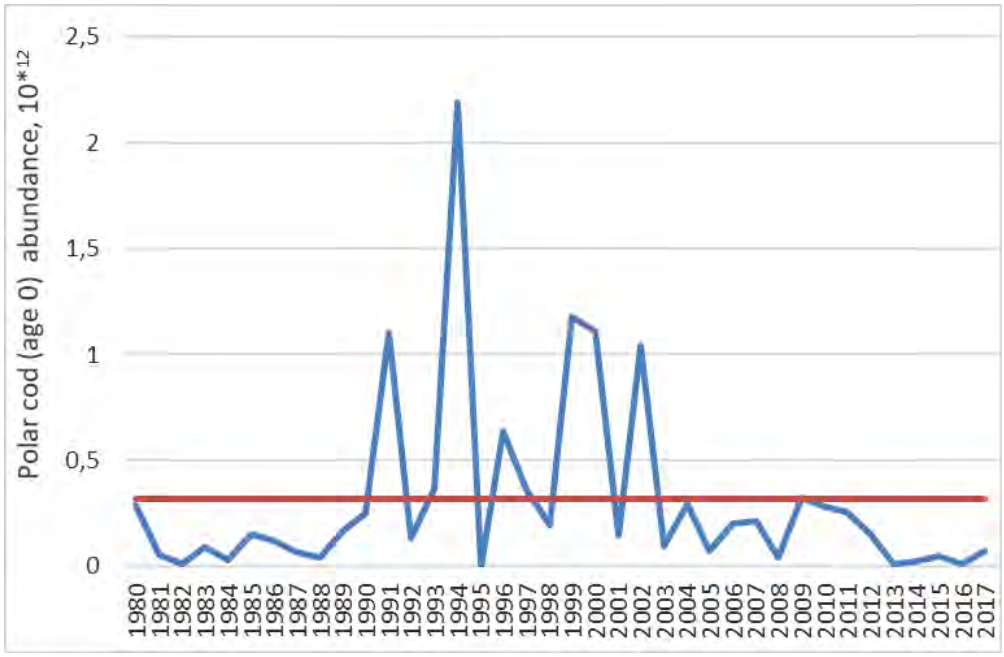

Figure 3.5.11. 0-group polar cod abundance, corrected for trawl efficiency, in the Barents Sea 1980–2017. Red line shows long-term mean for the period 1980–2017, while the blue line indicates 0-group abundance fluctuation

Young of the year

In 2017, as in previous years, distribution of 0-group polar cod was split into two components: western (around Svalbard-Spitsbergen); and eastern (off the western coast of Novaya Zemlya). The eastern component is usually distributed along the southwestern coast of Novaya Zemlya; in 2017, however, part of the area west of Novaya Zemlya was not covered by the survey. Thus, 2017 distribution and abundance indices are likely underestimated due to lack of complete coverage. The length of polar cod varied between 2 and 7.4 cm, and most were between 4.0 and 5.9 cm. The mean length of 0-group polar cod (5.0 cm) was higher than the long-term mean (4.1 cm). The abundance index for the western component was lower than in 2016; approximately 1/8th of the long-term mean. Estimated biomass for 0-group polar cod was only 4 thousand tonnes; 1/24th of the long-term mean (Figure 3.5.11). Abundance indices of 0-group polar cod have been extremely low for several years; indicating a lack of spawning success and/or that a large proportion of the 0-group are distributed outside the standard survey area.

Adult polar cod

In 2017, estimated total abundance and biomass of polar cod in the Barents Sea decreased significantly. Estimated total-stock biomass (TSB) was only 357 thousand tonnes; approximately 38% of the 2016 estimate. Total stock number (TSN) was only about 23% of the 2016 estimate. The 2015 year class decreased from an estimated 95 billion in 2016 to 8.27 billion individuals in 2017. Nevertheless, fish in the 2015 year class contributed most (56%) to stock biomass. Estimated abundance of the 2016 year class was low (13.81 billion individuals, Figure 3.5.12).

Such significant fluctuations in the polar cod stock may be the consequence of variations in natural mortality due to consumption by cod and other predators, but possibly also because part of polar cod stock was distributed outside the standard survey area in 2017. Overestimation of the polar cod stock in 2016 should not be ruled out.

According to the 2016 BESS, there was a significant increase in the number of polar cod in 2016. However, the dramatic decline stock in 2017 cast doubt as to the quality of the 2016 survey. Accordingly, acoustic and trawl data from 2016 will be further investigated, and this work presented at the Russian-Norwegian Symposium in June 2018.

As in previous years, the main concentrations of polar cod were found in the northeastern parts of the survey area, north of 78°N (Figure 3.5.13). Scattered concentrations were observed along the southern coast of Novaya Zemlya and near the Svalbard (Spitsbergen) archipelago.

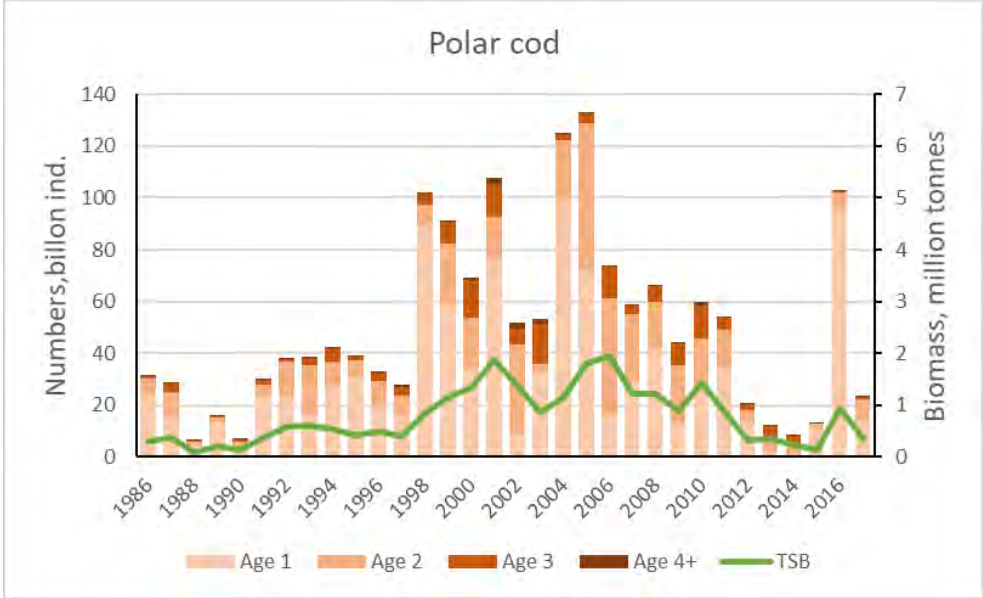

Figure 3.5.12. Total abundance in billions (colored bars and left axis), and biomass (green line and right axis) of polar cod in the Barents Sea (acoustic survey and BESS data), August-September 1986–2017. (2003 numbers based on VPA due to poor coverage in survey).

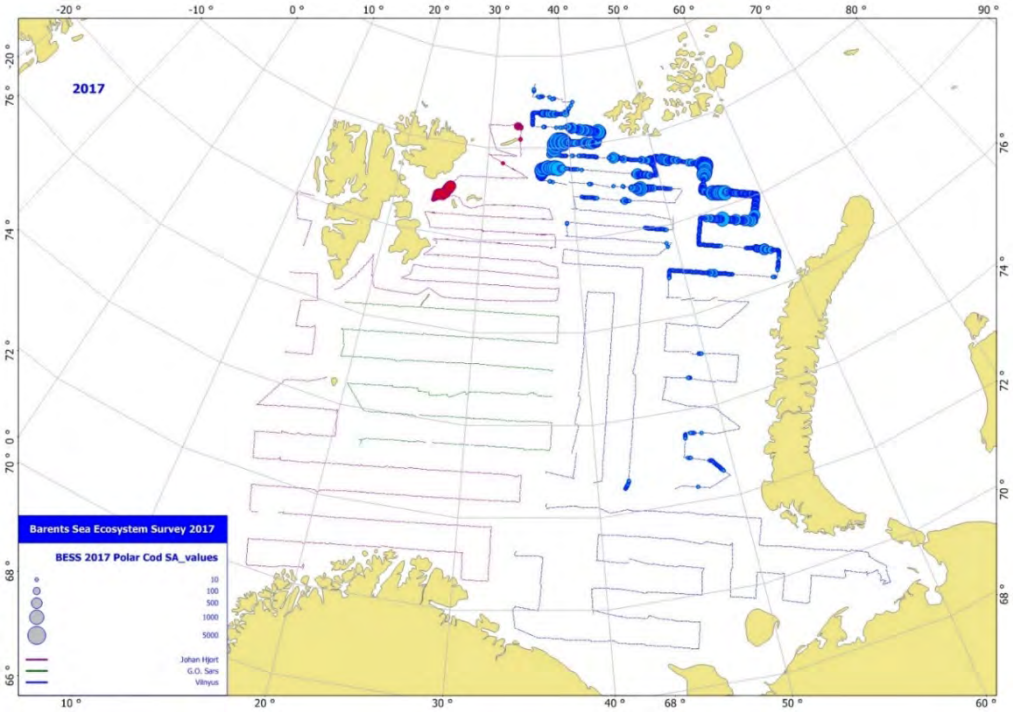

Figure 3.5.13. Estimated total density distribution of polar cod, August–October 2017. Circle sizes corresponding to S_A values per nautical mile.

Blue whiting

Acoustic estimates of the Barents Sea blue whiting stock have been made since 2004. After 2017 the BESS data time-series was recalculated applying a new target strength equation (Pedersen *et al.*, 2011), and a standardized area; this resulted in an overall reduction in estimated biomass to about 1/3rd of previous estimates. During 2004–2007, estimated biomass of blue whiting in the Barents Sea was >200 000 tonnes (Figure 3.5.14), but decreased abruptly in 2008 and stayed low until 2012; after which time it has been variable. In 2017, blue whiting biomass was estimated at about 115 000 tonnes;

a decrease from 2016 (Figure 3.5.14). Blue whiting migrate from the Norwegian Sea into deeper parts of the Barents Sea (Figure 3.5.15) when the stock is large and when sea temperatures are high.

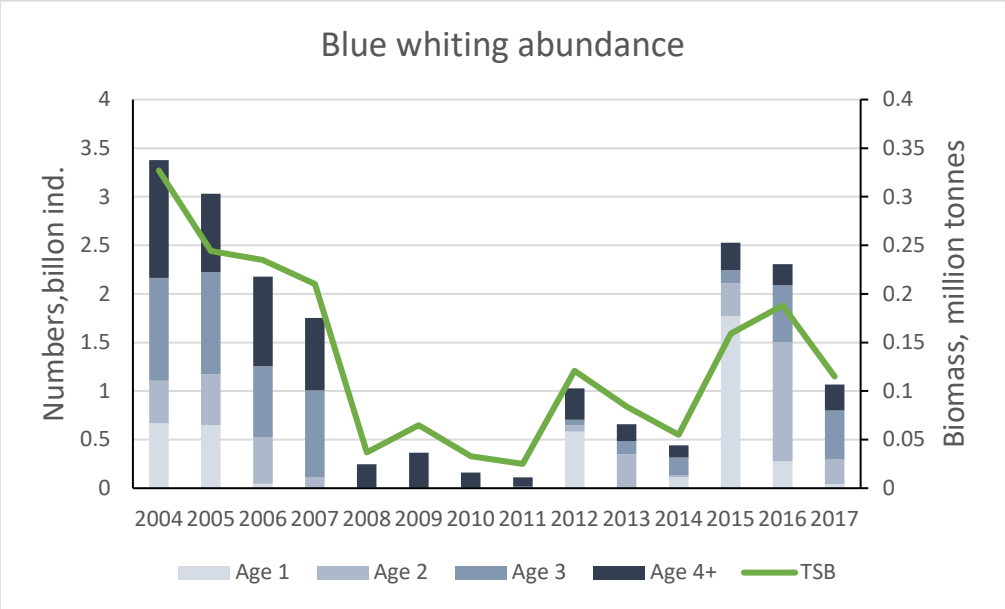

Figure 3.5.14. Total abundance in billions (colored bars and left axis), and biomass (green line and right axis) of blue whiting in the Barents Sea (BESS data revised in 2017), August–September 2004 –2017.

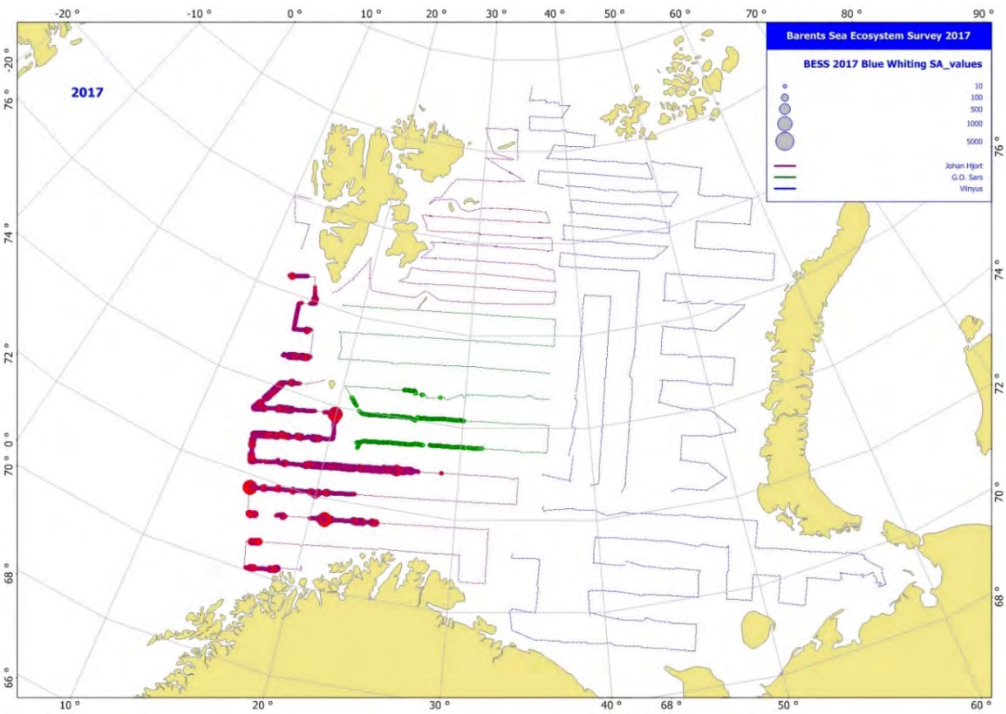

Figure 3.5.15. Estimated distribution of blue whiting, August-October 2017. Circle sizes corresponding to S_A values per nautical mile.

3.6 Demersal fish

Most Barents Sea fish species are demersal (Dolgov *et al.,* 2011); this fish community consists of about 70–90 regularly occurring species which have been classified into zoogeographical groups. About 25% are Arctic or mainly Arctic species. The commercial species are all boreal or mainly boreal (Andriashev and Chernova, 1995), except for Greenland halibut (*Reinhardtius hippoglossoides*) that is classified as either Arcto-boreal (Mecklenburg *et al.,* 2013) or mainly Arctic (Andriashev and Chernova, 1995).

Distribution maps for cod, haddock, long rough dab, Greenland halibut, redfish, and six other demersal fish species can be found at: http://www.imr.no/tokt/okosystemtokt_i_barentshavet/utbredelseskart/en, and are based on data from the BESS.

Abundance estimates are available for the commercial species that are assessed. Figure 3.6.1 shows biomass of cod, haddock, and saithe (*Pollachius virens*) from the ICES AFWG assessments made in 2017. Saithe occurs mainly along the Norwegian coast and off the coast south of the Barents Sea; few occur in the Barents Sea itself. Total biomass of these three species is close to the highest recorded in time-series dating back to 1960. Greenland halibut and redfish, in particular *S. mentella,* are important commercial species with large part of their distribution within the Barents Sea. Time-series of biomass estimates for *S. mentella* and Greenland halibut are much shorter than those for haddock, cod, and saithe. Other than these main commercial stocks, long rough dab is the demersal stock with the highest biomass. Overall, cod is the dominant demersal species.

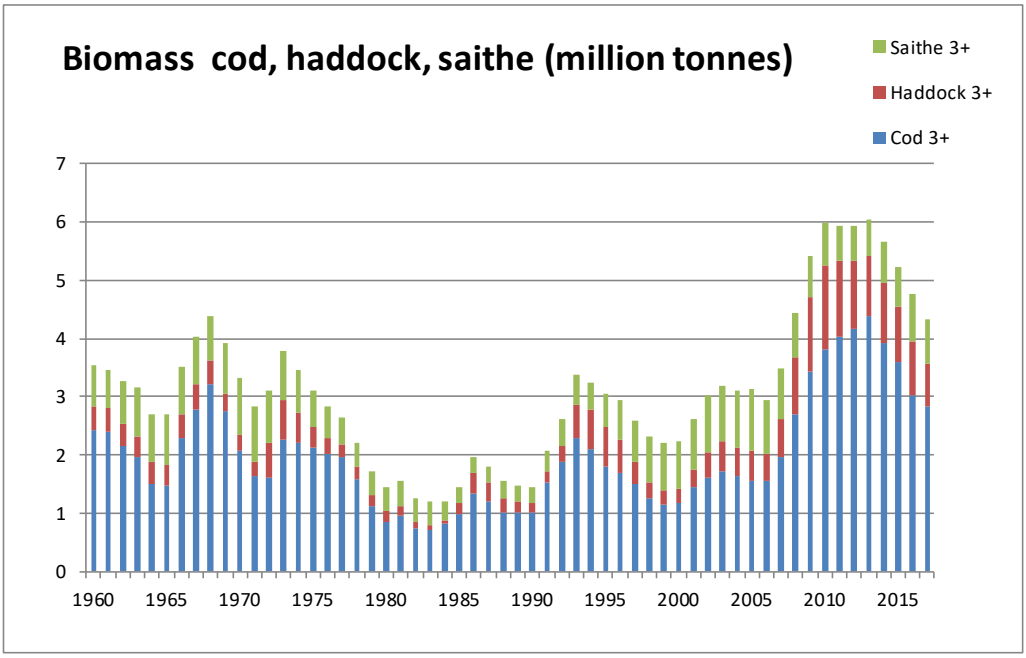

Figure 3.6.1 Biomass estimates of cod, haddock and saithe 1960–2017 from AFWG 2016 (ICES 2017c). Please note that saithe is only partly distributed in the Barents Sea.

Cod

Young of the year

0-group cod were widely distributed within the 2017 surveyed area. The main dense concentrations were observed in the central part of the Barents Sea. The 2017 cod abundance index is underestimated as the northeastern region was not covered. estimated 0-group cod biomass (961 thousand tonnes) is higher than for 2015 and 2016 and higher

than the long-term mean (618 thousand tonnes). The abundance index for the 2017 year class is twice the long-term mean, and may be characterized as strong (Figure 3.6.2). Lengths of 0-group cod were between 4 and 14.4 cm; with a mean length of 8.3 cm, higher than the long term (7.6 cm). Most fish (89%) were between 7.0 and 9.9 cm; indicating good growth, and sufficient feeding and living conditions during the first summer.

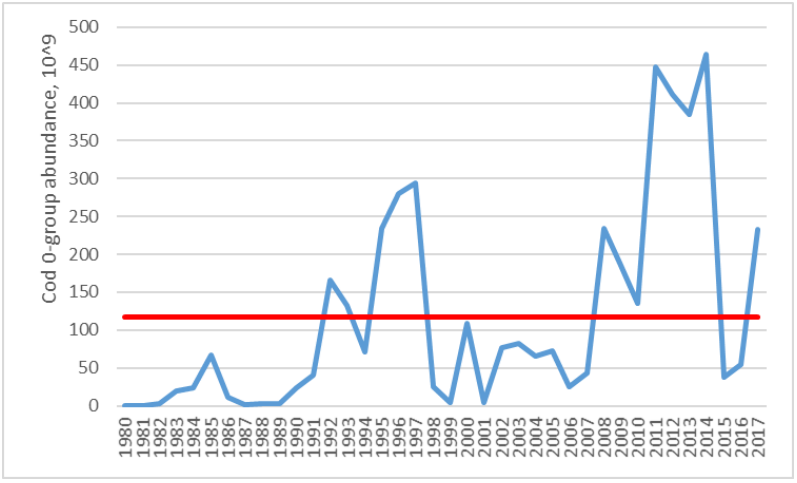

Figure 3.6.2. 0-group cod abundance, corrected for trawl efficiency, in the Barents Sea 1980–2017. Red line shows the long-term mean for the period 1980–2017, while the blue line indicates 0-group abundance fluctuation.

Older cod

The northeast Arctic cod stock is currently in good condition, with high total stock size, and spawning-stock biomass (Figure 3.6.3). The 2004 and 2005 year classes were very strong, but subsequent recruitment-at-age 3 returned to an average level (Figure 3.6.4). 0-group abundance has been very high in recent years (2011–2014); but thus far, this has not resulted in strong year classes.

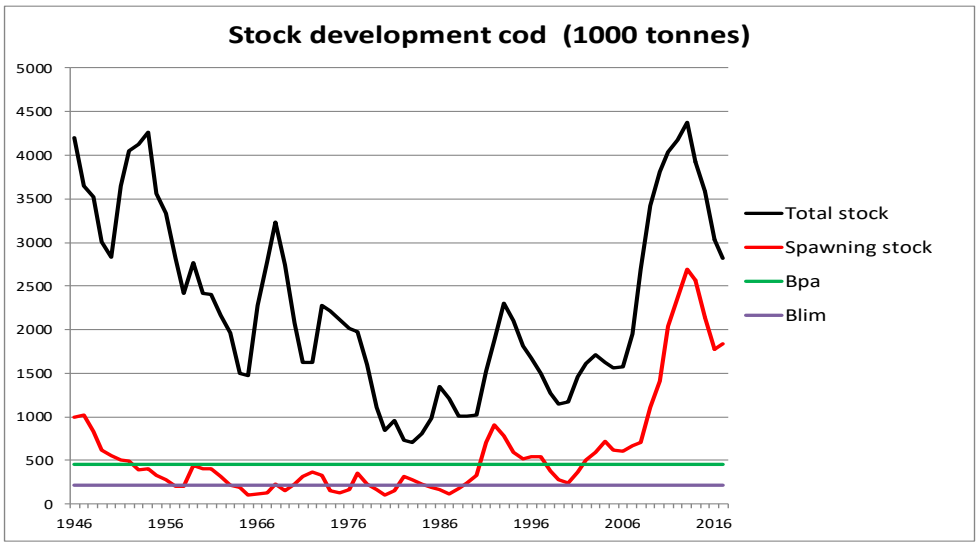

Figure 3.6.3. Cod total stock and spawning stock development – from AFWG 2017 (ICES 2017c).

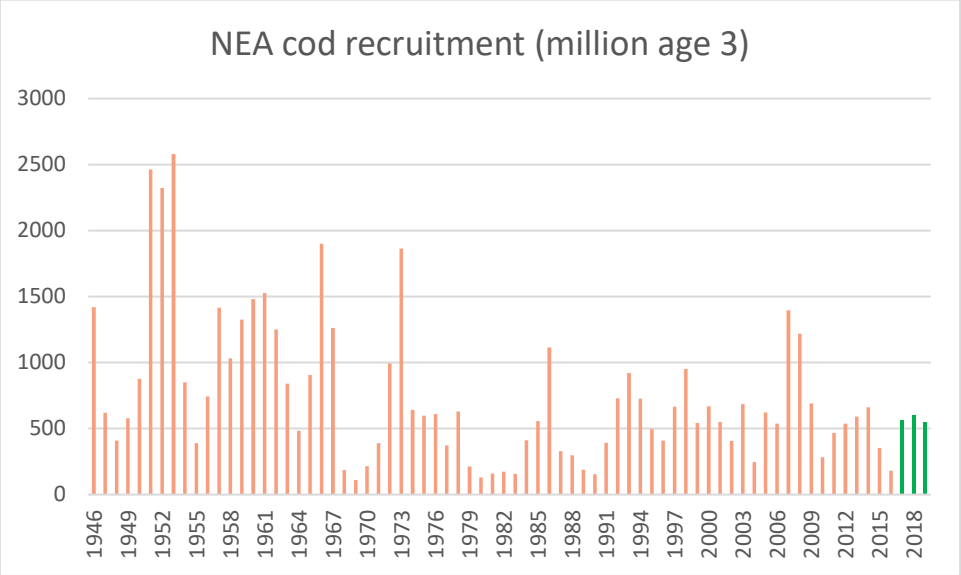

Figure 3.6.4. Cod recruitment-at-age 3 from AFWG 2017 (ICES 2017c).

The strong 2004 and 2005 year classes have, together with a low fishing mortality, led to rebuilding of the cod age structure to that seen in the late 1940s (Figure 3.6.5).

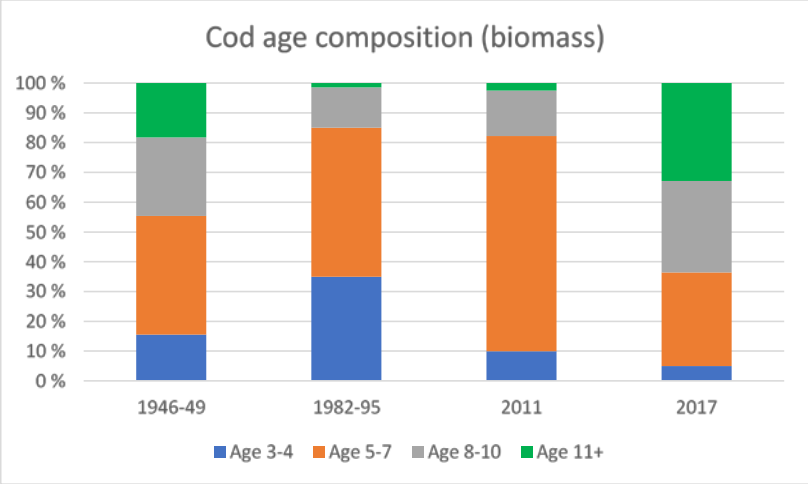

Figure 3.6.5. Cod age-group distribution (biomass). From data in ICES 2017c.

NEA haddock

Young of the year

In 2017, haddock had relatively wide distribution in the western, central, and north-western areas of the Barents Sea. Haddock biomass was 258 thousand tonnes; close to the 2016 estimate, and higher than the 1993–2017 long-term mean (176 thousand tonnes). Estimated 0-group abundance is 1.7 times higher than the long-term mean; the 2017 year class can be characterized as strong (Figure 3.6.6). The length of 0-group haddock varied between 4.5 and 16.9 cm, with an average of 10.7 cm; most fish (61%) had lengths between 9.0 and 11.9 cm; indications are that young haddock had suitable living conditions in 2017.

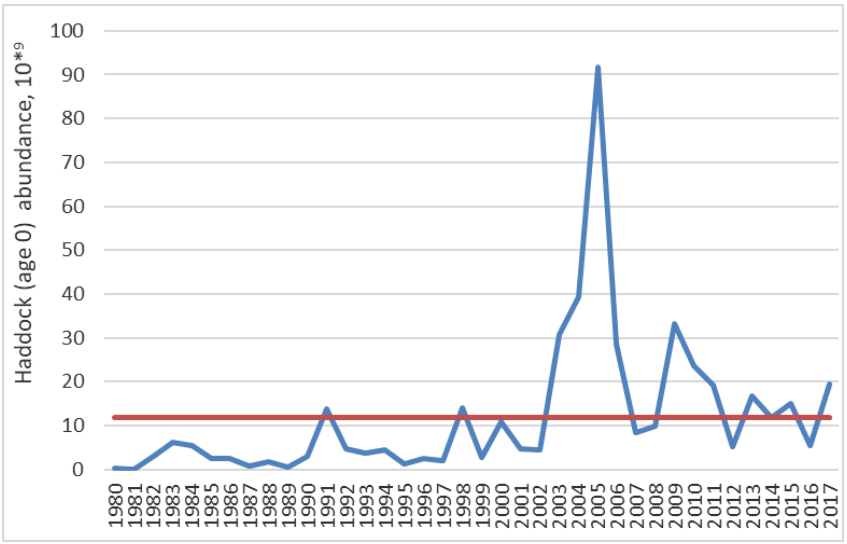

Figure 3.6.6. 0-group haddock abundance, corrected for trawl efficiency, in the Barents Sea 1980–2017. Red line shows long-term mean for the period 1980–2017, while the blue line indicates 0-group abundance fluctuation.

Older haddock

The Northeast Arctic haddock stock reached record levels in 2009–2013, due to the very strong 2004–2006 year classes. Subsequently, recruitment has normalized; the stock is still at a relatively high level, but has declined in recent years (Figures 3.6.7 and 3.6.8).

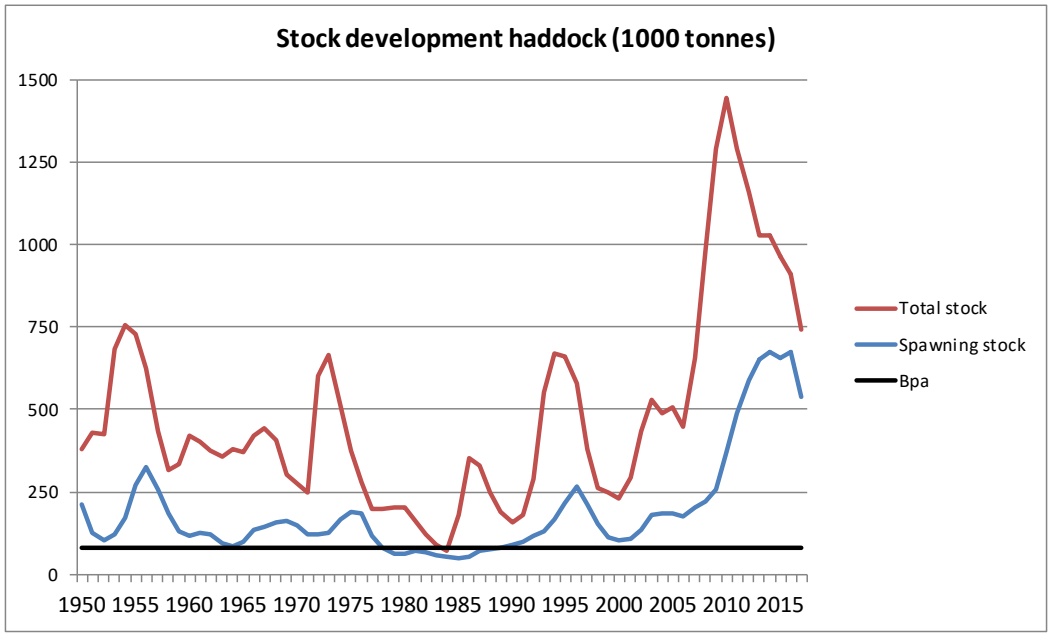

Figure 3.6.7. Haddock total stock and spawning stock development – from AFWG 2017 (ICES 2017c).

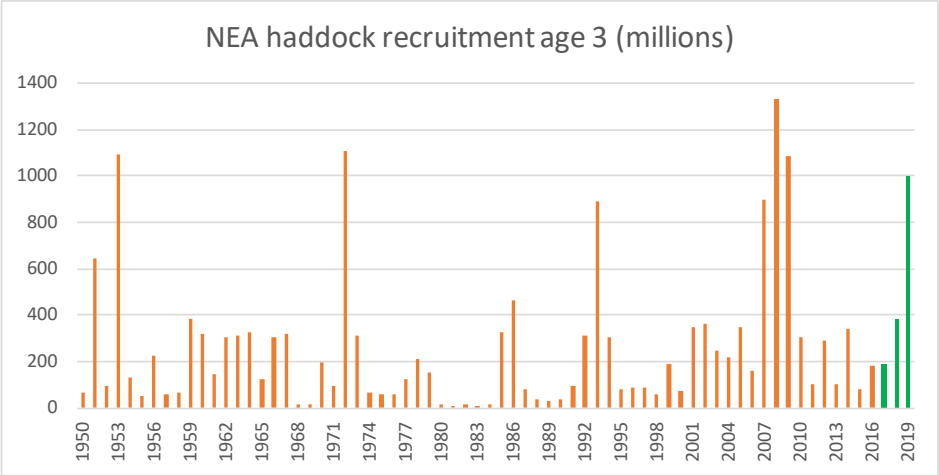

Figure 3.6.8 Recruitment of haddock (ICES 2017c).

Long rough dab

Young of the year

In 2017, 0-group long rough dab were observed at survey boundary areas. The largest catches were taken in the southeastern Barents Sea. Some 0-group individuals were taken by bottom trawl; this indicates that settlement to the bottom has begun, and that abundance indices will be slightly underestimated in 2017. The long rough dab index was the lowest since 2014, and lower than the long-term mean (Figure 3.6.9). Fish length varied between 1.0 and 5.4 cm, with a mean length of 2.9 cm; this was lower than the long-term average (3.3 cm).

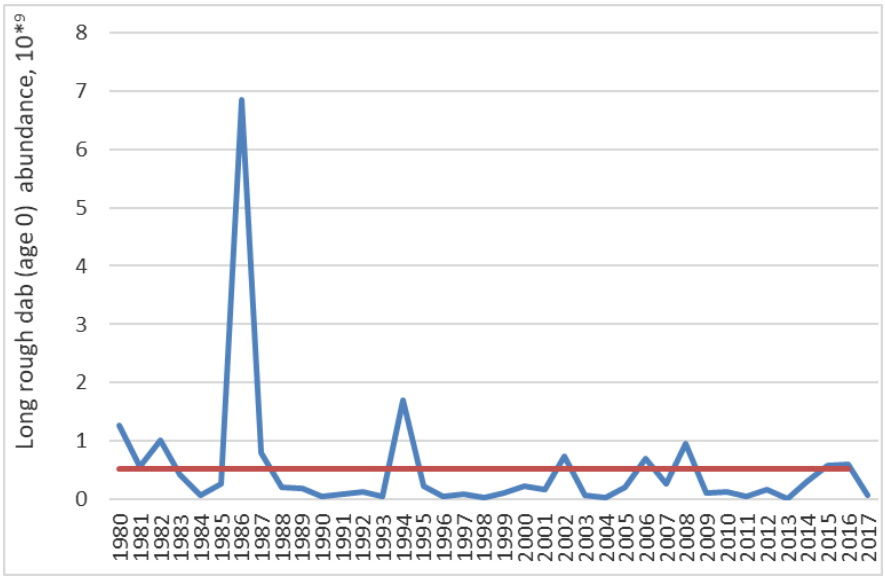

Figure 3.6.9. 0-group long rough dab abundance, corrected for trawl efficiency, in the Barents Sea 1980-2017. Red line shows long-term mean for the period 1980-2017, while the blue line indicates 0-group abundance fluctuation.

Older long rough dab

Older long rough dab (age 1+) are widely distributed in the Barents Sea. During the Russian Autumn-Winter Survey (October-December) and the BESS (August–September), major concentrations of long rough dab were observed in the central-northern

and eastern areas and were dominated by numbers in the bottom-trawl catches in surveys. Many small fish were observed in trawl catches especially in the eastern areas at the 2015-2016 BESS. Long rough dab abundance has been somewhat stable over last decade according to both the Russian Autumn-Winter Survey and the BESS time-series (Figure 3.6.10 and 3.6.11).

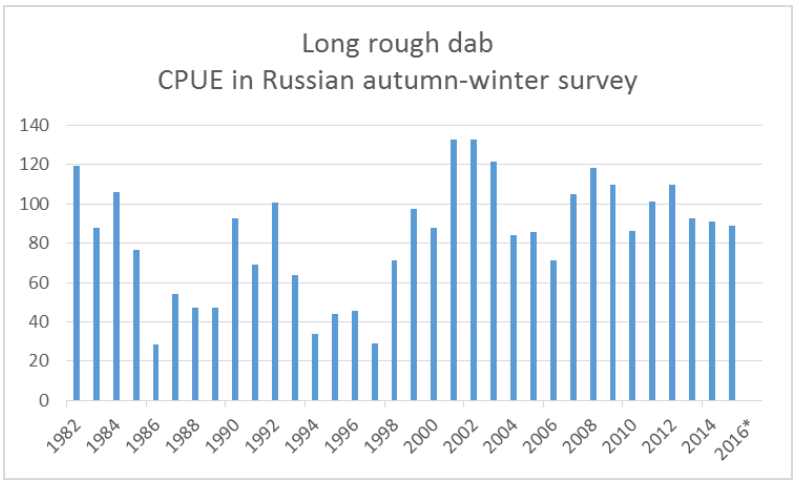

Figure 3.6.10. Catch-per-unit-effort of long rough dab at the Russian Autumn-Winter Survey 1982–2015 (October-December). **2016 – no survey*

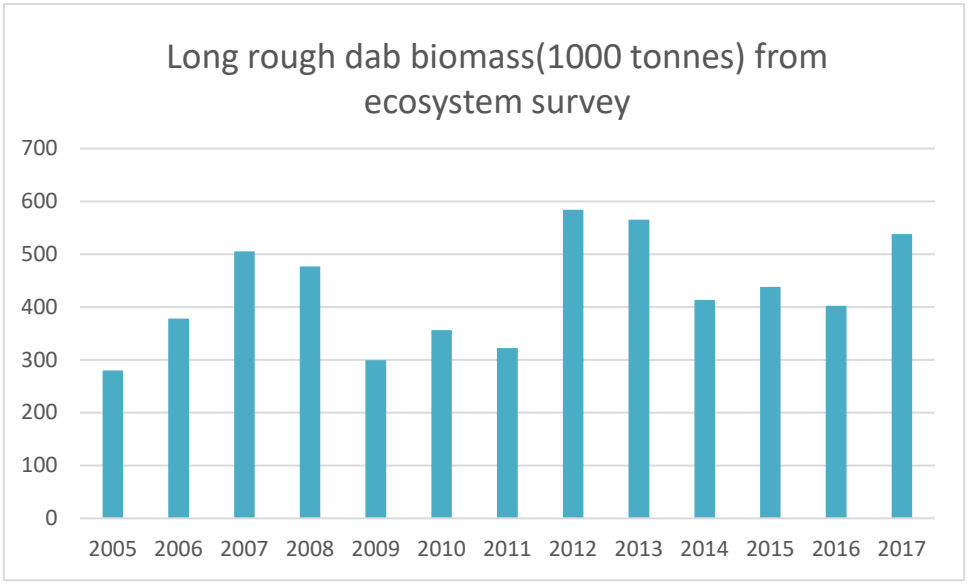

Figure 3.6.11. Stock biomass of long rough dab during the 2005–2017 BESS, calculated using bottom-trawl estimates (swept-area).

Greenland halibut

Young of the year

Since 2005, only low concentrations of 0-group Greenland halibut were found. In 2017, they were observed north and south of the Svalbard/Spitsbergen where only few small catches were taken. The BESS survey does not cover the numerous Svalbard/Spitsbergen fjords, where 0-group Greenland halibut are abundant; therefore, this index does not reliably reflect recruitment to the stock at age 0; however, it may reflect the minimum abundance of the year-class strength in the standard long-term surveyed area. During 2012–2017, abundance of Greenland halibut continuously declined, the 2017

year-class index is also low. Fish length varied between 6 and 8.9 cm, while most fish (67%) were between 7.5 and 8.4 cm. The mean length was 7.7 cm; higher than the long-term mean (6.3 cm).

Older Greenland halibut

The adult component of the stock was, as usual, mainly distributed outside the ecosystem survey area. On the other hand, in recent years an increasing number of large Greenland halibut has been captured in deeper waters of the area surveyed by the BESS (Figure 3.6.12). Northern and northeastern areas of the Barents Sea serve as nursery grounds for the stock. Greenland halibut are also relatively abundant in deep channels running between the shallowest fishing banks. Figure 3.6.13 shows an index for Greenland halibut at the nursery grounds, based on the BESS results north of 76.5°N from northwest of Svalbard and east to Franz Josef Land (for details see Hallfredsson and Vollen 2015, WD 1 ICES IBPhali 2015).

The fishable component of the population (length ≥45 cm) increased from 1992 to 2012, and has been stable since then (Figure 3.6.14). The harvest rate has been low and relatively stable since 1992.

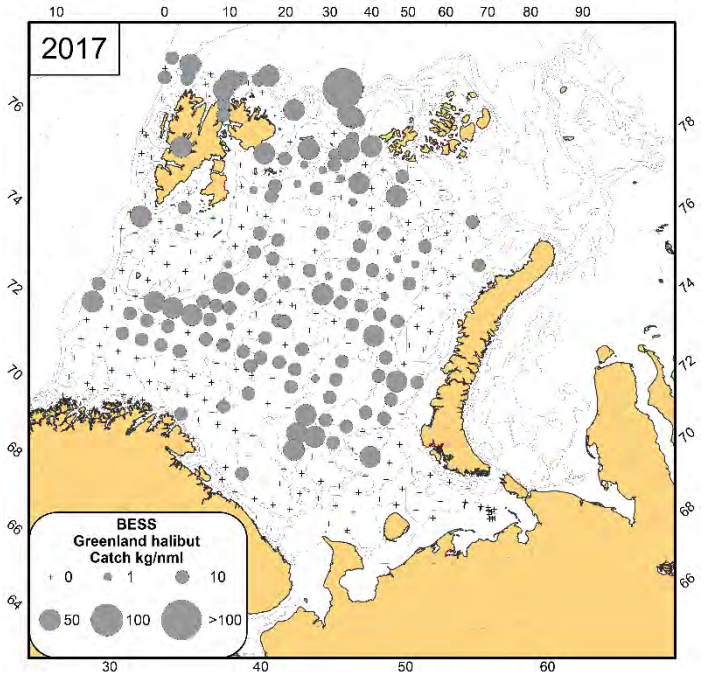

Figure 3.6.12 Greenland halibut distribution (specimens/nautical mile) during August–September 2017 based on the BESS data.

Figure 3.6.13. Biomass index for Greenland halibut at the nursery areas; 2014 excluded due to poor area coverage.

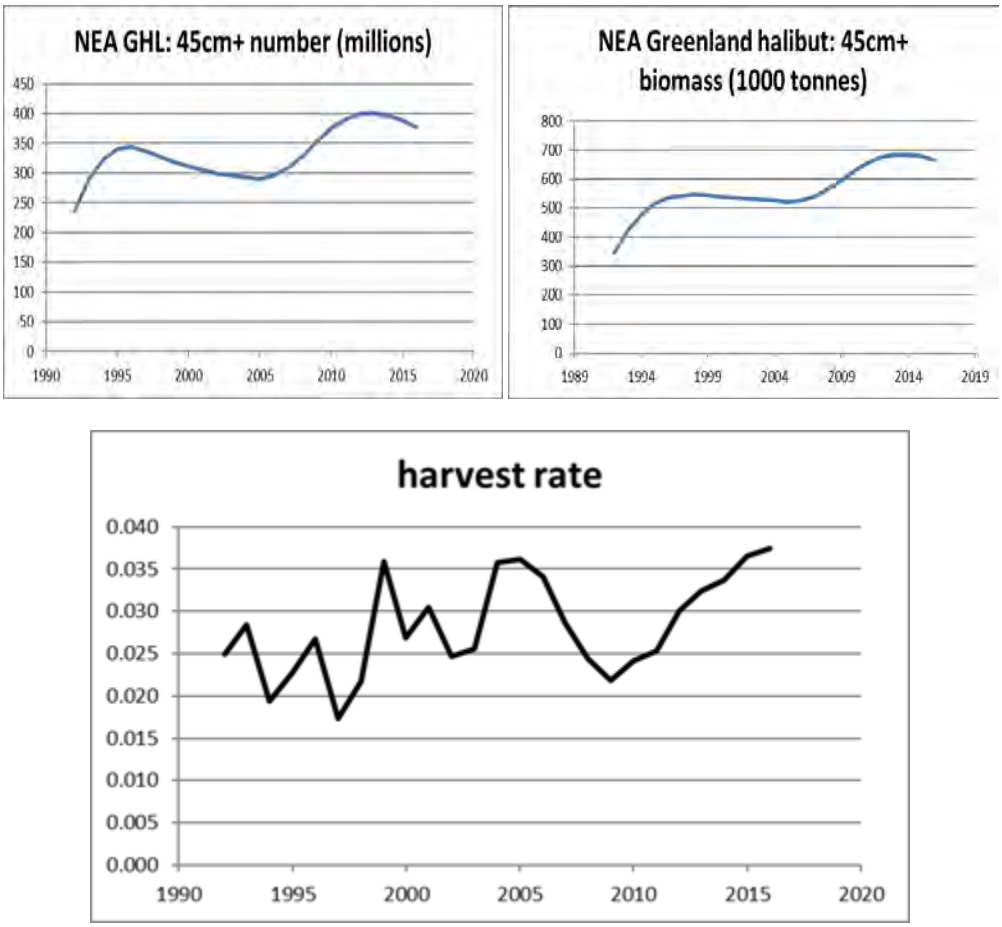

Figure 3.6.14 Northeast Arctic Greenland halibut. Numbers (upper left) and biomass (upper right) 1992–2016 for 45+ cm Greenland halibut as estimated by the GADGET model, and estimated exploitation rates (below) (ICES 2017c).

Deep-water redfish

Young of the year

In 2017, redfish, mostly *Sebastes mentella*, were distributed in western and northern areas of the Barents Sea, with the densest concentration west of Svalbard/Spitsbergen Archipelago. Estimated 0-group redfish biomass (100 thousand tonnes) was lower than the long-term mean (168 thousand tonnes). Abundance of 0-group redfish was lower than the long-term mean; thus, the 2017 year class can be characterized as weak. However, some 0-group fish may occur outside the area surveyed. The estimated index of 0-group redfish represents only shelf areas of the Barents Sea and, therefore, an unknown proportion of total 0-group abundance.

Older redfish

In 2017, deep-water redfish were widely distributed in the Barents Sea. During the ecosystem survey and the winter survey, the largest concentrations were observed, as usual, in the western and northwestern parts of the Barents Sea. Biomass was at a higher level during 2013–2017 than in preceding years. Geographical distribution of deep-water redfish during the 2017 ecosystem survey is shown in Figure 3.6.15. Most adult fish are found in the Norwegian Sea. Stock development from the latest ICES AFWG assessment is shown in Figure 3.6.16.

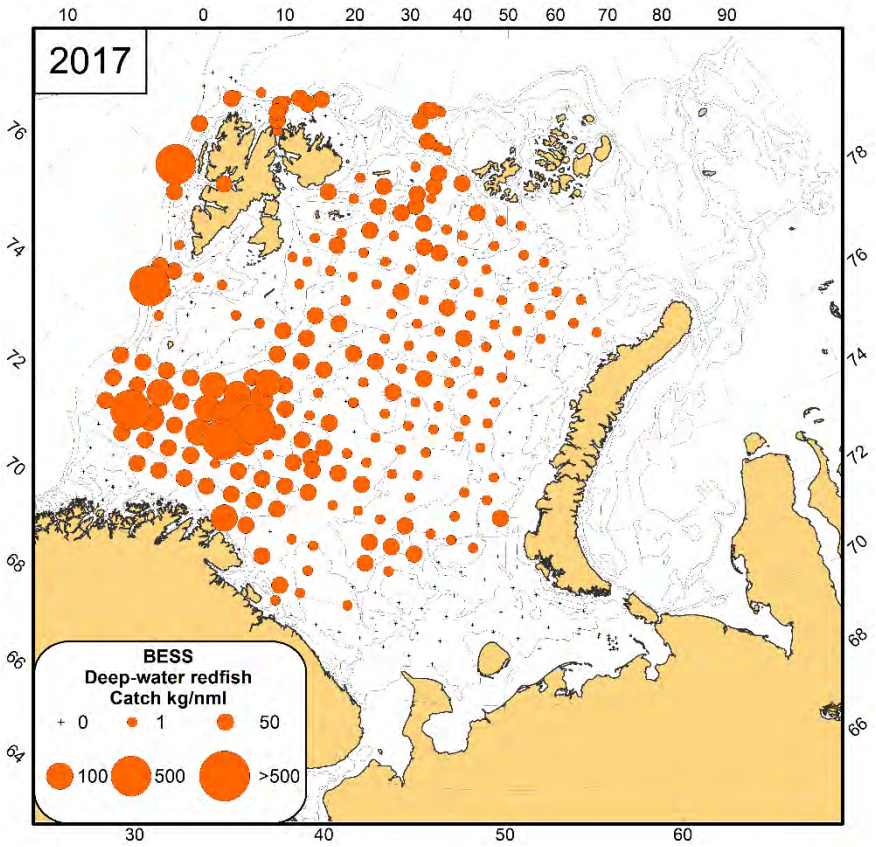

Figure 3.6.15. Geographical distribution of deep-water redfish during the 2017 BESS survey.

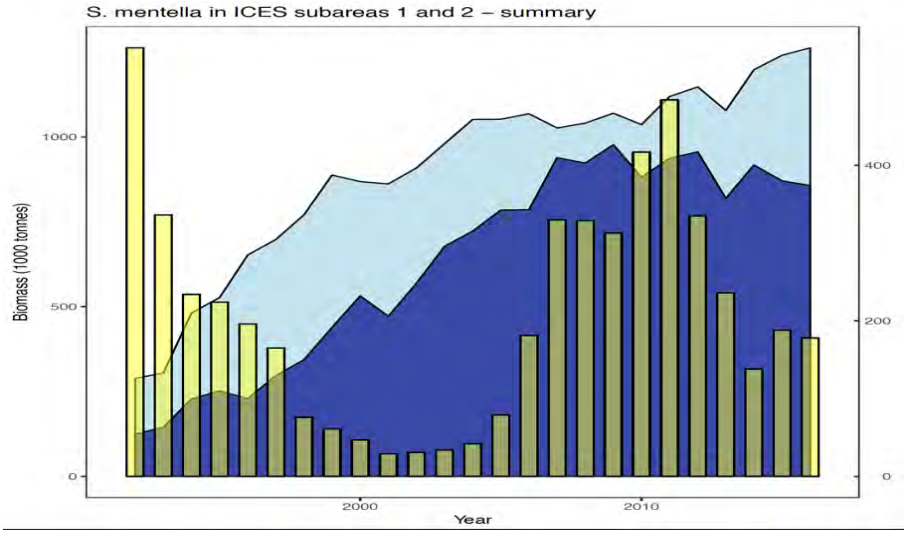

Figure 3.6.16 Results from the statistical catch-at-age model showing the development of total biomass ('000s), spawning-stock biomass and recruitment-at-age 2 for the period 1992–2016, for *S. mentella* in subareas 1 and 2. (ICES 2017c).

3.7 Zoogeographical groups of non-commercial species

Zoogeographical groups of fish species are associated with specific water masses. Relative distribution and abundance of fish species belonging to different zoogeographic groups are of interest because these fish will respond differently to climate variability and change. Since they are not commercial species, fishing does not directly contribute to changes in abundance and distribution of these species. Different zoogeographic groups also tend to differ in their trophic ecology: many of the Arctic species are small, resident, and feed mainly on invertebrates; whereas, most boreal and mainly boreal species are migratory and piscivorous. Therefore, the relative abundance of these species should influence foodweb structure and dynamics. Comparing changes in relative abundance and distribution of species classified into zoogeographical groups based on established criteria from the literature, is relatively simple and does not rely on sophisticated statistical methods — like those used to study changes in the Barents Sea fish community, e.g. Fossheim *et al.,* 2015 and Frainer *et al.,* 2017.

Andriashev and Chernova (1995) classified Barents Sea fish species into seven zoogeographical groups: widely distributed, south boreal, mainly boreal, Arctic-boreal, mainly Arctic, and Arctic. In the recent publication, "Marine Fishes of the Arctic Region" (Mecklenburg *et al.,* 2018), some fish species were reclassified into six zoogeographical groups: **widely distributed, boreal, boreal, mainly boreal, Arctic-boreal, mainly Arctic and Arctic**. We use the Andrashev and Chernova classification scheme here, since it is more comprehensive and includes a larger number of species occurring in the Barents Sea. We give the change in distribution of different zoogeographic group species from the BESS survey 2004–2017 (Figure 3.7.1).

It was found that each year south boreal and boreal species occurred in southern and southwestern areas of the Barents Sea, while Arctic and mainly Arctic species occur in northern and northeastern areas. Arctic-boreal species were observed in central, northern, and northeastern areas. Mainly boreal species were observed throughout survey areas during 2004–2017 (Figure 3.7.1).

Generally, since the onset of the ecosystem survey in 2004, a decrease of the area of species from Arctic, mainly Arctic, and Arctic-boreal group has been observed (Figure 3.7.1). This may be due to change in the direction of survey from south to north in 2017;

whereas, the direction was from north to south in 2016. Northern areas were sampled during September in 2017; whereas they were sampled during August (one month earlier) in 2016. Southern areas were sampled during August in 2017; whereas they were sampled during September in 2016. Water mass temperature differs between August and September, and species distribution may shift with changing water mass temperature; this might explain the differences observed between 2016 and 2017.

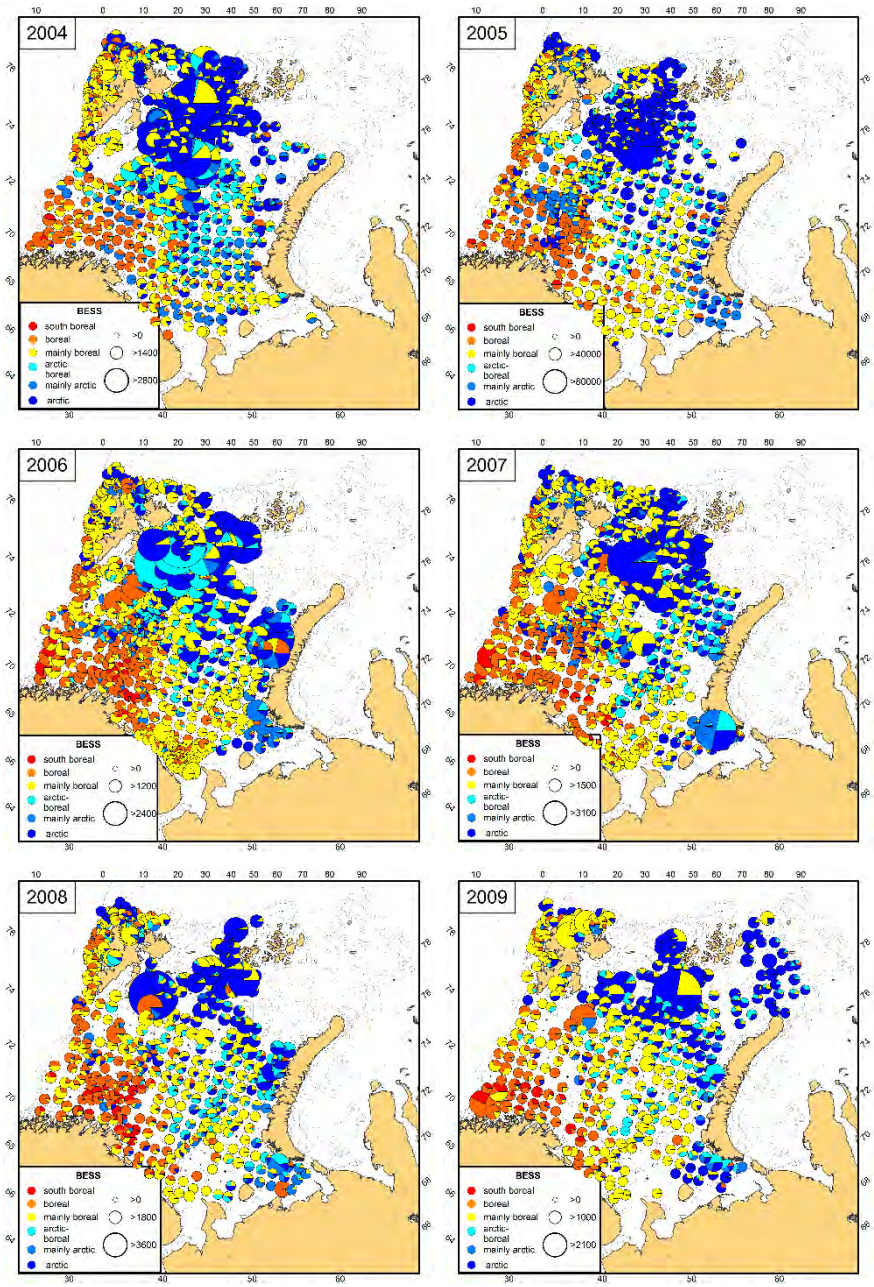

Figure 3.7.1. Distribution of non-commercial fish species from different zoogeographic groups during the ecosystem survey 2004–2009. Size of circle corresponds to abundance (individuals per nautical mile, only bottom-trawl stations were used, both pelagic and demersal species are included).

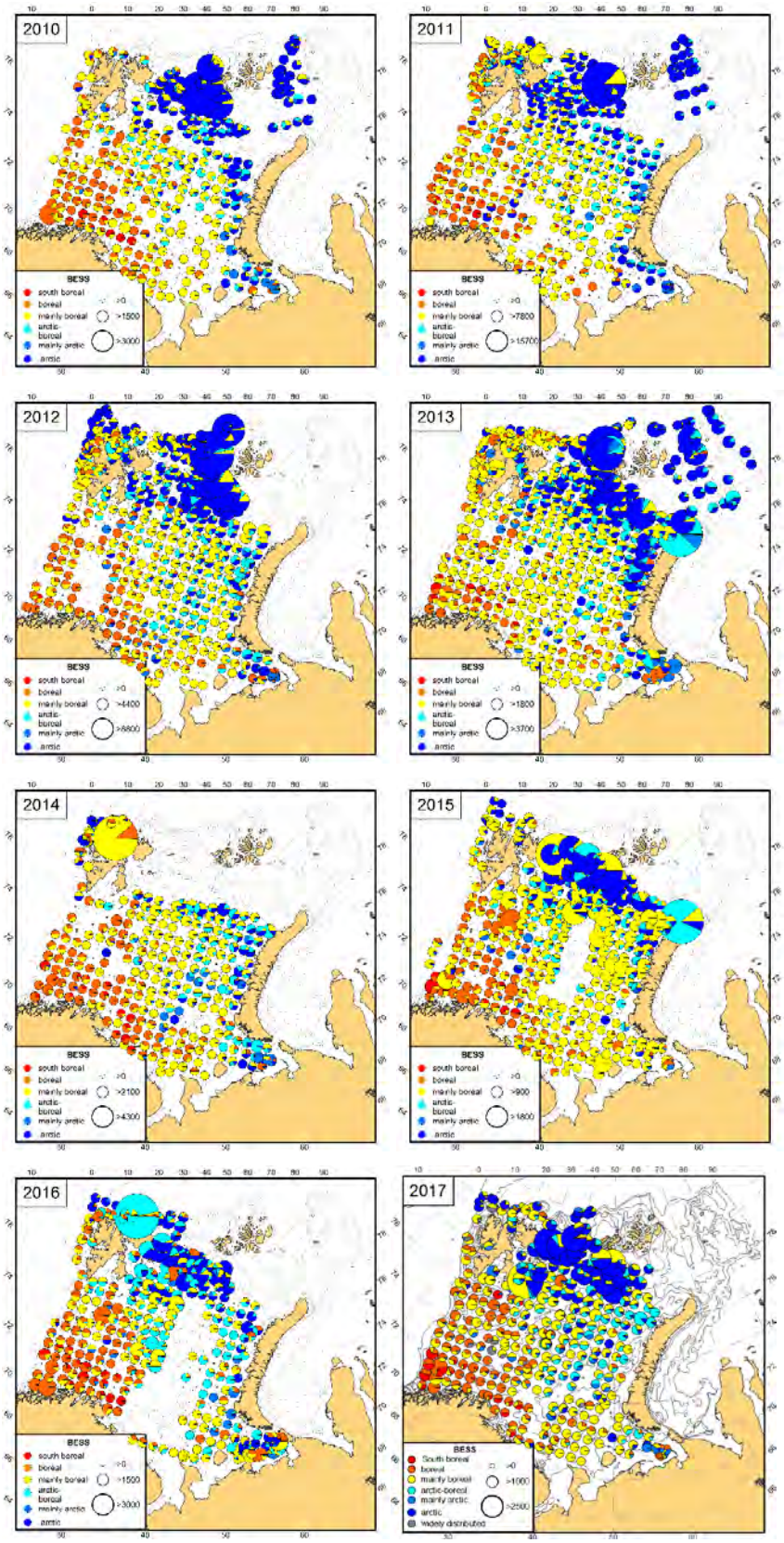

Figure 3.7.1 (continued). Distribution of non-commercial fish species from different zoogeographic groups during the ecosystem survey 2010–2017. Size of circle corresponds to abundance (individuals per nautical mile, only bottom-trawl stations were used, both pelagic and demersal species are included).

Conclusions:

Since the onset of BESS in 2004, a decrease in the distribution area of species from Arctic, mainly Arctic, and Arctic-boreal zoogeographic groups have been observed.

In 2017, both distribution area and abundance of species, categorized as Arctic and mainly Arctic zoogeographic groups, increased relative to 2016. The ecosystem survey covered the northern area during September in 2017, but during August in 2016. Conversely, the survey covered the southern area during August in 2017 and during September in 2016. Water mass temperature differs between August and September, and since species distribution may shift with water mass distribution, this might explain the difference between 2016 and 2017.

Due to different survey area coverage from year-to-year, it is difficult to analyse interannual variability. It is therefore necessary to choose areas that have been sampled consistently each year, and use these data to evaluate trends and determine how well the new zoogeographic classification system (Mecklenburg *et al.,* 2018) applies to species in the Barents Sea ecosystem.

Benthos: Interannual fluctuation of the fauna biogeographical structure.

To visualize the border areas between prevailing Boreal and Arctic fauna, the biogeographical index (BGI) was developed (Manuchin *et al.,* 2012); boreal-arctic fauna are not included. The index can be calculated with different parameters (biomass, abundance, number of the species etc.) using the following equation:

$$BGI=(Pb-Pa)/(Pb+Pa)$$

where: Pa – quantitative parameter of arctic species; Pb – quantitative parameter of boreal species.

BGI ranges from 1 (only boreal species are present at the trawl station) to -1 (only arctic species are present); 0 value indicates an equal ratio between boreal and arctic species. Situations where neither boreal nor arctic species are present will result a "0" BGI value (equal ratio between boreal and arctic species).

The BGI distribution in in 2017 indicates that the southern Barents Sea- southern part of Svalbard, Svalbard Bank, and the Pechora Sea in the East- is dominated by boreal fauna (Figure 3.7.2).

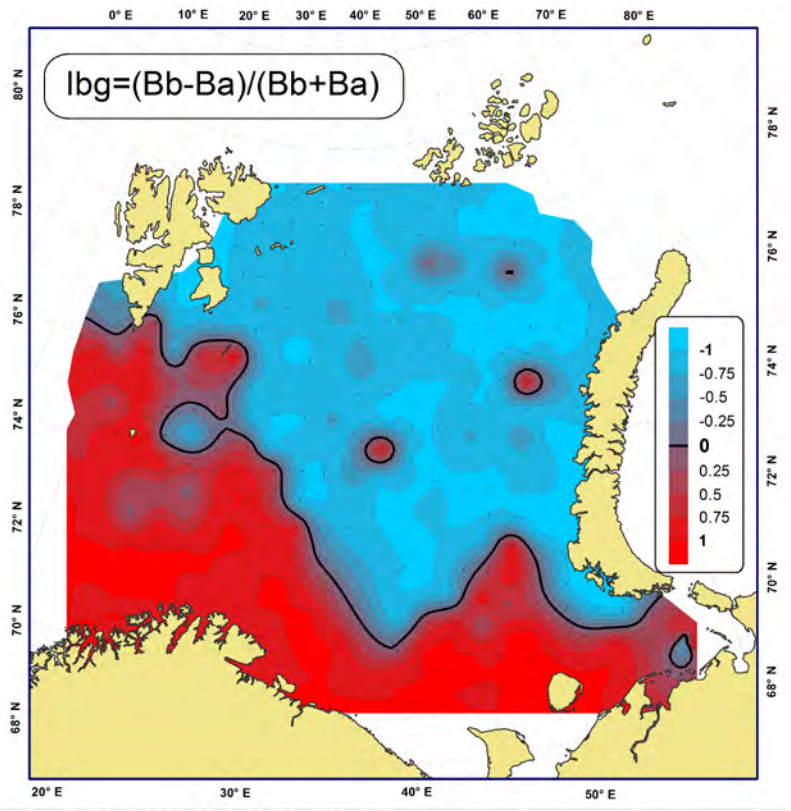

Figure 3.7.2. The distribution of the biogeographical Index (BGI) of the megabenthos in the Barents Sea according to ecosystem data from 2017.

Ba – biomass of arctic species; Bb – biomass of boreal species; black line is the border of the equal ratio of the boreal and arctic species in the terms of biomass

Interannual fluctuation in the BGI, calculated using total biomass, show the same dynamic as biomass anomalies (Figure 3.7.3). The lowest BGI value (2009) corresponds to the coldest year (2003) with a 6-year time delay.

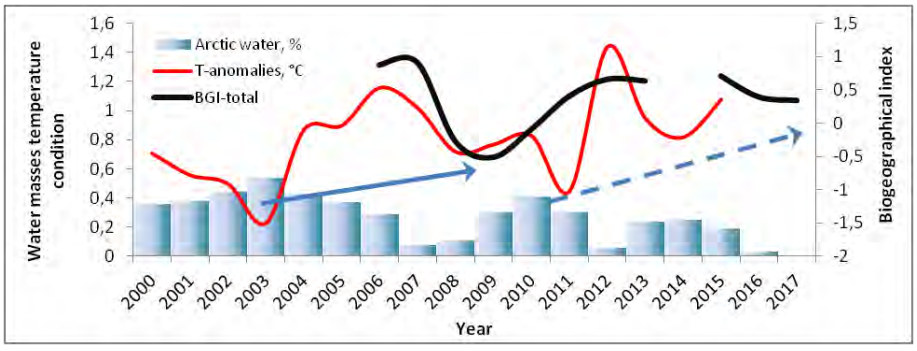

Figure 3.7.3. Dynamics of the Biogeographical index (BGI) during 2006–2017 (black line) and indicators of the oceanographic condition of the Barents Sea: % area of the Barents Sea bottom covered by arctic water (blue bars) (WGIBAR report 2017, Figure 3.1.17), and the temperature anomalies in the Kola sections (red line) (http://www.pinro.ru).

In summary, the short timeline of benthic monitoring, combined with technical issues and data gaps/poor coverage, make it difficult to determine long time-trends. But, interannual fluctuations in the hydrological and biological parameters suggest that a decrease in benthic biomass may be recorded 6-7 years after a cold period.

3.8 Marine mammals and seabirds

3.8.1 Marine mammals

During the 20 June to 14 August 2017 period, a sighting survey was conducted in the Barents Sea east of 28°E as part of a six-year mosaic survey of the Northeast Atlantic to estimate the regional abundance of minke whales and other cetaceans during summer. Coverage was adequate, except in the southeastern area where military restrictions restricted survey activity. The most often observed species was minke whale, followed by white-beaked dolphins, harbour porpoises, humpback whales, and fin whales. A few observations were also made of bowhead whales and beluga whales. Data have not yet been analysed but the qualitative impression was that minke whales were abundant in northern and eastern areas (Figure 3.8.1.1). Harbour porpoises were observed mostly in the southern parts of the area covered, and they are associated with the coastal areas along Kola and fjord systems. Humpback whales were sighted in the northwest, which is considered an early appearance in waters where they usually occur later in autumn in association with capelin distribution. White-beaked dolphins were, as usual, observed in southern and central parts of the survey area, especially over the Central Bank. It is noteworthy that a considerable number of harp seal observations — single animals and groups — were made in open waters north of about 74°N. During summer, ime harp seals are usually closely associated with the ice edge in the north.

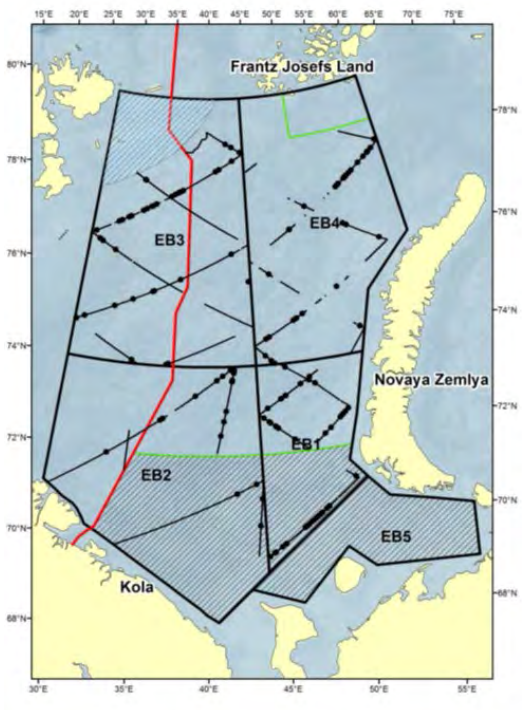

Figure 3.8.1.1. The survey area summer 2017. Black lines are transects conducted in primary search mode and black dots are minke whale sightings.

Although an estimate of minke whale abundance from the 2017 summer survey is not yet available, we have a series of abundance estimates from earlier surveys, which can be compiled to illustrate the status over a time of nearly 30 years (Figure 3.8.1.2). The summer abundance of minke whales in the Barents Sea is now about 50 000 animals and has been quite stable or increasing over the period. The sighting rate from the 2017 survey is the highest recorded which may confirm the apparent increasing trend at present.

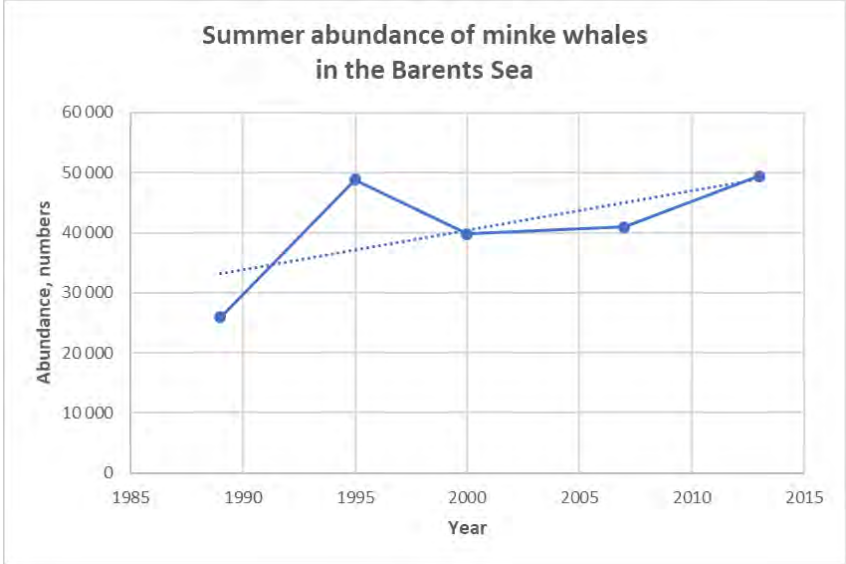

Figure 3.8.1.2. Summer abundance of minke whales in the Barents Sea over the past nearly 30 years.

During the ecosystem surveys in the Barents Sea in August–October 2017 marine mammal observers were on all vessels. In total, 1518 individuals of 9 species of marine mammals were observed and an additional 46 individuals were not identified to species. The observations are presented in Table 3.8.1 and distributions in the Figures 3.8.1.3 (toothed whales) and 3.8.1.4 (baleen whales).

As in previous years, white-beaked dolphins were most common (more than 50% of all registrations). This species was widely distributed in the research area. Most records of white-beaked dolphin overlap with distribution of capelin and cod in the central area, and herring in the coastal area. The largest groups of white-beaked dolphin included up to 20–40 individuals.

In addition to white-beaked dolphins, other observed species of toothed whales included: sperm whale (*Physeter macrocephalus*); harbour porpoise (*Phocoena phocoena*); and killer whale (*Orcinus orca*). Sperm whales were observed in deeper waters along the continental slope in the western part of the survey area. Harbour porpoises were mainly observed in the southeastern area between 70° and 73°13'N; their distribution overlapped with recorded herring aggregations. Killer whales were only observed in the western part of the 2017 survey area.

Table 3.8.1.1. Number of marine mammal individuals observed from the RV "Johan Hjort", "G.O. Sars", "Vilnyus" during the ecosystem survey in 2017.

Order/ suborder	Name of species (english)	G.O.Sars	J. Hjort	Vilnyus	Total	%
Cetacea/ Baleen whales	Fin whale	22	148	4	174	11.5
	Humpback whale	11	159	7	177	11.7
	Minke whale	21	205	22	248	16.3
	Unidentified whale	3	37	-	40	2.6
Cetacea/ Toothed whales	White-beaked dolphin	280	354	220	854	56.2
	Harbour porpoise	-	-	5	5	0.3
	Killer whale	-	4	-	4	0.3
	Sperm whale	-	7	-	7	0.5
	Unidentified dolphin	5	-	-	5	0.3
	Unidentified cetacean	-	1	-	1	0.1
Pinnipedia	Harp seal	-	2	-	2	0.1
	Bearded seal	-	1	-	1	0.1
Total sum		342	918	258	1518	100

Baleen whales — minke (*Balaenoptera acutorostrata*), humpback (*Megaptera novaeangliae*), and fin whales (*Balaenoptera physalus*) — were also abundant in the Barents Sea, and comprised 39% of all marine mammals observed. Minke whales were widely distributed in the survey area; dense concentrations in the northwestern areas overlapped with capelin aggregations. In southern areas, minke whales overlapped with herring and juvenile cod aggregations. In 2017, minke whale abundance exceeded levels observed during the 2012–2015 period.

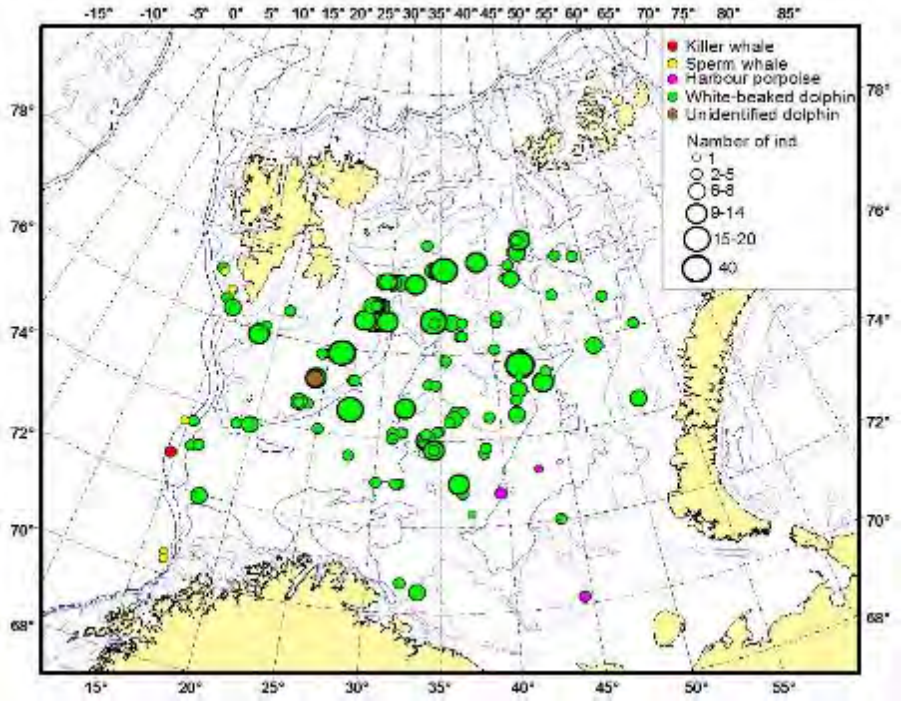

Figure 3.8.1.3. Distribution of toothed whales in August–October 2017.

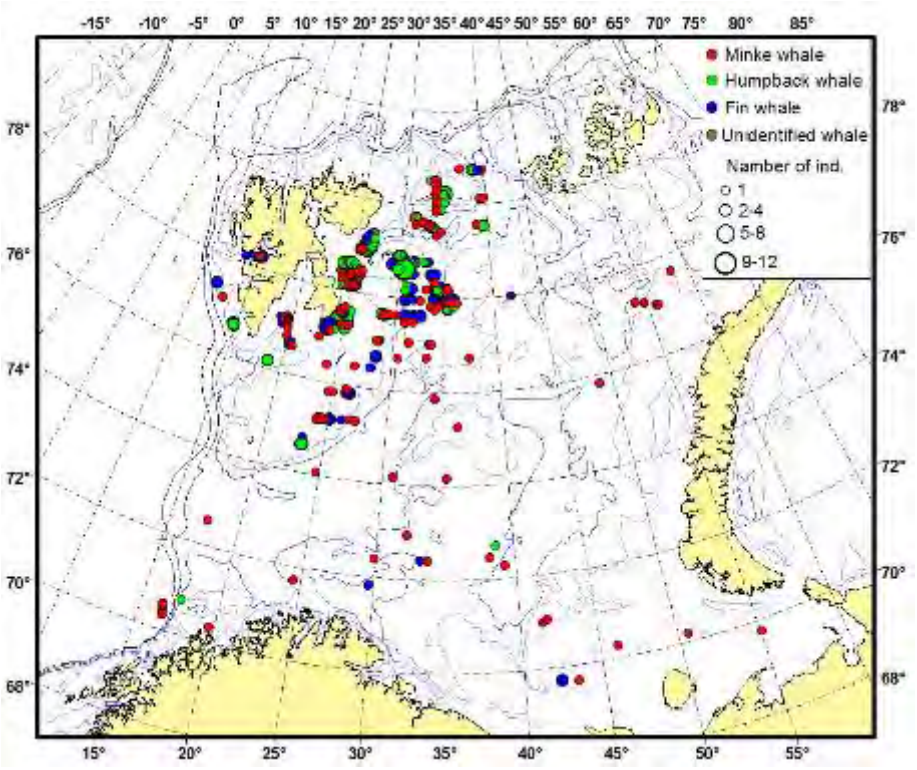

Figure 3.8.1.4. Distribution of baleen whales in August–October 2017.

In 2017, humpback whale abundance was lower than observed in 2013 and 2015. Most humpback whales were observed — in groups of up to 12 individuals or as single specimens — on Great Bank and at White Island, and overlapped with dense concentrations of capelin. Minke whales and fin whales were recorded in the same area. More fin whales were observed during the 2017 survey; mostly in capelin areas east of Svalbard Archipelago and Great Bank.

In 2017, the only pinnipeds observed were harp seals and bearded seals (*Erignathus barbatus*). Harp seals were recorded on Great Bank, while bearded seals occurred northward of White Island. Polar bears (*Ursus maritimus*) were not observed during the 2017 survey, most likely due lack of the ice in the surveyed area.

3.8.2 Seabirds

About six million pairs from 36 seabird species breed regularly in the Barents Sea (Barrett et al. (2002), Table 3.8.2.1). Allowing for immature birds and non-breeders, the total number of seabirds in the area during spring and summer is about 20 million individuals. 90% of the birds belong to only 5 species; Brünnich's guillemot, little auk, Atlantic puffin, northern fulmar and black-legged kittiwake. The distribution of colonies is shown in Figure 3.8.2.1. Colonies in the high-Arctic archipelago are dominated by little auks, Brünnich's guillemots and kittiwakes. These birds utilize the intense secondary production that follows the retreating sea ice. Little auks feed mainly on lipid rich Calanus species, amphipods and krill while Brünnich's guillemots and black-legged kittiwakes feed on polar cod, capelin, amphipods and krill. The seabird communities, as well as their diet change markedly south of the polar front. In the Atlantic part of the Barents Sea, the seabirds depend more heavily fish, including fish larvae, capelin, I-group herring and sandeels. The shift in diet is accompanied by a shift in species composition. In the south, Brünnichs' guillemots are replaced its sibling species, the

common guillemot. Large colonies of puffins that largely sustain on the drift of fish larvae along the Norwegian coast, are found in the southwestern areas.

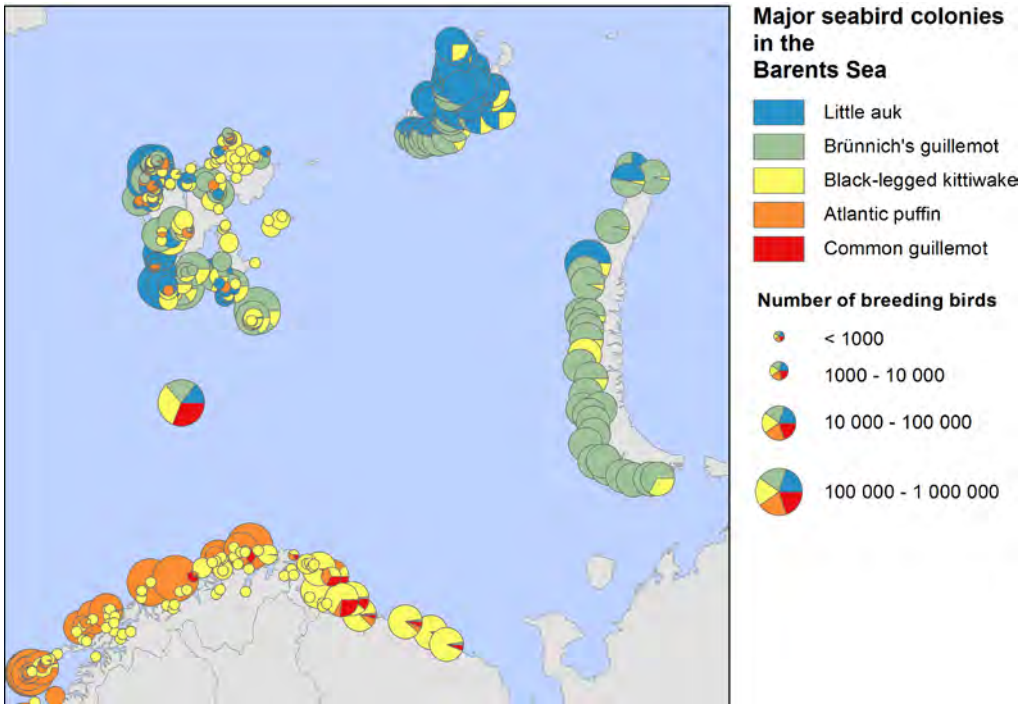

Figure 3.8.2.1. Major seabird colonies in the Barents Sea. Data compiled from SEAPOP (www.seapop.no), Fauchald et al. (2015), Anker-Nilssen et al. 2000 and The Seabird Colony Registry of the Barents and White Seas.

Table 3.8.2.1. Seabirds in the Barents Sea sorted by breeding population size in decreasing number. Breeding pairs are from Strøm et al. (2009). Observations on BESS 2017 are the observations from Norwegian and Russian vessels during the ecosystem survey in 2017.

Species name	Scientific name	Breeding pairs	Observations on BESS 2017
Brünnich's guillemot	*Uria lomvia*	1 250 000	14084
Little auk	*Alle alle*	>1 010 000	3342
Atlantic puffin	*Fratercula arctica*	910 000	779
Northern fulmar	*Fulmarus glacialis*	500 000-1 000 000	62786
Black-legged kittiwake	*Rissa tridactyla*	682 000	11264
Common eider	*Somateria mollisima*	157 000-159 000	16
Herring gull	*Larus argentatus*	122 600	402
Common guillemot	*Uria aalge*	104 000	182
Arctic tern	*Sterna paradisaea*	65 000	378
Black guillemot	*Cepphus grylle*	58 000	75
Great black-backed gull	*Larus marinus*	22 930	610
Razorbill	*Alca torda*	19 600	20
Mew gull	*Larus canus*	14 200	6
Glaucous gull	*Larus hyperboreus*	9 000-15 000	1277
Great cormorant	*Phalacrocorax carbo*	11 570	3
European shag	*Phalacrocorax aristotelis*	6 350-6 400	0
European storm-petrel	*Hydrobates pelagicus*	1 000-10 000	0
Lesser Black-backed gull	*Larus fuscus*	3 500	6
Ivory gull	*Pagophila eburnea*	2 200-3 750	109

Northern gannet	*Morus bassanus*	1 900-2 150	39
Arctic skua	*Stercorarius parasiticus*	1 150	116
King eider	*Somateria spectabilis*	1 000	0
Common tern	*Sterna hirundo*	>1 000	0
Heuglin's Gull	*Larus heuglini*	600-1 100	27
Great skua	*Stercorarius skua*	540-1 100	33
Leach's storm petrel	*Oceanodroma leucorhoa*	100-1 000	0
Steller's eider	*Polysticta stelleri*	10-100	0
Sabine's gull	*Xema sabini*	1-10	3
Great northern diver	*Gavia immer*	0-3	5
Long-tailed duck	*Clangula hyemalis*	?	0
Black scoter	*Melanitta nigra*	?	0
Velvet scoter	*Melanitta fusca*	?	0
Red-breasted merganser	*Mergus serrator*	?	0
Black-throated loon	*Gavia arctica*	?	3
Long-tailed skua	*Stercorarius longicaudus*	?	0
Pomarine skua	*Stercorarius pomarinus*	?	260
Sooty shearwater	*Puffinus griseus*	0	14
Ross's gull	*Rhodostethia rosea*	0	1

Population monitoring in Norway and Svalbard has revealed a marked downward trend for several important seabird species the last 30 years, including puffin, Brünnich's guillemot and kittiwake (Figure 3.8.2.2). The population of common guillemot was decimated in the 1980s mainly due to a collapse in the capelin stock combined with low abundance of alternative prey. The population has increased steadily since then. The status and trends of the large populations of seabirds in the Eastern Barents Sea is less known.

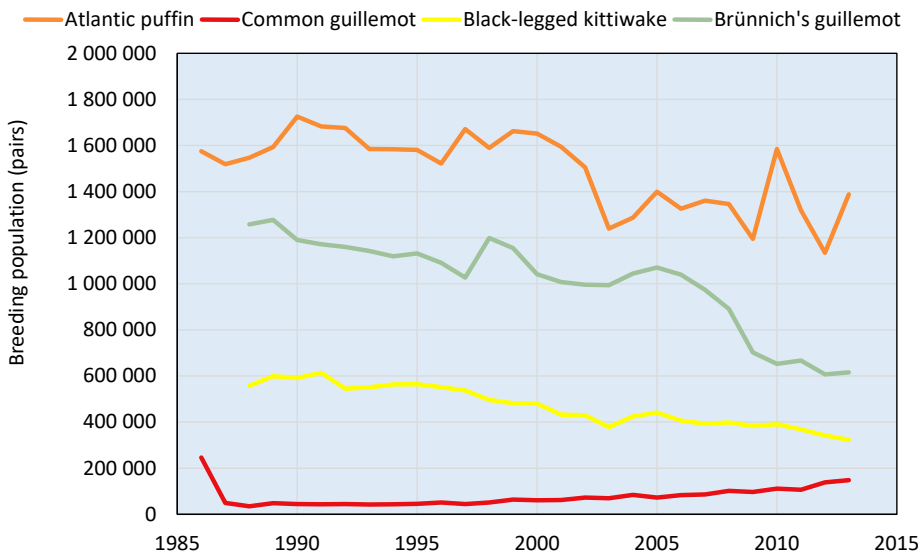

Figure 3.8.2.2: Size and trends of puffin, guillemots and kittiwake populations in the Western Barents Sea (Norway and Svalbard incl. Bjørnøya). Data from Fauchald et al. (2015).

Recent tracking studies (see www.seatrack.no) show that after the breeding season, parts of the adult populations of kittiwakes, puffins and common guillemots from colonies along the Norwegian coast migrate into Barents Sea to feed, possibly increasing the number of birds in the area in August and September. However, during September and October the populations of Brünnich's guillemots and little auks from colonies in West-Spitsbergen and Bjørnøya start their migration westward, crossing the Norwegian Sea to reach their wintering grounds in the Northwest Atlantic. The large eastern populations (birds breeding in East Spitsbergen, Franz Josef Land and Novaya Zemlya), however, seem to over-winter in the southern Barents Sea. Kittiwakes do also migrate out of the Barents Sea during winter, while common guillemots stay in the southeastern part of the Barents Sea throughout the non-breeding period. Finally, only a few puffins from the eastern colonies over-winter in the southern Barents Sea, while the rest of the population roam over large areas in the central North Atlantic. Most seabird populations return to the colonies in late winter or early spring.

Broadly, the spatial distribution of seabirds during the ecosystem survey reflects the climatic gradient from a boreal Atlantic climate with common guillemots, puffins, herring and black-backed gull in the south and west, to an Arctic climate with little auks, Brünnich's guillemots and kittiwakes in the north and east (Figure 3.8.2.3). Seabirds have been surveyed uninterruptedly on Norwegian vessels in the western part of the Barents Sea since 2004. Based on the minimum annual survey extent, the abundance (Figure 3.8.2.4) of different species and the centre of gravity of the spatial distribution (Figure 3.8.2.5) was calculated for each year.

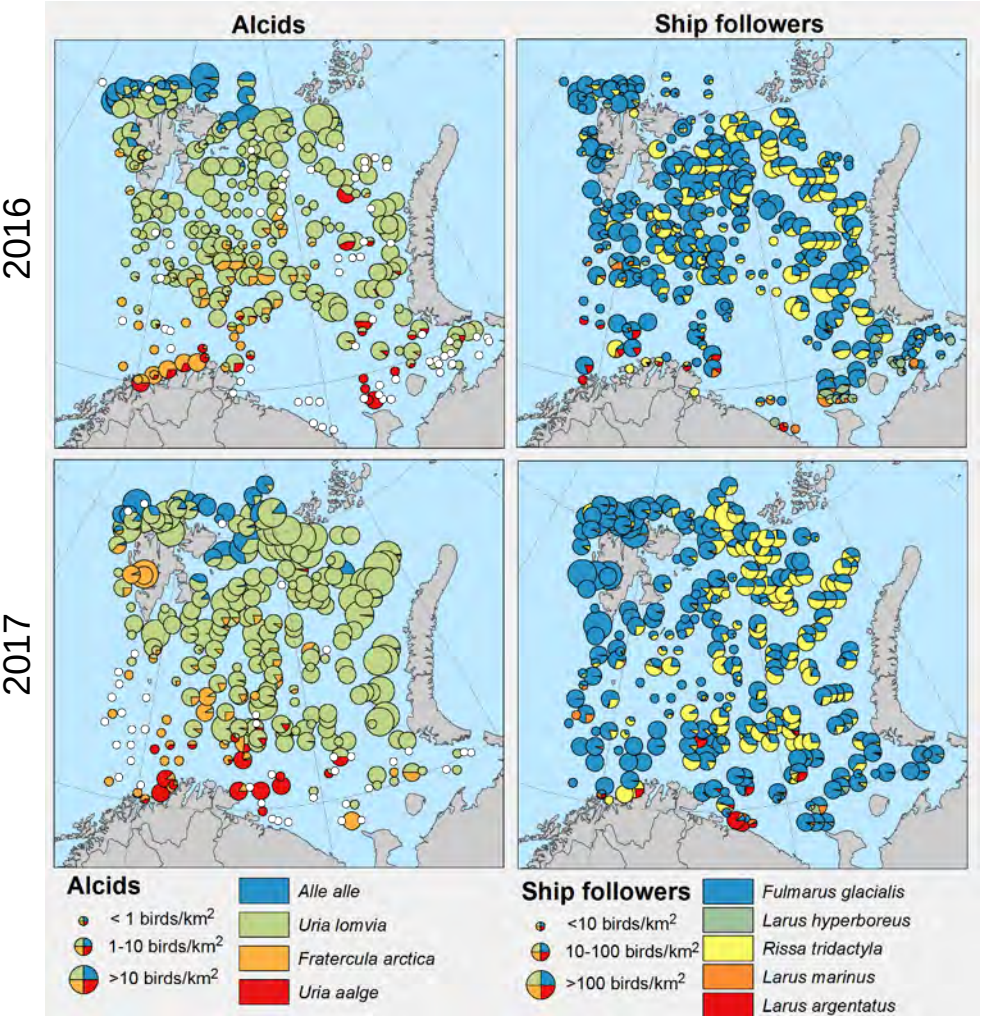

Figure 3.8.2.3. Density of seabirds during the Barents Sea ecosystem surveys in 2016 (top) and 2017 (bottom). Left panel is the distribution of auks (little auk, Bünnich's guillemot, puffin and common guillemot). Right panel is the distribution of shipfollowers (fulmar, glaucous gull. Kittiwake, black-backed gull and herring gull).

Note the large fluctuations in the abundance estimates from the at-sea surveys (Figure 3.8.2.4). These fluctuations do not necessarily reflect the observed population trends from the colonies (cf. Figure 2). This discrepancy could be related to the fact that the at-sea abundances are influenced by annual differences in migration pattern which would mask the general population trends. There is not yet an evidence for a widespread "borealization" (Fossheim et al. 2015) of the seabird communities in the Barents Sea, although there is a tendency for a slight northward displacement of puffins, kittiwakes and glaucous gull (Figure 3.8.2.5). During the last 14 years, the different seabird species seem to stay relatively fixed within their respective geographic niche.

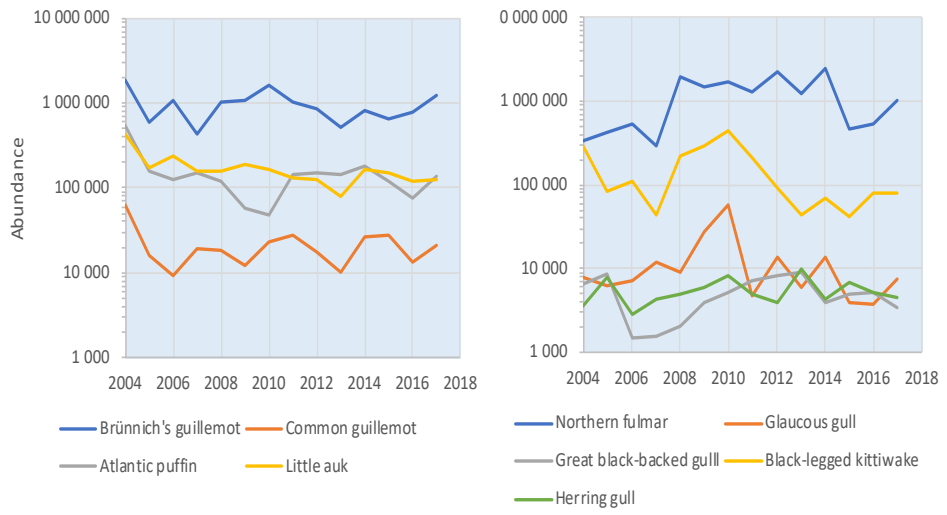

Figure 3.8.2.4. Abundance of auks (left) and shipfollowers (right) in the Western Barents Sea during the ecosystem surveys 2004-2017.

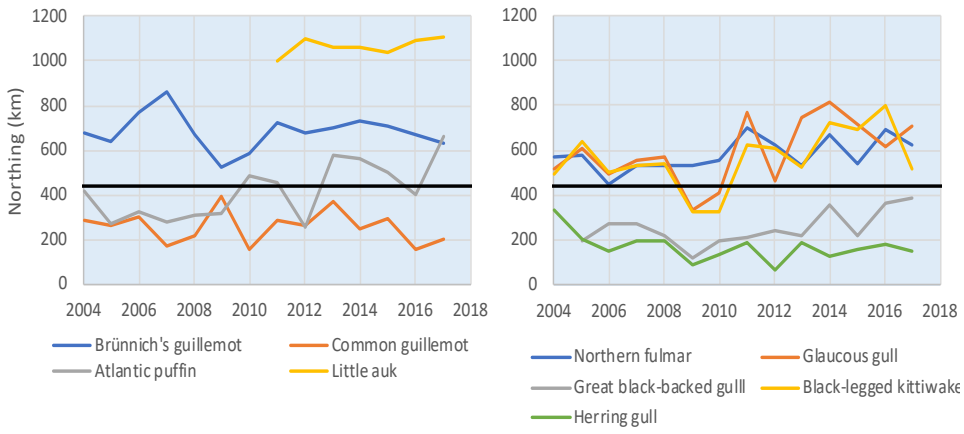

Figure 3.8.2.5. Center of gravity in the north direction of the distribution of auks (left) and shipfollowers (right) in the Western Barents Sea during the ecosystem surveys 2004-2017. Black line indicates the position of Bjørnøya.

3.9 Anthropogenic impact

3.9.1 Fisheries

Total catches

Fishing has the largest anthropogenic impact on fish stocks in the Barents Sea, and thereby, on the functioning of the entire ecosystem. However, observed variations in

both fish species and ecosystem are also strongly affected by climate and trophic interactions. During the last decade, catches of most important commercial species in the Barents Sea and adjacent waters of Norwegian and Greenland Sea varied around 1.5–3 million tonnes and has decreased in the last years (Figure 3.9.1.1).

Catch variation within the region depends on both the ecosystem dynamics effecting commercial stocks and management considerations. Agreed-upon harvest control rules exist for all major species, which are usually applied when setting TACs; actual catch removals tend to be very close to the agreed TACs.

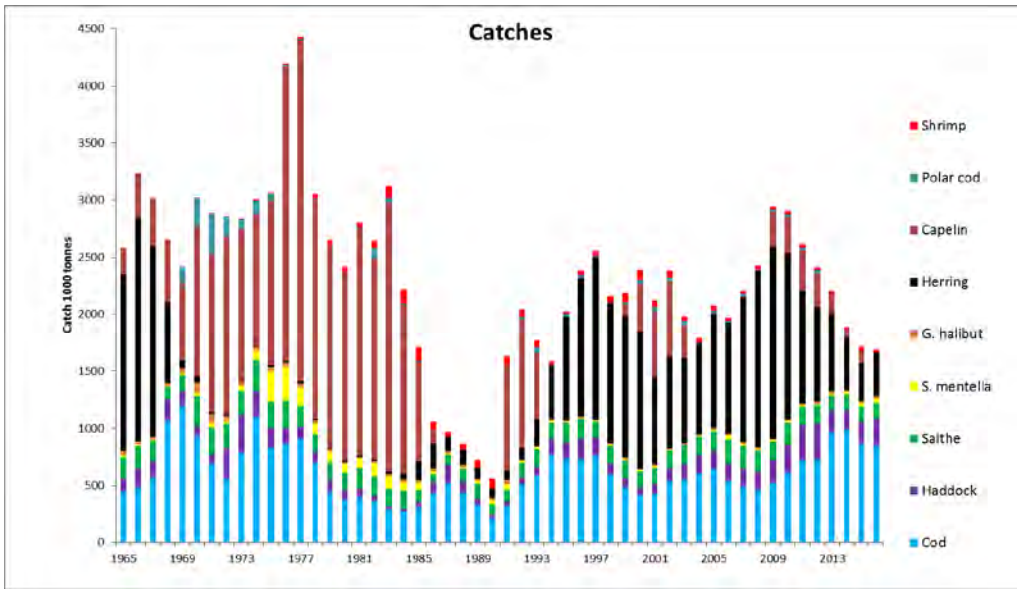

Figure 3.9.1.1. Total catches of the most important stocks in the Barents Sea and adjacent waters of Norwegian and Greenland Sea (including catches in all of ICES Division 2.a, i.e. along the Norwegian coast south to 62°N) from 1965–2017. Catches of Norwegian spring-spawning herring outside ICES Division 2.a are also included. Minor catches of other stocks are taken in the Barents Sea (see ICES website).

Fishing mortalities and harvesting strategies

Fisheries influence the ecosystem by removing substantial quantities of fish for human consumption and for other purposes. A fishery is not considered sustainable if it impairs recruitment to the fish stock. Single species management often focuses on measuring stock status through benchmarks called biological reference points (BRPs). BRPs for single species management are usually defined in terms of fishing mortality rate (F), total-stock biomass (TSB), spawning-stock biomass (SSB), and in terms of target and limit reference points. Limit BRPs suggest maximum F levels and minimum B levels that should adhered to. These BRPs are then compared to estimates of F and B from stock assessments to determine the state of the fishery and suggest management actions.

Fishing above the limiting reference point for fishing mortality (F_{lim}) will eventually bring the spawning stock down to B_{lim}; below which recruitment will be impaired. As such, F_{lim} may hence be used as an indicator for unsustainable exploitation which may negatively influence both the stock and the ecosystem. Keeping F below F_{lim} and the stock above B_{lim} may, however, not provide sufficient protection. Proliferation of smaller and younger adults within a stock as result of high fishing pressure, results in a lower stock reproductive potential; compared to a stock having adults with a wider

range of sizes and ages. The harvest rate and fishing pattern should hence fit with these biological requirements.

Recently the Maximum Sustainable Yield (MSY) concept was implemented in ICES advisory work. The ICES approach to fisheries advice integrates the precautionary approach, maximum sustainable yield, and an ecosystem approach into one advisory framework. The goal is, in accordance with the aggregate of international guidelines, to inform policies on sustainable fisheries removals from productive fish stocks within healthy marine ecosystems. Maximum sustainable yield is a broad conceptual objective aimed at achieving the highest possible yield over an infinitely long period of time. For several stocks, MSY reference points have been identified and implemented into fishery management strategies.

Furthermore, a fishery may not be considered optimal if the fish are caught too early, i.e. if the net natural growth potential is not utilized. This is called growth overfishing and makes the total yield less than it would be if the fish had been allowed to grow to a reproductive size/age. Introduction of minimum fish catch size limits and selective gears are the most common management measures to avoid growth overfishing.

Larvae and juveniles of all groundfish species are important predators on zooplankton. Accordingly, it is important that a healthy marine foodweb have sufficient plankton production to support plankton-eating invertebrate and fish species, as well as production at higher trophic levels, including: fish species; seabirds; marine mammals; and humans. For an ecosystem approach to management of commercial fish stocks it is essential to consider production at all trophic levels from a multispecies perspective.

Cod, haddock, and saithe

Barents Sea stocks of cod, haddock, and saithe all have fishing mortality (F) based management plans which are largely followed by managers when setting TACs; all are currently harvested close to or below MSY (Figure 3.9.1.2), and all are above B_{pa} at present. Several variants of harvest control rules (HCR) for cod and haddock were tested by ICES in 2016. A new harvest control rule for cod, with increasing F at high stock sizes, was adopted by the joint Russian-Norwegian Fisheries Commission in autumn 2016. The HCR for haddock was not changed. The current HCR for saithe was set by Norway in 2013.

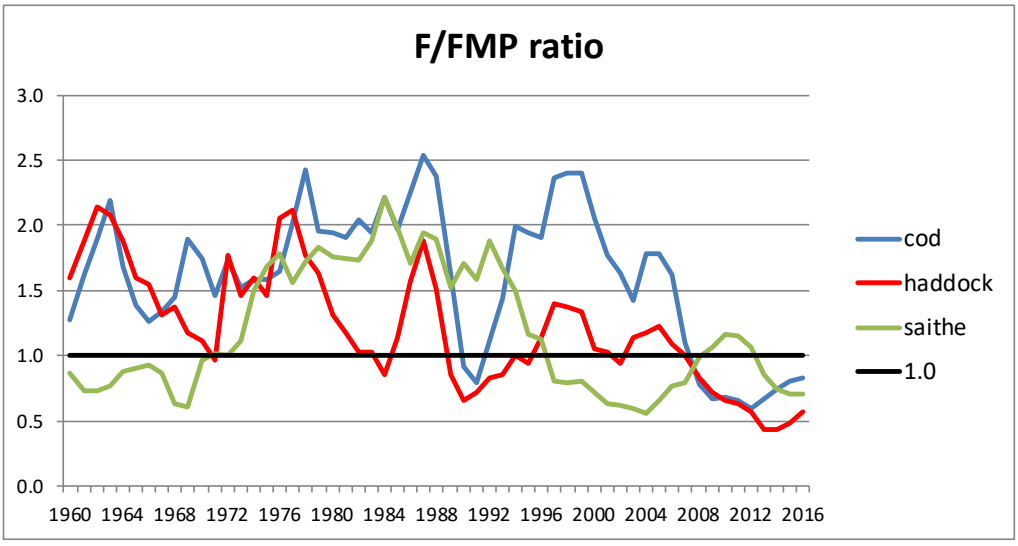

Figure 3.9.1.2. Annual fishing mortalities of the northeast Arctic cod, haddock and saithe stocks relative to fisheries management plan (FMP), i.e. the level used in the management plans for these

stocks when SSB>B_{pa} (and SSB<2*B_{pa} for cod) (ICES 2017). Note that saithe is mainly found along the Norwegian coast and off the coast south of the Barents Sea – little in the Barents Sea itself.

The exploitation rate has during some periods been critically high. Because of the harvest control rules, better regulation, and enforcement, this problem has been reduced in recent years. However, the recent increased exploitation rate for cod requires careful monitoring. The 2018 TAC for cod was set 63 kt above the advice from ICES and corresponds to an expected fishing mortality of 0.49 (not shown in Figure 3.9.1.2).

The current large cod stock has caused concern about it being 'too large' relative to food availability, and ecosystem carrying capacity. Thus far, cod population dynamics appear little affected by the large stock size, but the question remains valid. The introduction of a harvest control rule to increase F levels at high stock sizes could be a step taking such concerns into account. However, the concept of a stock being 'too large' is not, at present, incorporated in the ICES advice framework; although, such issues are well recognized, e.g. in management of freshwater fisheries and wildlife.

Capelin

The capelin fishery is managed through a target escapement strategy. MSY for capelin will depend strongly on size of the cod stock, and offers little meaning within a single-species context. There was no fishery for capelin in the Barents Sea during 2004–2008 due to poor stock condition. During 2009–2013 the stock was sufficiently large to support a quota between 200 000 and 400 000 tonnes. After which time, both stock and catch decreased, and there was a 'mini-collapse' of the stock; the fishery was closed during 2016–2017. The fishery reopened in 2018 with TAC set at 205 000 tonnes. Since 1979, the capelin fishery has been regulated through quotas set using a harvest control rule enforced by the Norwegian-Russian Fishery Commission. The harvest control rule is considered by ICES to be in accordance with precautionary and ecosystem approaches to fisheries management. Being a forage fish in an ecosystem where two top predators (cod and haddock) are currently at high levels, the capelin stock is now under heavy predation pressure. The fishery is restricted to the prespawning period (mainly February–March) and exploitation is regulated based on a model that incorporates natural mortality, including predation from cod. A minimum landing size of 11 cm has been in force since 1979. The management plan's harvest control rule is designed to ensure that SSB remains above the proposed B_{lim} of 200 000 metric tonnes (with 95% probability).

Greenland halibut

For Greenland halibut, no limit reference points have been suggested or adopted. The assessment is still considered to be uncertain due to problems with the age-reading and input data quality. The exploratory assessment is accepted as indicative for stock trends. Although many aspects of the assessment remain uncertain, fishery-independent indices of stock size from research surveys indicate an increase in stock size over the last decade, which now appears to be levelling off. Due to poor recruitment, some decrease in stock size is expected in the coming years. Therefore, it is important not to increase the exploitation rate and catch above the present level. Reconstruction of historical (pre-1992) stock and exploitation levels is needed to provide a stronger basis to determine reference points and develop sound of harvest control rules.

Beaked redfish (*Sebastes mentella*)

Analytical assessments and advice are provided for ICES Divisions 1 and 2 combined. The fishery for *S. mentella* (beaked redfish) operates in national and international waters, and is managed under different schemes and by different management organizations. A pelagic fishery for *S. mentella* has been conducted since 2004 in the Norwegian Sea outside the EEZ. This fishery is managed by the Northeast Atlantic Fisheries Commission (NEAFC). A new directed demersal and pelagic fishery has been permitted in the Norwegian Economic Zone since 2014, and is managed by Norway and Russia. This is mostly a directed fishery; while part of the TAC is set aside to cover bycatch by Norway, Russia, and third-party countries. The geographical distribution of Norwegian catches during 2016 is shown in Figure 3.9.1.4.

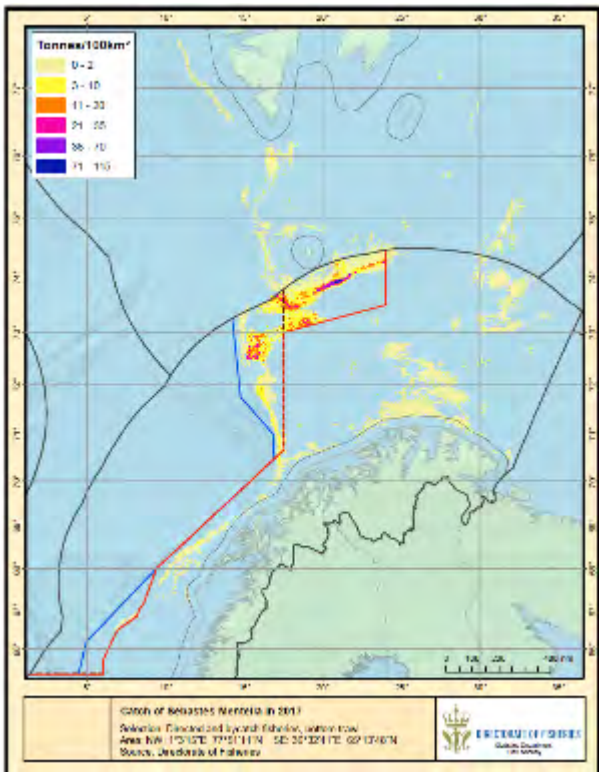

Figure 3.9.1.3. ***Sebastes mentella*** **in Divisions 1 and 2. Location of** ***S. mentella*** **catches by Norwegian fishing vessels in 2017, both in a directed fishery and as bycatch.**

An ICES Benchmark Workshop was held for this stock at the beginning of 2018 to evaluate the current data and assessment methodology and propose improvements. $F_{0.1}$ (19+) = 0.080 was considered a good proxy for F_{MSY}. Biomass trigger points of 600–800 kt are suggested. The current estimate of fishing mortality is below the F_{MSY} proxy, while the current SSB is estimated to be well above the range suggested for trigger points.

The Joint Norwegian-Russian Fisheries Commission requested that an evaluation of possible management plans for this stock be carried out during 2018. In the absence of a management plan, ICES advised a precautionary basis that an annual catch in 2015, 2016, and 2017 be set at no more than 30 000 tonnes below the MSY catch level, and that measures currently in place to protect juveniles should be maintained. Accordingly, Norway and Russia set a quota of 30 000 t for those years. For 2018 the quota was set to 32 658 t, corresponding to status quo F.

Golden redfish (Sebastes norvegicus)

An ICES Benchmark Workshop was also held for *Sebastes norvegicus* (golden redfish) at the beginning of 2018. No limit reference points have yet been adopted. SSB has been decreasing since the 1990s and is currently at the lowest level in the time-series. Fishing mortality is high, but there are some signs of improved recruitment. For many years, ICES has advised no fishing on this stock, given the very low SSB (below any possible reference points) and poor recruitment. Most catch of this stock is bycatch. A stock rebuilding plan is needed.

Polar cod (Boreogadus saida)

There has been little economic interest in developing a fishery for polar cod; no fishery has been conducted in recent years. Stock size as measured in the BESS survey, has also been at very low levels, except for a one-year peak in 2016. The historical fishery conducted mainly by Russia, took place in late autumn when concentrations of polar cod were targeted during southward spawning migrations along the coast of Novaya Zemlya.

Wolffish (Catfish)

Three species of wolffish: Atlantic wolffish (*Anarhichas lupus*), Spotted wolffish (*Anarhichas minor*), and Northern wolffish (*Anarhichas denticulatus*) are taken mostly as bycatch in fisheries for gadoids in the Barents Sea, but also in a directed longline fishery. From 1905 to 1950, international catches of wolffish in the Barents Sea and along the northern Norwegian coast increased from 100 to 14 000 tonnes. Until 1998, annual landings were between 6000 and 44 500 tonnes. Large catches during 1997–2001 were primarily due to intensive targeted fishing for northern wolffish related to bycatch regulations on other valuable species (e.g. Greenland halibut) and a growing Russian market. After 2001, total wolffish catch north of 62°N decreased; but has improved slightly in recent years, reaching 25 862 tonnes in 2017. Russian catches increased from about 13 000 tonnes — a level maintained over several years — to 18 000 tonnes in the past two years. Norwegian catches have been aroundt 6000 tonnes in recent years (Figure 3.9.1.6). Northern and spotted wolffish comprise more than 90% of total wolffish catch in the Barents Sea. Atlantic wolffish are mainly caught in the coastal zone, but also beyond the coastal region.

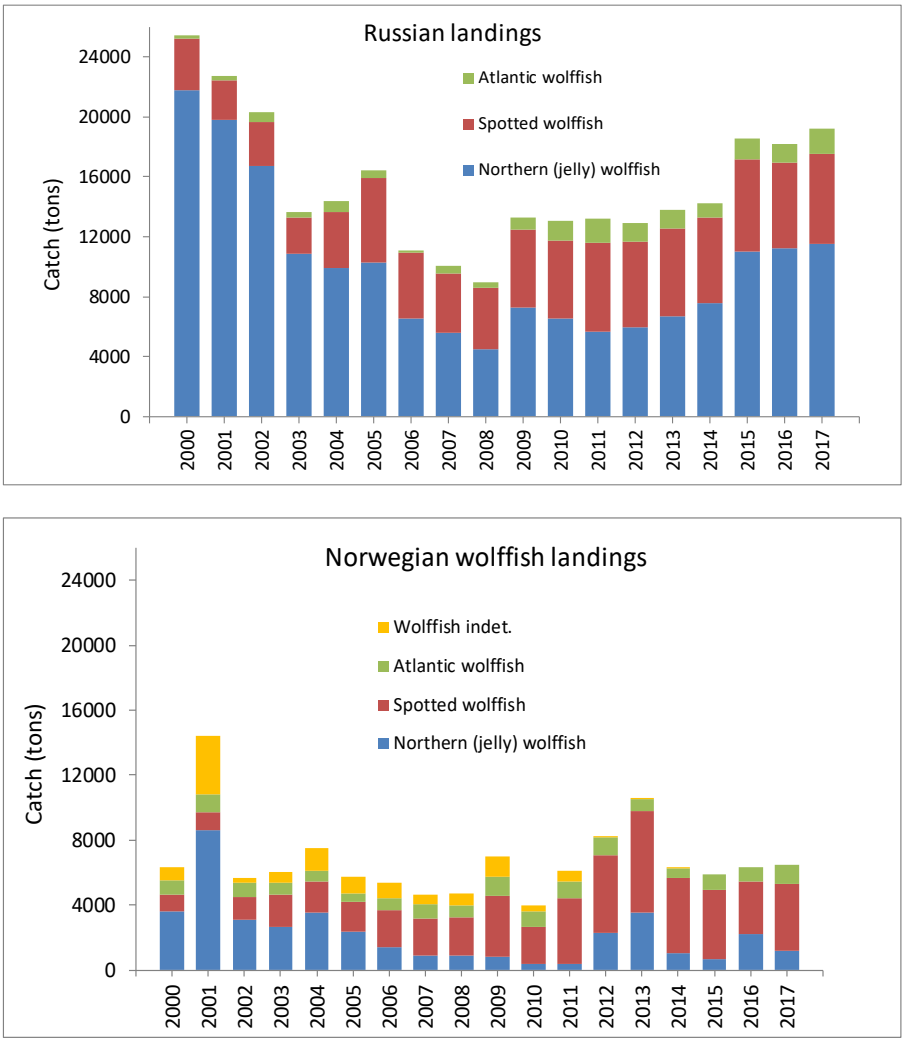

Figure 3.9.1.4. Russian (above) and Norwegian (below) official landings of the different wolffish species north of 62°N in 2000–2017.

Other fish species

Information on the species composition of the Norwegian fisheries north of 67°N is available from the Norwegian Reference Fleet (NRF), i.e. 15 high seas and 24 coastal fishing vessels contracted by the Institute of Marine Research. Such data are now routinely collected from these vessels' fishery each day or every other day. The impact of fishing activity on non-regulated species and on the ecosystem will be a subject for further research.

Gullestad *et al.* (2017) presents practical implementation of the Ecosystem Approach to Fisheries Management (EAFM) in Norway. This involves defining management objectives and developing simple and efficient tools to: obtain an overview of management needs; prioritize these needs; integrate broader conservation issues; and ensure stakeholder involvement.

Species of economic interest not mentioned in this chapter, include: tusk, ling, f grenadiers, Atlantic halibut, other flatfish, lumpsucker, hake, pollack, whiting, Norway pout, argentines, salmon, dogfish, skates, and molluscs.

3.9.2 Catches of shellfish

Northern shrimp (*Pandalus borealis*)

Norwegian and Russian vessels harvest northern shrimp over the stock's entire area of distribution in the Barents Sea. Vessels from other nations are restricted to trawling shrimp only in the Svalbard zone and the Loophole — a piece of international waters surrounded by the EEZs of Norway and Russia. No overall TAC has been set for northern shrimp, and the fishery is regulated through effort control, licensing, and a partial TAC in the Russian zone only. The regulated minimum mesh size is 35 mm. Bycatch is constrained by mandatory sorting grids, and by temporary closures in areas with high bycatch of juvenile cod, haddock, Greenland halibut, redfish, and shrimp (<15 mm carapace length or <6 cm total length). Catches have varied between 19 000 and 128 000 tonnes per year since 1977. Since the mid-1990s, a major restructuring of the fleet toward fewer and larger vessels has taken place. Since 1995, average engine size of a shrimp vessel in ICES Divisions 1 and 2 increased from 1000 HP (horse power) to more than 6000 HP in the early 2010s, and the number of fishing vessels has declined markedly. Overall catch decreased from approximately 83 000 tonnes since 2000, reflecting reduced economic profitability in the fishery. After a low of about 20 000 tonnes in 2013, catches again began to increase and reached about 34 000 tonnes in 2015, but decreased to 30 000 tonnes in 2016 and 2017. The 2017 stock assessment indicated that the stock has been fished sustainably, and has remained well above precautionary reference limits throughout the history of the fishery. Accordingly, ICES used the MSY-approach to advice a 2018 TAC of 70 000 metric tonnes (ICES 2017a).

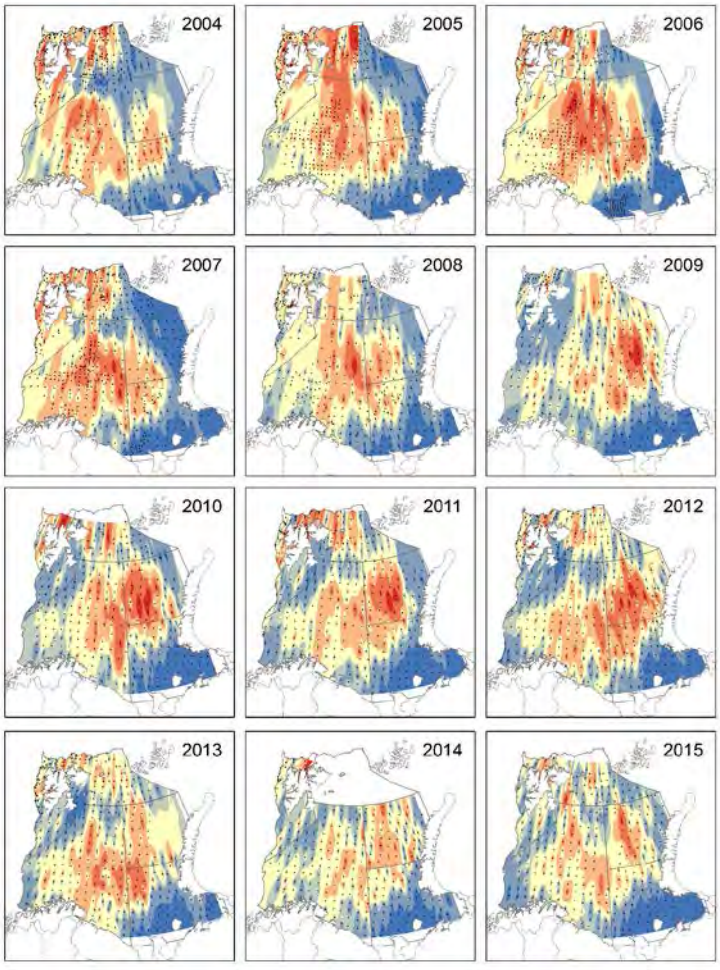

Figure 3.9.2.1 Shrimp density by year from inverse distance weighted interpolation (e.g. Fisher *et al.*, 1987) between trawl stations (black dots) for the Joint Russian-Norwegian Ecosystem survey (Europe Albers Equal Area Conic projection). No map for 2016–2017 available

Geographical distribution of the stock in 2009–2015 was more easterly compared to previous years (Figure 3.9.2.1). As results, catch levels from some of the more traditional western fishing grounds have declined. Recent reports indicate lower catch rates than would be expected given the overall good stock condition. This may be related to operation costs for a relatively small fleet to move away from more traditional fishing grounds, and to find new grounds with commercially viable shrimp concentrations.

Fisheries for northern shrimp in the Barents Sea and waters adjacent to Spitsbergen Archipelago have been carried out since the 1950s; the Russian fishery was started in 1976. The largest catches were recorded in the mid-1980s (more than 120 000 tonnes) and during 1990–1991, 2000 (approximately 80 000tonnes). Since 2005, total annual catch of northern shrimp in this area have remained at the 20 40 thousand tonnes level (Figure 3.9.2.2).

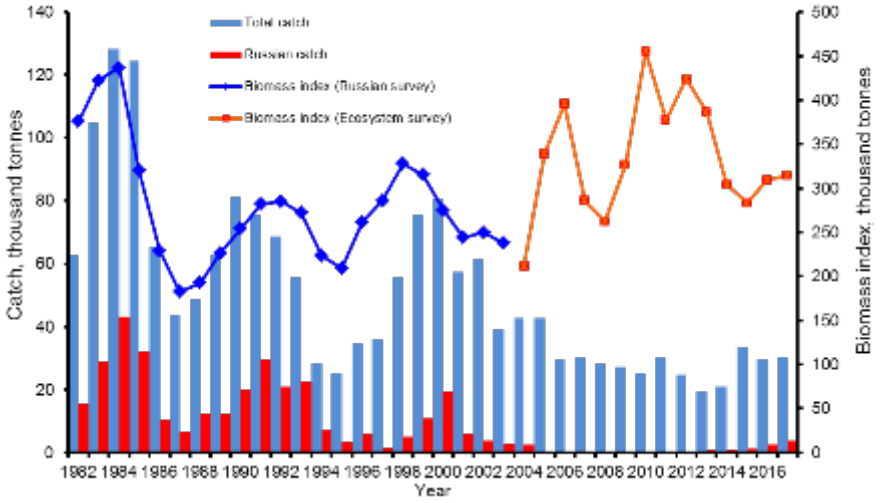

Figure 3.9.2.2 Total biomass index and catch of the northern shrimp in the Barents Sea and waters around Svalbard archipelago in 1982–2017 (Zakharov, 2017 with editions)

The catch of northern shrimp by Russian vessels in 2017 was about 4000 tonnes and conducted mainly in the Central Basin, near Novaya Zemlya and Franz Josef Land.

Trawl surveys of northern shrimp stocks have been carried out in the Barents Sea since 1982. During the 2005–2016 period, the stock was relatively stable (Figure 3.9.2.2).

In 2017, estimated total biomass (method of squares) of northern shrimp was 314.2 thousand tonnes; 1.5% higher than in 2016, and 8% lower than the long-term average. Annual assessments of total catch of northern shrimp in the Barents Sea and waters around Spitsbergen Archipelago can typically reach 70 000 tonnes (Zakharov, 2017).

Red king crab (Paralithodes camtschaticus)

The commercial fishery for red king crab in the Russian Economic Zone of the Barents Sea has been carries out since 2004. Russian Fisheries Regulations stipulate that males with carapace width greater than or equal to 150 mm can only be caught using traps.

Heavy exploitation of the stock during 2005–2006 led to a decrease in the commercial component of the red king crab population, and reduced productivity in the fishery. In 2011, decreased fishery pressure prompted population growth, and subsequent stabilization of the commercial stock. Total catch also increased in subsequent years (Figure 3.9.2.3); in 2016, total catch of red king crabs in Russian Economic Zone was 8.3 thousand tonnes (Table 3.9.2.1).

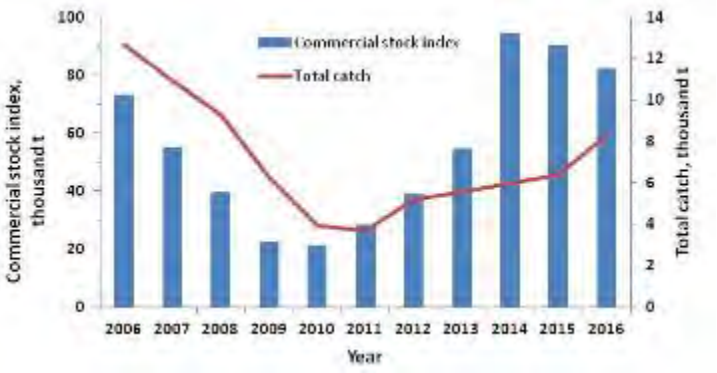

Figure 3.9.2.3. Commercial stock index and the total catch of the red king crab in the Russian Economic Zone of the Barents Sea in 2006–2016 (Bakanev and Stesko, 2017)

Table 3.9.2.1. The main parameters of the red king crab Russian fishery in 2006–2016 (Bakanev and Stesko, 2017)

Year	Commercial stock index, thousand tonnes	Total catch		Mean weight of commercial crab, kg
		thousand ind.	thousand tonnes	
2006	73.3	3 082	12.639	4.1
2007	54.9	2 667	10.934	4.1
2008	39.6	2 266	9.291	4.1
2009	22.5	1 971	6.309	3.2
2010	21.4	1 313	3.940	3.0
2011	28.4	1 276	3.702	2.9
2012	39.0	1 736	5.209	3.0
2013	54.8	1 784	5.531	3.1
2014	94.8	1 712	5.995	3.5
2015	90.4	1 725	6.381	3.7
2016	82.5	2 075	8.300	4.0

One of the most detailed trap surveys to assess distribution of the red king crab commercial stockwas conducted in 2013. Results from this survey indicated the densest concentrations of commercial sized male crabs (more than 1000 ind./km^2) was recorded on Rybachya Bank and Kildinskaya Bank, in the eastern part of Murmansk Rise, and in the southern part of North Kanin Bank (Figure 3.9.2.4). In other parts of this area, the abundance of commercial sized males varied from 100 to 500 ind./km^2 (Figure 3.9.2.4). Subsequently, aggregations of fishable crabs shifted eastward to the western part of the Kanin-Kolguev Shallow. The most eastern extent of red king crab distribution was recorded in 2015 and 2017. Two adult individuals (male and female with clutch) in eastern Pechora Sea near Vaygach Island, and the southwestern coast of Novaya Zemlya Archipelago. This change in distribution could be caused by both migration to find new food resources and climatic warming.

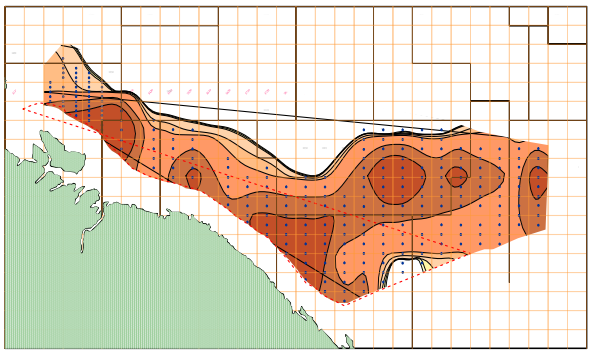

Figure 3.9.2.4. Distribution of the commercial stock of the red king crab (commercial males, ind./km²) in autumn 2013 in Russian Economic Zone of the Barents Sea according to assessment trap's survey (Bakanev and Stesko, 2017).

In 2016, ten Russian vessels fished red king crabs in the eastern Barents Sea, the Murmansk Rise, and Kanin Bank using rectangular and trapezoidal traps. The largest catches were obtained at southeastern Murmansk Rise outside the 12-mile coastal zone. In 2016, the commercial stock index for red king crab was 82.5 thousand tonnes (Table 3.9.2.1, Bakanev and Stesko, 2017).

Snow crab (Chionoecetes opilio)

The snow crab fishery carried out by Norwegian, Spanish, and Russian vessels began in international waters of the Barents Sea (Loop Hole) in 2013. Russian vessels fished crabs in this area until 2016. In 2016, Russian vessels started fishing snow crabs in Russian waters (Figure 3.9.2.5). In 2017, the Russian fishery for snow crabs was conducted only within the Russian EEZ.

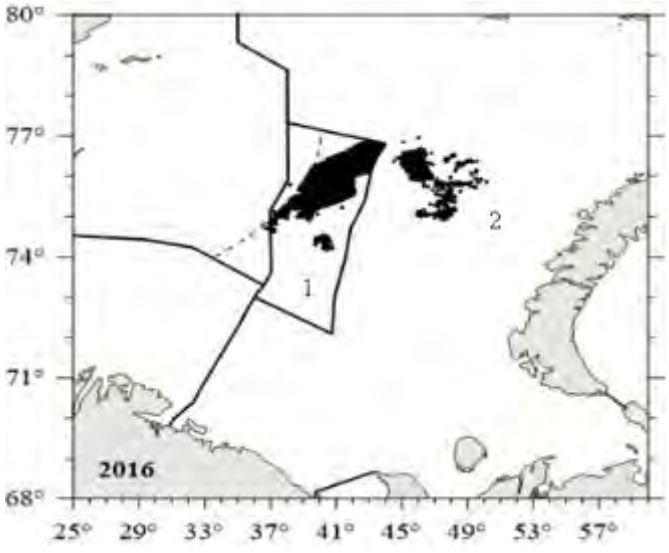

Figure 3.9.2.5. Russian fishery of the snow crab location in the Barents Sea in the international waters in 2013-2016 (1) and nationality waters in 2016 (2) (Bakanev and Pavlov, 2017)

Russian vessels mainly use conical traps for the snow crab fishery. Statistics for the Russian snow crab fishery in the Barents Sea during 2013–2016 are shown in Table 3.9.2.2.

Table 3.9.2.2. Russian fishery statistics for the snow crabs in the Barents Sea during 2013-2016 (Bakanev, Pavlov, 2017)

Year	Number of vessels	Total fishery days	Numbers of traps, th.	Total catch, tonnes
International waters (Loop Hole)				
2013	2	22	2,4*	62.0
2014	12	1 153	788.7	4 104.2
2015	20	3 119	2894.7	8 894.6
2016	18	2 576	2687.5	6 486.7
Russian waters				
2016	5	178	91.7	1 499.9

During the 2003–2016 period of unregulated fishing in Loop Hole, the total international catch of snow crabs exceeded 55 thousand tonnes. During 2015–2016, average daily catch declined by 10–20% from the 2014 estimate. (Bakanev and Pavlov, 2017).

Decreased fishery productivity indicated significant overfishing of the Barents Sea snow crab stock. To address this situation, Russia and Norway agreed in 2016 on joint management of the snow crab fishery in the international waters (Loop Hole area) to prevent illegal, unreported, and unregulated fishing.

3.9.3 Whaling and seal hunting

Minke whale (Balaenoptera acutorostrata)

Management of the minke whale is based on the Revised Management Procedure (RMP) developed by the Scientific Committee of the International Whaling Commission. Inputs to this procedure are catch statistics and absolute abundance estimates. The present quotas are based on abundance estimates from survey data collected in 1989, 1995, 1996–2001, 2002–2007, and 2008–2013. The most recent estimates (2008–2013) are 89 600 animals in the Northeastern stock, and 11 000 animals for the Jan Mayen area, which is exploited by Norwegian whalers. The present (2016–2021) RMP quota of 880 animals annually is considered precautious, conservative, and protective for the minke whale population in the Northeast Atlantic. At present only Norway utilizes this quota.

Harp seals (Pagophilus groenlandicus)

Northeast Atlantic stocks of harp seals are assessed every second year by the ICES Working Group on Harp and Hooded Seals (WGHARP). The assessments are based on modelling, which provides ICES with sufficient information to give advice on both status and catch potential of the stocks. The applied population model estimates current total population size, incorporating historical catch data, estimates of pup production and historical values of reproductive rates. Modelled abundance is projected into the future to provide an estimate of future population size for which statistical uncertainty is provided for various sets of catch options. Russian aerial surveys of White Sea harp seal pup production conducted during the period 1998–2013 indicate a severe reduction in pup production after 2003. This could be due to changes in fecundity and/or changes in survival. The Barents Sea/White Sea population of harp seals is now considered data poor (available data for stock assessment older than 5 years). The population model provided a poor fit to pup production survey data; primarily due to the

abrupt reduction after 2003. Nevertheless, to the model results were used to provide advice in 2017 (ICES 2016d). The total size of the population was estimated to be 1 408 200 (95% C.I. 1 251 680–1 564 320). A catch of 10 090 age 1+ animals, or an equivalent number of pups (where one 1+ seal is balanced by 2 pups), per year would sustain the 1+ population at present level over the 15-year period (2017–2032). Catches in recent years have been much lower than the quotas. Particularly after 2008, the last year that Russia hunted this population.

3.9.4 Fishing activity

Fishing activity in the Barents Sea is tracked by the Vessel Monitoring System (VMS). Figures 3.9.4.1 and 3.9.4.2 show fishing activity in 2017 based on Russian and Norwegian data. VMS data offer valuable information about temporal and spatial changes in fishing activity. The most widespread gear used in the Barents Sea is bottom trawl; but longlines, gillnets, Danish seines, and handlines are also used in demersal fisheries. Pelagic fisheries use purse-seines and pelagic trawls. The shrimp fishery used special bottom trawls.

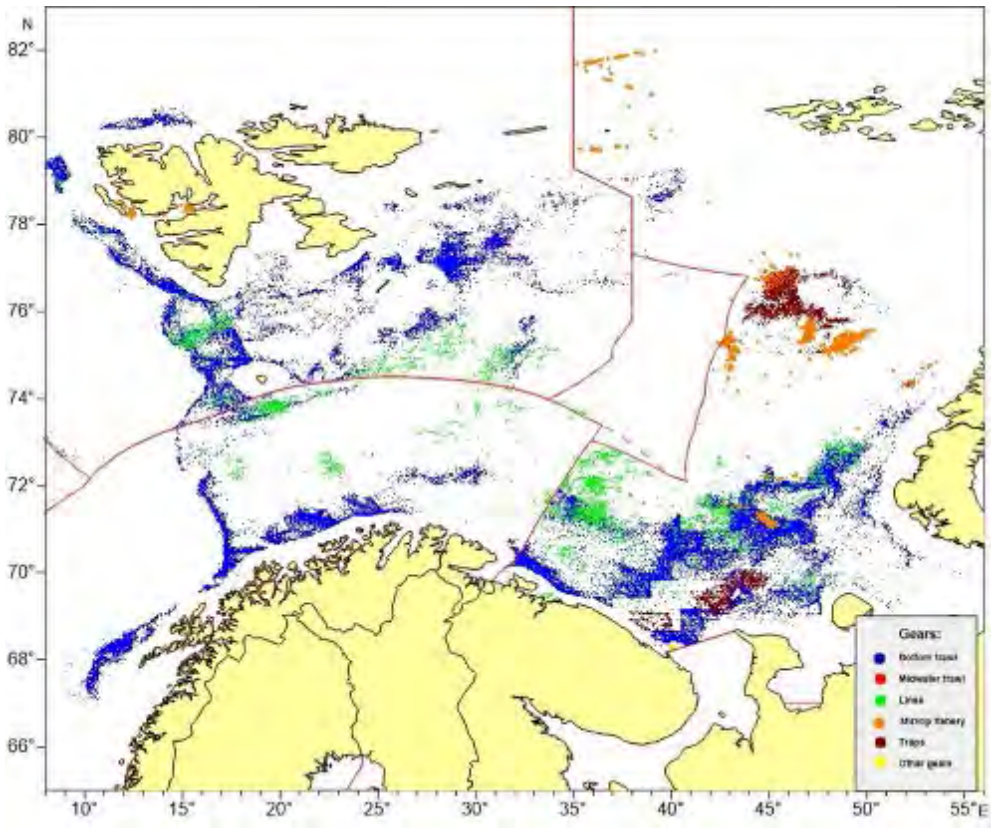

Figure 3.9.4.1. Location of Russian and foreign fishing activity from commercial fleets and fishing vessels used for research purposes in 2017 as reported (VMS) to Russian authorities. These are VMS data linked with logbook data (source: PINRO Fishery statistics database).

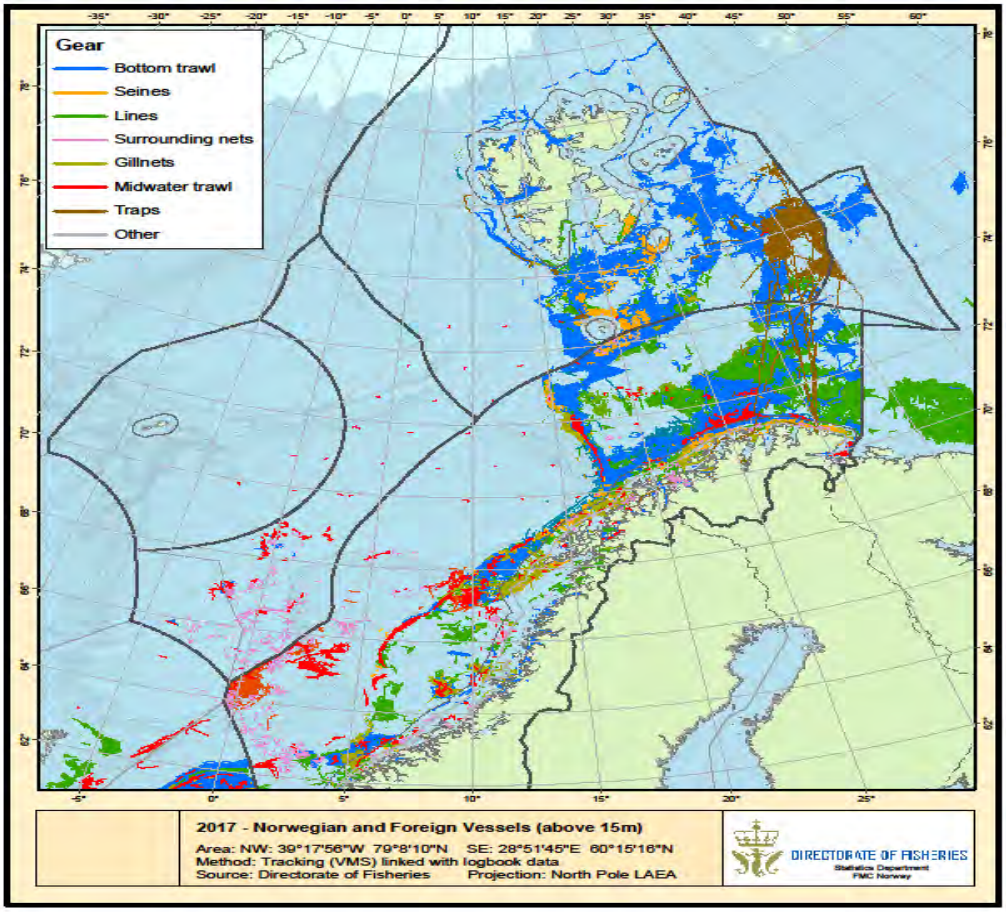

Figure 3.9.4.2 Location of Norwegian and foreign fishing activity from commercial fleets (larger than 15 m) and fishing vessels used for research purposes in 2017 as reported (VMS) to Norwegian authorities. These are VMS data linked with logbook data. Surrounding nets = Danish seine (source: Norwegian Directorate of Fisheries).

From 2011 onwards, minimum mesh size for bottom-trawl fisheries for cod and haddock is 130 mm for the entire Barents Sea; previously the minimum mesh size was 135 mm in the Norwegian EEZ and 125 mm in the Russian EEZ. It is still mandatory to use sorting grids. Minimum legal catch size was harmonized at the same time: for cod from 47 cm (Norway) and 42 cm (Russia) to 44 cm for all, and for haddock from 44 cm (Norway) and 39 cm (Russia) to 40 cm for all.

3.9.5 Discards

The level of discarding in fisheries is not estimated, and discards are not accounted for in stock assessments. Both undersized fish and bycatch of other species can lead to discarding; fish of legal size but low market value are also subject to discarding to fill the quota with larger and more valuable species (known as highgrading).

Discarding is a (varying) problem, e.g. in haddock fisheries where discards are highly related to the abundance of haddock close to, but below, the minimum legal catch size. Dingsør (2001) estimated discards in the commercial trawl fishery for northeast Arctic cod during 1946–1998, and the effects on the assessment. Sokolov (2004) estimated cod discard in the Russian bottom-trawl fishery in the Barents Sea during 1983–2002. The lack of discard estimates leads to less precise and accurate stock assessments. The influence of the fishery on the ecosystem is, therefore, not fully understood. A possible

way to estimate discard is through analysis of landing information (size/weight composition of landings relative to observations made onboard fishing vessels). Norway is conducting a pilot project to estimate discards in selected fisheries to test and establish methods for estimating discards in all Norwegian fisheries on a routine basis.

Since 1984, documentation of redfish (mainly *S. mentella*) taken as bycatch and then discarded in the Norwegian shrimp fishery, shows that shrimp trawlers removed significant numbers of juvenile redfish during the early 1980s. This discarding peaked in 1984, when bycatch amounted to about 640 million individuals; a number comparable to a good year class in this stock (Figure 3.9.5.1). After sorting grids became mandatory in 1993, bycatch of redfish was reduced dramatically. It was also shown that areal closure are necessary to protect small juvenile redfish, since they are not sufficiently protected by sorting grids. The bycatch and discard of cod consists mainly of 1- and 2-year-olds, but is generally small compared to other reported sources of mortality like catches, discards in the groundfish fisheries and cannibalism.

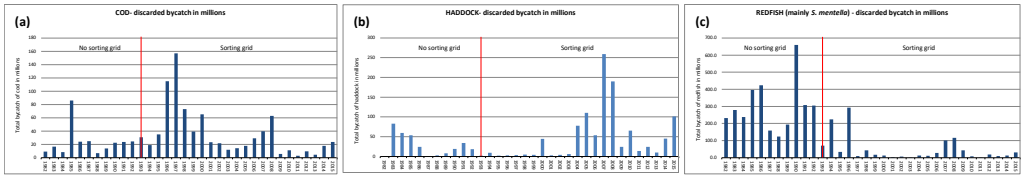

Figure 3.9.5.1. Revised bycatch (discards) estimates of small a) cod, b) haddock and c) redfish during the Barents Sea shrimp fishery 1982–2015 (ICES 2016c).

Noticeable discard of cod in the shrimp fishery occurred in 1985 and 1996–1998. The highest recorded number of discarded cod was 157 million in in 1997. Cod bycatch has declined in recent years (<20 million). Discards of haddock in the Barents Sea shrimp fishery have been estimated for the period 2000–2005, and show the highest discard in 2007–2008 (about 200 millions). Discard of Greenland halibut in the Barents Sea shrimp fishery was estimated for the 2000–2005 period; highest discard occurred in 2002 and 2000 (approximately 13 million specimens).

Even if the sorting grid prevents discarding of fish larger than 18 cm, it becomes obvious that only effective surveillance and closing areas for shrimp fishing can prevent bycatch and discard of smaller specimens.

3.9.6 Marine litter

3.9.6.1 The Barents Sea

Marine litter is defined as "any persistent, manufactured or processed solid material discarded, disposed or abandoned in the marine and coastal environment".

Large-scale monitoring of marine litter was conducted by the BESS survey during the 2010–2017 period, and helped to document the extent of marine litter in the Barents Sea (the BESS survey reports, Grøsvik *et al.*, 2018). Distribution and abundance of marine litter were estimated using data from: pelagic trawling in upper 60 m; trawling close to the seabed; and visual observations of floating marine debris at surface.

The study, done by Grøsvik *et al.*, 2018, had comprehensive, with data collected from 2265 pelagic trawls and 1860 bottom trawls, and surface observations made between stations. Marine litter was recorded from 301 pelagic- and 624 bottom-trawl catches. In total, 784 visual observations of floating marine debris were recorded during the period. Marine litter was categorized according to volume or weight of material type:

plastic; wood; metal; rubber; glass; paper; or textile. Marine litter is observed in the entire Barents Sea and distribution varied with material densities, ocean currents, and water depth. Plastic was the dominant type of marine litter observed at: 72% of surface observations; 94% of pelagic trawl stations; and 86% of bottom-trawl stations (Figure 3.9.6.1.1, Grøsvik *et al.*, 2018). Wood constituted 19% of marine litter observed at the surface, 1% in pelagic trawls, and 17% in bottom trawls. Materials from other categories — metal, rubber, paper, textile, and glass — were observed less frequently.

Floating marine debris was widely distributed; highest volume was observed in central, eastern, and northern areas (Figure 3.9.6.1). Wood dominated observations in this category (61.9 ±21.6% by volume), while plastic constituted 34.6 ±22.3% by volume. Metal, rubber, and paper were recorded less frequently.

Pelagic marine litter was observed in 13% of all pelagic trawls with a mean of 58 grammes per trawl catch, and was widely distributed (Figure 3.9.6.1.1). Plastic formed the bulk (85.1%) of pelagic marine litter observed with a mean of 0.011 mg m-3; paper formed 9.4%; textile formed 3.9%, and was more seldom observed; other materials were only observed sporadically. Pelagic plastic was significantly correlated with latitude and longitude during some years, and indicated northeastern distribution in 2010, and northern distribution in 2011 and 2014.

Marine litter as bycatch from bottom trawling was observed in 33.5% of all bottom-trawl hauls, with a mean of 772 g per haul. Marine litter from bottom trawls was distributed widely; highest levels were observed in western, southeastern, north eastern parts, and around Svalbard. Plastic was observed in the entire Barents Sea, processed wood in eastern and northern parts, and metal and rubber in the southeast (Figure 3.9.6.1.1 and 3.9.6.1.2). Processed wood dominated marine litter from bottom trawls, with 66% of mean weight in all catches with any type of marine litter. Plastic constituted 11.4% of the mean weight; but dominated in the number of observations. Metal and rubber constituted ~10% of the mean weight, but the number of observations was limited. On average, 26 kg km^{-2} of marine litter was observed in the Barents Sea; with an average of 2.9 kg km^{-2} of plastic litter alone (Grøsvik *et al.*, 2018).

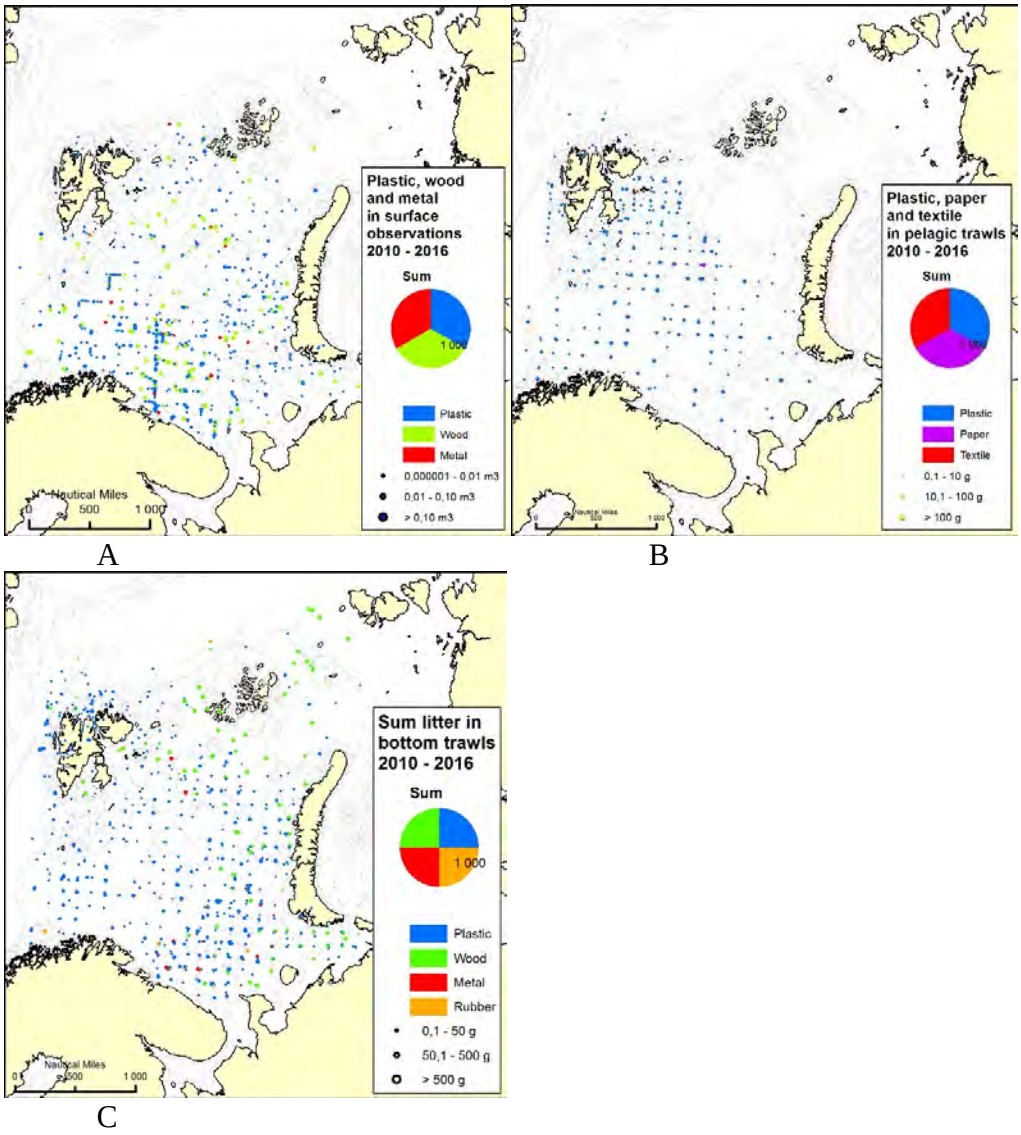

Figure 3.9.6.1.1 A: Sum marine litter from (A) surface observations, (B) pelagic trawls and (C) bottom trawls from 2010 to 2016.

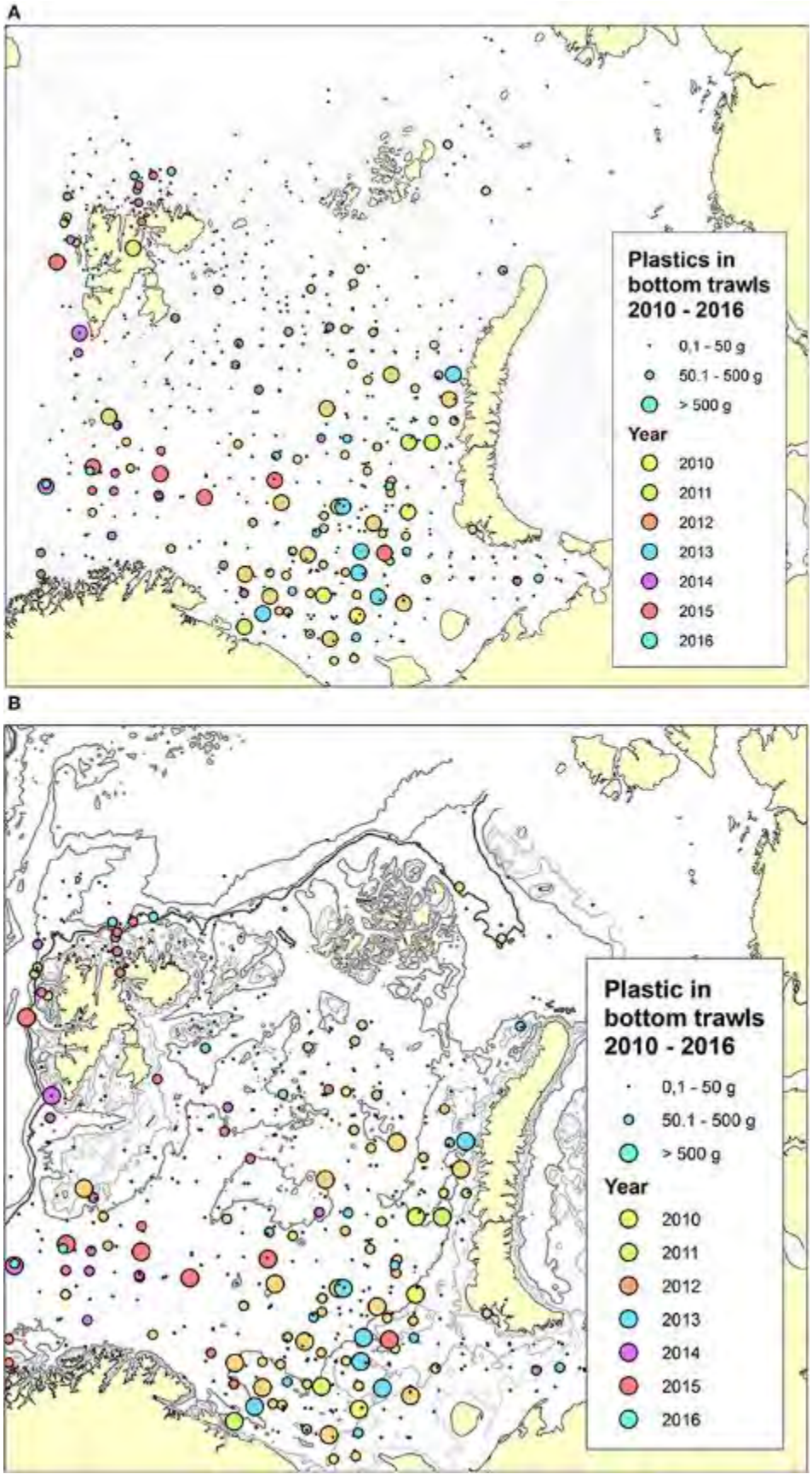

Figure 3.9.6.1.2. Plastic and wood in bottom trawls from 2010 to 2016, (A) Plastic only. (B) Wood only. Different colors indicated per year.

In 2017, anthropogenic marine litter floating on the surface and captured in trawls was observed on board all Russian and all Norwegian vessels during the ecosystem survey. Plastic dominated this category in 71.3% of all observations (Figure 3.9.6.1.3). Due to currents, it is uncertain whether polluting objects were dumped directly into some areas or had been transported in from other areas. Wood was observed in the 28.4% of all observations. Dispersed amounts of textile, paper, rubber, and metal were observed less frequently, but on occasion. Litter from fishing operations was observed in 23.5% of observations of plastic litter at the surface (Figure 3.9.6.1.3). Types of fishery litter largely consisted of ropes (OSPAR code 31), string and cord (32), pieces of nets (115), floats/buoys (37), etc.

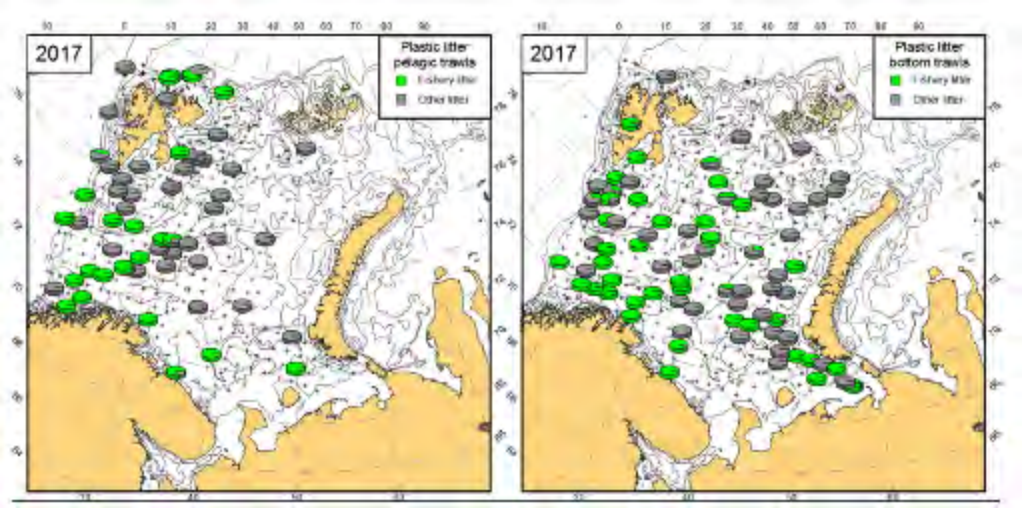

Figure 3.9.6.1.3. Proportion of fishery plastic among total plastic litter collected in pelagic (left) and bottom trawls (right) during the 2017 BESS survey (crosses – trawl stations).

3.9.6.2 Video recording of marine litter

Buhl-Mortensen and Buhl-Mortensen (2017) reported litter from 1778 video transects. Each video transect is 700 m long; the average field of view is 3 m. Video recording of the seabed was performed with a tethered video platform that is equipped with a high definition color video camera (Sony HDC-X300) tilted forward at a 45° angle during transect survey mode. Two analogue CCD video cameras were also deployed: one directed forward for navigation; and one for surveillance of the cable. Two laser beams (10 cm apart) were used to determine width of the field view. The video rig is towed by the survey vessel at a speed of 0.7 knots and controlled manually using a winch operator ~1.5 m above the seabed.

The percentage of video transects showing litter is comparable for the Barents Sea and the Norwegian Sea; 27% and 29%, respectively. Mean density of litter for the Barents Sea and Norwegian Sea was 202 and 279 items/km^2, respectively. Mean density of litter near the coast and offshore was 268 and 194 items/km^2, respectively. A conservative estimate of the total amount of marine litter in the Barents Sea south of Svalbard (523 600 km^2) — using mean litter densities in offshore areas (194 items/km^2) — is ~101 million items, corresponding to 79 thousand tonnes (Buhl-Mortensen and Buhl-Mortensen, 2017).

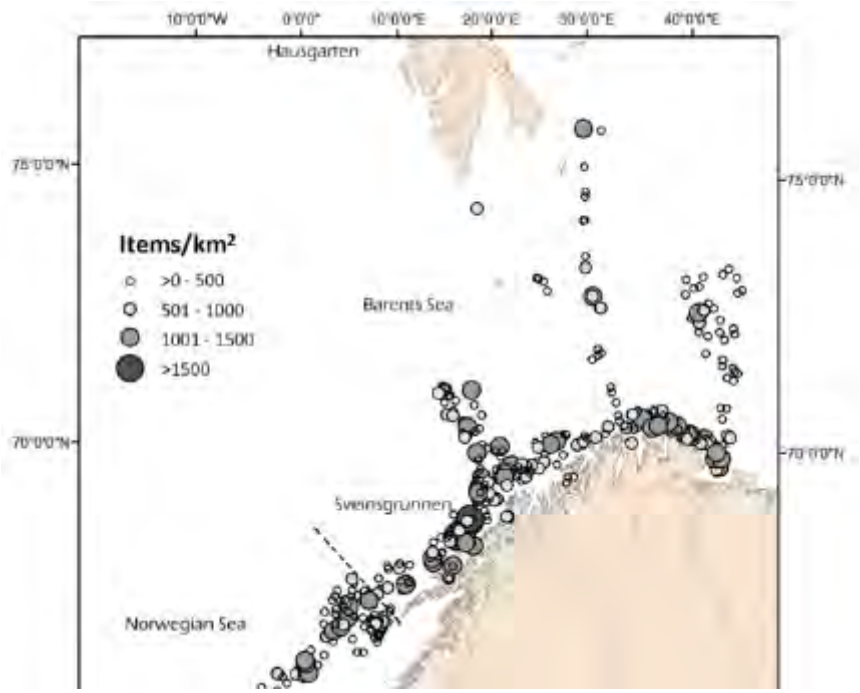

Figure 3.9.6.2.1. Litter densities (kg/km²) based on Mareano programme from 2006–2007. Dashed lines mark the border between the Barents Sea and Norwegian Sea.

Dividing video observations of litter into three categories of density: 23% of video transects had low densities of litter (>0–1000 items/km²); 3.0% of video transects had medium densities (1000–2000 items/km²); and only 1.9% of video transects had high densities (>2000 items/km²) (Figure 3.9.6.2.2, Buhl-Mortensen and Buhl-Mortensen, 2017).

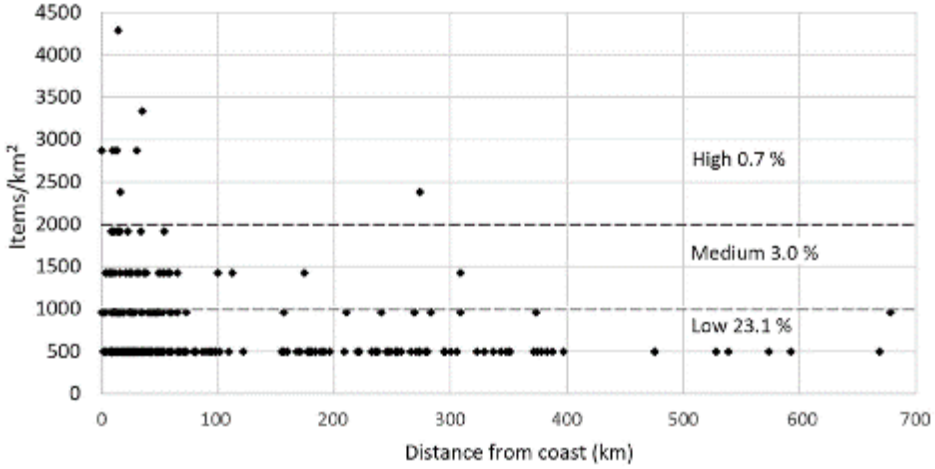

Figure 3.9.6.2.2. Litter density (items/km²) in relation to distance to coast and in the Barents Sea. Dashed lines indicate density group: high >2000, medium 1000–2000, and > 0–1000 items/km² and percentage of video transects within each group is provided.

Abundance and composition of marine litter and the density of bottom-trawl marks (TM) varied with depth, type of sediment and marine landscapes (Buhl-Mortensen and Buhl-Mortensen, 2018). Lost or discarded fishing gear (especially lines and nets), and plastics (soft and hard plastic and rubber) were dominant types of litter. Distribution of litter reflected the distribution of fishing intensity (density of Vessel Monitoring System (VMS) records) and density of TM at a regional scale; highest abundance was observed near the coast and in areas with high fishing intensity — indicated by VMS data.

It is likely that deliberate dumping of discarded fishing gear occurs away from good fishing grounds. Extensive litter, observed close to the coast is probably the result of discarded fishing gear, but input from aggregated populations on land is also indicated from the types of litter observed (Buhl-Mortensen and Buhl-Mortensen, 2018).

3.9.6.3 Beach litter

In Norway, beach litter has been surveyed annually for the Norwegian Environment Agency since 2011. Ingestion of marine plastics by northern fulmars (*Fulmarus glacialis*) has been surveyed in Svalbard twice (1987 and 2013); in northern Norway (2011–2015); and every winter in southern Norway since 2002–2003. These data have been used in a study to compare litter composition and density on beaches with stomach contents of northern fulmars from the same region to indicate the transfer of litter to marine foodwebs.

In total, 186 168 litter items were collected from seven Norwegian beaches during the period 2011–2017 with a mean of 3650 items per 100 meters of beach. In general, the amount of litter decreased moving northward; the largest difference was between the mainland (with 4000–5000 litter items per 100 meters) and Svalbard (with 145 litter items). The litter was dominated by plastic (96%); large plastic items were more common on Svalbard, while small plastics and strings contributed a larger proportion in the south. Large and small fishnets contributed most to fisheries related litter, and the proportion was larger on Svalbard (13%) than on the mainland (5–6%).

Fulmars residing in Arctic areas had ingested less plastic than those breeding further south. In both regions, most fulmars had ingested plastic, but the proportion of birds that exceeded the EcoQO of <0.1 g of stomach plastic decreased from 55% in the North Sea to 35% in Northern Norway, and 24% in Svalbard. Amounts of plastic in fulmar stomachs correspond to what is known about plastic pollution in their overwintering areas, with lowest amounts related to the Spitsbergen population.

4 Interactions, drivers and pressures

4.1 Feeding and growth of capelin and polar cod

Capelin

Eleven years (2006–2016) of capelin diet were examined from the Barents Sea where capelin is a key forage species, especially of cod. The PINRO/IMR mesozooplankton distribution shows low plankton biomass in the central Barents Sea, most likely due to predation pressure from capelin and other pelagic fish. This pattern was also observed in 2017. In the Barents Sea, a pronounced shift in the diet from smaller (<14 cm) to larger capelin (≥14 cm) is observed. With increasing size, capelin shift their diet from predominantly copepods to euphausiids, (mostly *Thysanoessa inermis* - not shown), with euphausiids being the largest contributor to the diet weight in most years (Figure 4.1.1). Hyperiid amphipods contributed a small amount to the diet of capelin.

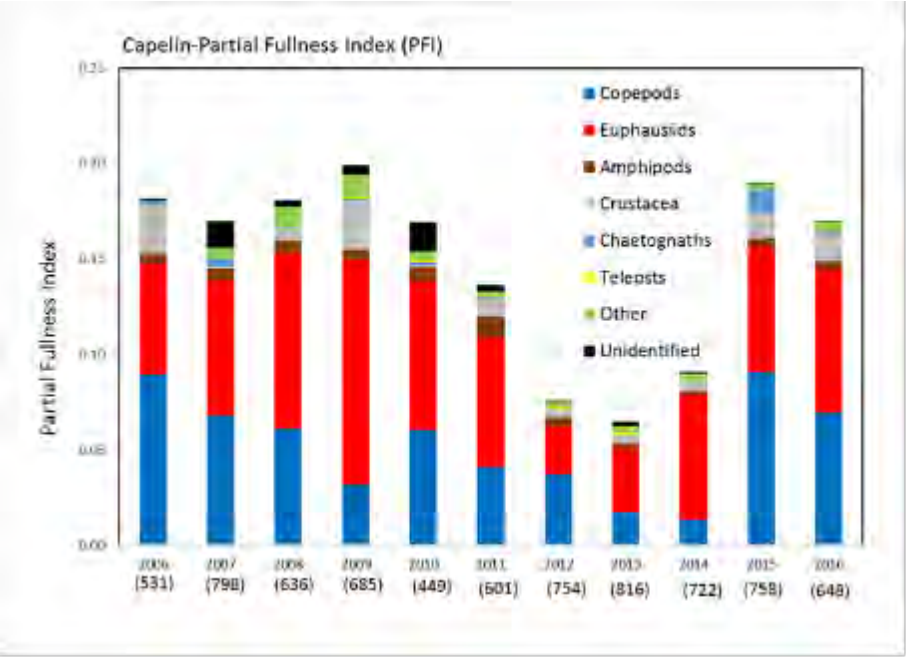

Figure 4.1.1. Stomach fullness of capelin during survey in August-September 2006-2016. Number of fish sampled each year in brackets

Capelin growth decreased from 2009 onwards in a way similar to earlier periods of relatively high capelin abundance (1990–1992, 1998–2002) (Figure 4.1.2). There was a corresponding decrease in stomach fullness of capelin from 2009 onwards. These trends were reversed in 2014; both weight-at-age and stomach fullness are now at relatively high levels.

The decrease in individual growth rate and condition of capelin observed before 2014 for the large capelin stock may have been caused by reduced food availability linked to strong grazing on the largest planktonic organisms; as suggested by reduction of the largest size fraction (>2 mm) in the Norwegian zone during the autumn survey (see section 3.3). Plankton species composition in the northeastern area has changed; abundance and biomass of large copepod species (*Calanus finmarchicus* and *C. glacialis*) — which are important prey items for capelin — decreased in recent years. While the abundance of small copepods (*Pseudocalanus minutus*) — which are not important to the capelin diet — has increased. This change species composition of the plankton community is most likely caused by warming in the Barents Sea, and high grazing pressure

from capelin and other species. Compared to 2015, the 2016 abundance of large copepods (*C. finmarchicus* and *C. glacialis*) increased, while that of the smaller copepod (*P. minutus*) decreased slightly. In 2016, increase biomass of *C. finmarchicus* was observed relative to 2015, while biomass of *C. glacialis* remained at the same level.

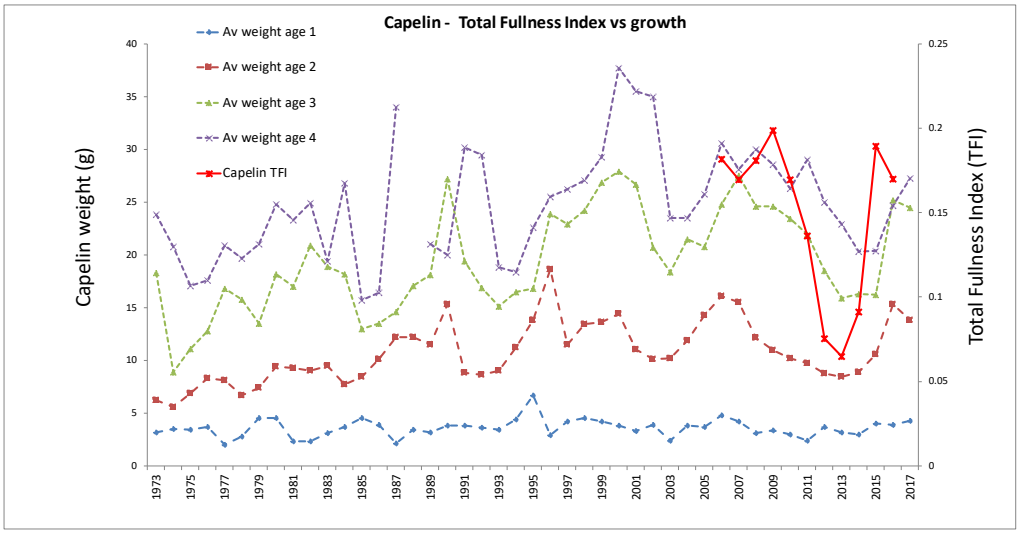

Figure 4.1.2 Growth (weight at age from ecosystem survey) and stomach fullness (TFI) of capelin in 1973–2017

Capelin growth depends on the state of the plankton community (Skjoldal *et al.*, 1992; Dalpadado *et al.*, 2002; Orlova *et al.*, 2010). Capelin produces a strong feedback mechanism on zooplankton stock levels through predation (Figure 4.1.3, Dalpadado *et al.*, 2003; Stige *et al.*, 2014); has been found to be particularly pronounced for krill in the central Barents Sea (Dalpadado and Skjoldal, 1996).

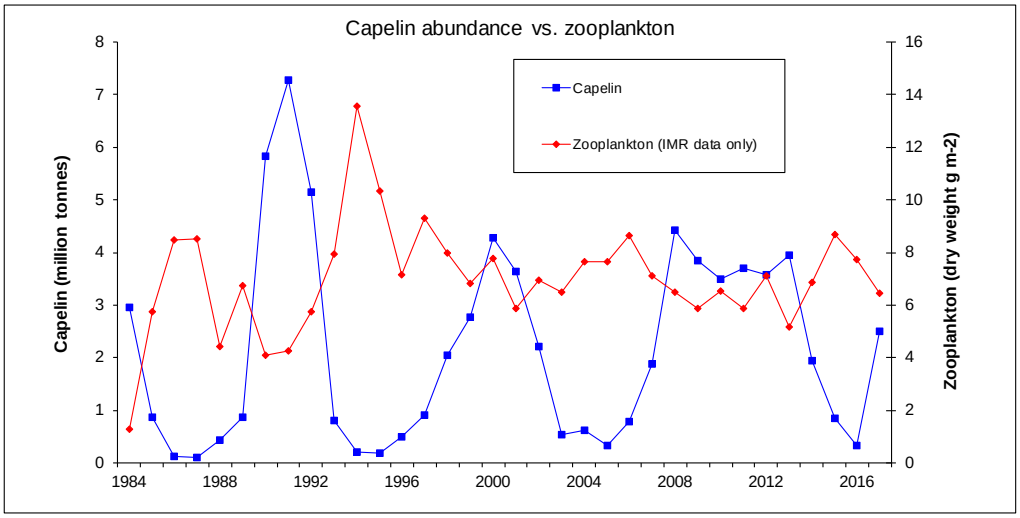

Figure 4.1.3. Fluctuation of capelin stock and zooplankton biomass in the Barents Sea in 1984–2017.

There is evidence of a density-dependent effect on capelin growth. This is reflected in decreasing length of individual (2- and 3-year old) capelin with increasing capelin abundance (Figure 4.1.4).

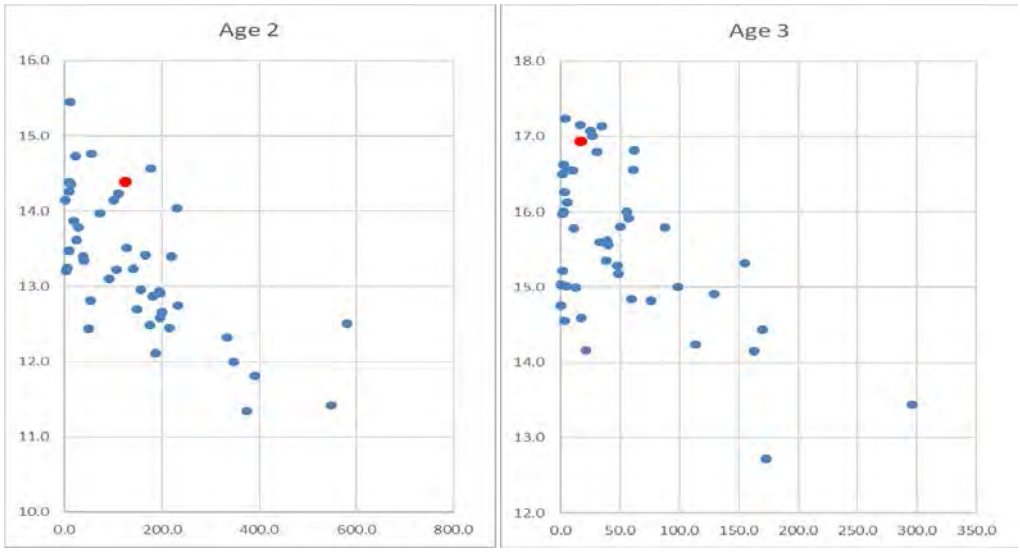

Figure 4.1.4. Average length as function of abundance for capelin at age 2 and 3. The data point from 2017 is marked in red.

Polar cod

Diet data from 2007–2016 indicate that polar cod mainly feed on copepods, amphipods (mainly hyperiids *Themisto libellula* and occasionally gammarids), euphausiids, and other invertebrates (to a lesser degree) (Figure 4.1.5). Large polar cod also prey on fish. The total stomach fullness index decreased after 2011, and was at a fairly low level in 2012–2015; the index increased again in 2016 to the highest level measured in this 10-year time-series (Figure 4.1.6). The growth rate of polar cod was low in 2016 and, thus, did thus not reflect the increased stomach fullness observed that year. It should be noted that spatial coverage for polar cod is incomplete during most years of the BESS; thus, growth and stomach fullness data may not reflect the status of the entire population.

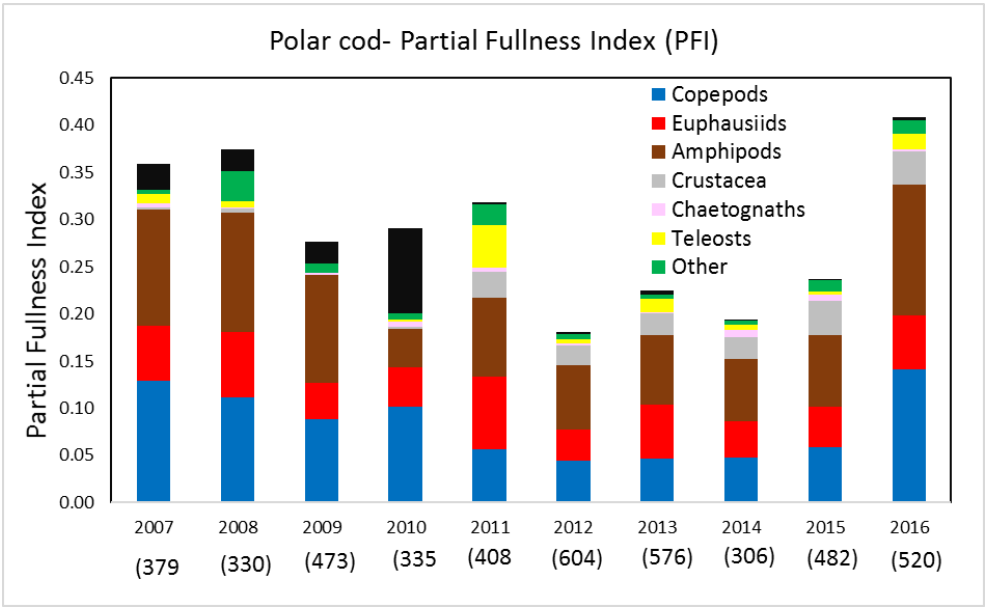

Figure 4.1.5. Stomach fullness of polar cod during survey in August–September 2007–2016. Number of fish sampled each year in brackets.

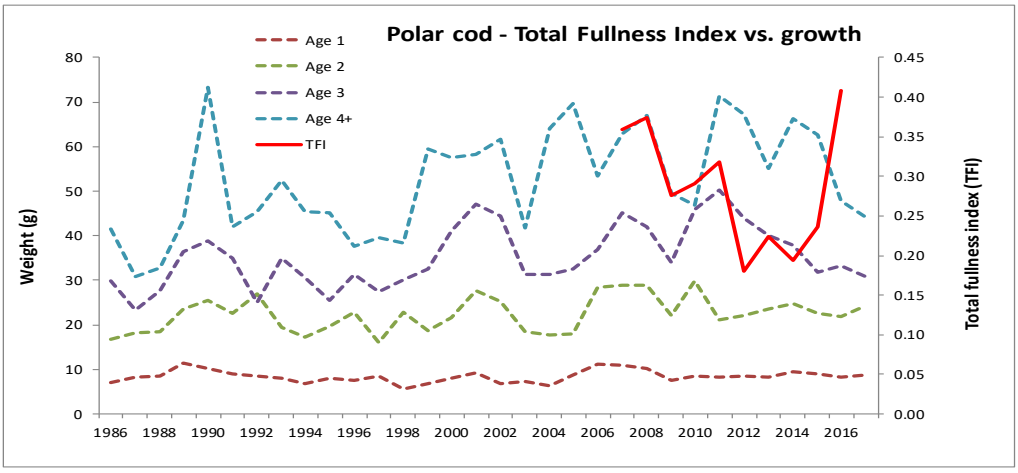

Figure 4.1.6 Growth (weight at age from ecosystem survey) and stomach fullness (TFI) of polar cod in 1986-2017

4.2 Feeding, growth, and maturation of cod

Feeding

Figures 4.2.1 and 4.2.2 show the consumption and diet composition of cod.

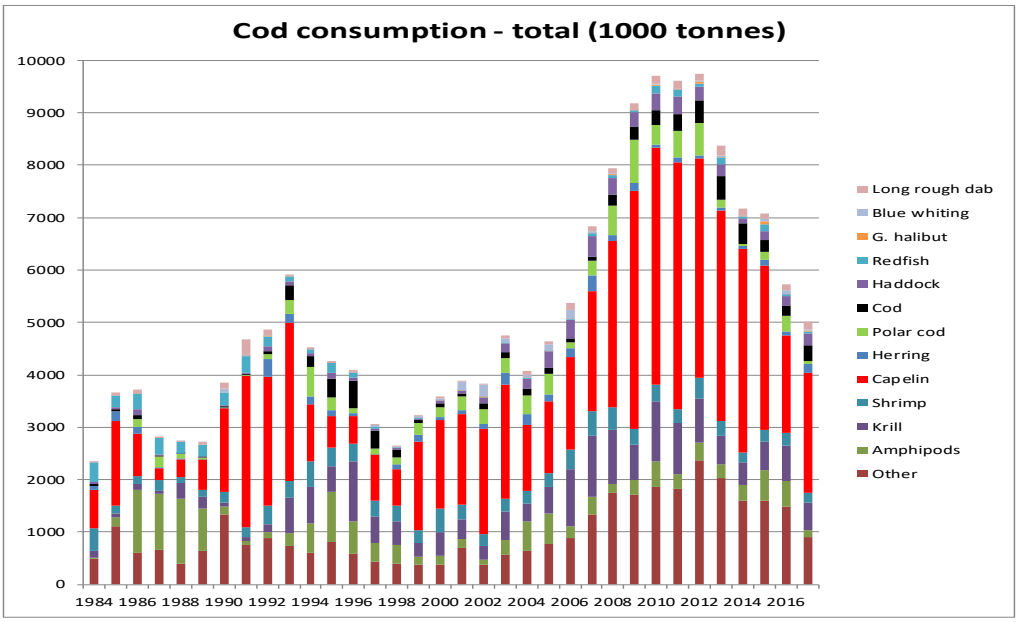

Figure 4.2.1 Cod consumption 1984–2017. Consumption by mature cod outside the Barents Sea (3 months during first half of year) not included. Norwegian calculations, preliminary figures, final numbers to be found in AFWG 2018.

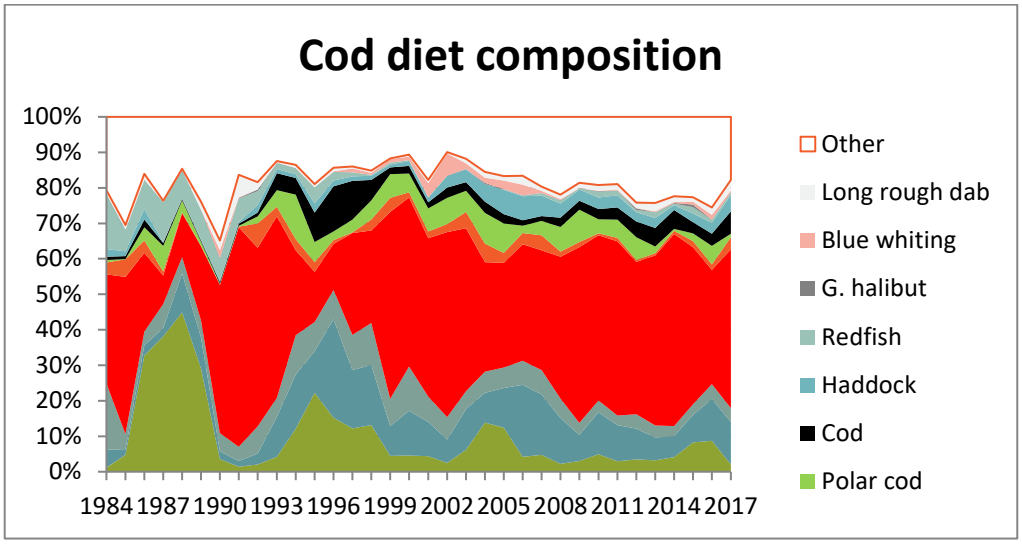

Figure 4.2.2. Cod consumption composition in the Barents Sea in 1984–2017, by weight

Cod is the major predator on capelin; although other fish species, seabirds and marine mammals are also important predators. In the last 6–7 years, cod stock levels have been extremely high in the Barents Sea. Estimated biomass of capelin consumed by cod in recent years has been close to the biomass of the entire capelin stock (Figure 4.2.3). Abundance levels of predators other than cod are also high and, to our knowledge, stable.

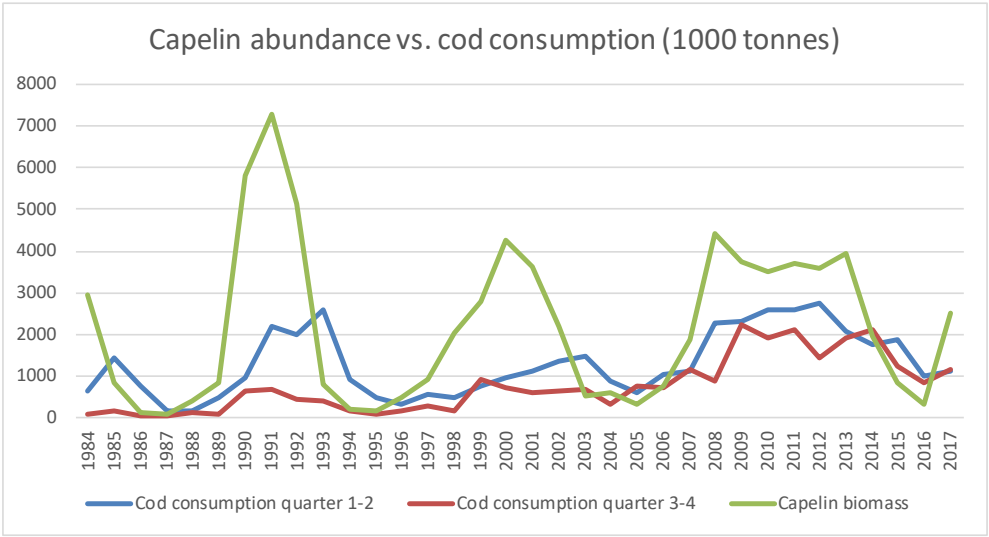

Figure 4.2.3 Size of the capelin stock and estimated consumption of capelin by cod.

Estimated consumption of capelin by cod during first and second parts of the year has indicated different temporal patterns. Consumption during the 1st and 2nd quarters has been high during earlier periods and includes consumption during the spawning period, and during spring and early summer prior to seasonal capelin feeding migrations. During the last decade, however, a major difference has been the pronounced increase to a much higher level of consumption in the 3rd and 4th quarters (Figure 4.2.3). This reflects the northward movement of cod stock, and a larger spatial overlap between cod and capelin under the recent warm conditions.

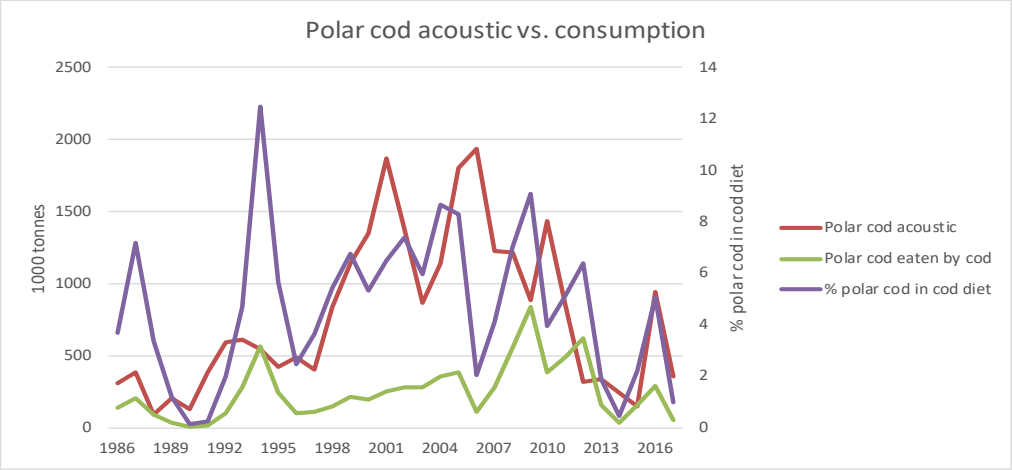

Figure 4.2.4 Acoustic estimates of polar cod compared to consumption of polar cod by cod and % of polar cod in cod diet.

Figure 4.2.5 shows that there is a reasonable correspondence between the proportion of polar cod in the cod diet and acoustic estimates of polar cod.

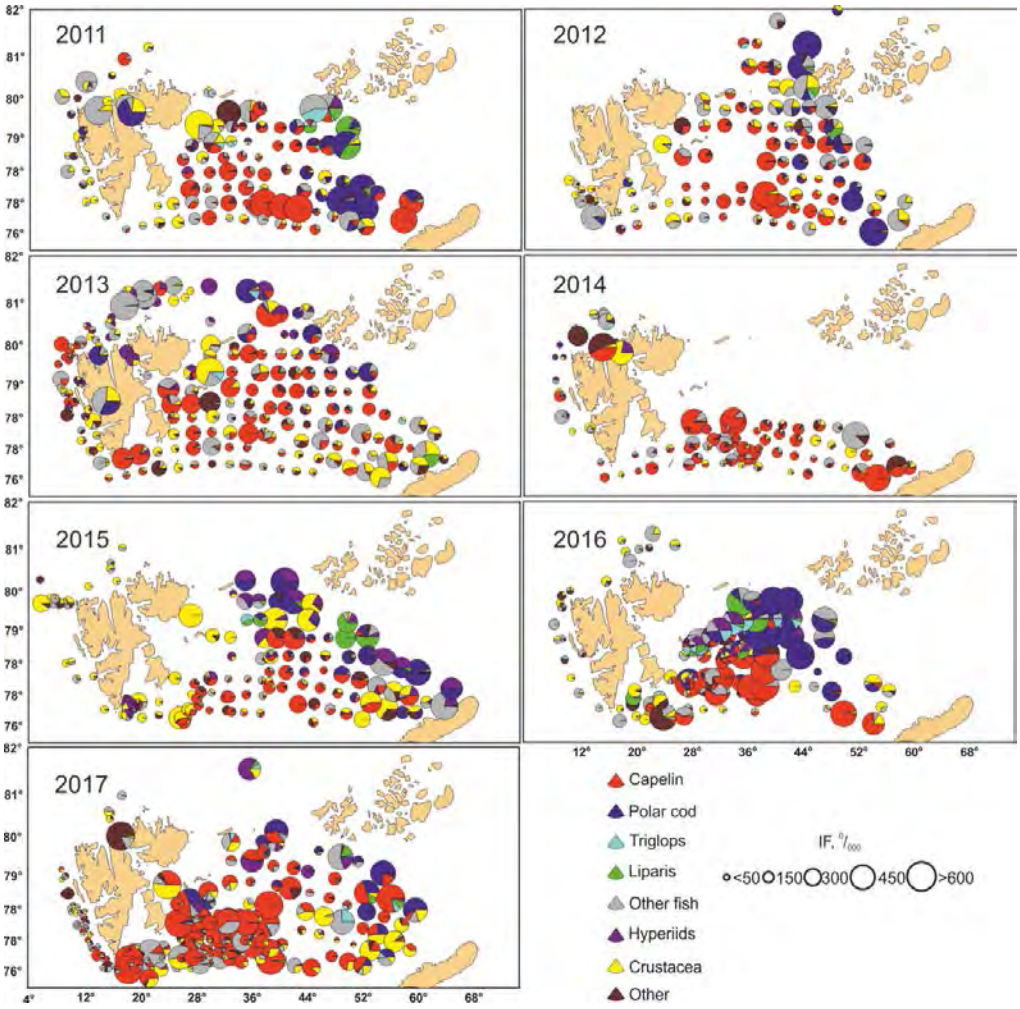

Figure 4.2.5. Cod diet composition during the ecosystem survey in August–September 2011–2017. Red dots indicate capelin, and blue dots polar cod.

During the first capelin collapse (1985–1989) the importance of capelin in cod diet decreased from 53% in 1985 to 20–22% (maximum) for the remainder of the collapse period. During that period, an increase of other prey was observed; in particular, hyperiids which constituted 7–23% of the capelin diet and redfish which constituted 3–18%.

During the second capelin collapse (1993–1997), the proportion (by weight) of capelin in the cod diet was high during the first 2 years (47% and 30%), followed by a decreased to 6–16%. During this period, cannibalism in cod increased sharply from 4–11% to 18–26% of the diet. In addition, more intensive consumption of hyperiids was observed (1–12%), but the proportion of hyperiids consumed was still much lower than during the first collapse.

During the third capelin collapse (2003–2006), consumption of capelin by cod was rather high (10–26%). Several alternative prey groups were present in the cod diet in similar quantities: juvenile haddock (6–11%) and cod (5–10%); herring (3–11%); blue whiting (1–5%); and hyperiids (1–12%). Consumption of capelin by cod during the most recent years has remained somewhat stable (17–31%), but has been much lower than during earlier periods of high capelin abundance (average 36–51%). In recent years, a relatively diverse cod diet has been recorded: with stable high consumption of juvenile cod and haddock (6–11 and 5–11%, respectively); other fish species (11–15%); and other food types (21–33%) (mainly ctenophores and crabs).

Investigations of cod diet in the area north of 76°N showed different types of feeding intensity in three different local areas (Dolgov and Benzik, 2014). Cod feeding intensity was low (149–169‰) in areas near western and southern Spitsbergen — where cod feed on non-commercial fish. Other local areas were characterized by high feeding intensity (MFI 214-251-169 ‰) with capelin as dominant; non-target species (snailfish and sculpins), polar cod, and hyperiids were also consumed. These two are traditional areas of cod distribution during summer. The third area (Franz Josef Land, northern Novaya Zemlya, and adjacent areas) has become available habitat for cod only since 2008; in this area, cod (MFI 284-340 ‰) feed intensively on polar cod and capelin. Northward expansion of cod distribution, and their movement into northeastern Barents Sea results in better feeding conditions for cod under their high stock biomass and decreasing of main prey (capelin and polar cod).

In addition, some new prey items appeared in the cod diet. The non-indigenous snow crab (*Chionoecetes opilio*) has become a rather important prey items for cod, especially in eastern Barents Sea alongside Novaya Zemlya (Dolgov and Benzik, 2016). The percentage (by weight) of snow crab in the cod diet sharply increased from 0.1-0.3% during 2009–2010 to 5.6–6.1% during 2014–2015; but decreased in 2016 and 2017 (5.2 and 3.9% respectively) (Figure 4.2.6). In contrast, two other non-indigenous crab species have not become more importance in the cod diet, the percentages weight of red king crab and *Geryon* spp. have not exceeded 1.0% and 0.2%, respectively. The difference is probably related to higher overlap between cod and snow crab, and more appropriate body shape and size of snow crab than the other crab species as prey for cod.

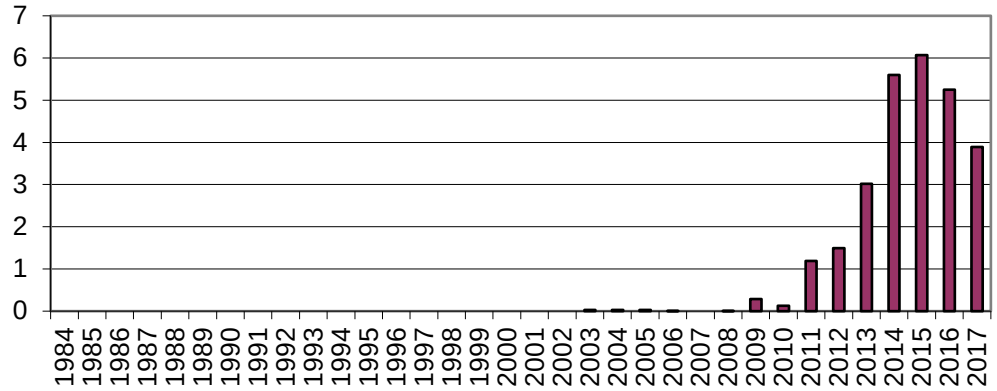

Figure 4.2.6. Importance of snow crab in cod diet (% weight) in 1984–2017.

Growth and maturation

Consumption and growth for young cod has been relatively stable in recent years (Figure 4.2.7); there has been a slight decrease for older cod (Figure 4.2.8). Maturity-at-age for cod has decreased considerably in recent years, particularly for ages 6-9. For 2017, there is a discrepancy between Norwegian and Russian data – Norwegian data indicate that age-a- maturity seems to have again increased for these age groups; while Russian data indicate no such reversal. The change from 2013 to 2016 was considerably larger than indicated by recent changes in weight-at-age estimates (Figures 4.2.9 and 4.2.10).

Biomass of the main prey species, relative to the cod stock size, has decreased somewhat in recent years (Figure 4.2.11). However, no consequences — of the 2015-2016 'mini-collapse' of the Barents Sea capelin stock on cod condition have been observed. This may be related to ongoing expansion of cod stock to the northern Barents Sea, making previously untapped food resources now available for cod consumption.

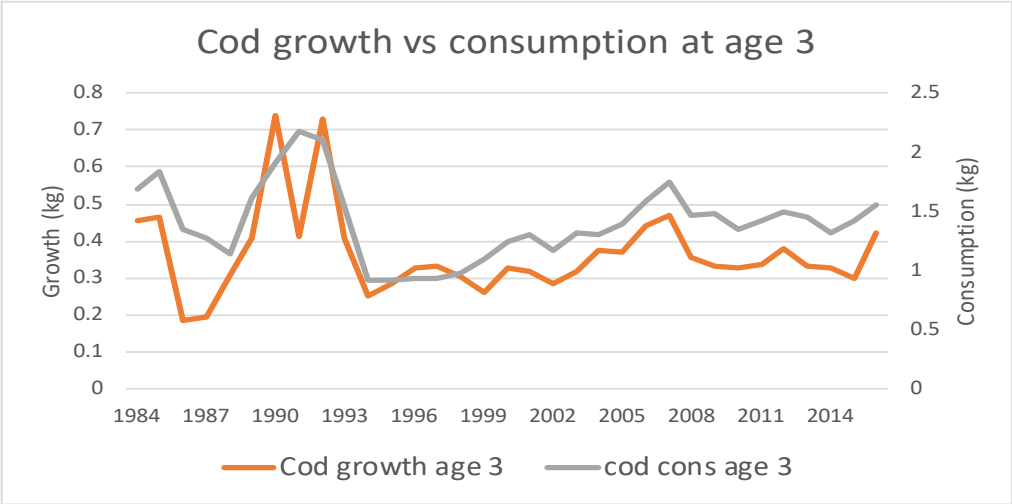

Figure 4.2.7 Cod growth and consumption at age 3 (ICES 2017c).

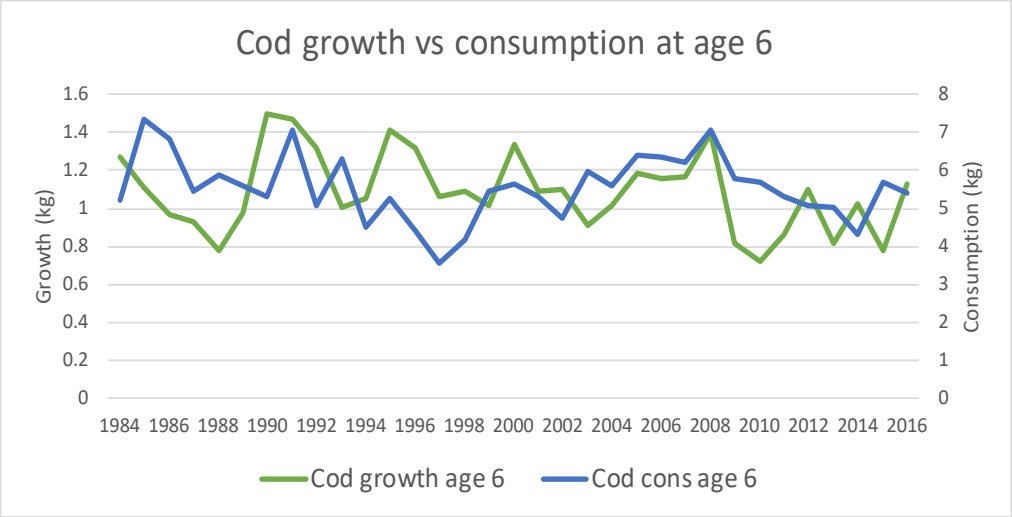

Figure 4.2.8 Cod growth and consumption at age 6 (ICES 2017c).

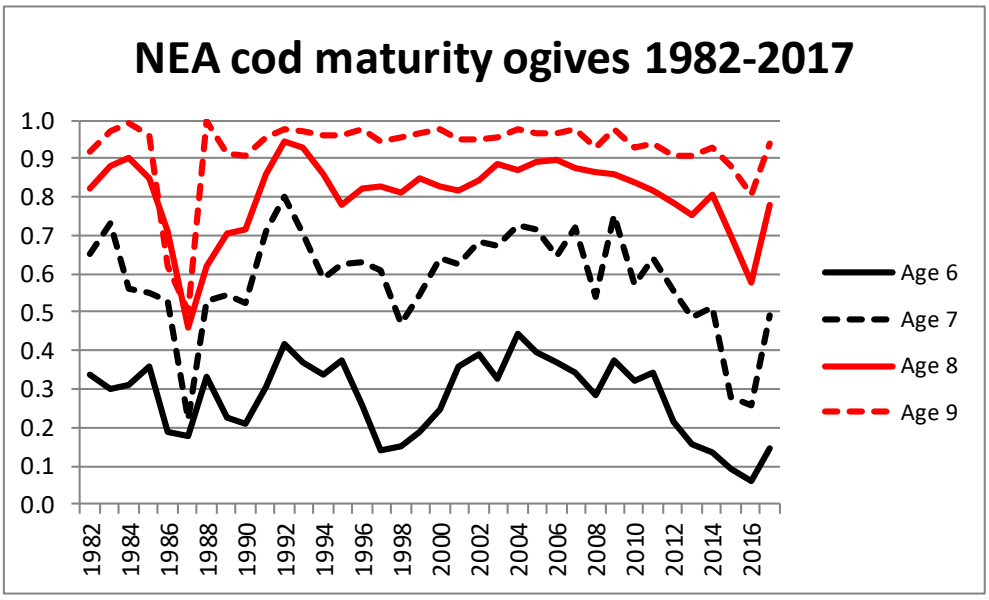

Figure 4.2.9 Maturity-at-age for cod ages 6-9 (ICES 2017c).

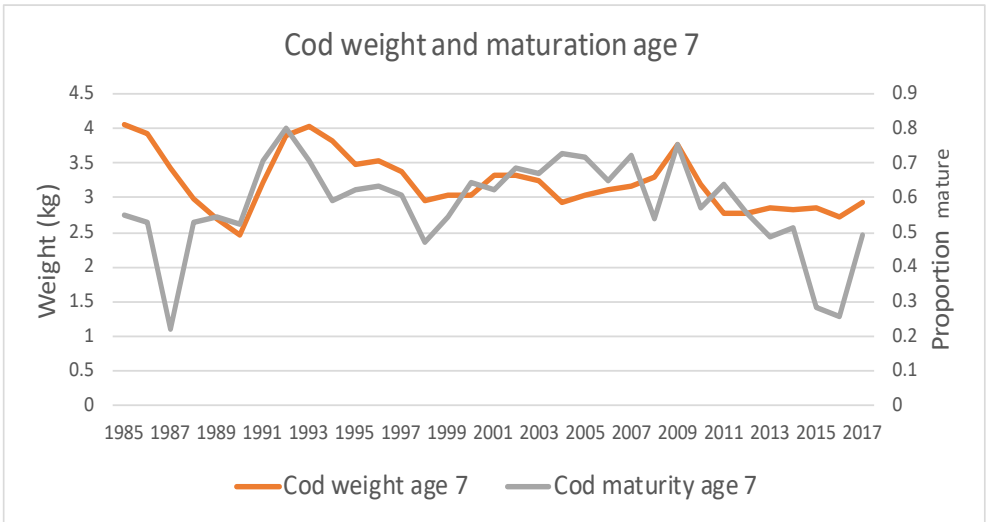

Figure 4.2.10 Cod maturity and weight at age 7 (ICES 2017c).

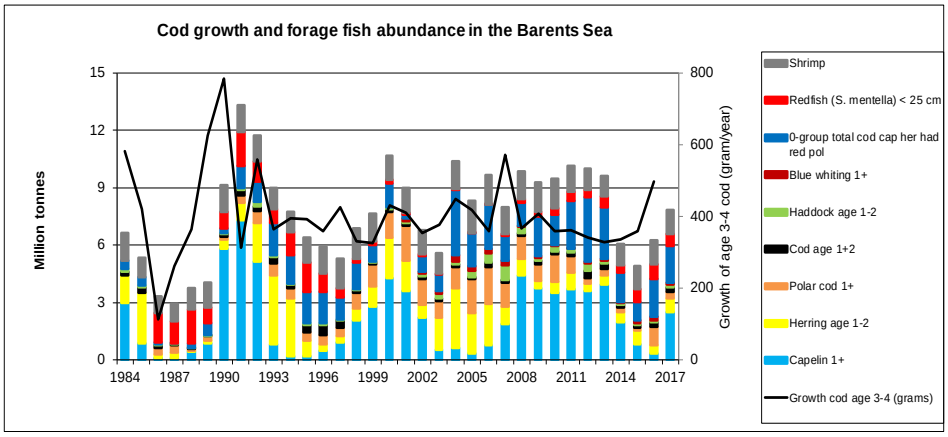

Figure 4.2.11. Abundance of major fish prey stocks and shrimp compared to cod growth.

4.3 Causes of capelin fluctuations

Stock size fluctuations

The Barents Sea capelin has undergone dramatic changes in stock size over the last three decades. Three stock collapses (when abundance was low and fishing moratoriums imposed) occurred during 1985–1989, 1993–1997, and 2003–2006. A sharp reduction in stock size was also observed during 2014–2016; followed by an unexpectedly strong increase during 2016–2017. Observed stock biomass in 2015 and 2016 was below 1 million tonnes, which previously was defined as the threshold of collapse. Despite indications that capelin stock size was underestimated in 2016, at present 2015–2016 is recognized as a 'mini-collapse'. However, the stock size development during the next couple of years will reveal whether this is indeed the case.

Previous collapses have had serious effects both up and down the foodweb. Reduced predation pressure from capelin has led to increased amounts of zooplankton during periods of capelin collapse. When capelin biomass was drastically reduced, its predators were affected in various ways. Cannibalism became more frequent in the cod stock, cod growth was reduced, and maturation delayed. Seabirds experienced increased rates of mortality, and total recruitment failures; breeding colonies were abandoned for several years. Harp seals experienced food shortages, and recruitment failure, and increased mortality; partly because they invaded coastal areas, and were caught in fishing gear. The effects were most serious during the 1985–1989 collapse, whereas, the effects could hardly be traced during the third collapse. Gjøsæter *et al.* (2009) concluded that these differences in effect likely resulted from increased availability of alternative food sources during the two most recent collapses (1990s and 2000s).

These collapses were caused by poor recruitment, most likely in combination with low growth and increased predation pressure. It is likely that high levels of fishing pressure during 1985–1986 amplified and prolonged the first collapse. After each collapse, the fishery has been closed and the stock has recovered within a few years due to good recruitment. Several authors have suggested that predation by young herring has had a strong negative influence on capelin recruitment and, thus, has been a significant factor contributing to these capelin collapses (Gjøsæter *et al.*, 2016).

Recruitment

Capelin is a short-lived species and thus the stock size variation is strongly influenced by the annual recruitment variability. This may indicate that the main reason of capelin stock collapses is poor recruitment (Figure 4.3.1).

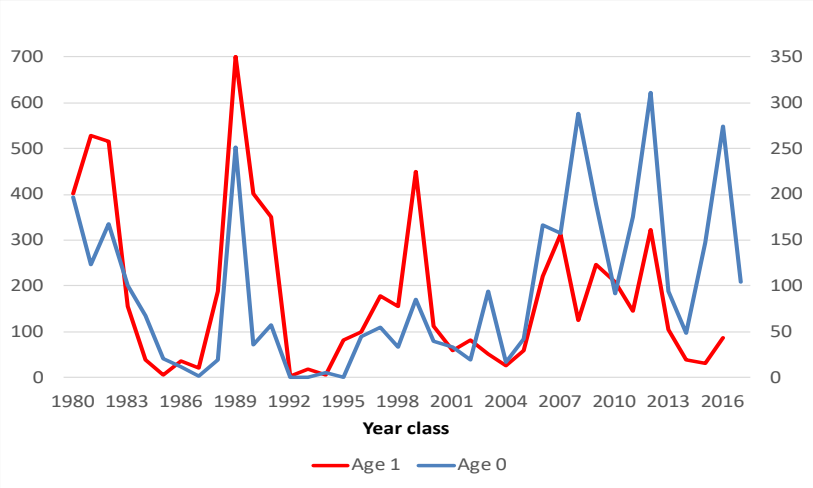

Figure 4.3.1. Fluctuation of capelin at age 0 (blue line) and 1 (red line) for the cohorts 1980–2017.

Mean length of 0-group capelin has varied somewhat during the data time-series. From a biological perspective, one may hypothesize that survival rates from age 0 to age 1 might be correlated with lengths-at-age 0. However, a plot of mean length-at-age 0 and total mortality, from age 0 to age 1, shows no such correlation; rather, this plot shows that 0-group and/or 1-group abundance estimates and, therefore also, mortality estimates from age 0 to age 1, are noisy; this could possibly mask possible relationships that might exist.

Figure 4.3.2 shows a stock–recruitment plot from Gjøsæter *et al.* (2016) going back to 1987. This plot shows that 1989 is still the strongest year class (age-1). An estimation of breakpoint from this plot could be attempted. This figure has not been updated since the 2016 report. Figure 4.3.3 shows an alternative approach where recruitment-at-age 0 is used, and SSB is estimated as the mature stock (>14 cm) in autumn (with fishery removals taken in January–March subtracted).

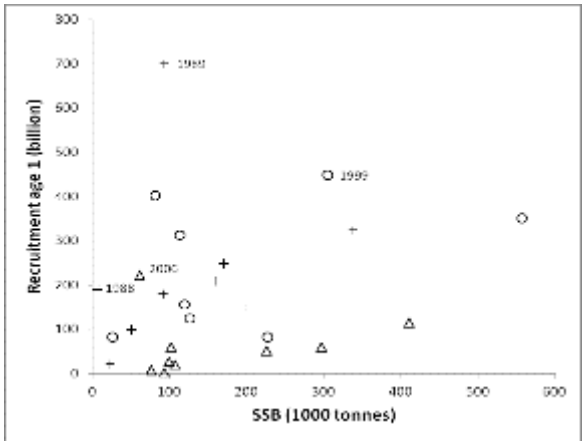

Figure 4.3.2. SSB/R plot for capelin. Cohorts 1987–2012. Points coded according to herring biomass age 1 + 2 in spawning year. Circles—herring biomass <450 000 tonnes, crosses—herring biomass between 450 000 tonnes and 1.3 million tonnes, triangles-herring biomass >1.3 million tonnes. (Figure 7. in Gjøsæter *et al.* 2016).

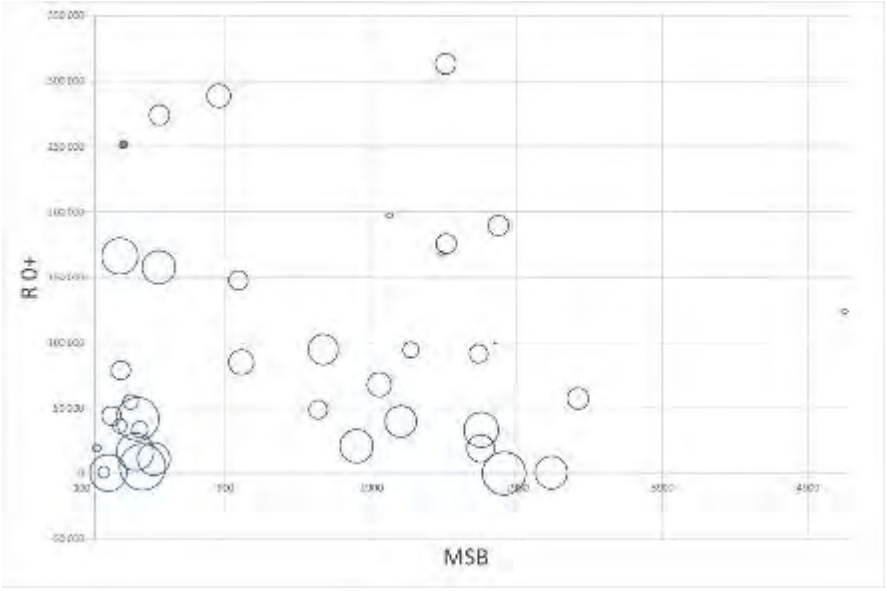

Figure 4.3.3. Relationship between mature stock biomass (>14 cm) with spring fishery subtracted (biomass at 1 Oct. Y, total landings from 1 January to 1 April.Y+1 are subtracted, 1000 tonnes) and 0-group index in billions (Y+1), covering the cohorts 1980–2017. The size of bubbles indicates the biomass of herring at age 1-3 (ICES WGIBAR data). Minimum diameter of bubble corresponds to 0.02 million tonnes of herring (1983), the maximum - 5.02 million tonnes. (1994). The red point is the 1989 cohort which is the basis for the current reference point (B_{lim}).

The Barents Sea polar cod stock also had a declining trend until 2015 (described in the next section). The decrease in polar cod abundance may have contributed to increased predation pressure on capelin since polar cod is also prey for cod. Predation pressure from seals and whales may also have changed, but data are limited. Assuming that the occurrence of predators, such as harp seal and minke whale, has been stable, their steady feeding on capelin would come in addition to the heavy predation by cod.

4.4 Causes of polar cod fluctuations

The Barents Sea polar cod stock was at a low level in 2017. Norway conducted commercial fisheries on polar cod during the 1970s; Russia has fished this stock on more-or-less a regular basis since 1970. However, the fishery has for many years been so small that it is believed to have very little impact on stock dynamics. Stock size has been measured acoustically since 1986, and has fluctuated between 0.1–1.9 million tonnes. Stock size declined from 2010 to a very low level in 2015, increased to 0.9 million tonnes in 2016, and again declined to 0.4 million tonnes in 2017. The rate of natural mortality for this stock appears to be quite high, relative to its importance as prey for cod and different stocks of seals.

It appears that polar cod mortality has increased in recent years. The recent warming in the Barents Sea has resulted in decreased sea ice distribution; several boreal species have moved northward, while the distribution area of Arctic species, such as polar cod, has decreased.

Since the mid-1990s, there has been a general trend of increase in both air and water temperature in the Barents Sea (See Section 3.1); record highs have been recorded during the 2000s. The areal extent of sea ice coverage has never lower, for both the Arctic and the Barents Sea, as in 2016. In the Barents Sea, the area of Arctic water decreased, while a larger portion has been dominated by warmer Atlantic water. These climatic

changes have likely affected the distribution and abundance of Arctic species like polar cod.

The reduction of sea ice in winter reduces spawning habitat, leading to unfavourable conditions for polar cod spawning (Eriksen *et al.,* 2015c). The eggs have long incubation time and float near the surface where they may be exposed to unstable temperatures and increased water mixing due to lack of ice. Most of the juveniles are found in waters with temperatures below 5°C and reduction of cold-water masses in summer and autumn reduces the nursery area for 0-group polar cod. 0-group polar cod prey on small plankton organisms such as copepods and euphausiids, while adults feed mainly on large Arctic plankton organisms such as *Calanus hyperboreus* and *C. glacialis* and hyperiids. The biomass of Arctic forms of zooplankton decreased in recent years and most likely influenced negatively the feeding conditions for 0-group polar cod. However, no significant changes in the condition of adults were observed in recent years. This indicates a high degree of adaptability of this species to changes in the environment and enough available food resources.

The current fishing pressure is negligible now compared to the 1970s, when total catches were as high as 350 thousand tonnes. Thus, the total mortality is close to the natural mortality. Most likely predation by cod has contributed to the high natural mortality. Cod is a boreal species and associated with the temperate waters. The Barents Sea warming has been beneficial for cod and it has spread further north. In the northern areas cod overlapped with polar cod, and thus predation pressure on polar cod has increased, contributing to the stock decline until 2015. In the overlapping area cod feeds efficiently on polar cod (see Section 4.2).

4.5 Cod-capelin-polar cod interaction

The interaction cod-capelin-polar cod is one of the key factors regulating the state of these stocks. Cod prey on capelin and polar cod, and the availability of these species for cod varies. In the years when the temperature was close to the long-term mean, the cod overlap with capelin and polar cod was lower than in the recent warm years. Cod typically consume most capelin during the capelin spawning migration in spring (quarters 1+2), but especially in recent years the consumption has been high also in autumn (quarters 3+4) in the northern areas (Figure 4.2.3). A decline in the consumption of capelin by cod was observed in the second half of 2015 and in 2016–2017, but the decline is less strong than indicated by the low stock estimates in 2015 and 2016.

With the recent warming of the Barents Sea, the cod stock increased and became distributed over larger area, overlapping with capelin and especially polar cod to a higher degree than before. Cod can prey intensely on polar cod. The polar cod are most likely more available for cod than the capelin, because they possibly have a lower swimming speed (confirmed by trawl catch analyses) and are distributed closer to the bottom. However, capelin is a fatter and energetically more valuable prey item. It should be noted, however, that the length of the period with cod and polar cod overlap is much shorter (September-December) compared to the overlapping time of cod and capelin.

4.6 Snow crab effect on benthos

In most of the measured years, the biomass in the northeast part of the Barents Sea was above the total Barents Sea mean (Figure 3.4.7), but from 2013 and ongoing, the mean biomass was reducing, and was record low (<20 kg/n.ml) in 2016, and below the total Barents Sea mean. This decrease could be explained by the maximum distribution of the snow crab predating on the benthos, and with increasing bottom temperatures

(Section 3.1). In 2017, the biomass increased to 116 kg/n.ml, the highest value recorded both with and without snow crab biomass. It is believed that this increase is an effect of changes in the technical trawl-sampling approach and should be considered as an error. The 2017 value will therefore not be used in an ordinary biomass comparison with previous year.

The spatial impact on benthos biomass done by the snow crab predation (Manushin, 2016) shows that the highest impact is located west of Novaya Zemlya (Figure 4.6.1) and in an area dominated by the polychaete *Spiochaetopterus typicus* (deeper areas with adult snow crabs) and the bivalve *Macoma calcarea* (shallower areas with juvenile snow crabs) (Zakharot *et al.*, 2016).

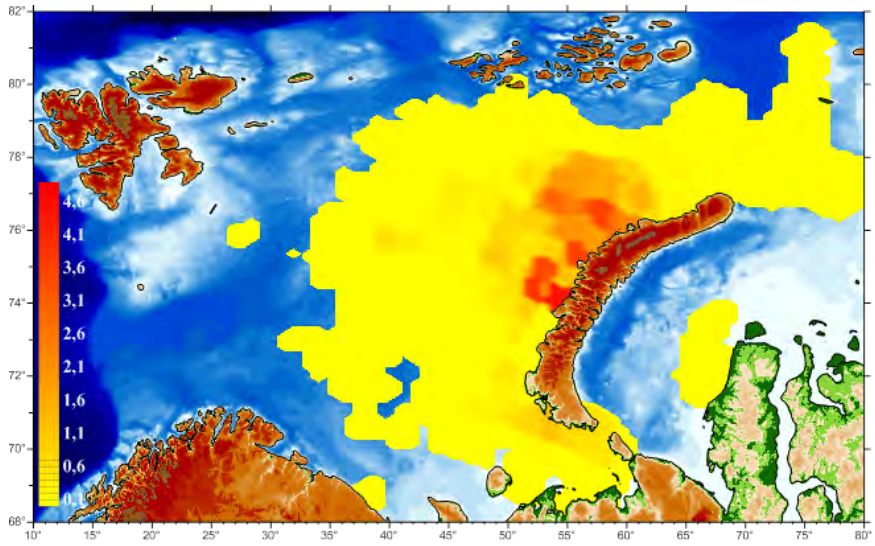

Figure 4.6.1. Total biomass (g/m²) of the benthos consumed/killed by the snow crab population during a nine-year period (2005–2014) (Manushin, 2016).

4.7 Environmental impact of fisheries

The impact of fisheries on the ecosystem is summarized in the chapter on Ecosystem considerations in the AFWG report (ICES 2016c), and some of the points are:

- The demersal fisheries are mixed, and currently have largest effect on coastal cod, and Golden redfish *(Sebastes norvegicus)* due to the poor condition of these stocks.
- The most widespread gear is bottom trawl. Trawling has largest effect on hard bottom habitats, whereas the effects on other habitats are not clear and consistent.
- Currently the possibility of using pelagic trawls when targeting demersal fish is explored, to avoid impact on bottom fauna and to reduce the mixture with other species. It will be mandatory to use sorting grids to avoid catches of undersized fish.
- Fishery induced mortality due to lost gillnets, contact with active fishing gears, etc. on fish is a potential problem but not quantified at present.

4.8 Important indirect effects of fisheries on the ecosystem

In order to conclude on the total impact of trawling, an extensive mapping of fishing effort and bottom habitat would be necessary. In general, the response of benthic organisms to disturbance differs with substratum, depth, gear, and type of organism (Collie *et al.*, 2000). Seabed characteristics from the Barents Sea are only scarcely known (Klages *et al.*, 2004) and the lack of high-resolution (~100 m) maps of benthic habitats and biota is currently the most serious impediment to effective protection of vulnerable habitats from fishing activities (Hall, 1999). An assessment of fishing intensity on fine spatial scales is critically important in evaluating the overall impact of fishing gear on different habitats and may be achieved, for example, by satellite tracking of fishing vessels (Jennings *et al.*, 2001). The challenge for management is to determine levels of fishing that are sustainable and not degradable for benthic habitats in the long run.

The qualitative effects of trawling have been studied to some degree. The most serious effects of otter trawling have been demonstrated for hard-bottom habitats dominated by large sessile fauna, where erected organisms such as sponges, anthozoans and corals have been shown to decrease considerably in abundance in the pass of the groundgear. Barents Sea hard bottom substrata, with associated attached large epifauna should therefore be identified.

Effects on soft bottom have been less studied, and consequently there are large uncertainties associated with what any effects of fisheries on these habitats might be. Studies on impacts of shrimp trawling on clay-silt bottoms have not demonstrated clear and consistent effects, but potential changes may be masked by the more pronounced temporal variability of these habitats. The impacts of experimental trawling have been studied on a high seas fishing ground in the Barents Sea (Kutti *et al.*, 2005.) Trawling seems to affect the benthic assemblage mainly through resuspension of surface sediment and through relocation of shallow burrowing infaunal species to the surface of the seabed.

During 2009–2011 work between Norway and Russia was conducted to explore the possibility of using pelagic trawls when targeting demersal fish. The purpose with pelagic trawl is to avoid impact on bottom fauna and to reduce the mixture of other species. During the exploratory fishery, it was mandatory to use sorting grids and/or a more stable four-panel trawl geometry with square mesh in the top panel of the codend to avoid catches of undersized fish. The efficiency of pelagic trawling was also tested compared with bottom trawling with regards to reduce the oil consumption per kilo of fish caught, i.e. to improve profitability and reduce NOx emissions.

After three years of exploratory fishing with pelagic trawls, pelagic trawling for cod, haddock and other demersal fish are still not allowed, mainly due to on average a smaller size of the fish and too big catches which are difficult to handle. The experiment has however led to a further development of the bottom trawls, including bigger trawl openings, better size selection and escapement windows to prevent too big catches.

Lost gears such as gillnets may continue to fish for a long time (ghost fishing). The catch efficiency of lost gillnets has been examined for some species and areas (, but at present no estimate of the total effect is available. Ghost fishing in depths shallower than 200 m is usually not a significant problem because lost, discarded, and abandoned nets have a limited fishing life owing to their high rate of biofouling and, in some areas, their tangling by tidal scouring. Investigations made by the Norwegian Institute of Marine Research of Bergen in 1999 and 2000 showed that the amount of gillnets lost increases with depth and out of all the Norwegian gillnet fisheries, the Greenland halibut

fishery is the métier where most nets are lost. The effect of ghost fishing in deeper water, e.g. for Greenland halibut, may be greater since such nets may continue to "fish" for periods of at least 2–3 years, and perhaps even longer (D. M. Furevik and J. E. Fosseidengen, unpublished data), largely because of lesser rates of biofouling and tidal scouring in deep water. The Norwegian Directorate of Fisheries has organized retrieval surveys annually since 1980. All together 10 784 gillnets of 30 meters standard length (approximately 320 km) have been removed from Norwegian fishing grounds during the period from 1983 to 2003. During the retrieval survey in 2011 the following were retrieved and brought to land: more than 1100 gillnets, 54 red king crab traps, 13 km trawlwire, 12 km of ropes, 40 km longlines, trawl codends, 14 tonnes of fish, and about 12000 crabs, mainly red king crab.

Other types of fishery-induced mortality include slipping (pelagic catch is released, but too late to survive), burst net, and mortality caused by contact with active fishing gear, such as escape mortality (Suuronen, 2005). Some small-scale effects are demonstrated, but the population effect is not known.

The harbour porpoise (*Phocoena phocoena*) is common in the Barents Sea region south of the polar front and is most abundant in coastal waters. The harbour porpoise is subject to bycatches in gillnet fisheries. Revised estimates of harbour porpoise bycatches in two Norwegian coastal gillnet fisheries suggest an annual bycatch of ~3000 harbour porpoises along the entire Norwegian coast.

Fisheries affect seabird populations in two different ways: 1) Directly through bycatch of seabirds in fishing equipment and 2) Indirectly through competition with fisheries for the same food sources.

Documentation of the scale of bycatch of seabirds in the Barents Sea is fragmentary. Special incidents like the bycatch of large numbers of guillemots during spring cod fisheries in Norwegian areas have been documented. Gillnet fishing affects primarily coastal and pelagic diving seabirds, while the surface-feeding species will be most affected by longline fishing. The population impact of direct mortality through bycatch will vary with the time of year, the status of the affected population, and the sex and age structure of the birds killed. Even a numerically low bycatch may be a threat to red-listed species such as Common guillemot, White-billed diver, and Steller's eider.

Several birds scaring devices has been tested for long-lining, and a simple one, the bird-scaring line, not only reduces significantly bird bycatch, but also increases fish catch, as bait loss is reduced. This way there is an economic incentive for the fishers to use it, and where bird bycatch is a problem, the bird-scaring line is used without any forced regulation.

In 2009, the Norwegian Institute for Nature Research (NINA) and the Institute of Marine Research (IMR) in Norway started a cooperation to develop methods for estimation of bird bycatch. Data on seabirds taken as bycatch from 2006 to 2009 in the coastal reference fleet program that is managed by IMR were analysed. These estimates suggest that a total of 4000 to 6000 seabirds are killed by these fisheries. More detailed studies of seabird bycatch in the lumpfish and Greenland halibut longline fisheries are in progress to provide more accurate data on bycatch and evaluate different measures to mitigate seabird bycatch.

4.9 Benthic habitat integrity and benthos vulnerability

With retreating sea ice, new areas in the northern Barents Sea become available for fisheries, including bottom trawlers. Of special interest to WGIBAR is therefore the

vulnerability analysis (Jørgensen *et al.,* 2015). Current knowledge of the response of benthic communities to the impact of trawling is still rudimentary. The benthos data from the ecosystem survey in 2011 have been used to assess the vulnerability of benthic species to trawling, based on the risk of being caught or damaged by a bottom trawl (WGIBAR report 2016). A clear decline in biomass was noted for all three categories when comparing trawled vs. untrawled areas. This suggests that trawling significantly affects the biomass of all species, but predominantly the "high-risk" taxa. Some Barents Sea regions were particularly susceptible to trawling (2016 WGIBAR Report).

5 Expected changes in the coming years

5.1 Sea temperature

Oceanic systems have a "longer memory" than atmospheric systems. Thus, a priori, it seems feasible to predict oceanic temperatures realistically and much further ahead than atmospheric weather predictions. However, the prediction is complicated due to variations being governed by processes originating both externally and locally, which operate at different time-scales. Thus, both slow-moving advective propagation and rapid barotropic responses resulting from large-scale changes in air pressure must be considered.

According to the expert evaluation based on the analysis of the internal structure of the long-term variations in hydrometeorological parameters, over the next two years (2018–2019), the Atlantic water temperature in the Murmansk Current is expected to decline slightly but remain typical of warm years.

Due to high temperatures and low sea-ice extent in recent years, the ice coverage is expected to remain below normal.

5.2 Possible development of the stocks

Most of the commercial fish stocks found in the Barents Sea stocks are at or above the long-term level. The exceptions are polar cod and *Sebastes norvegicus*. In addition, the abundance of blue whiting in the Barents Sea is at present very low, but for this stock only a minor part of the younger age groups and negligible parts of the mature stock are found in the Barents Sea.

Concerning shellfish, the shrimp abundance is relatively stable and above the long-term meanwhile, the abundance and distribution area of snow crab is increasing.

Based on the current abundance and age structure of the main commercial stocks, the following lines of development are possible:

A new haddock outburst may take place, as the 2016 and 2017 year classes so far seem to be of the same order of magnitude as the strong 2004–2006 year classes.

The abundance of young herring is currently the highest since 2005, and this may affect the capelin recruitment in 2018–2019 negatively.

The westward expansion of snow crab leads to higher overlap between cod and snow crab and thus predation by cod on snow crab may slow down the rate of increase of the snow crab stock.

If the sea temperature increases further, this may allow further north and eastwards expansion of several stocks, while e.g. cod has almost reached it maximal distribution and polar cod will be negatively affected by other species moving into typical polar cod areas. The strong 2015 year class of polar cod may be strongly reduced by predation from cod.

6 References

Anker-Nilssen, T., Bakken, V., Strøm, H., Golovkin, A.N., Bianki, V.V. and Tatarinkova, I.P. 2000. The Status of Marine Birds Breeding in the Barents Sea Region. Norsk Polarinstitutt Rapportserie, 113. 213 pp.

Arrigo KR, van Dijken G, Pabi S (2008) Impact of a shrinking Arctic ice cover on marine primary production. Geophys Res Lett 35: L19603, doi:10.1029/2008GL035028,2208.

Arrigo KR, van Dijken GL 2011. Secular trends in Arctic Ocean net primary production. J Geophys Res 116: C09011, doi:10.1029/2011JC007151

Arrigo K.R. and van Dijken G. 2015. Continued increases in Arctic Ocean primary production. Progress in Oceanography 136:60-70

Andriyashev, A.P. and Chernova, N.V. 1995. Annotated list of fish-like vertebrates and fishes of the Arctic Seas and adjacent waters. Journal of Icthyology, 34: 435-456.

Anisimova, N.A., Jørgensen, L.L., Ljubin, P., Manushin, I. 2011. Benthos. In The Barents Sea Ecosystem Resources and Management. Half a century of Russian-Norwegian Cooperation. Pp 121-159. Ed by T. Jakobsen, V. Ozhigin. Tapir Academic Press, Trondheim Norway.

Bakanev S.V., Pavlov V.A. Snow crab. In: The state of the biological resources of the Barents Sea and the North Atlantic in 2017 (Edited by E.A. Chamray). Murmansk: PINRO, 2017. P. 47-50. (In Russian).

Bakanev S.V., Stesko A. Red king crab. In: The state of the biological resources of the Barents Sea and the North Atlantic in 2017 (Edited by E.A. Chamray). Murmansk: PINRO, 2017. P. 44-46. (In Russian).

Barrett, R.T., Anker-Nilssen, T., Gabrielsen, G.W. and Chapdelaine, G. 2002. Food consumption by seabirds in Norwegian waters. - ICES Journal of Marine Science, 59: 43-57.

Bjørge, A. and Moan, A. 2016. Revised estimates of harbour porpoise (Phocoena phocoena) bycatches in two Norwegian coastal gillnet fisheries. International whaling commission, SC/66b/SM/03, 16 pp.

Blacker R.W. Benthic animals as indicators of hydrographic conditions and climatic changes in Swalbard waters // Fish. Invest. Ser. 1957a. Vol. 20, № 10. P. 5–12.

Blacker R.W. Recent changes in the benthos of the west Spitsbergen fishinggrounds // Int. Comm. N.W. Atl. Fish. Spec. Publ. 1957b. Vol. 6. P. 791–794.

Buhl-Mortensen L, Buhl-Mortensen P. 2017. Marine Litter in the Nordic Seas: distribution composition and abundance. Marine Pollution Bulletin 125:260-270. http://dx.doi.org/10.1016/j.marpolbul.2017.08.048

Buhl-Mortensen P, Buhl-Mortensen L. 2018. Impacts of Bottom Trawling and Litter on the

Seabed in Norwegian Waters. Front. Mar. Sci. 5:42. doi: 10.3389/fmars.2018.00042

Buhl-Mortensen L,Wing Gabrielsen G, Anker-Nilssen T, Standal E. 2018. Plastic on beaches and in seabirds: Preliminary results from a comparative study in the Norwegian Arctic and North Sea, Sixth International Marine Debris Conference, San Diego, 12 – 16 March (Poster) Dalpadado, P., and Skjoldal, H.R., 1996. Abundance, maturity and growth of the krill species, Thysanoessa inermis and T. longicaudata in the Barents Sea. Marine Ecology Progress Series 144, 175–183.

Collie *et al*. 2000. A quantitative analysis of fishing impacts on shelf-sea benthos. Journal of Animal Ecology 2000, 69, 785-798

Dalpadado, P., Bogstad, B., Gjøsæter, H., Mehl, S., and Skjoldal, H. R. 2002. Zooplankton–fish interactions in the Barents Sea. In Large Marine Ecosystems of the North Atlantic, pp. 269–291. Ed. by K. Sherman, and H. R. Skjoldal. Elsevier Science, Amsterdam.

Dalpadado, P., R. Ingvaldsen and A. Hassel. 2003. Zooplankton biomass variation in relation to climatic conditions in the Barents Sea. Polar Biol. 26: 233–241.

Dalpadado P., Ingvaldsen R.B., Stige L.C, Bogstad B., Knutsen T., Ottersen G. Ellertsen B. 2012. Climate effects on Barents Sea ecosystem dynamics. ICES J. Mar. Sci. 69(7): 1303–1316.

Dalpadado, P., Arrigo, K.R., Hjøllo, S.S., Rey, F., Ingvaldsen, R.B., Sperfeld, E., *et al*. 2014. Productivity in the Barents Sea - Response to Recent Climate Variability. PLoS ONE 9(5): e95273. doi:10.1371/journal.pone.0095273

Denisenko S.G. 2013. Biodiversity and bioresources of macrozoobenthos in the Barents Sea, structure and long-term changes. Nauka, St Petersburg. Pp 284.

Dingsør, G. E. 2001. Estimation of discards in the commercial trawl fishery for Northeast Arctic cod (Gadus morhua L.) and some effects on assessment. Cand. Scient thesis, University of Bergen, 2001

Dolgov, A.V., Johannesen, E., and Høines, Å. 2011. Main species and ecological importance. In The Barents Sea Ecosystem Resources and Management. Half a century of Russian-Norwegian Cooperation. Pp 193-200. Ed by T. Jakobsen, V. Ozhigin. Tapir Academic Press, Trondheim Norway.

Dolgov A.V., Benzik A.N. 2014. Feeding of cod in the northern Barents Sea. In : A.B. Karasev (ed.) The formation of bioproductivity in the northern Barents Sea in the period of warming in the Arctic. Murmansk: PINRO Press, P. 138-154. (in Russian)

Dolgov A.V., Benzik A.N. 2016. Snow crab as a component of fish diet in the Barents Sea. In : K.M. Sokolov (ed.) Snow crab Chionoecetes opilio in the Barents and Kara seas. Murmansk:PINRO Press. P.140-153. (in Russian)

Eriksen, E., Ingvaldsen, R. B., Nedreaas, K. and Prozorkevich, D. 2015c. The effect of recent warming on polar cod and beaked redfish juveniles in the Barents Sea. Regional Studies in Marine Science 2: 105–112.

Eriksen, E., Dalpadado. P., Prokhorova T. and Dolgov, A. 2017. Biomass indices and distribution of krill and amphipods. In: Prozorkevich, D. Sunnanå K. 2017. (Ed.) Survey report from the joint Norwegian/Russian ecosystem survey in the Barents Sea and adjacent waters, August-October 2016. IMR/PINRO Joint Report Series, No. 1/2017. ISSN (in press)

Fauchald, P., Ziryanov, S. V., Strøm, H., Barrett, R. T. 2011. Seabirds of the Barents Sea. Pages 373-394 in Jakobsen T, Ozhigin VK (Eds) The Barents Sea. Ecosystem, Resources, Management. Tapir Academic Press, Trondheim, Norway.

Fauchald, P., Anker-Nilssen, T., Barrett, R., Bustnes, J. O., Bårdsen, B. J., Christensen-Dalsgaard, S., Descamps, S., Engen, S., Erikstad, K. E., Hanssen, S. A., Lorentsen, S.-H., Moe, B., Reiertsen, T., Strøm, H., Systad, G. H. (2015). The status and trends of seabirds breeding in Norway and Svalbard. NINA report 1151: 84 pp.

Fossheim M, Primicerio R, Johannesen E, Ingvaldsen RB, Aschan M and Dolgov AV. 2015. Recent warming leads to a rapid borealization of fish communities in the Arctic. Nature Climate Change 5, 673–677

Frainer A, Primicerio R, Kortsch S, Aune M, Dolgov AV, Fossheim M and Aschan MM. 2017. Climate-driven changes in functional biogeography of Arctic marine fish com-munities. PNAS

Gjøsæter, H., Bogstad, B., and Tjelmeland, S. 2009. Ecosystem effects of the three capelin stock col-lapses in the Barents Sea. Mar. Biol. Res.: 40-53.

Gjøsæter, H., Hallfredsson, E. H., Mikkelsen, N., Bogstad, B., and Pedersen, T. 2016. Predation on early life stages is decisive for year-class strength in the Barents Sea capelin (Mallotus villosus) stock. – ICES J. Mar. Sci., 73: 182–195.

Grøsvik BE, Prokhorova T, Eriksen E, Krivosheya P, Horneland PA, Prozorkevich D. 2018. Assessment of marine litter in the Barents Sea, a part of the joint Norwegian-Russian ecosystem survey. Front. Mar. Sci., 06 March 2018. https://doi.org/10.3389/fmars.2018.00072

Gullestad, P., Abotnes, A.M., Bakke, G., Skern-Mauritzen, M., Nedreaas, K., and Søvik, G. 2017. To-wards ecosystem-based fisheries management in Norway – Practical tools for keeping track of relevant issues and prioritising management efforts. Marine Policy, Volume 77, March 2017, Pages 104–110. http://dx.doi.org/10.1016/j.marpol.2016.11.032

Hall 1999. Managing fisheries within ecosystems: can the role of reference points be expanded? Aquatic Conser Mar. Freshw. Ecosyst. 9: 579–583

Humborstad, O.B., Løkkeborg, S., Hareide, N.R., and Furevik, D.M. 2003. Catches of Greenland halibut (Reinhardtius hippoglossoides) in deepwater ghostfishing gillnets on the Norwegian continental slope. Fisheries Research 64 (2-3): 163-170

Hunt G.L., Blanchard A.L., Boveng P., Dalpadado P., Drinkwater K., Eisner L., Hopcroft R., Kovacs K.M., Norcross B.L., Renaud P., Reigstad M., Renner M., Skjoldal H.R, Whitehouse A., Woodgate R. A 2012. The Barents and Chukchi Seas: Comparison of two Arctic shelf ecosystems. Journal of Marine Systems: 43-68

ICES 2016a. Report of the NAFO/ICES Pandalus Assessment Group (NIPAG), 7-14 September 2016, Bergen, Norway. ICES CM 2016/ACOM: 15. 113 pp.

ICES. 2016b. Report of the Working Group on Widely Distributed Stocks (WGWIDE), 31 August-6 September 2016, ICES HQ, Copenhagen, Denmark. ICES CM 2016/ACOM:16. 500 pp.

ICES. 2016c. Report of the Arctic Fisheries Working Group (AFWG), Dates 19-25 April 2016, ICES HQ, Copenhagen, Denmark. ICES CM 2016/ACOM:06. 621 pp.

ICES. 2016d. Report of the ICES/NAFO/NAMMCO Working Group on Harp and Hooded Seals (WGHARP), 26-30 September 2016, ICES HQ, Copenhagen, Denmark. ICES CM 2016/ACOM:21. 85 pp.

ICES. 2017. Report of the Working Group on Widely Distributed Stocks (WGWIDE), 30 August -5 September 2017, ICES Headquarters, Copenhagen, Denmark. ICES CM 2017/ACOM:23. 1111 pp.

Jennings S, Dinmore TA, Duplisea DE, Warr KJ, Lancaster JE. 2001. Trawling disturbance can modify benthic production processes. J Anim Ecol 70:459–475

Jørgensen, L.L., Ljubin, P., Skjoldal, H.R., Ingvaldsen, R.B., Anisimova, N., Manushin, I. 2015a. Distribution of benthic megafauna in the Barents Sea: baseline for an ecosystem approach to management. ICES J Mar Sci, 72: 595-613

Jørgensen, L.L., Planque, B., Thangstad, T.H., Certain, G. 2015b. Vulnerability of megabenthic species to trawling in the Barents Sea. ICES J Mar Sci. doi: 10.1093/icesjms/fsv107. 14 pp.

Kutti, T., Høysæter, T., rapp, H.T., Humbistad, O.B., Løkkeborg, S., Nøttestad, L. 2005. Immediate Effects of Experimental Otter trawling on a Sub-Arctic Benthic Assemblage inside inside Bear Island Protection Zone in the Barents Sea. American Fisheries Society Symposium 41:519–528.

Klages M. *et al.* (2004) The Benthos of Arctic Seas and its Role for the Organic Carbon Cycle at the Seafloor. In: Stein R., MacDonald R.W. (eds) The Organic Carbon Cycle in the Arctic Ocean. Springer, Berlin, Heidelberg

Large, P. A., Graham, N. G., Hareide, N-R., Misund, R., Rihan, D. J., Mulligan, M. C., Randall, P. J., Peach, D. J., McMullen, P. H., and Harlay, X. 2009. Lost and abandoned nets in deepwater gillnet fisheries in the Northeast Atlantic: retrieval exercises and outcomes. ICES Journal of Marine Science, 66: 323–333.

Lien, V.S., Y. Gusdal, J. Albretsen, A. Melsom, and F.B. Vikebø, 2013: Evaluation of a Nordic Seas 4 km numerical ocean model archive. Fisken og Havet, 7, 79pp

Lyubin, P. A., Anisimova, A. A., and Manushin, I. E. 2011. Long-term effects on benthos of the use of bottom fishing gears. In The Barents Sea: Ecosystem, Resources and Management: Half a Century of Russian-Norwegian Cooperation, pp. 768–775. Ed. By T. Jakobsen, and V. K. Ozhigin. Fagbokforlaget, Bergen, Norway. 832 pp.

Lyubina O.S., Strelkova (Anisimova) N.A., Lubin P.A., Frolova E.A., Dikaeva D.R., Zimina O.L., Akhmetchina O.Yu., Manushin I.E., Nekhaev I.O., Frolov A.A., Zakharov D.V., Garbul E.A., Vyaznikova V.S. Modern quantitative distribution of zoobenthos along the transect Kola Section / Transactions of the Kola Science Centre. Series 3 Oceanology, 2/2016 (36). P. 64-91 (In Rusian)

Løkkeborg, S. 2003. Review and evaluation of three mitigation measures - bird-scaring line, underwater setting and line shooter - to reduce seabird bycatch in the North Atlantic longline fishery. Fisheries Research 60 (1): 11-16

Løkkeborg, S. 2005. Impacts of trawling and scallop dredging on benthic habitats and communities. FAO Fisheries Technical Paper. No. 472. Rome, FAO. 2005. 58p.

Manushin I.E. (2016) Food consumption by the snow crabs in the Barents and Kara Seas. In: Snow crabs Chionoecetes opilio in the Barents and Kara Seas (eds by K.M. Sokolov, Pavlov V.A., Strelkova N.A. *et al*.). Murmansk: PINRO press: 136-139. (In Russian).

Manuchin I.E., Anisimova N.A., Lubin P.A., Dahle S., Cochrane S. Long-term changes in the macrozoobenthos of the southeaster part of the Barents Sea / Materials of XIV scientific workshop "Reading in memorian of K.M. Derjugin". Sankt-Petersburg: University, 2012. P. 33-45. (In Russian)

Mecklenburg, C.W., I. Byrkjedal, J.S. Christiansen, O.V. Karamushko, A. Lynghammar and P. R. Møller. 2013. List of marine fishes of the arctic region annotated with common names and zoogeographic characterizations. Conservation of Arctic Flora and Fauna, Akureyri, Iceland

Mecklenburg, C.W., A. Lynghammar, E. Johannesen, I. Byrkjedal. J.S. Christiansen, A.V. Dolgov, O.V. Karamushko, T.A. Mecklenburg, P.R. Møller, D. Steinke, and R.M. Wie-nerroither. 2018. Marine Fishes of the Arctic Region. Conservation of Arctic Flora and Fauna, Akureyri, Iceland. ISBN: ISBN 978-9935-431-70-7.

Nesis K.N. Changes in the bottom fauna of the Barents Sea under the influence of the hydrological regime fluctuations // Soviet fisheries research in the seas of the European North. Moscow: Fisheries, 1960. P. 129-138 (In Russian).

Orlova, E. L., Rudneva, G. B., Renaud, P. E., Eiane, K., Vladimir, S., and Alexander, S. Y. 2010. Cli-mate impacts on feeding and condition of capelin, Mallotus villosus in the Barents Sea. Evidence and mechanisms from a 30 year data set. Aquatic Biology, 10: 105–118.

Rey *et al.* (in prep). Interannual variability of new and net primary production in the Barents Sea.

Sirenko BI (2001) Introduction. In List of species of free-living invertebrates of Eurasian Arctic Seas and adjacent waters. pp. 3-8. Ed by Sirenko B.I. Explorations of the fauna of the seas, 51. Zoological Institute of the Rus.Ac. of Sci.: Saint Petersburg.

Sokolov, K. 2004. Estimation of cod discards in the Barents Sea and adjacent waters during the Russian bottom trawl fishery in 1983-2002. Working Document no. 7. ICES Arctic Fisheries Working Group, ICES CM 2004/ACFM:28.

Skjoldal, H.R., Rey, F., 1989. pelagic production and variability of the Barents Sea ecosystem. In: Sherman, K., Alexander, L.M. (Eds.), Biomass yields and geography of large marine ecosystems, AAAS Selected Symposium, vol. 111. Westview Press, pp. 241–286.

Skjoldal, H.R., Gjøsæter, H., Loeng, H., 1992. The Barents Sea ecosystem in the 1980s: ocean climate, plankton and capelin growth. ICES Marine Science Symposia 195, 278–290.

Stige, L.C., Dalpadado, P., Orlova, E., Boulay, A.C., Durant, J.M., *et al.* 2014. Spatiotemporal statistical analyses reveal predator-driven zooplankton fluctuations in the Barents Sea. Progr Oceanogr, 120: 243–253.

Strelkova, N.A. About acclimatization of snow crabs in the Barents Sea and Kara Sea. 2016. PINRO press, Murmansk. Pp 17-35

Strøm, H., Gavrilo, M.V., Krasnov, J.V. and Systad, G.H. 2009. Seabirds. In Joint Norwegian-Russian Environmental Status 2008 Report on the Barents Sea Ecosystem. Part II – Complete report, pp. 67-73. Ed. by J.E. Stiansen, O. Korneev, O. Titov, P. Arneberg, A. Filin, J.R. Hansen, Å. Høines and S. Marasaev. IMR/PINRO Joint Report Series, 3/2009

Suuronen, P., 2005. Mortality of fish escaping trawl gears. FAO Fisheries Technical Paper No. 478. Tschernij, V., Suuronen, P., 2002. Improving trawl selectivity in the Baltic. Nordic Council of Ministers (TemaNord 2002. No. 512).

Zakharov D.V., Strelkova N.A., Lyubin P.A., Manushin I.E. (2016) Macrobenthic communities in the area of the snow crab distribution in the Barents and Kara Sea. In: Snow crabs Chionoecetes opilio in the Barents and Kara Seas (eds by K.M. Sokolov, Pavlov V.A., Strelkova N.A. *et al*.). Murmansk: PINRO press: 59-73. (In Russian).

Zakharov D.V. Northern shrimp. In: The state of the biological resources of the Barents Sea and the North Atlantic in 2017 (Edited by E.A. Chamray). Murmansk: PINRO, 2017. P. 41-42. (In Russian).

Annex 6: Time-series used in WGIBAR

Description of the time-series used in the Integrated multivariate analysis, grouped into abiotic, biotic and pressures (see below and Table 1).

A PCA analysis was run with 13 abiotic variables reflecting oceanographic conditions.

A PCA analysis was done on a set of variables including zooplankton biomass in three size fractions and sum total for the Barents Sea (Figure 2.2.3), 3 time-series of krill, and abundance of 0-group fish of 8 species (capelin, cod, haddock, herring, polar cod, Greenland halibut, long-rough dab, redfish, and saithe).

A PCA analysis was run with 23 variables reflecting stock size, growth and maturation of cod (7 variables), haddock (6 variables), capelin (5 variables), polar cod (2 variables), and herring, long-rough dab and shrimp (1 variable each).

a. Abiotic

Atmosphere and Air:

Winter North Atlantic Oscillation (NAO) index (PC-based) from December January February March. TaAnom_East and TaAnom_West - Air temperature anomalies in the eastern (69–77°N, 35–55°E) and western (70–76°N, 15–35°E) Barents Sea based on monthly data from the ERA Interim (ECMWF).

Ice:

IceareamaxApril and IceareaminSept - Ice area in the Barents Sea (10–60°E, 72-82°N) at maximum (April) and minimum (September) ice coverage. Sea ice concentration was obtained from the National Snow and Ice Data Center (NSIDC)

Fluxes:

The Barents Sea is a through-flow system with Atlantic water entering from the Norwegian Sea in southwest and leaving modified between Novaya Zemlya and Franz Josef Land in northeast. Here, we use modelled volume transports from a 4 km resolution model hindcast for the Barents Sea. BSO is the modelled net eastward volume transport between Norway and Bear Island (positive into the Barents Sea). BSX is the modelled net eastward volume transport between Franz Josefs land and Novaya Zemlya (positive out of the Barents Sea). NBSO is the modelled net southward volume transport between Svalbard and Franz Josef Land (positive into the Barents Sea). SBSO is the modelled net eastward volume transport between Kola and Novaya Zemlya (positive out of the Barents Sea).

Water masses:

Areas of Arctic Water (Area_ArW, T<0°C), Atlantic Water (Area_AW, T>3°C) and Mixed water (Area_MW 0°C<T<3°C) were calculated based on the mean 50-200 temperature fields from temperature measurements taken during the annual scientific surveys in the third quarter. To ensure complete data coverage each year, the area calculations were restricted to the area 72–80°N, 20–50°E.

Ocean temperatures:

TempNE and TempNW - Average temperature in two boxes representing the northern and northeastern Barents Sea based on data from the annual scientific surveys in the third quarter. FB-aug - The temperature averaged over the 50–200 meter depth range between 71.5°N and 73.5°N in the Barents Sea Opening in August. Kola_Temperature

- The temperature averaged over the 50–200 meter depth range between 70.5°N and 72.5°N in the Kola Section.

Salinity:

Kola_Salinity- The salinity averaged over the 0–200 meter depth range between 70.5°N and 72.5°N in the Kola Section

b. Biotic

Plankton

Meso-zooplankton – Biomass estimate (interpolated from catches by WP2 plankton nests) from survey in August-September, total and by three size fractions (Zoopl_Total, Zoopl180, Zoopl1000, Zoopl2000). The mesozooplankton biomass data consist mainly of copepods.

Krill- There are four species of krill in the BS, our data are not separated by species We include two krill biomass index series Krill_S is from the Russian winter survey (October-December), sampled with a plankton net attached to the demersal trawl, this survey covers mostly the ice free BS. The dataseries is the longest time-series of zooplankton in the Barents Sea, going back to the 1950s. The series was discontinued in 2016. The second series is from 0-group survey (now the ecosystem survey) covering most of the BS shelf in August-September (Krill). A pelagic trawl is used, and only larger (>15 mm) specimens are retained in the trawls.

Jellyfish - This is a biomass index based on data from 0-group survey (now the ecosystem survey) covering most of the BS shelf in August-September (Jelly).

Benthic invertebrates - *Pandalus borealis* index (Shrimp) from stock assessment.

Pelagic fish

Mallotus villosus- Capelin is a key species in the BS, capelin total-stock biomass (age 1+) acoustic estimate from survey in August-September (Capelin_TSB), length growth from age 1 to 2 (Capelin_gr12), condition at age 2 (Capelin_cond), % mature age 2 (Capelin_Mat2). 0-group abundance is from the ecosystem survey/0-group survey, pelagic trawl (Capelin_0).

Boreogadus saida – Polar cod is a true arctic species. Polarcod_biom is acoustic estimate of biomass from the acoustic survey in August-September. The acoustic survey was originally targeted towards capelin, and the polar cod distribution area extends northeast outside the survey area, so the estimate of the polar cod is uncertain, especially before 2004. 0-group abundance is from the ecosystem survey/0-group survey, pelagic trawl (Polarcod_0).

Juvenile *Clupea harengus*. Juvenile herring is a key species in the Bs, and strong year classes of herring are often associated with recruitment failure of capelin: VPA data age 1 and 2 on herring multiplied with individual weight by age (Herring1-2_biom). 0-group abundance is from the ecosystem survey/0-group survey, pelagic trawl (Herring_0).

Demersal fish

Gadus morhua – Cod is the most important piscovore in the BS and a very important commercial species. Cod total-stock biomass (Cod3+_biom), recruitment-at-age 3 (Cod _Rec3), weigth at age (Cod_w3y, Cod_w5y, Cod_w8y), weight at age 3, proportion mature at age 7 (Cod _mat7), all these series are obtained from assessment. 0-group abundance is from the 0-group survey, pelagic trawl (Cod_0).

Melanogrammus aeglefinus – Haddock is an important commercial species, and is more benthivor than cod. Haddock total-stock biomass (Haddock3+_biom), spawning-stock biomass ages 6–8 (Haddock_SSB68), recruitment-at-age 3 (Haddcok_R3), and predation mortality age 3 from cod (Haddock_M_age3). Data from assessments (ICES 2016c) 0-group abundance is from the ecosystem 0-group survey, pelagic trawl (Haddock_0).

Hippoglossoides platessoides – long rough dab is of limited commercial importance but one of the most abundant and widespread fish in the BS. We used a cpue index from the Russain demersal survey in Nov-Dec (LRD) 0-group abundance is from the ecosystem survey/0-group survey, pelagic trawl (LRD_0).

c. Pressures

Fishing mortality of shrimp (Relative_F_Shrimp) is from the last shrimp assessment (ICES 2016a)

Fishing mortality and haddock (Cod_F510 and Haddock_F47) are from the last stock assessments (ICES 2016c)

Fishing Mortality of Capelin (Relative_F_Capelin) in year y was calculated as the sum of catches in autumn year y-1 and the next spring (year y) divided by biomass in autumn year y-1. This was shifted one year compared to the analyses done last year, to reflect that most of the catches are taken in spring.